STUDYING TRYPANOSOMAL PEPTIDASE ANTIGEN TARGETS FOR THE DIAGNOSIS OF ANIMAL AFRICAN TRYPANOSOMIASIS

by

Lauren Elizabeth-Ann Eyssen

B.Sc (Hons)

Submitted in the fulfilment of the
academic requirements for the
MSc degree
in
Biochemistry
School of Life Sciences
University of KwaZulu-Natal
Pietermaritzburg

2013

PREFACE

The experimental work described in this dissertation was carried out in the School of Life Science, University of KwaZulu-Natal, Pietermaritzburg, from January 2011 to December 2013, under the supervision of Professor THT Coetzer. The studies represent original work by the author and have not otherwise been submitted in any other form to another University. Where use has been made of the work of others, it has been duly acknowledged in the text.

_____

Lauren Eyssen
March 2014

As the candidate's Supervisor I agree to the submission of this dissertation.

_____

Prof. Theresa H. T. Coetzer

DECLARATION - PLAGIARISM

I, Lauren Elizabeth-Ann Eyssen, declare that

1. The research reported in this dissertation, except where otherwise indicated, is my original research.

2. This dissertation has not been submitted for any degree or examination at any other university.

3. This dissertation does not contain other persons' data, pictures, graphs or other information, unless specifically acknowledged as being sourced from other persons.

4. This dissertation does not contain other persons' writing, unless specifically acknowledged as being sourced from other researchers. Where other written sources have been quoted, then:

    a. Their words have been re-written but the general information attributed to them has been referenced
    b. Where their exact words have been used, then their writing has been placed in italics and inside quotation marks, and referenced.

5. This dissertation does not contain text, graphics or tables copied and pasted from the Internet, unless specifically acknowledged, and the source being detailed in the dissertation and in the Reference section.

_____

Lauren Eyssen
March 2014

AKNOWLEDGEMENTS

I can do all things through God who strengthens me (Phil. 4:13).

I would like to express my heartfelt thanks and appreciation to the following persons:

Firstly to Prof Coetzer for the opportunity to complete this degree under your guidance, your time and belief in my ability. To Prof Goldring for your advice and thought provoking questions.

To Dr Phillia Vukea for your vast knowledge of just about every experimental method in the laboratory and your time spent assisting when needed.

To Dr Pillay and Dr Watson for all things cloning and your advice regarding the murky world of genetics. To Charmaine Ahrens, Tanya Karalic, Natalie Jones and Jane Flockhart for their tireless administration work which makes our lives as post graduate students much easier.

To Pat Joubert, my other mom, for all the ordering of our desperately needed lab reagents and all the other small, but very necessary things you do. Along with Megan Brunkhorst, thank you both for your time and friendship.

To my fellow post graduates: Faith Ndluvo, Phindili Ximba, Sanele Mnkandla, Omolara Adekunle, Kayleen Brien and those from the neighbouring laboratories: Mellissa Govender, Rob Krause, Kelvin Adicott, Faiz Shaik, Celia Snyman, Nick Walker, Rhys McColl, Kyle Groechst and to Jacky Viljoen, thank you all. Each of you have, in some way or other, shaped me into the researcher that I am today with your advice, encouragement and even your presence.

To Shelley Barnsley for your help and support throughout my prostgraduate studies.

To the National Research Foundation (NRF) for their financial assistance.

To Grant Napier at Galvmed for allowing me the opportunity to work on the trypanosomiasis diagnostics project. To the friendly staff at ClinVet: Annesca, Werner, Alec and Heidi for making my trips to Bloemfontein a pleasant one.

Finally to my family, my Mom, Bartholomew, Dad, Nana, Grampa and everyone else, as well as to Gavin and his family, a huge thank you for your never ending love and support which I so truly needed during this time.

ABSTRACT

The lack of a vaccine candidate due to antigenic variation by trypanosomal parasites, the causative agents of human and animal African trypanosomiasis, requires the disease to be controlled by surveillance, diagnosis and appropriate treatment schedules. Due to the non-specific symptoms along with the toxicity and side effects of the current trypanocides, diagnosis needs to be accurate, cost effective and applicable to active case finding in mostly rural settings. Trypanosomal proteases have been identified as virulence factors as they are essential to the parasites' survival. Here the diagnostic potential of previously described virulence factors, oligopeptidase B (OPB), pyroglutamyl peptidase (PGP) and the full length and catalytic domain of the cathepsin L-like peptidases ($CATL_{FL}$ and CATL respectively) from *T. congolense* (Tc) as well as OPB and CATL from *T. vivax* (Tv), was determined. These antigens were recombinantly expressed, purified and used to generate antibodies in chickens. The purified recombinant antigens were tested in an inhibition and indirect ELISA format using two separate blinded serum panels consisting of sera from non-infected and experimentally infected cattle, one each for *T. congolense* and for *T. vivax.* The tested sera were diluted 1:10 for the $TcCATL_{FL}$, TcCATL antigens whilst the TvCATL antigen used a 1:100 serum dilution. The $TcCATL_{FL}$, TcCATL and TvCATL antigens had the highest diagnostic potential in the indirect ELISA format with a 90.91, 92.21% accuracy at the second cut-off and a 77.22% accuracy at the third cut-off along with 0.8084, 0.7785 and 0.8813 area under curve (AUC) values respectively. These antigens show potential for development of lateral flow tests to detect *T. congolense* and *T. vivax* infections in cattle.

The recently discovered metacaspases (MCAs) have been implicated in caspase-like activity and differentiation in *T. b. brucei*, *T. cruzi* and *L. major* and are considered to be virulence factors. The putative metacaspase 5 gene from *T. congolense* (*TcMCA5*) was successfully cloned, expressed within inclusion bodies, resolubilised and refolded using immobilised metal affinity chromatography. Recombinant TcMCA5 was successfully refolded as evident by the hydrolysis of the synthetic peptide substrate, Z-Gly-Gly-Arg-AMC. Autocatalytic processing was observed within the inclusion bodies and the products were purified along with the full length recombinant protein. Anti-TcMCA5 IgY antibodies, raised in chickens, were able to detect the native TcMCA5 along with the autocatalytic processed products within the lysate of the procyclic *T. congolense* (strain IL 3000) parasites. The diagnostic potential of TcMCA5 still requires verification.

TABLE OF CONTENTS

LIST OF FIGURES

LIST OF TABLES

ABBREVIATIONS

2 x YT	2 x yeast extract, tryptone
3D	three dimensional
AAT	animal African trypanosomiasis
ABTS	2,2-azino-di-[3-ethylbenzthiazoline sulfonate]
AMC	7-amino-4-methylcoumarin
ANF	atrial naturiuretic factor
AT	African trypanosomiasis
AUC	area under curve
BARP	brucei alanine rich protein
BCA	bicinchoninic acid
BCM	buffy coat method
BMGY	buffered media glycerol yeast
BMM	buffered minimal media
bp	base pair
BPT	0.5% (w/v) BSA-PBS, 0.1% (v/v) Tween-20
BSA	bovine serum albumin
BSF	bloodstream form
CATL	cathepsin-L
CATT	card agglutination test
CCB	carbonate coating buffer
CI	confidence interval
CIATT	card indirect agglutination test for trypanosomiasis
CSF	cerebral spinal fluid
DALYS	disability-adjusted life years
dH_2O	distilled H_2O
DFMO	eflornithine
DMSO	dimethylsulfoxide
DNA	deoxyribonucleic acid
dNTP	deoxynucleotide triphosphate
DTT	dithiothreitol
ECL	enhanced chemiluminescence
EDTA	ethylenediaminetetra-acetic acid
ELISA	enzyme-linked immunosorbent assay
EMEM	eagle's minimal essential medium
EMF	epimastigote form

ES	expression sites
ESAG	expression site-associated gene
FN	false negative
FP	false positive
FBS	foetal bovine serum
FIND	Foundation for Innovative New Diagnostics
g	relative centrifugal force
GLB	gel loading buffer
GnRH	gonadotropin-releasing hormone
GPI	glycosylphosphatidylinositol
GPI-PLC	GPI-specific phospholipase C
GRESAG	related to expression site associated gene
GST	glutathione S-transferase
h	hour
HAT	human African trypanosomiasis
HRPO	horseradish peroxidise
HSP	1% (v/v) horse serum-PBS
IC	intermediate chromosomes
IFA	immunofluorescence assay
IFN-γ	gamma interferon
Ig	immunoglobulin
ICP	inhibitor of cysteine peptidase
IL	interleukin
IMAC	immobilised metal ion affinity chromatography
IPTG	isopropyl-β -D-thiogalactopyranoside
ISG	invariant surface glycoprotein
J	Youden index
kDa	kiloDalton
LAMP	loop-mediated isothermal amplification
LHRH	luteinizing hormone releasing hormone
mAECT	mini-anion-exchange centrifugation technique
MBP	maltose-binding protein
MBS	M-maleimidobenzoyl acod N-hydroxy succinimide ester
MC	minichromosomes
MCA	metacaspase
MCF	metacyclic form
MEC	molecular exclusion chromatography

mHCT	microhaemocrit centrifugation test
min	minute
M_r	molecular mass
MSP	surface metalloprotease
NASBA	nucleic acid sequence based amplification
ND	not determined
NECT	eflornithine-nufurtimox combination theray
NO	nitric oxide
NPV	negative predictive value
OC	oligochromatographic
OIE	International Office of Epizootics
OPB	oligopeptidase
PAGE	polyacrylamide gel electrophoresis
PARP	procyclic acidic repetitive protein
PBS	phosphate buffered saline
PCD	programmed cell death
PCE	sarkosyl elution buffer
PCF	procyclic form
PCL	sarkosyl lysis buffer
PCR	polymerase chain reaction
PCV	packed cell volume
PCW	sarkosyl wash buffer
PDB	Protein Database
PEG	polyethylene glycol
PfrA	paraflagellar rod protein A
L-pGlu	L-pyroglutamyl residue
PGP	pryoglutamyl peptidase
pI	isoelectric point
PLC	phospholipase C
POP	prolyl oligopeptidase
PPV	positive predictive value
QBC	quantitative buffy coat
QSPR	quantitative structure-property relationship
RIME	ribosomal mobile element
RNAi	RNA interference
ROC	receiver-operating characteristic
RT	room temperature

sarkosyl	N-lauroylsarsocine sodium salt
SBTI	soya bean trypsin inhibitor
SD	standard deviation
SDS	sodium dodecyl sulphate
SRA	serum resistance-associated
SOC	super optimal catabolizer
TAE	tris-acetate-EDTA
TBS	tris buffered saline
TB	terrific broth
TL	immune trypanolysis
TLCK	N-tosyl-L-lysyl chloromethylketone
TN	true negative
TNF	tumor necrosis factor
TP	true positive
TPP	three phase partitioning
TRH	thyrotropin-releasing hormone
Tris	2-amino-2-(hydroxymethyl)-1,3-propandiol
UPH_2O	ultra pure H_2O
VAT	variant antigen type
V_e	elution volume
V_o	void volume
VSG	variant surface glycoprotein
V_t	total column volume
WBC	white blood cell
WHO	World Health Organisation
X-gal	isopropyl-β-D-thiogalactopyranoside
YNB	yeast nitrogen base
YPD	yeast extract peptone dextrose
Z	benzyloxycarbonyl

CHAPTER 1

LITERATURE REVIEW

1.1 African trypanosomiasis, the disease

Approximately 60 million people spread across 200 separate active foci from 36 sub-Saharan countries are estimated to be exposed to human African trypanosomiasis (HAT) and of these, only 4 to 5 million are under surveillance (WHO, 1998; Cattand *et al.*, 2001). In 2004, the WHO estimated an incidence of HAT to be between 50 000 to 70 000, however 17 500 new cases were reported (WHO, 2006) The locations of these active foci are mostly rural and follow the geographic distribution of the tsetse belt which stretches north of the Kalahari desert to the south of the Sahara (Barrett *et al.*, 2003). Within this region, it is estimated that 46 to 62 million head of cattle and other livestock species are at risk of animal African trypanosomiasis (AAT) (Swallow, 2000). In 2011, 6 631 cases of *Trypanosoma brucei gambiense* and 112 cases of *T. brucei rhodesiense* HAT infections were reported (Simarro *et al.*, 2013). This number is estimated to be higher due to the limitations of diagnostic methods combined with the rural locations of disease incidence. The disease was estimated to have a health burden on the African continent of approximately 1.6 million disability-adjusted life years (DALYS) in 2004 (Févre *et al.*, 2008) which results in a situation of repressed economic development in central Africa (WHO, 1986; Molyneux *et al.*, 1996). The impact of AT in Africa results in an excess of US $4.5 billion annually in economic losses (Swallow, 2000).

The tsetse fly (*Glossina* spp.) is the insect vector for the transmission of trypanosomal parasites between vertebrate hosts as the parasite relies on the host for survival and replication (Kuzoe, 1993; Steverding, 2008). Tsetse flies are found in approximately 10 000 million km^2 of Africa (Mattioli *et al.*, 2004). Trypanosomes are unicellular protozoan parasites from the genus *Trypanosoma* and are the causative agents of AT. The *Palpalis* group are the insect vectors for the human infective trypanosomal parasites, whilst the animal infective parasites are of the *Morsitans* group (Stuart *et al.*, 2008; Hargrove *et al.*, 2012) (Fig. 1.1, panel A). Human infections by *T. b. gambiense* is known to occur in 24 countries across the west and central regions of Africa (Simarro *et al.*, 2008; Simarro *et al.*, 2012) (Fig. 1.1, panel B). This species is responsible for over 90% of reported HAT infections with the remainder of infections being caused by the *T. b. rhodesiense* species in east and southern Africa (Simarro *et al.*, 2008; Simarro *et al.*, 2011) (Fig. 1.1, panel A). The former causes chronic infection, where death can

occur within years, and the latter causes acute infection with death occurring within months (Steverding, 2008).

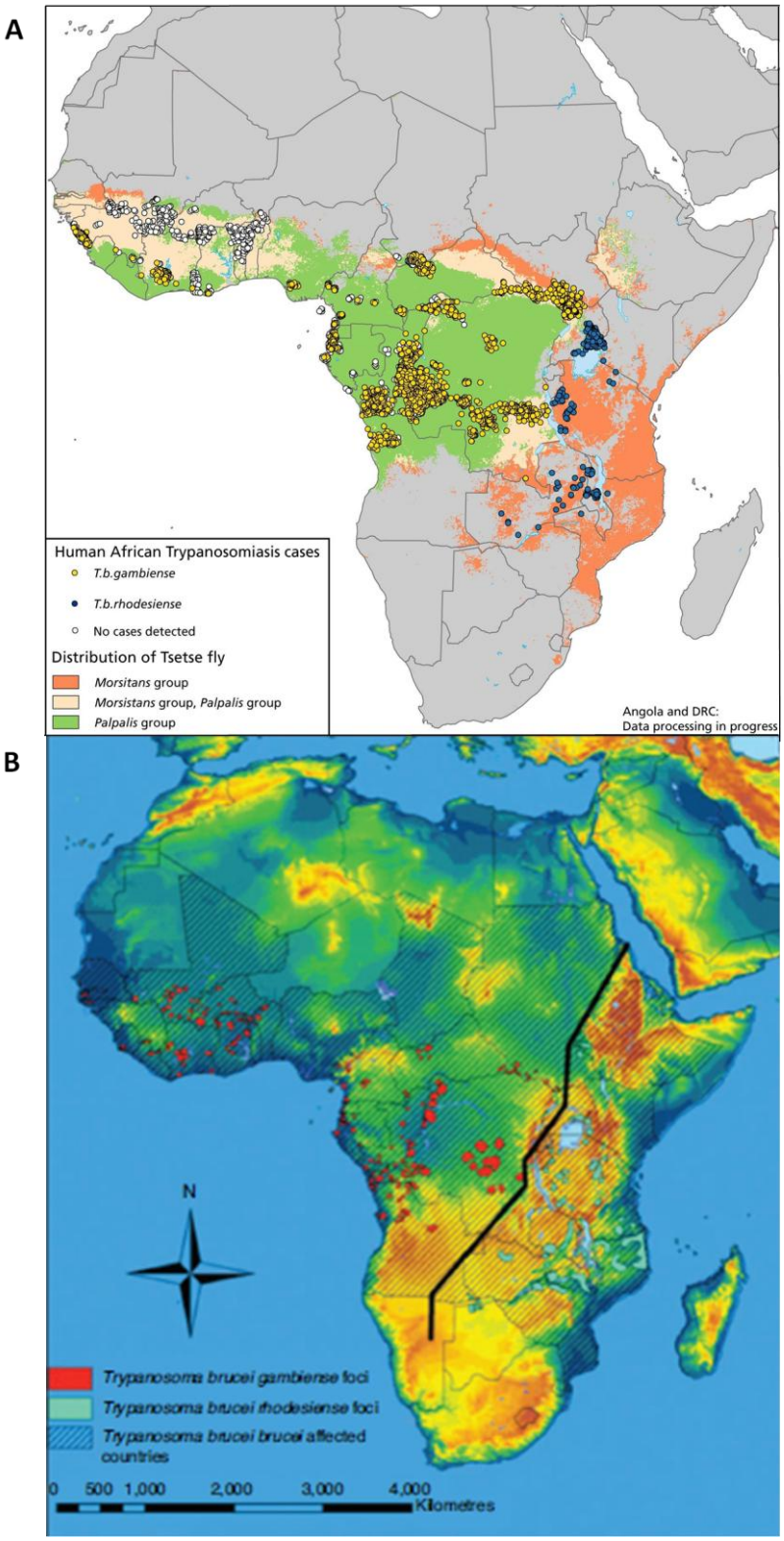

Figure 1.1: Distribution of tsetse flies in Africa and their impact on the human population. (A) The geographical locations of the reported HAT cases along with the tsetse fly distribution [Taken from the Atlas of Human Infectious Diseases (2012)] and **(B)** the foci of the *T. brucei* species throughout Africa (Wastling and Welburn, 2011).

Trypanosomal infections in livestock are 100 to 150 times more likely to occur than human infections (Jordan, 1976). Infections brought about by the *T. b. brucei* species are characterised by necrosis, oedema and numerous inflammatory disease symptoms (Facer *et al.*, 1982). Infections by the *T. congolense and T. vivax* species cause extra-vascular haemolytic anaemia in infected cattle and is responsible for the development of chronic anaemia and results in decreased productivity and losses of livestock (Facer *et al.*, 1982; Authié, 1994). N'dama cattle (*Bos taurus*) are able to limit parasitaemia and the disease symptoms caused by *T. congolense* infection and are known as trypanotolerant (Authié, 1994). African Zebu cattle (*Bos indicus*) are not able to limit the parasite infection and are thus susceptible to the disease (Authié, 1994).

1.2 Classification of trypanosomes

Trypanosomes form part of the *Kinetoplastida* order and can be further defined, according to the life cycle within the insect vector, into the *Salivaria* and *Stercoraria* groups (Smith and Sherman, 1994) (Fig. 1.2). The parasites of the *Stercoraria* group develop within the intestinal tract of the insect vector and infection occurs via the faeces whilst the parasites of the *Salivarian* group develop within the stomach of the vector with infection occurring via the saliva during the acquisition of a blood meal. A prime example of the *Stercoraria* group is *T. cruzi*, whilst *T. b. brucei, T. congolense, T. vivax, T. evansi* and *T. equiperdum* are of the *Salivaria* group (Haag *et al.*, 1998). The causative agents of Nagana are *T. b. brucei, T. congolense* and *T. vivax* which belong to the *Trypanozoon, Nannomas* and *Duttonella* groups respectively (Facer *et al.*, 1982). Nagana infections in wild animals are often mild whilst severe and often fatal infection is displayed in domestic animals (Steverding, 2008). Of the *Salivaria* group, *T. congolense* and *T. b. brucei* are transmitted only by the tsetse fly (*Glossina* spp.) whilst the other species are either transmitted by the tsetse fly or by mechanical transmission by hematophagus insects as is the case for *T. vivax* (Smith and Sherman, 1994). Surra, a livestock disease, in Africa, Central and South America, the Middle East and Asia is caused by *T. evansi* (Wuyts *et al.*, 1994). The equine veneral disease, dourine, is caused by *T. equiperdum*. Transmission for *T. evansi* and *T. equiperdum* occurs mechanically by biting flies and sexually, respectively (Smith and Sherman, 1994).

1.3 The life cycle and distribution of African trypanosomes

Due to a trypanolytic factor in their serum, humans and some primates are resistant to most species of trypanosomal parasites, however *T. b. gambiense* and

T. b. rhodesiense are resistant to this factor and are thus the only trypanosomal species to cause HAT infections (Poelvoorde *et al.*, 2004; Baral, 2010). Due to the expression of the serum resistance-associated (*SRA*) gene, *T. b. rhodesiense* is resistant to the trypanolytic factor in human serum and thus cause acute rather than chronic infections (De Greef *et al.*, 1992; Pays, 2006).

Trypanosomal parasites have a dual host life cycle and require special adaptations such as kinetoplast DNA, unique gene regulation, RNA editing, glycosomes and a flagellum along with a flagellar pocket (Clayton *et al.*, 1995). Due to the parasites' dual life cycle, they require the various morphological and gene expression changes, which are involved in the various life cycle stages, to be effectively coordinated (Matthews, 1999) (Fig. 1.3). Mammalian infection commences upon the acquisition of a blood meal by an infected tsetse fly whereby metacyclic form (MCF) parasites are injected. The MCF parasites transform into proliferative bloodstream form (BSF) trypomastigotes which are entirely coated with a continuous layer of variant surface glycoprotein (VSG) homodimers (Vickerman and Luckins, 1969; Cross, 1975). The BSF trypomastigotes are long and slender in appearance, during the ascending phase of parasitaemia. At the peak of parasitaemia, the BSF trypomastigotes, which are now short and stumpy in appearance, are no longer proliferative (Barry and McCulloch, 2001; Matthews *et al.*, 2004). Upon the transformation into the stumpy form, the parasites subsequently transform into insect vector infectious procyclic form (PCF) parasites which are able to colonise and proliferate within the midgut of the insect vector (McLintock *et al.*, 1993; Redpath *et al.*, 2000). The transformation from stumpy BSF into PCF is accompanied by a change in metabolism, whereby ATP is generated by glycolysis to being generated by oxidative phosphorylation (Clayton, 1992; Vassella *et al.*, 2004; Matthews, 2005). Within the midgut of the insect vector, once colonised by PCF stumpy forms, metabolic changes occur within the parasite. The loss of the VSG surface coat along with the expression of new surface proteins, procyclic acidic repetitive proteins (PARPs) or procyclins which are glycosylphosphatidylinositol (GPI)-anchored proteins (Urwyler *et al.*, 2005), characterise the parasite's transformation into proliferative PCF (Ziegelbauer and Overath, 1993; Gruszynski *et al.*, 2003).

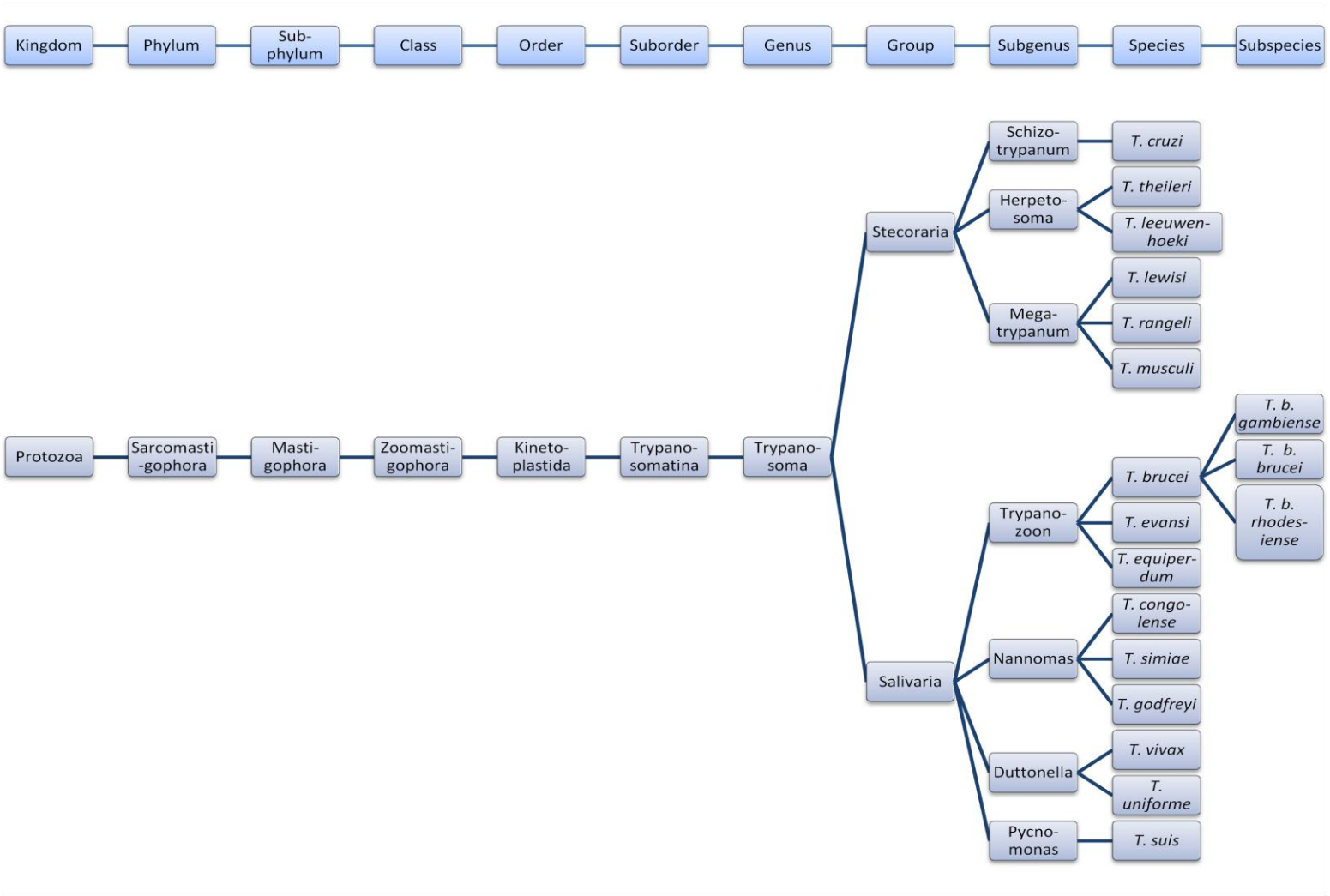

Figure 1.2: Classification of trypanosomes within the protozoan kingdom. Adapted from Baral (2010).

The rapid loss of the VSG surface coat of the PCF stumpy form requires the combined action of GPI-specific phospholipase C (GPI-PLC) and a surface zinc metalloprotease (MSP-B) (Ziegelbauer and Overath, 1993; Gruszynski *et al.*, 2003). After the proliferation of PCF parasites within the midgut, migration towards the salivary glands occurs where they undergo asymmetric cell division to form stumpy and slender epimastigote form (EMF) parasites (Van Den Abbeele *et al.*, 1999). Only the stumpy EMF parasites possess a brucei alanine rich protein (BARP) surface coat which replaces the procyclin coat. These stumpy EMF parasites are able to attach, proliferate and mature into MCF parasites within the salivary glands of the insect vector, where they re-acquire their VSG surface coat (Tetley *et al.*, 1987; Urwyler *et al.*, 2005; Urwyler *et al.*, 2007). Once colonised, the salivary glands are the generation site of the MCF which are infectious to mammals (Sbicego *et al.*, 1999). The MCF parasites have a larger repertoire of VSG genes compared to that of the BSF parasites (Barry and McCulloch, 2001).

The BSF of the *T. b. brucei* parasites are pleomorphic, with two different physical forms being present at any one given time (Vickerman, 1985). The slender forms replicate by asexual division and are susceptible to elimination by host proteases (Sbicego *et al.*, 1999). The stumpy forms, which are non-proliferative, are resistant to elimination by host peptidases and are able to differentiate into PCF parasites which are then able to colonise the salivary glands of the insect vector (Clayton, 1992; Sbicego *et al.*, 1999). The non-proliferative character of the stumpy forms acts to prevent the uncontrolled growth of the slender forms which would result in the rapid killing of the infected mammalian host. This would result in the reduction of the transmission potential of the invading parasites (Matthews and Gull, 1994).

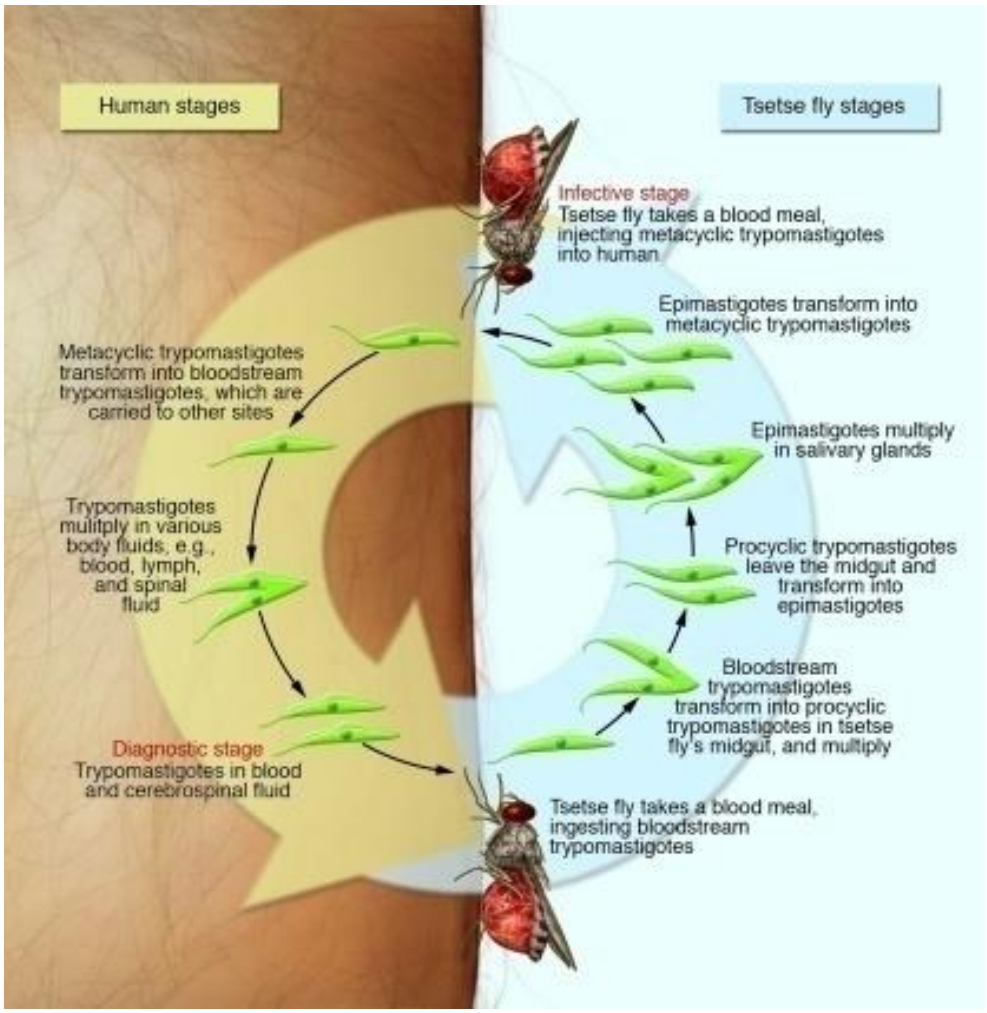

Figure 1.3: Life cycle of a *Trypanosoma brucei brucei* parasite showing the human host and tsetse fly insect vector stages. (Stuart *et al.*, 2008).

1.4 The genomic organisation of trypanosomes

The trypanosome karyotype, which is able to undergo genetic variation, is characterised by the presence of minichromosomes (MCs) and intermediate chromosomes (ICs) which are absent in all other kinetoplastids (Ersfeld, 2011). The ICs and MCs are only found in the genome of *T. b. brucei* and are solely responsible for the provision of the genes necessary for antigenic variation (Berriman *et al.*, 2005). An estimated 15% of the *T. b. brucei* genome is dedicated to the reservoir of VSG genes (Barry *et al.*, 2005). Many of these VSG genes are pseudogenes, and by genetic recombination, are responsible for the generation of functional mosaic genes (Marcello and Barry, 2007). The variable surface glycoprotein expression sites (VSG-ES) are found within the ICs. These VSG-ESs are activated by the *in situ* VSG expression switching (Van der Ploeg *et al.*, 1984). The MCs constitute an important source of VSG genes and are predicted to encode for almost 200 VSGs (Ersfeld, 2011). In the BSF

parasites, only a single ES is transcribed in an individual parasite at any given time (Ersfeld, 2011). However in the PCF parasites, all ESs are silent, as the PCF parasites lack the VSG coat and are coated rather with PARPs and procyclins (Ersfeld, 2011). An ES is either switched off, a different ES is activated or an existing VSG gene in an active ES is replaced with a different VSG gene via genetic recombination and results in the expression of a new variant of VSG (Horn and Cross, 1997).

1.5 Immune response to trypanosomal infection

The innate immune system is the first defence against trypanosomal infection (Stijlemans *et al.*, 2007; Baral, 2010). Trypanolytic factors present in the serum of humans serve as their primary defence against trypanosomal infection (Poelvoorde *et al.*, 2004).

Antigenic variation occurs due to the differential expression of VSG genes to evade the host's immune response (Haag *et al.*, 1998; Barry and McCulloch, 2001). Trypanosomal parasites have various methods by which they evade the host immune system. One such method is by the process of antigenic variation (Cross, 1990) and immune-suppression by the elimination of B-cell memory as suggested by Magez and co-workers (2010). A typical immune response to trypanosomal infection is the non-specific activation of polyclonal B-cells to produce immunoglobulin M and G (IgM and IgG) against the VSG coat, as well as the generalised suppression of some humoral and cellular immune functions (Sacks and Askonas, 1980; Pépin and Donelson, 2006). The anti-VSG IgM antibodies are used in the capture of C3b complement fragments for liver mediated clearance of the infecting trypanosomal parasites (Shi *et al.*, 2005; Pan *et al.*, 2006). The MCF parasites are able to evade this method of clearance by removing the VSG binding IgM from the surface (Shi *et al.*, 2005). Macromolecular trafficking of endocytosed VSG-complexed IgM antibodies occurs and results in protection against complement mediated killing (Engstler *et al.*, 2007; Field *et al.*, 2009).

Anti-VSG IgM antibodies are produced during the early stages of infection with IgG antibodies being the dominant response in the later stages, and facilitate the destruction and clearance of the invading parasites (Sacks and Askonas, 1980; Crowe *et al.*, 1984). This process occurs in successive waves as new VSG coats, and in turn, new antibodies are produced (Black *et al.*, 1986). This process is thought to be a contributing factor in antibody mediated trypanotolerance (Uzonna *et al.*, 1999). In addition, these anti-VSG IgM antibodies are responsible for the neutralisation of

parasite metabolic waste and debris from parasite lysis, however, a significant portion of these antibodies are polyspecific (Ellis *et al.*, 1987; Williams *et al.*, 1996). The waves of parasitaemia explain the ever changing levels of circulating trypanosomal parasites in the blood stream (Ross and Thomson, 1910) which in turn affect the limited sensitivity of parasitological detection methods in clinical practice (Chappuis *et al.*, 2005a).

1.6 Control strategies for trypanosomiasis

In order to target, monitor and evaluate the interventions against AT, accurate geographical information, in the form of disease distribution maps, is required (Cattand *et al.*, 2001; Simarro *et al.*, 2010). Since the main reservoir for *T. b. gambiense* is found in humans, active case finding and treatment of infections are the strategies implemented for the control of *T. b. gambiense* infections (Stuart *et al.*, 2008). The control of *T. b. rhodesiense* infections is accomplished by the treatment of the patients as well as the animal reservoir which includes wild and domestic animals (Welburn *et al.*, 2006). In addition to the control of the insect vector and the management of the mammalian host and insect vector reservoirs, the incidence of AT should decrease due to the resulting reduction of disease incidence, vector density and the mammalian reservoir (Simarro *et al.*, 2010). There are currently four strategies implemented for the control of trypanosomal transmission in cattle, namely curative drugs, vector control, breeding with trypanotolerant cattle and the development of potential vaccination strategies (McDermott and Coleman, 2001).

The current trypanocidal drug therapy used for AAT include isometamidium chloride, dimazene aceturate or homidium chloride which comprise 40, 33 and 26% of the market respectively (McDermott and Coleman, 2001). The treatment of AT with trypanocidal drugs is the main control strategy, whilst less attention is given to the control of the insect vector and the parasite (Hargrove *et al.*, 2012).

The use of insecticide spraying, sterile insects, odour-baited traps and pesticide treated targets and livestock, which have been treated with a pour-on insecticide, are effective measures to reduce trypanosomal transmission by the tsetse fly insect vector to the mammalian host (McDermott and Coleman, 2001). Insecticides are either applied directly onto the cattle, used for aerial and ground spraying or for the treatment of odour-baited traps. The use of insecticide treated odour baited traps is a more environmentally friendly control strategy than game destruction, habitat clearance and insecticidal ground spraying (Hargrove *et al.*, 2003). Odour-baited traps are effective

against AAT insect vectors (Torr *et al.*, 2005), but less so for the HAT insect vectors (Rayaisse *et al.*, 2010) due to the difference in the host and insect vector relationships between the causative agents of AAT and those of HAT (Hargrove *et al.*, 2012). Research has shown that the treatment of livestock with insecticide has resulted in the same degree of tsetse control that can be achieved with the use of odour-baited traps, however, this method was less effective in areas where wild animals were the food source for the tsetse fly (Hargrove *et al.*, 2003).

1.7 The clinical features of human and animal African trypanosomiasis

Animal trypanosomiasis is the model of a neglected disease which affects the poorest people in Africa (Trouiller *et al.*, 2002). It is due to this neglect that the development of new diagnostic tests and trypanocidal drugs has been negatively affected.

Chronic illness which lasts for years characterises HAT infections caused by *T. b. gambiense*, whilst *T. b. rhodesiense* infections are characterised by acute febrile illness which, if left untreated, is fatal within months. During the course of AT infection, two stages are observed, namely the haemolymphatic or initial and the meningo-encephalitic or final stage (Dumas and Bisser, 1999). The presented clinical features are neither specific nor sensitive enough to be able to correctly diagnose and stage the disease with confidence and as a result invasive procedures must be carried out to obtain cerebral spinal fluid (CSF) and lymph for analysis (Apted, 1970). Other diseases such as malaria and tuberculosis have been found to mimic and even coexist with HAT infection, thus clinical suspicions must be confirmed by laboratory tests (Chappuis *et al.*, 2005a).

After 15 days of an infecting bite, a chancre is formed due to the proliferation of parasites which are generally absent at the time of diagnosis (Buyst, 1975). Rubbery, painless cervical lymph nodes, which are enlarged, occur in the posterior cervical triangle and may not always be present or caused by trypanosomal infection (Pépin and Milord, 1994). In the initial stage of HAT infection, the trypanosomal parasites are found only in the blood and lymph system, whilst in the final stage of infection, parasites are found in the CSF (Kennedy, 2008).

Non-specific symptoms such as headaches, fatigue, joint pains and intermittent fever are characteristic of the initial stage of *T. b. gambiense* infections (Apted, 1970). The clinical features of final stage *T. b*. *gambiense* infection are characterised by motor,

sensory, psychiatric and sleep abnormalities and the appearance of mononuclear inflammatory cells in the CSF (Chappuis *et al.*, 2005b). Based on symptoms, infections caused by *T. b. rhodesiense* cannot be distinguished from other tropical diseases such as malaria, bacterial meningitis and enteric fever (Chappuis *et al.*, 2005a). When compared to *T. b. gambiense* infections, febrile episodes are more frequent and more distinct with *T. b. rhodesiense* infections. Within six months after trypanosomal infection, most cases (> 80%) result in death (Odiit *et al.*, 1997).

The final stages of HAT infections are usually treated with melarsoprol (Schmid *et al.*, 2004; Chappuis *et al.*, 2005b), an arsenate, which is toxic and is known to cause reactive arsenical encephalopathy in patients (Pépin and Milord, 1994; WHO, 1998). It is due to this reason that diagnosis and staging of the disease needs to be highly accurate and sensitive (Van Nieuwenhove, 1999). However, to date there are no blood tests or specific clinical signs which are able to give an indication of HAT progression.

Due to the infecting AAT trypanosomal species, the species of the infected host and the virulence of the particular isolate, the clinical signs may vary widely. Symptoms of AAT are weight loss, anaemia, abortion, reduced productivity and death if left untreated (Taylor and Authié, 2004). Infected animals might not display these symptoms and when stressed can succumb to the trypanosomal infection. Livestock which recover from infections are less productive and are generally left infertile (Luckins, 1988).

The *T. congolense* and *T. vivax* species are haematic parasites, which are found in the blood vessels whilst the *T. b. brucei, T. evansi* and *T. equiperdium* species are humoral parasites and are found within the tissues (Lonsdale-Eccles and Grab, 2002). Due to the ability to cross the blood-brain barrier, the humoral parasite species are able to cause neurological symptoms during the course of the disease (Lonsdale-Eccles and Grab, 2002; Antoine-Moussiaux *et al.*, 2008). In addition, infections with *T. b. brucei* and *T. congolense* are characterised by low levels of parasitaemia when compared to that in *T. vivax* infections which results in difficulties in parasitological detection (Taylor and Authié, 2004).

Three stages of infection occur in AAT progression, namely acute, stabilisation and chronic. In the acute phase, enlarged lymph nodes and spleen, reduced milk production, abortion, weakness and immunodepression are common symptoms and is accompanied by a continuous drop in packed cell volume (PCV) (Uilenberg and Boyt, 1998). Within six to eight weeks post infection, during the stabilisation stage, the PCV

becomes stable. Thereafter chronic infection sets in and is characterised by infertility, anaemia, immunodepression and intermittent parasitaemia (Uilenberg and Boyt, 1998).

1.8 Techiques used for diagnosis of African trypanosomiasis

Due to the toxic nature of melarsprol together with the improbability of developing a vaccine due to antigenic variation, the control of the disease relies heavily on early case detection, diagnosis and stage determination followed by the appropriate treatment. A three step strategy for the diagnosis of *T. b. gambiense* HAT is used for control programmes to detect active HAT cases: screening, diagnostic confirmation and staging (Chappuis *et al.*, 2005a). Screening tools need to be robust, cost effective, practical, rapid, sensitive and be able to discriminate between different parasite species (Chappuis *et al.*, 2005a; Stuart *et al.*, 2008). The ideal format of a trypanosomal diagnostic test would be a lateral flow test whereby a membrane "strip" is dipped in the blood sample and an instant result is visualised (Deborggraeve *et al.*, 2006). Lateral flow tests have the ability to detect nanogram amounts of antibodies or antigens in a small amount of blood, usually from a finger prick, without the need for any other equipment or specialised training (Posthuma-Trumpie *et al.*, 2009).

The most widely used serological screening test, based on the detection of anti-trypanosomal antibodies, in endemic infection areas, is the card agglutination test for *T. b. gambiense* (CATT/*T. b. gambiense*), which has been found to be more efficient than cervical lymph node palpation and puncture (Robays *et al.*, 2004). Parasitological diagnostic confirmation is performed by locating of the parasites in the blood, lymph nodes or CSF and is estimated to fail to detect 20 to 30% of trypanosomal infections (Robays *et al.*, 2004).

Disease staging allows for the classification of HAT into either the first or final stage of infection. Staging is performed by the examination of the CSF due to the lack of reliable blood tests to detect trypanosomal invasion of the central nervous system (Lejon and Büscher, 2001). Infected patients are treated according to the stage of infection and are monitored over a two year period to determine the success of the treatment (Chappuis *et al.*, 2005a).

1.8.1 Serological screening

The detection of anti-trypanosomal antibodies in the blood, serum or plasma of infected hosts can be indirect evidence for infection (Rebeski *et al.*, 1999c; Chappuis *et al.*, 2005a). The complex antigenic structure of the trypanosomal parasite elicits an

immune response resulting in a large number of antibodies being produced. The host's immune response is directed strongly against the VSG antigens and as a result a high concentration of specific IgG and IgM antibodies are produced (Crowe *et al.*, 1984). The sensitivity and specificity of a diagnostic test is determined by the choice of antigen and the detection format used.

The serological tests which are currently in use can detect anti-trypanosomal antibodies three to four weeks after the onset of infection (Vanhamme *et al.*, 2001). Anti-trypansomal antibodies can persist in previously treated hosts for up to three years after cure and thus must be considered before a diagnosis is made (Paquet *et al.*, 1992; Lejon *et al.*, 2010). Antigenic variation, co-infections, the identity of the infecting parasite, localisation of the parasite, the nutritional status of the patient and level of parasitaemia are all important factors to be taken into consideration as they complicate detection in diagnostic techniques (Stuart *et al.*, 2008).

The mass population screening for the diagnosis of *T. b. gambiense* infection has been revolutionised by the introduction of the CATT/*T. b. gambiense* (Magnus *et al.*, 1978) (Fig. 1.4). The CATT is a fast and simple agglutination assay for the detection of *T. b. gambiense*-specific antibodies present in the blood, plasma or serum of infected patients (Magnus *et al.*, 1978). The lysed *T. b. gambiense* BSF parasites of the variable antigen type (VAT) LiTat 1.3 are used as the CATT antigen. Infections with trypanosomal strains which lack the LiTat 1.3 gene may lead to false negative CATT results (Dukes *et al.*, 1992; Enyaru *et al.*, 1998).

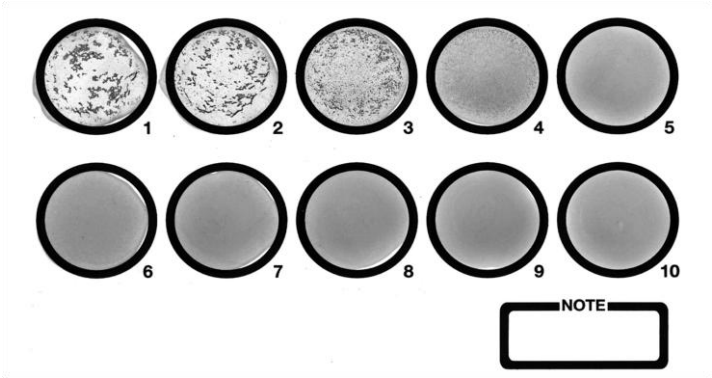

Figure 1.4: An example of a card agglutination test example using a 1:4 dilution of blood samples. A strongly positive reaction is visible for samples 1 to 3, a weakly positive reaction is present in sample 4 whilst the remainder of the samples are negative for trypanosomal infection (Chappuis *et al.*, 2005a).

A field alternative to CATT, the LATEX/*T. b. gambiense*, was developed using three purified VAT antigens, LiTaT 1.3, 1.5 and 1.6 which were coupled to latex beads. The

VAT antigens are obtained from parasites which have been propagated in rats or *in vitro* cultures in specialised laboratories (Greiner *et al.*, 1997; Hopkins *et al.*, 1998). A higher specificity (96 to 99% compared to 80%) and a lower sensitivity (71 to 100% compared to 80%) was obtained when comparing the performance of the LATEX/*T. b. gambiense* to the CATT/*T. b. gambiense* in field evaluations (Jamonneau *et al.*, 2000; Penchenier *et al.*, 2000; Truc *et al.*, 2002). This is as a direct result of the detection of three VATs by the LATEX/*T. g. gambiense*, whilst the CATT can only detect one (Kennedy, 2004). This allows for the LATEX/*T. g. gambiense* test to incur fewer false negatives. However, in foci where strains of trypanosomal parasites express high levels of LiTat 1.3, decreased sensitivity has been reported (Truc *et al.*, 2002). Antibody diagnostic tools, such as the CATT and LATEX, are limited to detection only and are not suitable for follow up evaluations due to the persistence of anti-trypanosomal antibodies after cure (Lejon *et al.*, 2010).

The immune trypanolysis (TL) test can be used as a surveillance tool as serum or blood impregnated filter paper eluate samples can be tested. The TL test is based on the complement mediated lysis of trypanosomal parasites (Chappuis *et al.*, 2005a). An infected patient will have anti-VSG IgM antibodies present in their serum, which will bind to the corresponding VSG on the cultured parasite surface. This results in complement mediated lysis of the trypanosomal parasites. Microscopic examination is performed at 250 x magnification, with a positive reaction being the absence of motile trypanosomes (Van Meirvenne *et al.*, 1995). The trypanosomes used for the test are of a determined VAT obtained from live cultured trypanosomal parasites, which poses a high infection risk to personnel and thus can only be performed in laboratories rather than in the field. Thus despite the TL test being considered the gold standard in the diagnosis of HAT and AAT infections (Van Meirvenne *et al.*, 1995), it is not a routine test as it is expensive and cannot be used in active case finding (OIE, 2013).

Immunofluorescence assays (IFA) can be performed using serum or blood impregnated filter paper eluates and have been shown to be highly sensitive and specific in field evaluations (Noireau *et al.*, 1988). Parasitised blood from mice inoculated with either *T. b. brucei* or *T. b. gambiense* is used as the antigen for the IFA (WHO, 1976). The IFA was one of the first serological tests used for the diagnosis of AAT and has been shown to be sensitive, specific but not species-specific (Luckins and Mehlitz, 1978). It, however, is not quantitative, requires sophisticated equipment and the lack of a standardised antigen makes it a poor choice for active case finding. The reliability of the IFA test has been improved due to the availability of standardised

antigen at a low cost (Nantulya, 1990). Comparison of IFA results is difficult due to the subjectivity of interpretation and the variations in the preparation of the slides. Due to cross-reactivity between the *T. b. brucei*, *T. congolense* and *T. vivax* species, it was found that the IFA was not species specific (Eisler *et al.*, 2004).

Serum, blood impregnated filter paper eluates and CSF, which must be accompanied by strict standardisation and quantification (Rebeski *et al.*, 2001), can be used in enzyme-linked immunosorbent assay (ELISA) methods (Lejon *et al.*, 1998). ELISA methods are able to detect antibodies against current and past infections and are characterised by high sensitivity and genus specificity (pan-*Trypanozoon*), with a generally low species specificity (OIE, 2008). This, however, can be improved by the use of a standardised set of species specific tests (Desquesnes, 2004). This results in the overestimation of the actual prevalence of trypanosomal infection. Two types of ELISAs are used for serological diagnosis, antibody detection using trypanosomal lysate (Luckins, 1997) and antigen detection using monoclonal antibodies (Nantulya, 1990; Eisler *et al.*, 1998). The antibody detection ELISA was first used for the diagnosis of *T. b. rhodesiense* infections (Voller *et al.*, 1975) and then for *T. evansi* infections (Luckins, 1997).

The antibody detection ELISA for *T. b. gambiense* diagnosis uses the same antigens as the LATEX/*T. b. gambiense* but the antigens are fixed on a microtitre plate instead (Hasker *et al.*, 2012). The sensitivity and specificity of the ELISA/*T. b. gambiense* varies from 82.8 to 100% and from 94.7 to 100%, respectively, when using different test samples (Nantulya and Doua, 1992; Hasker *et al.*, 2012). Despite the high sensitivities and specificities associated with the ELISA/*T. b. gambiense*, the test is time consuming, requires specific training of personnel and is expensive to perform. The requirement for sophisticated equipment and trained staff limits the IFA and ELISA methods to the laboratory as they are unsuitable for field diagnosis.

The ELISA is ideal for surveillance as numerous samples could be tested at a time, the process can be automated (Cabrera *et al.*, 2009) and blood impregnated filter paper, collected during active case findings, can be used (Chappuis *et al.*, 2005a). Rebeski and co-workers (1998; 1999c; 2000a; 2000b) have developed a standardised control system which monitors the ELISA performance using strong positive, moderate positive and negative serum controls, in triplicate, along with a no serum control in quadruplicate (Wright *et al.*, 1993). Antigen detection ELISAs have application in the monitoring of the programmes for the elimination and eradication of the tsetse fly (Rebeski *et al.*, 1999c).

To distinguish between active and cured HAT, a serological diagnostic test would have to detect the antigens produced by the parasite rather than the IgM antibodies produced against the parasite (Tiberti *et al.*, 2013). This can be achieved by the detection of antigens released by non-circulating trypanosomal parasites present in the spleen, liver, central nervous system or lymph nodes (Tiberti *et al.*, 2013). After promising results were obtained with the use of monoclonal antibodies in the antigen detection ELISA (Nantulya and Doua, 1992), the development of the card indirect agglutination test for trypanosomiasis (TrypTect CIATT) was undertaken by Brentec Diagnostics, Nairobi, Kenya for field use. Despite high sensitivities compared to other parasitological techniques indicated by preliminary evaluations, further studies indicated low specificities (Asonganyi *et al.*, 1998).

A recent development for the serological diagnosis of *T. b. gambiense* has resulted in the SD BIOLINE HAT (http://www.finddiagnostics.org/media/press/121206.html, accessed 7/06/2013), the HAT SERO K-SeT and the HAT SeroStrip rapid test serodiagnostic tools which are currently being evaluated in the Democratic Republic of Congo (Büscher *et al.*, 2013). Since lateral flow tests are quick, easy to use and requires no training of personnel nor sophisticated equipment, they are ideal for active case finding in rural settings.

Anti-trypanosomal antibodies in the saliva from a group of 23 patients with confirmed *T. b. gambiense* HAT infections were detected using an antibody detection ELISA which used the same antigens as for the LATEX/*T. b. gambiense* (Lejon *et al.*, 2003). The anti-trypanosomal antibodies present in the salvia were 250-fold lower than in the serum and both the CATT and the LATEX/*T. b. gambiense* tests failed to detect them. The use of saliva is a less invasive procedure than collecting blood or CSF.

Since ISG75 is not subject to antigenic variation and is present in all the species comprising the *Trypanozoon* subgenus, it was thought to have diagnostic potential (Tran *et al.*, 2009). Using an indirect antibody detection ELISA format, the ELISA/ISG75 was compared to the CATT/*T. evansi*, the ELISA/*T. evansi* (RoTat 1.2) and the TL assay towards the development of a new serodiagnostic test for the diagnosis of surra in camels (Tran *et al.*, 2009). The results obtained from the ELISA/ISG75 were almost in perfect agreement with the already established *T. evansi* diagnostic tools and the TL assay (Tran *et al.*, 2009).

The ISG64, -65 and -75 along with the gene related to expression site associated gene-4 (*GRESAG-4)* were identified as diagnostic targets and were tested in an

indirect antibody detection ELISA to develop a pan-*Trypanozoon* diagnostic test (Sullivan *et al.*, 2013). The ISG75 was the most promising antigen in the indirect antibody detection ELISA format and when used in a prototype lateral flow format was characteried by a 88% sensitivity and 93% specificity for the detection of *T. b. gambiense* infections (Sullivan *et al.*, 2013).

1.8.2 Parasitological confirmation

After screening by antibody detection methods, parasite infection needs to be confirmed in sero-positive cases. Microscopic examination of lymph node aspirate, blood or CSF provides direct evidence for trypanosomal infection and results in a definite diagnosis (Chappuis *et al.*, 2005a). Parasite detection can be labour intensive and failure to detect parasites does not rule out infection. The parasite numbers for *T. b. gambiense* infections can vary from more than 10 000 parasites/ml to less than 100 parasites/ml, the former being easily detectable, whilst the latter being below the detection limit of even the most sensitive parasitological and serodiagnostic tools (Chappuis *et al.*, 2005a). Discrimination between *T. b. gambiense* and *T. b. rhodesiense* cannot be made using parasitological techniques due to the similarity in their morphologies (Wastling and Welburn, 2011).

The gold standard for the diagnosis of AAT is microscopic examination of blood, with the aid of centrifugation techniques before analysis, the sensitivity of which can be improved (Woo, 1970). Due to the low levels of parasitaemia in chronic infections, diagnosis based on parasitological analysis is ineffective as false negatives may result due to the waves of parasitaemia during disease progression (Nantulya, 1990).

Palpation of the enlarged cervical lymph nodes, when present, is performed on every CATT sero-positive case. The cervical lymph node is punctured and aspirate is expelled onto a microscope slide which is examined microscopically at 200 x magnification for the presence of motile trypanosomal parasites and is characterised by a sensitivity of 40 to 80% (Van Meirvenne, 1999).

In the absence of a centrifuge, wet and thin blood films are the method of choice for the confirmation of AT infection (Fig. 1.5). Wet blood films entail the microscopic examination of finger-prick blood at 200 x magnification. This parasitological method has an upper detection limit of 10 000 trypanosomes/ml and despite its low sensitivity, is still used in some HAT control centres due to its simplicity and low cost. Similarly low sensitivities are obtained with Giemsa- or Field's-stained blood films which are visualised at 500 x magnification using an oil immersion objective lens. The method,

however, is time consuming and requires trained staff to identify the parasites which can become deformed upon preparation. In addition to trypanosomes, other parasites such as microfilaria and *Plasmodium* can be detected and subsequent action can be taken (Chappuis *et al.*, 2005a).

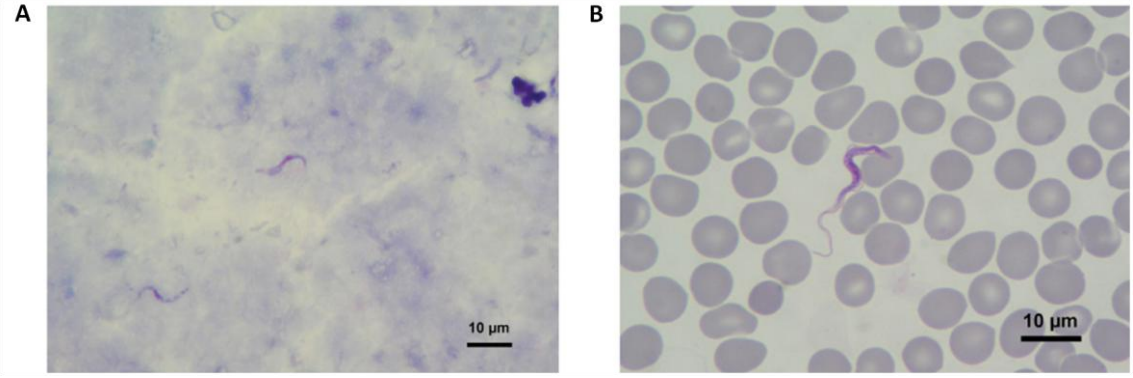

Figure 1.5: Giemsa stained blood smears from a Belgian traveller returning from Masai Mara area, Kenya. (A) Thick and **(B)** thin blood smears used for the parasitological confirmation of the diagnosis of trypanosomal infection (Clerinx *et al.*, 2012).

Blood concentration techniques such as the microhaemocrit centrifugation test (mHCT), or the Woo test, developed more than 40 years ago, are still currently in use in many HAT control programmes (Woo, 1970; Woo, 1971). Trypanosomal parasites are located between the plasma and the red blood cells after centrifugation of the blood sample in capillary tubes which are examined microscopically at 100 to 200 x magnification for motile parasites. The detection threshold of the mHCT is 500 parasites/ml with the sensitivity increasing with the number of tubes prepared. The presence of microfilaria hampers the visualisation of the much smaller trypanosomal parasites. This is a simple, yet moderately time consuming technique employed during mass screening by mobile teams.

The dark-ground/phase-contrast buffy coat method (BCM) or Murray's technique is very similar to the mHCT (Murray *et al.*, 1977) whereby the buffy coat layer from the capillary tubes are expelled onto a coverslip, mounted and examined at 200 to 500 x magnification using dark-ground or phase-contrast microscopy. Both the mHCT and the BCM techniques additionally allow anaemia to be estimated by measuring the PCV (OIE, 2013).

Initially developed for the rapid assessment of differential cell counts, the quantitative buffy coat technique (QBC; Beckton-Dickinson) has been adapted for the diagnosis of haemoparasite infections, including those by trypanosomal parasites (Levine *et al.*,

1989; Bailey and Smith, 1992). This technique allows for the concentration of the parasites as well as the fluorescent staining of the nucleus and kinetoplast with acridine orange which allows for better discrimination from white blood cells (WBCs). After centrifugation the trypanosomes are visualised microscopically at 400 x magnification, in a dark room, under UV light (Fig. 1.6). The equipment is sophisticated and thus the QBC cannot be used for active case finding. The QBC technique is characterised by a 95% sensitivity and with a detection threshold of 450 parasites/ml, can detect more infections with low levels of parasitaemia than the mHCT when fewer than 8 capillary tubes are prepared at a time. In addition, the QBC technique can simultaneously diagnose malaria along with AT infections (Chappuis *et al.*, 2005a).

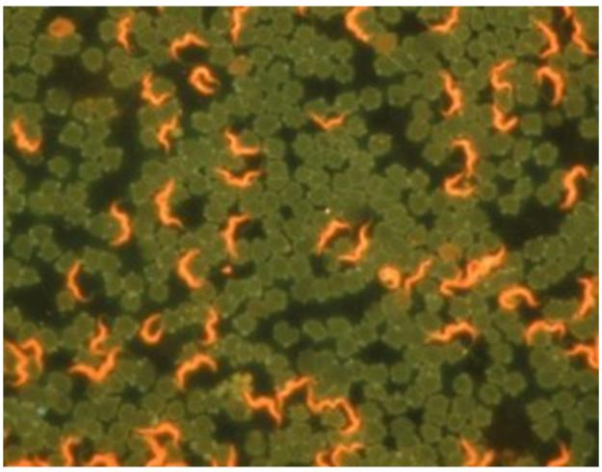

Figure 1.6: Acridine orange stained trypanosomal parasites using a thin blood smear and visualised at 400 x magnification using a LED fluorescence microscope. The microscope was developed by Foundation for innovative new Diagnostics (FIND) and Carl Zeiss with the photo as courtesy of Carl Zeiss (http://www.finddiagnostics.org/programs/hat-ond/hat/parasite_detection/, accessed 7/06/2013).

Based on the technique developed by Lanham and Godfrey (1970), where the less negatively charged trypansomal parasites are separated from red blood cells by anion exchange chromatography, the mini-anion-exchange centrifugation technique (mAECT) was introduced (Lumsden *et al.*, 1979). Initial studies indicated that the mAECT was a more sensitive technique for the detection of trypanosomal parasites than the thick blood films and the mHCT (Lumsden *et al.*, 1981). Zillmann and co-workers (1996) have since developed an improved version which allows for the detection of less than 100 parasites/ml at 100 x or 200 x magnification (Truc *et al.*, 2002). The mAECT is, however, time consuming and the manipulations are tedious.

The effectiveness of parasitological tools is limited by the levels of parasites present in the bodily fluids (Donelson, 2003; Field *et al.*, 2009). Due to the low levels of

parasitaemia in *T. b. gambiense* infections, compared with that found in *T. b. rhodesiense* infections, it is estimated that 20 to 30% of *T. b. gambiense* infections go undiagnosed (Robays *et al.*, 2004).

1.8.3 Stage determination

Due to the lack of specific clinical signs and blood tests for the differentiation between the first and the final stages of HAT infection, CSF obtained from a lumbar puncture is still used for the staging of the disease in patients. The guidelines for the definition of the final stage of HAT infections are set by the World Health Organisation (WHO) (1998). Should the CSF contain any of the following: (i) raised WBC count (>5 cells/µl), (ii) trypanosomal parasites and (iii) increased protein content (>370 mg/L), as measured by the dye-binding protein assay, the disease is considered to be in the final stage.

The sensitivity of parasitological examination of the CSF is limited, even after centrifugation techniques, due to the low numbers of parasites present in the CSF which may result in a false stage determination (Cattand *et al.*, 1988; Miezan *et al.*, 2000). In an attempt to increase the sensitivity of final stage determination, counting of the WBC is performed. Diagnosis made by a WBC count is complicated by the poor reproducibility of WBC counting and the controversy of the protein content limit (Lejon and Büscher, 2001; Kennedy, 2008; Simarro *et al.*, 2008).

1.8.4 Other molecular diagnostic approaches to screening and confirmation of trypanosome infection

Biomarkers of HAT have the potential to be applied in the development of novel diagnostic tests. According to Hölzmuller and co-workers (2008), the interactions between the host, the insect vector and the parasite may be the crucial factors for the onset of infection and the development of disease symptoms. Investigation into the parasite proteome, pathogeno-proteomics, has facilitated the identification of new potential therapeutic agents as well as diagnostic targets (Biron *et al.*, 2005; Hölzmuller *et al.*, 2008).

Various PCR assays exist for the proposed diagnosis of HAT and species identification but none have been validated for diagnostic purposes. In theory, a PCR assay which targets repetitive sequences is more sensitive than those which target single copy or low copy sequences such as those developed for the distinction between *T. b. gambiense* and *T. b. rhodesiense*. High specificities have been reported by most

PCR studies; however comparisons of their diagnostic abilities to those of commonly used diagnostic tests were not made (Tiberti *et al.*, 2013). The detection of pan-*Trypanozoon* species was confirmed by the amplification of the minicircles of the kinetoplast DNA (Mathieu-Daude *et al.*, 1994) and the ribosomal RNA genes (Desquesnes *et al.*, 2001). The detection of *T. b. gambiense* species was confirmed by the amplification of a *T. b. gambiense* specific glycoprotein gene (Radwanska *et al.*, 2002) and the *T. b. rhodesiense* species, by the amplification of the gene coding for the SRA protein (Gibson *et al.*, 2002).

The isothermal amplification of trypanosomal DNA has recently gained favour and various approaches and amplification targets have been investigated. Various diagnostic targets using the loop-mediated isothermal amplification (LAMP) (Wastling *et al.*, 2010) and nucleic acid sequence based amplification (NASBA) (Chan and Fox, 1999) have been developed for HAT diagnostics. The results of LAMP and NASBA are fluorescently visualised after the isothermal amplification of specific DNA sequences present in the parasites (Iwamoto *et al.*, 2003) (Fig. 1.7). The diagnosis of the pan-*Trypanozoon* species was achieved using LAMP of the *paraflagellar rod protein A* (*Pfr*A) gene (Kuboki *et al.*, 2003) and of the ribosomal mobile element (RIME) (Njiru *et al.*, 2008a) where fluorescence indicates a positive test. The diagnosis of *T. b. rhodesiense* infections was confirmed by the LAMP of the SRA gene (Njiru *et al.*, 2008b).

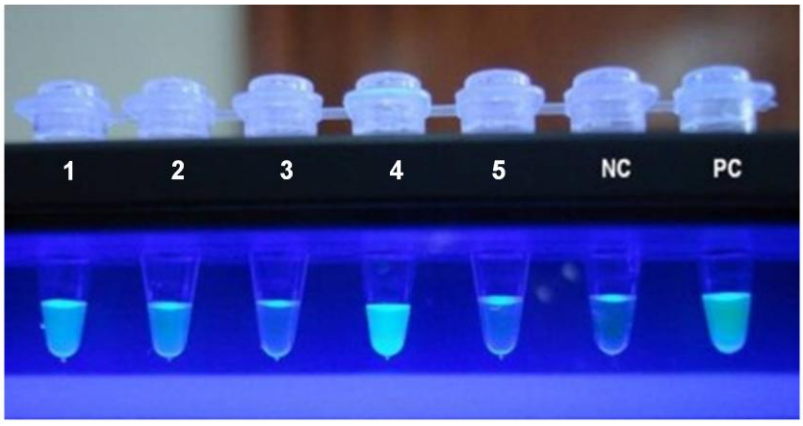

Figure 1.7: Seropositive samples tested using loop-mediated isothermal amplification (LAMP). The negative control is denotated as NC with the positive control by PC. A positive reaction is evident in tubes 1, 2 and 4, whilst tubes 3 and 5 are negative. The photo is courtesy of Dr. Enock Matovu (http://www.finddiagnostics.org/programs/hat-ond/hat/molecular_diagnosis.html, accessed 7/06/2013).

The diagnosis of HAT infections using either PCR, LAMP, or NABSA is not suitable for active case finding diagnosis due to the requirement for sophisticated equipment and

trained personnel and is thus restricted to laboratory and research use (Deborggraeve and Büscher, 2010).

The NASBA and PCR assays targeting the 18S rRNA has been coupled to an oligochromatographic (OC) dipstick detection format (NASBA-OC and PCR-OC) and was found to be more sensitive than parasitological techniques when blood instead of CSF was used (Matovu *et al.*, 2010). The specificity and sensitivity of the NASBA-OC was higher than the PCR-OC for the same gene, but was not compared to the *T. b. rhodesiense* PCR-OC (Matovu *et al.*, 2010). CORIS BioConcept recently launched an oligochromatography dipstick test for the serodiagnosis of *T. cruzi* infections, the *T. cruzi* OligoC-TesT. It is based on the amplification of selected antigens and the oligochromatographic detection thereof and is able to detect 1 parasite per 180 µl of blood.

1.9 Drug therapy for African trypanosomiasis

The ideal trypanocide should be affordable, safe, effective and require simple administration (orally vs. intravenously) (Kuzoe, 1993). When a treatment plan is made consideration of the identity of the infecting parasite needs to be made along with the infection stage due to the high toxicity of the trypanocidal drugs used for the treatment of final stage HAT. Initial stage infections by *T. b. gambiense* and *T. b. rhodesiense* are treated with pentamidine and sumarin respectively which are associated with a less than 1% mortality rate (Kinabo, 1993; Stuart *et al.*, 2008; Baral, 2010). The drugs used for the treatment of final stage HAT infections are plagued by adverse side effects and problems are encountered regarding their efficacy, administration as well as patient compliance (Burri *et al.*, 2004).

The most commonly used drug for final stage infections is melarsoprol, which is an organo-arsenic compound. Treatment of *T. b. gambiense* and *T. b. rhodesiense* final stage infections with melarsoprol causes the deaths of 44 and 5% of treated patients respectively (Pépin and Milord, 1994; Burri, 2010). The majority of these deaths are due to acute encephalopathies, which is a severe side effect of the melarsoprol treatment (Pépin and Milord, 1994; WHO, 1998; Burri, 2010). Due to development of drug resistance by the trypanosomal parasites, the rate of treatment failure is increasing (Brun *et al.*, 2001). When treatment with melarsoprol fails, eflornithine (DFMO) or nifurtimox-eflornithine combination therapy (NECT) is followed and provides a safer treatment alternative to melarsoprol (Chappuis *et al.*, 2005a; Bisser *et al.*, 2007; Simarro *et al.*, 2012). Despite being a safer drug treatment, DFMO and NECT both

require a complicated treatment schedule at a high cost, which prevents these from being the treatment of choice for final stage HAT infections (Chappuis *et al.*, 2005b).

Isometamidium chloride (Samorin®) and homidium chloride (Novidium®) possess prophylactic and therapeutic properties whilst diminazene aceturate (Berenil®) possesses only therapeutic properties and are used for the treatment of AAT (Geerts *et al.*, 2001). Due to the ease of availability and low cost of trypanocides, they are often administered indiscriminately without accurate diagnosis in tsetse infected areas thus reducing the effectiveness of the trypanocide and leading to the emergence of drug resistance (Van den Bossche *et al.*, 2000b; Geerts *et al.*, 2001; Delespaux *et al.*, 2002). Due to the extended use of trypanocides, it is no surprise that drug resistance has emerged (Geerts and Holmes, 1998) in 21 African countries (Delespaux *et al.*, 2008; Chitanga *et al.*, 2011).

Diminazene aceturate resistance has been reported in *T. b. brucei* in endemic areas (Anene *et al.*, 2001; Anene *et al.*, 2006) which is the most commonly used drug for animal infections. In a study done by Kagira and Maina (2007), it was found that out of six *T. b. rhodesiense* isolates used to infect mice, five were resistant to melarsoprol, homidium chloride and diminazene aceturate. However, each strain was sensitive to isometamidium chloride (Kagira and Maina, 2007). Since isometamidium chloride is a hybrid of homidium chloride and diminazene aceturate (Wragg *et al.*, 1958), it follows that the combined properties might be the reason for the observed sensitivity (Kagira and Maina, 2007). The use of a sanative pair for the treatment of AAT, consisting of isometamidium chloride and diminazene aceturate, is unlikely to induce cross-resistance (Whitesand, 1960; Chitanga *et al.*, 2011).

1.10 An anti-disease strategy for the control of African trypanosomiasis

Due to the improbability of an AT vaccine as a result of antigenic variation, an alternative strategy in combating the disease needed to be formulated. The anti-disease strategy focuses on the neutralisation of the host-parasite interactions and the parasite factors involved in pathogenesis rather than the elimination of the parasite itself (Antoine-Moussiaux *et al.*, 2009). An anti-disease vaccine strategy should be aimed at inducing a state that mimics trypanotolerant animals which are able to limit the levels of parasitaemia and reduce the disease symptoms, and as a result are able to survive longer than their trypanosusceptible counterparts (Authié *et al.*, 2001). The resistance to trypanosomal infection in genetically susceptible cattle has been shown to

be increased upon their immunisation against pathogenic/virulence factors of the parasite (Authié *et al.*, 2001). The identification of novel chemotherapeutic and diagnostic targets which should be unique to the parasites and essential for their growth and survival (Stuart *et al.*, 2008), has been achieved due to the completion of the TriTryp genome database (Berriman *et al.*, 2005).

By targeting the pathogenic factors released by the invading trypanosomal parasites, it is possible to induce immune recognition of these and could thus allow for protection against the pathological effects of trypanosomal infection (Playfair *et al.*, 1990). It is thought that N'dama cattle, which are trypanotolerant, are able to fight off infection by inducing an immune response against the invariant antigens which are released by the trypanosomal parasites upon lysis in the host bloodstream (Authié *et al.*, 1993b; Taylor, 1998).

When an anti-disease strategy is developed, various aspects need to be taken into consideration. When using bacterial derived recombinant material, bacterial contamination is possible, the time period between immunisation and challenge needs to be carefully selected as long term studies are required to assess the effect that immunisation has on B-cell memory (Radwanska *et al.*, 2008).

Since VSGs are found on the cell surface of the trypanosomal parasites they were the targets of early vaccine attempts before the process of antigenic variation was discovered (Cornelissen *et al.*, 1985). Vaccination against the VSG molecules is unlikely due to the nature of the gene rearrangements to produce new VSGs and the short-lived induced IgM response to VSGs (La Greca and Magez, 2011). Since vaccination with antigens present in the flagellar pocket provided partial, but temporary protection (Mkunza *et al.*, 1995) these antigens were deemed unsuitable for vaccines (Radwanska *et al.*, 2000). Attention then focused on the invariant surface antigens such as transferring receptors from the expression site-associated genes 6/7 (ESAG6/7) (Steverding *et al.*, 1994) and ISGs (Ziegelbauer and Overath, 1993) with partial protection reported upon vaccination with a DNA plasmid encoding a BSF specific ISG (Lança *et al.*, 2011). Despite numerous attempts using vaccines targeting the surface proteins together with the limited B-cell memory based protection from VSG and ISG vaccinations, the elimination of the entire parasite seems impossible and thus the attention turned towards an anti-disease approach (Magez *et al.*, 2010; La Greca and Magez, 2011).

Peptidases of the trypanosomal parasite have been shown to be virulence factors and are thus ideal chemotherapeutic targets and diagnostic candidates (Antoine-Moussiaux *et al.*, 2009). Numerous researchers have investigated the suitability of the identified virulence factors, some of which are peptidases, for the development of an anti-disease strategy; the cell surface metallopeptidase, GP63 (Jaffe and Dwyer, 2003), various cysteine proteases such as cathepsin-L like peptidases (CATL) (Authié *et al.*, 2001), oligopeptidase B (OPB) (Morty *et al.*, 1999), VSG, GIP anchors (Antoine-Moussiaux *et al.*, 2009) and various ISGs (Jackson *et al.*, 1993; Ziegelbauer and Overath, 1993).

1.11 Protozoan peptidases

Eight classes of peptidases have been identified, serine, cysteine, aspartic, glutamic, metallo, threonine, asparagine and a mixed type. Each class is further organised into clans and families by hierarchy (Rawlings *et al.*, 2012). The MEROPS database uses a hierarchical, structure-based classification of the peptidases. Protein sequences which are homologous are classified into families which are grouped into 27 clans (Rawlings *et al.*, 2012). Research has shown that despite the lack of sequence identity, structural similarity is observed between related proteins (Chothia and Lesk, 1986). The similarities in the tertiary protein structure allows for classification into clans as they will possess a similar protein fold (Rawlings *et al.*, 2012). Various classes of cysteine and serine peptidases have been identified in trypanosomes and these will be discussed in further detail.

Due to the fact that the *T. b. brucei, T. congolense* and *T. vivax* parasites localise to different tissues, it is proposed that their respective proteases will cause different pathological effects (Ssenyonga, 1980). The *T. b. brucei* and *T. congolense* species have unique and different interactions with the host immune system and thus are not similar from an immunological point of view (Magez *et al.*, 1997; Magez *et al.*, 2010). In the control of trypanosomal infection, the contribution of cytokine based immune response cannot be ignored (Noël *et al.*, 2002). Previous research has suggested that cytokine immune responses are able to influence the outcome of AT infection (Hertz *et al.*, 1998; Uzonna *et al.*, 1999). Resistance to *T. congolense* infections have been demonstrated to be correlated to the predominant secretion of type I cytokines in early infections and to a more pronounced secretion of type II cytokines during the late stages of infection (Namangala *et al.*, 2001). It has been previously demonstrated that resistance to murine models of *T. b. rhodesiense* and *T. b. brucei* infections are based on the secretion of gamma interferon (IFN-γ) by the activation of macrophages (Hertz *et al.*, 1998). In the case of *T. b. brucei* infections, tumor necrosis factor (TNF) has

been shown to play a crucial role in the control of parasitaemia and the development of pathology (Magez *et al.*, 1993; Magez *et al.*, 1999). In *T. congolense* infections, it has been shown that interleukin-12 (IL-12) -dependent synthesis of IgG2a against the parasite antigens (Kaushik *et al.*, 1999), along with the IFN-γ and nitric oxide (NO) immune responses, are crucial for resistance (Magez *et al.*, 2006).

1.11.1 Serine peptidases

Serine peptidases play a vital role in various physiological functions such as digestion, immune responses, fibrinolysis to name but a few (Polgár, 2005). These peptidases are characterised by a Ser, His, Asp catalytic triad (Polgár, 2005). The mechanism by which classical serine peptidases act is detailed in Fig. 1.8.

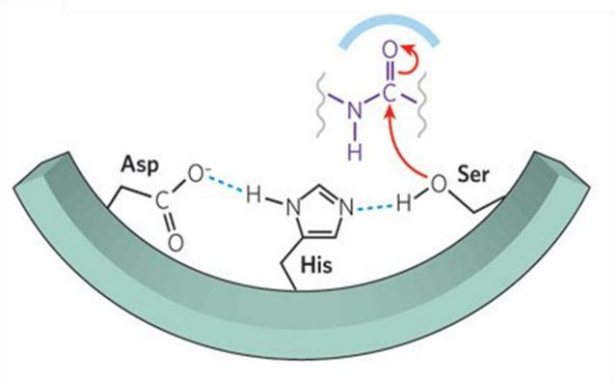

Figure 1.8: The reaction mechanism and amino acid orientation during serine peptidase mediated proteolysis. The catalytic triad consists of Asp, His and Ser residues whereby the serine nucleophile attacks the substrate carbonyl carbon (Erez *et al.*, 2009).

The serine hydroxyl nucleophile attacks the carbonyl carbon of the substrate whereby a tetrahedral intermediate and an imidazolium ion is formed (Polgár, 2005). The tetrahedral intermediate is stabilised by an oxyanion hole in the enzyme, which provides the hydrogen bonds to the oxygen atom, and is formed by the backbone amide of the Gly193 and Ser195 residues (Polgár, 1987; Hedstrom, 2002). The formation of the acyl enzyme and the amine product, from the intermediate, is achieved by acid catalysis (Polgár, 2005). The acyl enzyme is subsequently deacylated by the attack of a water molecule rather than the serine nucleophile (Polgár, 2005).

Serine peptidases are classed in 12 clans, namely SB, SC, SE, SF, SH, SJ, SK, SO, SP, SR, SS and ST along with 7 families which have not yet been assigned. Prolyl oligopeptidase (POP) and oligopeptidase B (OPB), present in trypanosomes, are members of the S9 family within the SC clan of serine peptidases (Coetzer *et al.*, 2008; Rawlings *et al.*, 2008). The SC clan possesses the same α/β-hydrolase fold containing the catalytic triad common to the classical serine peptidases with the exception in the

reverse of handedness (Fülöp *et al.*, 1998). Whereas POP cleaves peptides, no bigger than 30 residues, after a proline residue (Rawlings *et al.*, 1991; Barrett and Rawlings, 1992), OPB belongs to a small subgroup of peptidases from the S9 family which are able to cleave peptides C-terminal to basic residues (Burleigh *et al.*, 1997; Polgár, 2002).

1.11.1.1 Oligopeptidase B

African trypanosomes possess an OPB enzyme which has been implicated in trypanosomiasis since the serine peptidase inhibitors (serpins) found in the host bloodstream are unable to inhibit their activity such as the degradation of host peptide hormones (Troeberg *et al.*, 1996; Morty *et al.*, 2005; Coetzer *et al.*, 2008). This enables the trypanosomal parasite to disrupt the hormone metabolism of the host during infection, as is illustrated by the decrease in hormone levels during the course of trypanosomal infection (Tizard *et al.*, 1978; Tetaert *et al.*, 1993; Brandenberger *et al.*, 1996). The OPB enzyme (EC 3.4.21.83) has a trypsin-like specificity for small peptide substrates and cleaves peptides after basic Arg or Lys residues (Troeberg *et al.*, 1996; Fülöp *et al.*, 1998; Morty *et al.*, 2005; Coetzer *et al.*, 2008). The peptidase's specificity for small peptides is due to the N-terminal β-propeller domain which restricts access to the catalytic triad (Fülöp *et al.*, 1998; Gérczei *et al.*, 2000). The invasion of the host cell by *T. cruzi* requires calcium signalling which is generated by the proteolytic activity of OPB (Burleigh *et al.*, 1997). Research has shown that OPB is able to hydrolyse and thus inactivate atrial natriuretic factor in the plasma of infected rats (Morty *et al.*, 2001; Morty *et al.*, 2005) which is a contributing factor for the characteristic hypervolemia symptoms in AT infections (Anosa and Isoun, 1976). The OPB from *T. b. brucei* has been shown to retain its catalytic activity in the bloodstream of the host and is responsible for the degradation of the host's peptide hormones whereby pathogenesis is promoted (Morty *et al.*, 1999; Morty *et al.*, 2001). Trypanocidal drugs, pentamidine, diminazene, and suramin, have been found to target the OPB enzyme (Morty *et al.*, 1998). Since there are no mammalian OPB orthologues, it is considered to be an attractive chemotherapeutic target (Coetzer *et al.*, 2008; Bastos *et al.*, 2013). The application of OPB as a diagnostic antigen, however, has yet to be investigated.

The OPB from *T. congolense* (TcOPB, CCD12722.1), *T. vivax* (TvOPB, CCC53885.1) and *T. cruzi* (TcrOPB, XP_809967.1), and *Leishmania major* OPB (LmjOPB, XP_001681251.1) have a 81, 75, 72 and 61% sequence identity to *T. b. brucei* OPB (TbOPB, AAC80459.1) respectively (Fig. 1.9). The 3D structure of kinetoplastid OPB has only been solved for *Leishmania major* (McLuskey *et al.*, 2010) and *T. b. brucei*

(Canning *et al.*, 2013) in an attempt to understand the catalytic mechanism and regulation of the peptidase activity (Fig. 1.10).

```
TbOPB           GKYLTKRNTFMDFIACAEHLISSGLTTPAQLSCEGRSAGGLLVGAVLNMRPDLFHVALAG
TcOPB           GKYLTKRNTFMDFISCAEHLISSGVTTPPQLACEGRSAGGLLVGAVLNMRPDLFRVAVAG
TvOPB           AKYLTKRNTFMDFIACAEHLISSGLTTPNQLACEGRSAGGLLIGAVLNMRPDLFHVALAG
TcrOPB          AKYLTKRNTFSDFIACAEYLIEIGLTTPSQLACEGRSAGGLLIGAVLNMRPDLFRVALAG
LmjOPB          AKYLTKRNTFSDFIAAAEFLVNAKLTTPSQLACEGRSAGGLLMGAVLNMRPDLFKVALAG
                .********* ***:.**.*:.  :*** **:**********:***********:**:**

TbOPB           VPFVDVMTTMCDPSIPLTTGEWEEWGNPNEYKFFDYMNSYSPIDNVRAQDYPHLMIQAGL
TcOPB           VPFVDVMTTMCDPSIPLTTGEWEEWGNPNEYKFFDYMNSYSPIDNVRPQDYPNLIIQAGL
TvOPB           VPFVDVMTTMCDPTIPLTTFEWEEWGNPNEYKYFDYMNSYSPIDNVRAQAYPHLMIQAGL
TcrOPB          VPFVDVMTTMCDPSIPLTTGEWEEWGNPNEYKFFDYMNSYSPVDNVRAQDYPHLMIQAGL
LmjOPB          VPFVDVMTTMCDPSIPLTTGEWEEWGNPNEYKYYDYMLSYSPMDNVRAQEYPNIMVQCGL
                *************:***** ************::*** ****:****.* **::::*.**

TbOPB           HDPRVAYWEPAKWASKLRELKTDSNEVLLKMDLESGHFSASDRYKYLRENAIQQAFVLKH
TcOPB           HDPRVAYWEPAKWASKLRELKTDNNEVLLKMDLDSGHFSASDRYKYLREHAIQQAFVLKH
TvOPB           HDPRVAYWEPVKWASRLRQLKTDGNEVLVKMDLDSGHFSSADRYKYWREMAIQQAFVLKH
TcrOPB          HDPRVAYWEPAKWASKLRALKTDSNEVLLKMDLESGHFSASDRYRYWREMSFQQAFVLKH
LmjOPB          HDPRVAYWEPAKWVSKLRECKTDNNEILLNIDMESGHFSAKDRYKFWKESAIQQAFVCKH
                **********.**.*:**  ***.**:*:::*::*****: ***:: :* ::***** **

TbOPB           LN--VRQLLRK
TcOPB           LG--VRRLLRH
TvOPB           LN--VRCLLRR
TcrOPB          LN--ARTLLRR
LmjOPB          LKSTVRLLVRR
                *   .* *:*:
```

Figure 1.9: A sequence comparison between the oligopeptidase B enzymes of the various animal and human infective *Trypanosoma* and a human infective *Leishmania* species. Multiple sequence alignment of the SC clan, S9A family of serine oligopeptidases generated using ClustalX (Larkin *et al.*, 2007). Protein sequences were obtained from UniProtKB (http://www.uniprot.org/help/uniprotkb, accessed 25/08/2013): *T. b. brucei,* O76728, *T. congolense,* F9W6B7*, T. vivax*, G0U8G0, *T. cruzi*, Q4D6H1, and *Leishmania major,* Q4QHU7. The amino acid residues involved in the catalytic site are highlighted in yellow. Alignment characters are annotated as follows: conserved residues (*), strongly similar properties (:) and weakly similar properties (.).

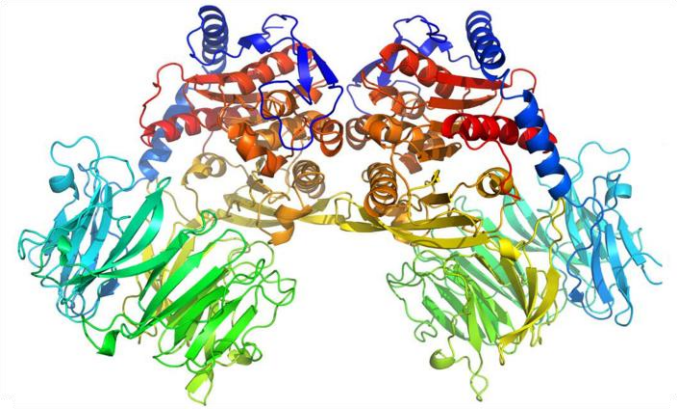

Figure 1.10: Structure of oligopeptidase B from *T. b. brucei*. The open state, non-ligand bound TbOPB is a dimer with a P3 symmetry which was resolved at a 2.4Å resolution (Canning *et al.*, 2013). The blue, green and yellow β sheets form the N-terminal β-propeller domain whilst the blue, red and orange α helices form the catalytic domain.

1.11.2 Cysteine peptidases

Research has shown that cysteine peptidases are essential to the survival of kinetoplastid parasites and function as important virulence factors (Mottram *et al.*, 1998; Mottram *et al.*, 2004). These peptidases are characterised by a Cys, His catalytic dyad with a Gln residue preceding the Cys residue to allow the formation of the oxyanion hole whilst an Asn residue follows the His residue in the primary structure to facilitate the correct orientation of the His imidazolium ring (Rawlings *et al.*, 2008). The catalytic mechanism of cysteine peptidases is similar to that of serine peptidases. Cysteine peptidases form a transient covalent bond between the carbonyl carbon of the substrate and the nucleophilic sulfur atom of the catalytic Cys residue, instead of the hydroxyl nucleophile of the catalytic Ser residue in serine peptidases (Atkinson *et al.*, 2009; Erez *et al.*, 2009) (Fig. 1.11).

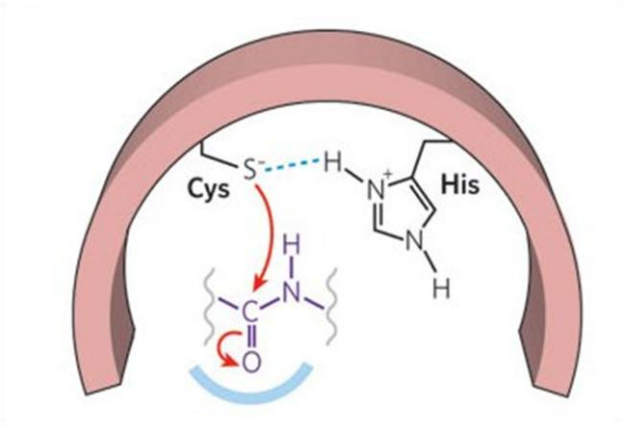

Figure 1.11: The reaction mechanism and amino acid orientation during cysteine peptidase mediated hydrolysis. The catalytic dyad consists of Cys and His catalytic residues whereby the Cys nucleophile attacks the substrate carbonyl carbon (Erez *et al.*, 2009).

Cysteine peptidases are classed into 10 clans, CA, CD, CE, CF, CL, CM, CN, CO, CP, CQ along with 8 families which have not yet been assigned (Rawlings *et al.*, 2012). The CA clan of cysteine peptidases consists of 84% of the known parasite cysteine proteases (Rawlings *et al.*, 2008). Of the CA clan, the C1 family is the best studied cysteine peptidase family of all the kinetoplastid peptidases (Rawlings *et al.*, 2008). The C1 family includes the model plant cysteine peptidase, papain and the mammalian cathepsins B, C, K, L and S (Rawlings *et al.*, 2008) Other important trypanosomal cysteine peptidases which are potential chemotherapeutic and diagnostic targets are found in families C13, C14 and C50 of the CD clan of cysteine peptidases which are comprised of the GPI:protein transamidases, metacaspases and separases respectively along with the calpains from the C2 family in the CA clan (Caffrey *et al.*,

2000; Caffrey and Steverding, 2009). Research has shown that the pyroglutamyl peptidase (PGP), which is found in the C15 family of the CF clan, is a potential virulence factor (Morty *et al.*, 2006; Mucache, 2012).

1.11.2.1 Cathepsin L- like peptidase

Two peptidases from the C1 family of the CA clan of cysteine peptidases are expressed by kinetoplastid parasites and are similar to mammalian cathepsins B and L, and were named cathepsin B- and L- like peptidases (CATB and CATL) (Cazzulo *et al.*, 1990; Caffrey *et al.*, 2000). The CATL peptidases are key factors in the trypanosomal infectivity, cell differentiation, metabolism and elicit prominent immune responses and as such are considered to be potential chemotherapeutic and diagnostic targets (Lalmanach *et al.*, 2002; Cortez *et al.*, 2009). All kinetoplastid derived CATL and CATB peptidases share the same characteristic of other cysteine proteases, where they possess the conserved Cys, His catalytic dyad (Lecaille *et al.*, 2002). In *T. congolense* infected cattle, it was found that TcCATB elicited a strong immune response and might be an appropriate antigen for the development of *T. congolense* specific diagnostic tests (Mendoza-Palomares *et al.*, 2008). The kinetoplastid CATL peptidases possess an additional, highly immunogenic 11 to 13 kDa C-terminal extension (Caffrey *et al.*, 2011). It has been recently shown that CATL is essential to the survival of the *T. b. brucei* parasite rather than CATB, and when completely inhibited the *in vitro* parasites died (Steverding *et al.*, 2012). Thus CATL is an important chemotherapeutic and thus diagnostic target.

Congopain (EC 3.4.22.15), a CATL peptidase from *T. congolense* (TcCATL), has previously been shown to be a pathogenic factor in *T. congolense* infected cattle (Authié *et al.*, 2001). It is a dominant antigen and as a result humoral and cellular responses are elicited against congopain (Lalmanach *et al.*, 2002). Trypanotolerance in these cattle was correlated to anti-congopain antibodies (Authié *et al.*, 1993a). Detection of TcCATL and its associated proteolytic activity has been detected in the plasma of infected cattle (Authié *et al.*, 1993a). Authié and co-workers (1993a; 1994) hypothesised that anti-TcCATL antibodies may alleviate disease symptoms and contribute to trypanotolerance in cattle.

Trypanopain (TbCATL) (Mackey *et al.*, 2004), congopain (TcCATL) (Mendoza-Palomares *et al.*, 2008) and rhodesian (TbrCATL) (Caffrey *et al.*, 2001) are expressed throughout each of the four life cycle stages, but most significantly in the BSF stage

where it is localised in the lysosomes (Mbawa *et al.*, 1991; Scory *et al.*, 1999; Caffrey *et al.*, 2001). The antigens used for serodiagnosis need to be expressed in the BSF and thus the CATL antigens are potential diagnostic antigens.

Many isoforms of congopain exist (Pillay *et al.*, 2010) and the same trend is observed in the CATL peptidases from *Leishmania mexicana* and *T. cruzi* (Mottram *et al.*, 1997; Lima *et al.*, 2001). Cruzipain is the major CATL lysosomal protease present in the *T. cruzi* parasite and is involved in the invasion process into mammalian smooth muscle and epithelial cells (Aparicio *et al.*, 2004; Yoshida, 2006). It is thought that cruzipain might be involved in the mechanism of evasion from the immune system by its digestion of the hinge region of the human IgG subclasses (Berasain *et al.*, 2003). It has been shown that along with TcrOPB and the metacyclic surface glycoprotein, gp82, that cruzipain plays a vital role in the mobilisation of Ca^{2+} which results in host cell invasion by the *T. cruzi* parasite (Dorta *et al.*, 1995; Burleigh *et al.*, 1997; Caler *et al.*, 1998).

The protozoan CATL enzymes have a similar 3D structure to that of papain-like cysteine peptidases and are comprised of an α-helical L-domain and an anti-parallel β-sheet R-domain with the propeptide settled in the substrate binding pocket (Lecaille *et al.*, 2002). The 3D structures of only two kinetoplastid CATL have been solved to date in the presence of different substrates and inhibitors, namely those from *T. cruzi* and *T. b. rhodesiense* (Fig. 1.12).

Figure 1.12: The cathepsin L-like peptidase from *T. b. rhodesiense* in the presence of the K777 inhibtitor. TbrCATL (PDB ID: 2P7U) is a monomer with P1 symmetry and was resolved at 1.65 Å (Kerr *et al.*, 2009).

The TDR targets database lists cruzipain and rhodesian as druggable targets (http://tdrtargets.org/targets/view?gene_id=48009, accessed 20/10/2103) and are thought to be potential diagnostic antigens. Rhodesian, the CATL from

T. b. rhodesiense, was thought to have diagnostic potential due to the fact that cruzipain was a diagnostic antigen and that it was highly expressed in BSF parasites, but was not recognised in infected human sera (Manful *et al.*, 2010).

Vivapain (TvCATL, CCD21670.1), congopain (TcCATL, CAA81061.1) and cruzipain (TcrCATL, P25779.1) share a 78%, 72% and 71% sequence identity to rhodesian (TbrCATL, CAC67416.1) respectively and thus should possess similar diagnostic and chemotherapeutic potential (Fig. 1.13).

```
TcCATL          MPRSEMTRTLRFSVGLLAVAACFVPVALGVLHAEQSLQQQFAAFKQKYSRSYKDATEEAF
TbrCATL         MPRTEMVRFVRLPVVLLAMAACLASVALGSLHVEESLEMRFAAFKKKYGKVYKDAKEEAF
TvCATL          -------MHAHALVTLLAAAVSVAPAAMAVLRADGPVEPLFAAFKQKYGRSYGTAAEEAF
TcrCATL         ---MSGWARALLLAAVLVVMACLVPAATASLHAEETLTSQFAEFKQKHGRVYESAAEEAF
                             . :*.  ......* . *:.: .:   ** **:*:.: *  * ****

TcCATL          RFRVFKQNMERAKEEAAANPYATFGVTRFSDMSPEEFRATYHNGAEYYAAALKRPRKVVN
TbrCATL         RFRAFEENMEQAKIQAAANPYATFGVTPFSDMTREEFRARYRNGASYFAAAQKRLRKTVN
TvCATL          RLRVFEDNMRRSRMYAAANPHATFGVTPFSDLTPEEFRTRYHNGERHFEAARGRVRTLVQ
TcrCATL         RLSVFRENLFLARLHAAANPHATFGVTPFSDLTREEFRSRYHNGAAHFAAAQERARVPVK
                *: .*.:*:  ::  *****:****** ***:: ****: *:**  :: **  * *  *:

TcCATL          VSTGKAPEAVDWRKKGAVTPVKDQGQCGSCWAFSAIGNIEGQWKVAGHELTSLSEQMLVS
TbrCATL         VTTGRAPAAVDWREKGAVTPVKDQGQCGSCWAFSTIGNIEGQWQVAGNPLVSLSEQMLVS
TvCATL          VPPGKAPAAVDWRRKGAVTPVKDQGTCGSCWSFSAIGNIEGQWAAAGNPLTSLSEQMLVS
TcrCATL         VEVVGAPAAVDWRARGAVTAVKDQGQCGSCWAFSAIGNVECQWFLAGHPLTNLSEQMLVS
                *    ** ***** :****.***** *****:**:***:* **  **: *..********

TcCATL          CDTNDFGCEGGLMDDAFKWIVSSNKGNVFTEQSYPYASGGGNVPTCDKSGKVVGAKIRDH
TbrCATL         CDTIDFGCGGGLMDNAFNWIVNSNGGNVFTEASYPYVSGNGEQPQCQMNGHEIGAAITDH
TvCATL          CDTKDNGCGGGLMDNAFEWIVKENSGKVYTEKSYPYVSGGGEEPPCKPRGHKVGATITGH
TcrCATL         CDKTDSGCSGGLMNNAFEWIVQENNGAVYTEDSYPYASGEGISPPCTTSGHTVGATITGH
                **. * ** ****::**:***..* * *:** ****.** *  * *   *: :** * .*

TcCATL          VDLPEDENAIAEWLAKNGPVAIAVDATSFQSYTGGVLTSCISEHLDHGVLLVGYDDTSKP
TbrCATL         VDLPQDEDAIAAYLAENGPLAIAVDATSFMDYNGGILTSCTSEQLDHGVLLVGYNDSSNP
TvCATL          VDIPHDEDAIAKYLADNGPVAVAVDATTFMSYSGGVVTSCTSEALNHGVLLVGYNDSSKP
TcrCATL         VELPQDEAQIAAWLAVNGPVAVAVDASSWMTYTGGVMTSCVSEQLDHGVLLVGYNDSAAV
                *::*.**  ** :** ***:*:****:::  *.**::*** ** *:********:*::

TcCATL          PYWIIKNSWSKGWGEEGYSALRR-HNQCLMKNLPSSAVVSG-----PPPPPPTPTFTQEL
TbrCATL         PYWIIKNSWSNMWGEDGYIRIEKGTNQCLMNQAVSSAVVGGPTPPPPPPPPPSATFTQDF
TvCATL          PYWIIKNSWSSSWGEKGYIRIEKGTNQCLVAQLASSAVVGG------PGPTPTPTPTTN-
TcrCATL         PYWIIKNSWTTQWGEEGYIRIAKGSNQCLVKEEASSAVVGGP----GPTPEPTTTTTTSA
                *********:. ***.**  : :  ****: :  *****.*      * * *:.* * .

TcCATL          ------------CEGAECQSKCTKATFPTGKCVQLSGAGSVIASCGSNNLTQIVYPLSSS
TbrCATL         ------------CEGKGCTKGCSHATFPTGECVQTTGVGSVIATCGASNLTQIIYPLSRS
TvCATL          -------------------NNNNNDRTWP-------------IVKLHEDALQR--------
TcrCATL         PGPSPSYFVQMSCTDAACIVGCENVTLPTGQCLLTTSGVSAIVTCGAETLTEEVFLTSTH
                                  . * *             *..   . * .

TcCATL          CSGFSVPLTVPLDKCLPIVIGSVMYECSDKAP---TESARLVRHE---------
TbrCATL         CSGLSVPITVPLDKCIPILIGSVEYHCSTNPP---TKAARLVPHQ---------
TvCATL          --------------------------------------------------------
TcrCATL         CSGPSVRSSVPLNKCNRLLRGSVEFFCGSSSSGRLADVDRQRRHQPYHSRHRRL
```

Figure 1.13: Sequence alignment of the cathepsin-L like peptidases from *T. congolense, T. b. rhodesiense, T. vivax and T. cruzi*. Multiple sequence alignment of the CA clan, C1 family of cysteine peptidases generated using ClustalX (Larkin *et al.*, 2007). Protein sequences were obtained from UniProtKB (http://www.uniprot.org/help/uniprotkb, accessed 25/08/2013): TcCATL from *T. congolense*, Q26895, TbrCATL from *T. b. rhodesiense,* Q95PM0, TvCATL from *T. vivax*, F9WRA9, and TcrCATL from *T. cruzi*, P25779. The amino acid residues involved in the signal peptide are highlighted in yellow, those in the propeptide in pink, the catalytic domain in blue, the catalytic site in grey, the C-terminal extension in green, and the 18-mer TcCATL N-terminal peptide in red and yellow. Alignment characters are annotated as follows: conserved residues (*), strongly similar properties (:) and weakly similar properties (.).

1.11.2.2 Pyroglutamyl peptidase

Also known as pyrrolidone carboxyl peptidase, two types of PGP are known to exist: type I which is a cysteine peptidase (EC 3.4.19.3) and type II which is a metallo peptidase (EC 3.4.19.6) (Cummins and O'Connor, 1998). The PGP type I has a Cys, His and Glu catalytic triad and lacks the oxyanion hole, differing from the classical cysteine peptidase Cys, His dyad, and is expressed as an intracellular, soluble peptidase belonging to the C15 family of the CF clan of cysteine peptidases (Cummins and O'Connor, 1998; Odagaki *et al.*, 1999; Barrett *et al.*, 2003). The type II PGP enzyme is membrane bound and belongs to the M1 family of metallo-peptidases (Rawlings *et al.*, 2012).

The activity of bioactive compounds, such as neuropeptides, is regulated by the cyclisation of the N-terminal glutamine residue to form L-pyroglutamyl residues (L-pGlu) (Doolittle and Armentrout, 1968; da Silva-Lopez *et al.*, 2008). This enables resistance to aminopeptidase degradation (Awadé *et al.*, 1994). The PGP type I peptidase is characterised by omega activity rather than aminopeptidase activity (Cummins and O'Connor, 1998; Atkinson *et al.*, 2009).

It is thought that certain trypanosomal proteins and enzymes are responsible for the hormonal degradation that is evident during the course of the disease (Tetaert *et al.*, 1993). Mammalian PGP type I has been shown to release L-pGlu from thyrotropin-releasing hormone (TRH), luteinizing hormone releasing hormone (LHRH), neurotensin, bombesin and leukopyrokinin (Dando *et al.*, 2003). From research done by Morty and co-workers (2006) is was evident that PGP type I was responsible for the reduction of the plasma half life of TRH and gonadotropin-releasing hormone (GnRH) in rats. Involvement of PGP type I has been demonstrated in the regulation of *Leishmania major* differentiation (Schaeffer *et al.*, 2006). The expression of PGP type I in *T. b. brucei* might be a contributing factor in the dysfunction of the endocrine system in AT infected patients. A common symptom of AAT is reproductive disorders (Seifert, 1995) which have been found to be associated with gonadal and endocrine abnormalities (Ng'wena *et al.*, 1997). It has been suggested that PGP type I is involved in protein metabolism in mammals but a definitive role has yet to be elucidated (Lauffart and Mantle, 1998). Mucache (2012) showed that PGP type I is expressed in the BSF and PCF parasites of *T. congolense* as is the case for *T. b. brucei* PGP type I (Morty *et al.*, 2006). When taking into account that PGP type I in *L. major* has been implicated in differentiation by regulating the action of L-pGlu-modified peptides

(Schaeffer *et al.*, 2006), this lends to the suggestion that PGP is a potential virulence factor.

The PGP from *T. b. brucei* (TbPGP, AAY40294.1), *T, cruzi* (TcrPGP, XP_814255.1), and *T. vivax* (TvPGP, CCC47591.1) share 54, 50 and 41% sequence identity respectively to that of *T. congolense* (TcPGP, HE57517.1). The sequences of the kinetoplastid PGP type I peptidases were obtained from the UniProtKB database (http://www.uniprot.org/help/uniprotkb, accessed 25/08/2013) and from GeneBank® (https://www.ncbi.nlm.nih.gov/genbank, accessed 25/08/2013) (Fig. 1.14).

```
TbPGP           MKPTKPLLYITGYGPFLEITENPSATIAQSVAEQVRQSGEADVHHETLDVNLEAVSKYFN
TcPGP           MSSVKPILHITGYGPFKDVVENPSDTIAQVVAKQMSQSGKTVTHHETLEVNLDAVTEYFD
TcrPGP          MRRSNLQLYMTGFGPFKSITVNPSAMIGESVSKRMMEDSELQVHYEKLEVGLEAVSAYFD
TvPGP           MRATSVQLYVTGFGPFKTITCNPSAAISAEVSRQMAEYGDLEVHYKELEVNLSATGTYFD
                *   .  *::**:***  :. ***  *.  *:.:: : ..  .*:: *:*.*.*.  **:

TbPGP           RLNESVTAHLEATHPENRVLLVNVGLHSREKEKVLRLEVRAFNELEGNPIDDELPLSTCK
TcPGP           RLDQLVDRQMAE-NPEQRVLLVHCGVHRREQSGLLRMEVRGFNELEGQPIDKHLPMDAFQ
TcrPGP          GLEGALAQHMED-NPDGCVLLLHIGLHSREEEGKMRLEVCGYNELEGSPIDESIPMDVCL
TvPGP           DLEERVAGHIKE-DAHQHVLLVHVGLHSPEEDGVMRLEVRGYNELEGSPIDSELPLDTFN
                 *:  :  ::   ...  ***:: *:*  *:.  :*:** .:*****.***. :*:..

TbPGP           DSAFVKG-------CKLETTTALIEELN----AIERNGSDHHEKPRWIISYDAGRYYCNY
TcPGP           ESTFGNE-------HMVQAVTALLEELNATMDANEKNEGDEQ-RPQWIVSRDAGRYYCNY
TcrPGP          ESMLVRDG-----CDESKATAELIEELNAAISKRGRREGDRQ-QPHWIISRDAGRYYCNY
TvPGP           ESLLVHSDDSDKDGSGAAVIEQLLDKLNREAHQLDTQRGIRK-RPRWIVSHAT-------
                :* : .            .   *:::**        . . .: :*:**:*  :

TbPGP           ALYRGVKMQEALNSRVFAVFLHIVASTVVC---MEEQVAQVRMLVSHLLK-HMEAVE-
TcPGP           ALYRSLKIQQRWEGRVFAVFLHVVNPHVVG---LDVQIPLVSSLVTGLLKIAMEGGAA
TcrPGP          TLYRSLKLQKKWRGRVFAVFVHVANPFTCNNPSLEEQTAQVLSLVSGLVRIVRNKHIV
TvPGP           ---RSA-----------------------------------------------------
                   *.
```

Figure 1.14: A sequence comparison between the pyroglutamyl peptidases of the various animal and human and animal infective *Trypanosoma* species. Multiple sequence alignment of the CF clan, C15 family of cysteine peptidases generated using ClustalX (Larkin *et al.*, 2007). Protein sequences were obtained from UniProtKB (http://www.uniprot.org/help/uniprotkb, accessed 25/08/2013): *T. b. brucei* PGP, Q4U338, *T. congolense* PGP, HE575317.1: 64647-65325bp (GeneDB), *T. cruzi* PGP, Q4DIQ6, and *T. vivax* PGP, G0TUF7. The amino acid residues involved in the catalytic site are highlighted in yellow. Alignment characters are annotated as follows: conserved residues (*), strongly similar properties (:) and weakly similar properties (.).

The α/β/α sandwich fold which characterises PGP type I is unlike any fold of the other cysteine peptidases which accounts for its classification into the CF clan (Singleton *et al.*, 1999). Archaean PGP exists as a tetramer whilst the mammalian and bacterial PGPs are monomeric (Singleton *et al.*, 1999). To date, only bacterial PGP has been crystallised and the 3D structure solved (Fig. 1.15).

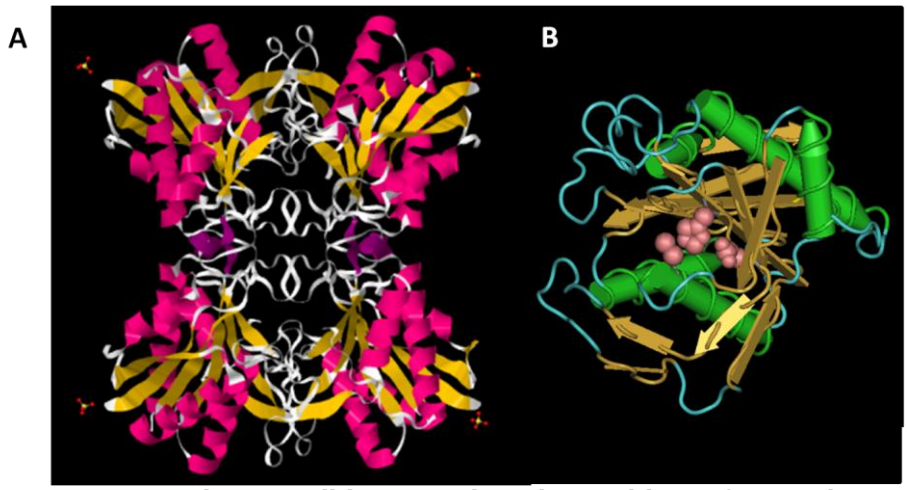

Figure 1.15: Tetrameric pyrrolidone carboxyl peptidase from *Thermococcus litoralis* and monomeric pyroglutamyl peptidase from *B. amyloliquefaciens*. (A) The PCP peptidase (PBD ID: 1A2Z) exists as a tetramer with a D2 symmetry and was resolved at 1.73 Å (Singleton *et al.*, 1999). **(B)** The monomeric form from *B. amyloliquefaciens* (Odagaki *et al.*, 1999).

1.11.2.3 Metacaspases

Caspases belong to the C14 family of the CD clan of cysteine peptidases and are synthesised as inactive pro-enzyme forms which, once activated, cleave substrates after an Asp residue (Rawlings *et al.*, 2008). In addition to apoptosis, caspases are involved in non-apoptotic events such as inflammation, cell proliferation and differentiation (Lamkanfi *et al.*, 2007). Programmed cell death (PCD) occurs for the maintenance of homeostatis and for the cellular development in multicellular organisms and is mediated by a cascade of caspases (Grutter, 2000). Processes, resembling that of PCD, have been described in a variety of plants, fungi and protozoa which lack the caspase gene with an increase in caspase-like proteolytic activity being observed (Bacchi, 1993; Das *et al.*, 2001; Bozhkov *et al.*, 2010).

The metacaspase gene present in protozoa, fungi and plants (Plantae, Fungi and Protozoa kingdoms) was identified based upon their predicted structural identities within the caspase catalytic domain (Uren *et al.*, 2000). The metacaspases (E.C. 3.4.22.-) share the caspase characteristic caspase-haemoglobinase fold (Vercammen *et al.*, 2007) and the conserved Cys, His catalytic dyad, were classified in the CD clan of cysteine proteases and are thought to be involved in PCD (Rawlings and Barrett, 1993; Aravind and Koonin, 2002).

The substrate specificity of metacaspases differs from that of the caspases, with cleavage at the C-terminal side of basic Arg or Lys residues rather than an acidic Asp

residue (Vercammen *et al.*, 2004; Watanabe and Lam, 2005). Based on research by Sundström and Vaculova (2009), it was shown that metacaspases and caspases share the same natural death related substrates and it was thus concluded that these peptidases evolved from a common origin and are variants of the same gene. This fact is evident as the metacaspase gene is present in every kingdom except for the animal, where the caspase gene is present (Sundström *et al.*, 2009). It has been proposed that metacaspases might function as caspase-like proteases and are involved in PCD (Debrabant *et al.*, 2003; Nguewa *et al.*, 2004; Chowdhury *et al.*, 2008) but due to their different substrate specificity, their function is not the same (Vercammen *et al.*, 2007).

The metacaspases from *L. major* (Abdulla *et al.*, 2007; Ambit *et al.*, 2008), *Saccharomyces cervisiae* (Madeo *et al.*, 2002) and *Arabidopsis thaliana* (Watanabe and Lam, 2011) all undergo caspase-like processing. The first reported metacaspase-dependent cell death was reported for the *S. cerevisiae* YCA1 mutant strain when subjected to oxidative stress (Madeo *et al.*, 2002). Exhibition of the metacaspase role in promoting cell death (pro-cell death) has also been confirmed in protozoa and plants. It has been shown that the *Leishmania* species require the action of metacaspases for oxidative stress induced cell death (Lee *et al.*, 2007; Zalila *et al.*, 2011). The conserved role of metacaspases in PCD regulation throughout the various non-metazoan eukaryote kingdoms, demonstrate the fact that they are a key element in the process of non-metazoan cell death, whereby cell death is carried out by molecules other than caspases and their effector molecules (Moss *et al.*, 2007; Tsiatsiani *et al.*, 2011).

It has been shown that most metacaspases are involved in the maturation of enzymes by autocatalytic processing of the pro-enzyme forms (Vercammen *et al.*, 2004; Gonzáles *et al.*, 2007; Watanabe and Lam, 2011). Metacaspases have been found to be involved in vesicle trafficking (Duszenko *et al.*, 2006), signalling to cells to enter into cytokinesis (Helms *et al.*, 2006) and are autocatalytically activated (Zalila *et al.*, 2011). The results of the RNAi of *TbMCA2/3/5* together negatively affected the process of cytokinesis and cell death (Helms *et al.*, 2006). No association was found between prostaglandin-induced PCD and TbMCA2, -3 and -5 expression but all were found to be involved in the recycling of endosomes and co-localised with Rab11 within recycling vesicles (Helms *et al.*, 2006).

Some exceptions have been found where the metacaspase contain the active site mutation of a Cys to a Ser and as a result are catalytically inactive (Szallies *et al.*, 2002). In oxygen rich blood, it is thought that the oxidation of the catalytic Cys residue

is moderated by its substitution to a Ser residue in the peptidases of haemoparasites (Atkinson *et al.*, 2009). Upon the over-expression of TbMCA4 which contains an active site substitution of Cys to a Ser residue, cell death in yeast was induced (Szallies *et al.*, 2002). The TbMCA4 might play a role in the control of cellular proliferation and is coupled to mitochondrial function (Szallies *et al.*, 2002). The functions of these inactive peptidases are unknown but might play a role in binding to natural peptidase inhibitors or might be substrates for endogenous enzymes which assist in the modulation of the activities of enzymatically active proteases (Mottram *et al.*, 2003).

Clan CD of cysteine proteases are better targets for the development of chemotherapeutics than those of the CA clan due to the greater specificity in their functions and the fact that they are unaffected by the classical cysteine protease inhibitor, E64, due to their strict P1 substrate specificity (Mottram *et al.*, 2003). The only kinetoplastid MCA to be crystallised, and the 3D structure solved, to date is MCA2 from *T. b. brucei* (Fig. 1.16).

Figure 1.16: The crystal structure of the metacaspase 2 from *T. b. brucei*. The monomeric TbMCA2 (PDB ID: 4AFR) has a C1 symmetry and was resolved at 1.40 Å (McLuskey *et al.*, 2012).

1.12 Objectives of current study

The first objective of this study was to clone, recombinantly express, resolubilise and refold the potential metacaspase 5 virulence factor from *T. congolense* for antibody production. These results are reported in chapter 2.

The second objective was to prepare selected antigens and their corresponding antibodies for optimisation of ELISA serodiagnostics of *T. congolense* and *T. vivax*. The selected antigens were previously described virulence factors, OPB, PGP as well as the full length and catalytic domain of CATL from *T. congolense*, along with OPB

and the catalytic domain of CATL from *T. vivax*. To this end these antigens were recombinantly expressed using the *Escherichia coli* and *Pichia pastoris* expression systems, followed by purification using immobilised metal affinity chromatography, three phase partitioning and molecular exclusion chromatography. Following purification, the purified antigens were used to raise antibodies in chickens. These results are reported in chapter 3.

The third objective was the evaluation of the diagnostic potential of the selected antigens using a *T. congolense* and *T. vivax* blinded serum panel. The results of the use of the purified antigens in the inhibition and indirect antibody detection ELISAs using infected and non-infected *T. congolense* and *T. vivax* sera are reported in chapter 4.

CHAPTER 2

CLONING AND EXPRESSION OF RECOMBINANT METACASPASE FROM *TRYPANOSOMA CONGOLENSE,* TcMCA5.

2.1 Introduction

African trypanosomiasis (AT) is a disease caused by trypanosomal parasites which affects both humans and animals in mostly rural communities in sub-Saharan Africa along the distribution of the tsetse belt which covers an area of approximately 10 million km^2 (Courtin *et al.*, 2010). *Trypanosoma brucei brucei, T. congolense* and *T. vivax* are of the *Salivaria* group within the *Kinetoplastida* order (Stevens, 2008) and are the causative agents of animal African trypanosomiasis (AAT) or Nagana in cattle (Facer *et al.*, 1982). While *T. b. brucei* and *T. congolense* are transmitted by the tsetse fly (*Glossina* spp.), *T. vivax* is transmitted by hematophagus insects (Smith and Sherman, 1994).

The expression of VSG coat proteins of trypanosomal parasites are periodically switched to that of different VATs to protect themselves from the host's immune system, a process known as antigenic variation (Radwanska *et al.*, 2008). Due to antigenic variation, the possibility of a vaccine for AT is very remote (Pays, 2006), thus an anti-disease strategy is followed by targeting parasite virulence factors (Antoine-Moussiaux *et al.*, 2009). Virulence factors are those which are essential to the parasite's survival within the host and are identified by studying the interaction between the two (Hölzmuller *et al.*, 2008). Pathogeno-proteomics have facilitated the identification of new potential therapeutic agents as well as diagnostic targets (Biron *et al.*, 2005; Hölzmuller *et al.*, 2008). A number of peptidases have been identified as virulence factors as they are responsible for a variety of cellular processes such as cell cycle progression and evasion of the host immune systems to name but a few (Klemba and Goldberg, 2002). After identification, these virulence factors have the potential to be used in the development of novel drug therapies and diagnostic tools for the treatment of AT (Mottram *et al.*, 2004).

Caspases are of the clan CD of cysteine peptidases and are synthesised as inactive zymogens which, once activated, cleave substrates C-terminal to Asp residues and play a crucial role in the PCD pathways of eukaryotes (Bozhkov *et al.*, 2010). The presence of metacaspases in protozoa, fungi and plants was detected based on their

predicted structural identities within the caspase catalytic domain (Uren *et al.*, 2000). The metacaspases share the same catalytic His-Cys dyad and the characteristic caspase-hemoglobinase fold with caspases and are part of the C14 family of cysteine proteases (Uren *et al.*, 2000; Aravind and Koonin, 2002). The most important difference between caspases and metacaspases is found in their P1 substrate specificity, with metacaspases having a strict basic Arg and Lys specificity and caspases having a strict acidic Asp specificity (Vercammen *et al.*, 2004; Watanabe and Lam, 2005; Vercammen *et al.*, 2006; Lee *et al.*, 2007). The fact that the metacaspases have distinct proteolytic properties from caspases and are not present in the metazoan genomes, make them ideal targets for the development of fungicides, herbicides and also drugs against protozoan parasites (Lam and Zhang, 2012).

Since regulated PCD pathways are absent in trypanosomatid parasites (Proto *et al.*, 2011), alternative pathways have evolved using metacaspase proteases (Helms *et al.*, 2006; Proto *et al.*, 2011). Based on research, it has been shown that metacaspases and caspases share the same natural death related substrates, evolved from a common origin and are variants of the same gene (Sundström *et al.*, 2009). This fact is evident as the metacaspase gene is present in every kingdom except for the animal kingdom, where the caspase gene is present (Sundström *et al.*, 2009). It is thus thought that metacaspases too, play a role in PCD. Research has shown that oxidative stress induced cell death in the *Leishmania* species requires the action of metacaspases (Lee *et al.*, 2007; Zalila *et al.*, 2011).

The best studied metacaspases are from *Arabidopsis thaliana* and *Picea abies* in plants and *T. b. brucei*, *T. cruzi* and *Leishmania major* in trypanosomatid parasites (Alvarez *et al.*, 2011). Research has been done regarding the metacaspases from *T. b. gambiense* and *T. b. rhodesiense,* which are the causative agents of HAT, however, less attention has been given to those from *T. congolense* or *T. vivax*, AAT causative agents.

Trypanosomatid metacaspases are characterised by their domain composition as well as their gene copy number (Alvarez *et al.*, 2011). Single copy metacaspases from *T. congolense*, TcMCA5 (TcIL3000.9.6120), *T. b. brucei*, TbMCA5 (Tb927.9.14220), *T. b. gambiense*, TbgMCA5 (Tbg972.9.8930), *T. vivax*, TvMCA (TvY486.0907120), *T.* cruzi, TcrMCA5 (TcCLB.510759.160), and *L. major*, LmMCA5 (LmjF35.1580), all possess a C-terminal extension which is rich in Pro, Glu and Tyr residues (Mottram *et al.*, 2003; Kosec *et al.*, 2006a). Multicopy metacaspase genes are found in *T. b. brucei*, TbMCA1, -2, -3 and -4 (Tb927.11.3320, Tb927.6.940, Tb927.6.930, Tb927.10.2440),

T. b. gambiense, TbgMCA1, -2, -3 and -4 (Tbg972.11.3560, Tbg972.6.710, Tbg972.6.700, Tbg972.10.300), *T. vivax*, TvMCA3 (TvY486.0019190) and *T. cruzi*, TcrMCA3, (TcCLB.506531.50). The above mentioned metacaspase proteins were aligned (Fig. 2.1) and the conserved residues involved in the S1 binding pocket, catalytic dyad and calcium binding were highlighted as based on the TbMCA2 alignment done by McLuskey and co-workers (2012). The protein sequences were sourced from the UniProtKB database (http://www.uniprot.org/help/uniprotkb, accessed 16/04/2012).

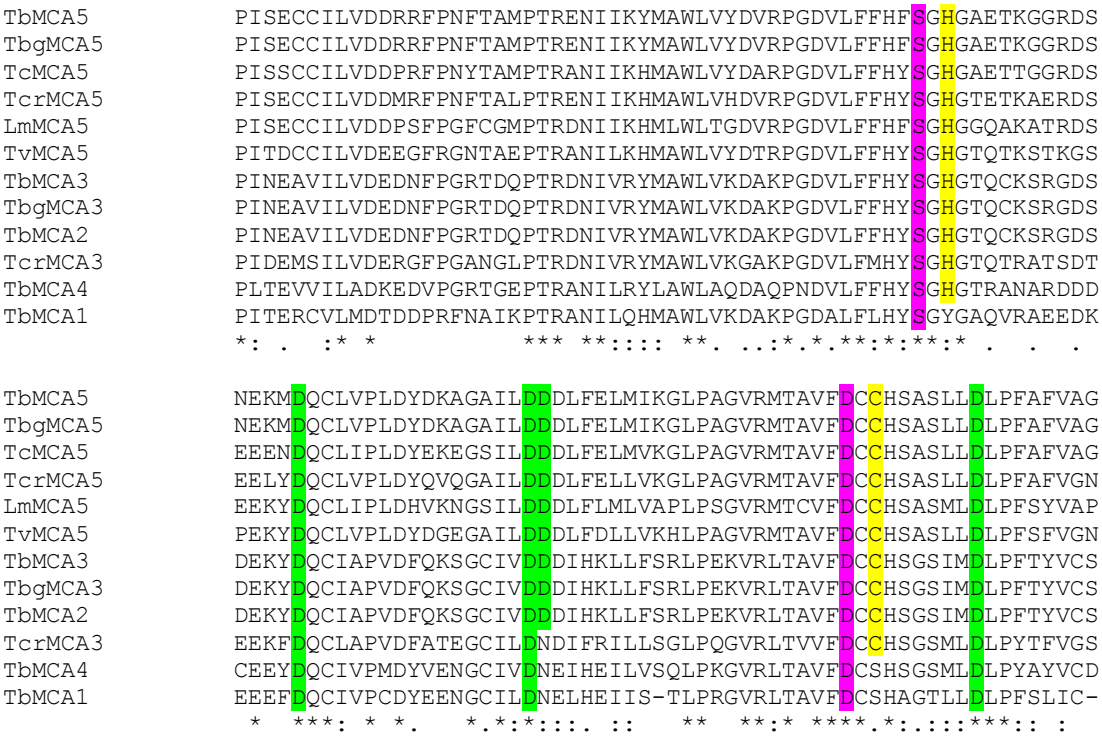

Figure 2.1: A sequence comparison between the metacaspases of the various animal and human infective *Trypanosoma* and *Leishmania* species. Multiple sequence alignment of the catalytic domain of the CD clan, C14 family of metacaspases generated using ClustalX (Larkin *et al.*, 2007). Protein sequences were obtained from UniProtKB (http://www.uniprot.org/help/uniprotkb, accessed 16/04/2012): *T. b. brucei* MCA5, Q8IEW1; *T. b. gambiense* MCA5, C9ZZG8; *T. congolense* MCA5, G0UUY6; *T. cruzi* MCA5, Q2VLK8; *T. vivax* MCA5, G0U3N4; *L. major* MCA5, E9AEY0; *T. b. brucei* MCA2, Q585F3; *T. b. brucei* MCA3, Q585F4; *T. b. brucei* MCA4, Q38C01; and *T. b. brucei* MCA1, Q8T8E8. The amino acid residues involved in the S1 binding pocket are highlighted in pink, those in the catalytic dyad in yellow and the calcium binding sites in green. Alignment characters are annotated as follows: conserved residues (*), strongly similar properties (:) and weakly similar properties (.).

From Fig. 2.1, it should be noted that TbMCA1 and -4 both have active site substitutions, i.e. a Ser instead of a Cys residue and are both catalytically inactive (Szallies *et al.*, 2002). Such homologues have been identified in various organisms and their biological functions are still to be determined (Merckelbach *et al.*, 1994). One such

example was found in one group of cathepsin L-like (CATL) cysteine proteases of *T. congolense* where the active site Cys had been replaced with a Ser (Pillay, 2010). It was determined, that although TbMCA4 was proteolytically inactive, it was responsible for the induction of cell death in yeast (Szallies *et al.*, 2002) and once released from the cell, it was specifically processed by TbMCA3 (Proto *et al.*, 2011). Deletion of TbMCA4 by RNA inhibition (RNAi) resulted in the disruption of the cell cycle which resulted in cell death (Proto *et al.*, 2011).

Since the BSF parasite is the mammalian infective form, it follows that the proteases and virulence factors expressed within this stage may have important diagnostic applications. The *T. b. brucei* metacaspases, TbMCA2 and -3 were found to be expressed only in the BSF stage whilst TbMCA5 was expressed throughout the life cycle of the parasite (Helms *et al.*, 2006). In addition, it was found that TbMCA2, -3 and -5 were essential to the BSF stage. Thus the homologous MCA5 gene in *T. congolense* might have diagnostic potential for AAT.

In the present study a metacaspase from *T. congolense* (strain IL 3000), TcMCA5, was identified as a potential target for the development of an ELISA based diagnostic test. The gene was cloned and recombinantly expressed in inclusion bodies. Thereafter solubilisation, on-column refolding and purification of TcMCA5 was performed using chaotropic and non-chaotropic methods. In addition, anti-TcMCA5 IgY antibodies were raised in chickens and the ELISA optimised for future application in inhibition and indirect diagnostic ELISA formats.

2.2 Materials and methods

2.2.1 Materials

Molecular biology: BamH1, EcoRI, [for nomenclature see Roberts *et al.* (2003)], Shrimp alkaline phosphatase (SAP), T4 DNA ligase, O'GeneRuler™ 1 kb DNA Ladder, 10 mM dNTPs, high fidelity PCR enzyme mix, GeneJet™ Plasmid Miniprep Kit, TransformAid™ Bacterial Transformation Kit, 5-bromo-4-chloro-3-indolyl-β-D-galactopyranoside (IPTG), isopropyl-β-D-thiogalactopyranoside (X-gal) and dithiothreitol (DTT) were obtained from Fermentas (Vilnius, Lithuania). The pGEM®-T cloning vector was purchased from Promega (Madison, WI, USA), the pET-28a and pET-32a expression vectors from Novagen (Darmstadt, Germany) and the pGEX4T-1 expression vector from GE Healthcare (Uppsala, Sweden). FIREpol® Taq polymerase, 10 x PCR reaction buffer and 25 mM $MgCl_2$ were from Solis Biodyne (Tartu, Estonia).

The ZymoResearch Clean and Concentrator™ kit was purchased from Zymo Research (Orange, CA, USA) and the E.Z.N.A® gel extraction kit from PEQlab (Erlangen, Germany). Seakem®LE agarose was purchased from Lonza (Rockland, ME, USA), ampicillin sodium salt from USB Corporation (Cleveland, OH, USA) and kanamycin from Gibco, (Paisley, UK). Bacteriological agar, tryptone and yeast extract were purchased from Merck Biolab (Darmstadt, Germany). Crystal violet and ethidium bromide were purchased from Sigma (St. Louis, MO, USA) and Whatman No. 1 filter paper from Whatman International Ltd (UK). Buffer salts and other common chemicals were purchased from Merck (Germany) and Sigma (St. Louis, MO, USA) and were of the highest purity available.

***E. coli* cells:** Competent *Escherichia coli* cells, JM 109 and BL21 (DE3) strains were purchased from New England Biolabs (Ipswitch, MA, USA). The JM 109 strain allowed for blue/white screening for transformants in the presence IPTG and X-gal. The BL21 (DE3) strain is deficient in both Lon and OmpT protease expression.

Purification and quantification of recombinant proteins: His-select® nickel affinity resin, dialysis tubing (10 kDa size cutoff), polyethylene glycol (PEG) M_r 20 000, 4-chloro-1-naphthol, blue dextran (200 kDa), phosphorylase B (97.4 kDa), bovine serum albumin (BSA, 68 kDa), ovalbumin (45 kDa), carbonic anhydrase (30 kDa), soyabean trypsin inhibitor (SBTI, 21.5 kDa), myoglobin (14 kDa), lysozyme (14 kDa), gelatin from porcine skin, the semi dry blotter and the Kodak BioMax light film were purchased from Sigma (St. Louis, MO, USA). The BCA™ Protein Assay Kit, the Pierce™ ECL western blotting substrate and the PageRuler™ prestained protein ladder were purchased from Pierce (Rockford, IL, USA), the Centricon® centrifugal concentrators from Merck Millipore (Billerica, MA, USA) and the BioTrace™ nitrocellulose was from PALL Corp (Ann Arbor, USA). The black Nunc 96-well plates were purchased from Nunc Intermed (Denmark).

Chicken IgY preparation and ELISA: Freund's complete and incomplete adjuvants along with bovine serum albumin (BSA, catalogue no.: A7906) were purchased from Sigma (St. Louis, MO. USA). Polyethylene glycol (PEG) M_r 6 000 was purchased from Merck (Darmstadt, Germany) and Nunc-Immuno™ Maxisorp 96-well plates from Nunc Intermed (Roskilde, Denmark). The 2, 2'-azinobis [3-ethyl-3, dihydrobenzithiazole-6-sulfonate] (ABTS) was purchased from Roche (Mannheim, Germany). The BIOTEK® ELx50™ Microplate washer was purchased from BioTek Instruments Inc. (USA).

Antibodies: The rabbit anti-chicken IgY HRPO conjugate was purchased from Sigma (Munich, Germany), the goat anti-mouse IgG HRPO conjugate from Novagen (Darmstadt, Germany) and mouse anti-6xHis IgG HRPO conjugate from Roche (Mannheim, Germany).

Peptides substrates and inhibitors: The peptide substrate benzyloxycarbonyl (Z)-Gly-Gly-Arg-amino-4-methylcoumarin (AMC), and the leupeptin, antipain and N-tosyl-L-lysyl chloromethylketone (TLCK) inhibitors were purchased from Sigma (Munich, Germany).

Trypanosome culture: Eagle's minimal essential medium (EMEM), Gln and Pro were purchased from Sigma (St. Louis, MO, USA) and foetal bovine serum (FBS) was from Gibco (Paisley, UK). Filters (0.2 µm) were purchased from PALL Corp (Ann Arbor, USA) and sterile disposable cell culture plasticware from Corning (NY, USA).

2.2.2 Molecular weight marker calibrations

Standard curves were constructed for molecular weight markers separated on a 1% (w/v) agarose gel (Fig. 2.2, panel A) and in a 12.5% reducing SDS-PAGE gel (Fig. 2.2, panel B). This was performed by relating the relative mobility of each of the marker proteins or DNA fragments to the log of its respective relative molecular mass (M_r) or number of base pairs (bp).

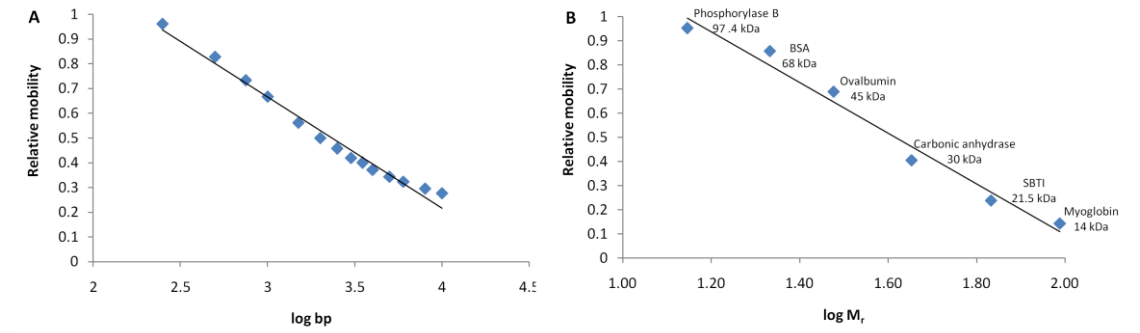

Figure 2.2: Standard curves relating relative mobility to the log of the base pairs and molecular weight markers used in agarose and SDS-PAGE gel electrophoresis. **(A)** The commercial O'GeneRuler™ 1 kb DNA ladder was used for agarose electrophoresis. The equation of the trendline is given by y = -0.449x + 2.102, with a correlation coefficient of 0.981. **(B)** The molecular weight marker used for SDS-PAGE consisted of phophorylase B (97.4 kDa), bovine serum albumin (BSA, 68 kDa), ovalbumin (45 kDa), carbonic anhydrase (30 kDa), soyabean trypsin inhibitor (SBTI, 21.5 kDa) and lysozyme (14 kDa). The equation of the trendline is given by y= -1.050x + 2.198, with a correlation coefficient of 0.977.

2.2.3 Protein quantititation

The biuret reaction is based upon the reaction of alkaline Cu^{2+} with proteins whereby the amount of cuprous ions (Cu^{1+}) produced is monitored (Rising *et al.*, 1930). Bicinchoninic acid (BCA) chelates the produced cuprous ions to form a stable, water soluble, purple coloured complex which over a broad range of protein concentrations, displays a linear increase in absorbance at 562 nm (Smith *et al.*, 1985). The protein content in samples of unknown concentration can thus be determined when compared to bovine serum albumin standards as the production of cuprous ions is directly proportional to the protein concentration in the samples (Walker, 1996). Interferences caused by detergents and denaturing reagents in the Bradford assay (Bradford, 1976) do not affect the bicinchoninate reagent (Smith *et al.*, 1985). The sensitivity and low protein-to-protein variation of proteins assayed with the BCA method are comparable to the Lowry technique (Smith *et al.*, 1985). The advantage of the BCA method over the Lowry technique is the stability of the bicinchoninate reagent in alkaline conditions which allows for the reaction to be simplified to a one-step rather than a two-step process which is required for the Lowry technique (Walker, 1996). Standard and microassays of the BCA assay are able to detect 0.1 to 1.0 mg/ml and 0.5 to 10 µg/ml respectively (Walker, 1996). According to the BCA manufacturer's instructions, the absorbance resulting from the BCA interaction with the protein samples can be measured between 540 to 595 nm should the spectrophotometer to be used not have a 562 nm filter. A standard curve using the BCA™ protein assay kit is shown in Fig. 2.3.

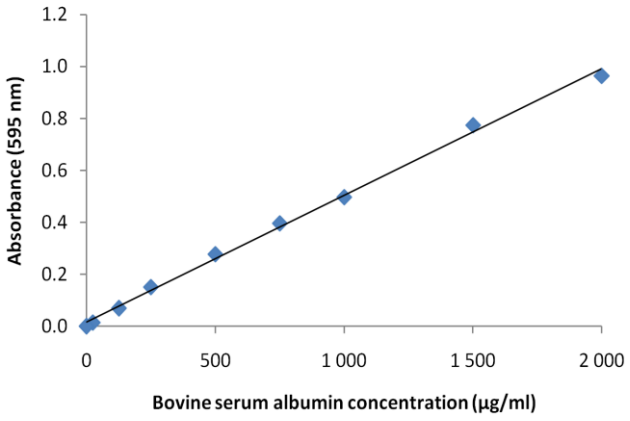

Figure 2.3: Standard curve for the BCA™ protein assay kit. Bovine serum albumin standards ranging from 25 to 2000 µg/ml were added to the BCA reagent and the resulting absorbance values measured at 595 nm after incubation at 37°C for 30 min. The equation of the trendline is given by y = 0.000x + 0.016 with a correlation coefficient of 0.997.

2.2.4 Cloning of *TcMCA5* into the pGEM®-T cloning vector

Genomic DNA was isolated from a pellet of procyclic *T. congolense* (strain IL 3000) parasites according to the method developed by Medina-Acosta and Cross (1993). Briefly, the trypanosome pellet was washed with PBS [100 mM Na_2HPO_4, 2 mM KH_2PO_4, 2.7 mM KCl and 137 mM NaCl, pH 7.2 (1 ml)] and centrifuged (2 000 *g*, 10 min, RT). The pellet was resuspended in TELT buffer [50 mM Tris-HCl buffer, pH 8.0, 62.5 mM Na_2EDTA, 2.5 M LiCl, 4% (v/v) Triton X-100 (150 µl)] and incubated at RT for 5 min. A phenol-chloroform [1:1 (v/v)] extraction with mixing using an end over end rotator at RT for 5 min was subsequently performed. The resulting top phase was recovered and 100% (v/v) ethanol was added (300 µl) and mixed using an end over end rotor at RT for 5 min to facilitate the precipitation of genomic DNA. The resulting sample was centrifuged (10 000 *g*, 10 min, RT) and the supernatant was discarded. The pellet was washed with 100% (v/v) ethanol (1 ml) and allowed to evaporate at 37°C for 30 min. The pellet was resuspended in TE buffer [100 mM Tris-HCl buffer, pH 7.5, 10 mM Na_2EDTA (30 µl)] with RNAse (20 µg/ml) and incubated at 37°C for 45 min. A sample of DNA extract (2 µl) was added to an equal volume of gel loading buffer (GLB) [30% (v/v) glycerol, 0.1 M EDTA, 1% (w/v) SDS, 0.25% (w/v) bromophenol blue] and electrophoresed on a 1% (w/v) agarose gel, containing ethidium bromide (0.5 µg/ml), in Tris-Acetate-EDTA (TAE) buffer (40 mM Tris-HCl buffer, 100 mM acetic acid, 1 mM Na_2EDTA, pH 8.0).

The coding DNA sequence for the MCA5 protein from *T. congolense* (strain IL 3 000) (GeneBank® accession number: CCC93200.1) was selected to design primers that amplified the 1 600 bp fragment using Primer 3 (Rozen and Skaletsky, 2000) (Fig. A.1). The introduction of BamHi and EcoRI restriction sites was factored into the primer design to facilitate the subsequent subcloning into expression vectors. The primers used for the PCR amplification of the *TcMCA5* gene as well as those required for colony PCR of the recombinant cloning and expression vectors are given in Table 2.1.

Table 2.1: Primer sequences used throughout the *TcMCA5* cloning process.

Primer	5' - 3'
TcMCA5 forward	AAG GAT CC**A TG**G ATC TTG CTG TTG GGC
TcMCA5 reverse	AAG AAT TCT C**AC T**TG GAG CCC TTC AAA A
T7 promoter	TAA TAC GAC TCA CTA TAG GG
T7 terminator	CTA GTT ATT GCT CAG CGG TG
SP6 promoter	ATT TAG GTG ACA CTA TAG

Underlined sequences correspond to the restriction sites.
Sequences in bold correspond to the start and the stop codon respectively.

The extracted DNA was used as the PCR template. Briefly, the final concentrations of the PCR master mix were: 0.25 µM of each gene primer, 1 x High Fidelity PCR enzyme mix buffer, 2.5 mM $MgCl_2$, 1 U High Fidelity PCR enzyme mix and 0.25 mM dNTPs in a total reaction volume of 20 µl. The PCR amplification of the *TcMCA5* gene was performed with incubation at 95°C for 2 min as the initial DNA denaturation step, followed by 40 cycles of 95°C for 10 s, 55°C for 15 s and 72°C for 1 min. A final elongation step at 72°C for 7 min was subsequently carried out. A sample of the PCR mixture produced (2 µl) was added to an equal volume of GLB and electrophoresed on a 1% (w/v) agarose gel, containing ethidium bromide (0.5 µg/ml), in TAE buffer. The remaining reaction mixture was purified using the Zymo Research Clean and Concentrator™ kit, as per the manufacturer's instructions. Ligation into the pGEM®-T cloning vector (Fig. 2.4) was performed using a 3:1 ratio of vector to purified PCR product and was subsequently incubated with 1 U of T4 DNA ligase at 37°C for 1 h, followed by a further incubation step at RT for 16 h.

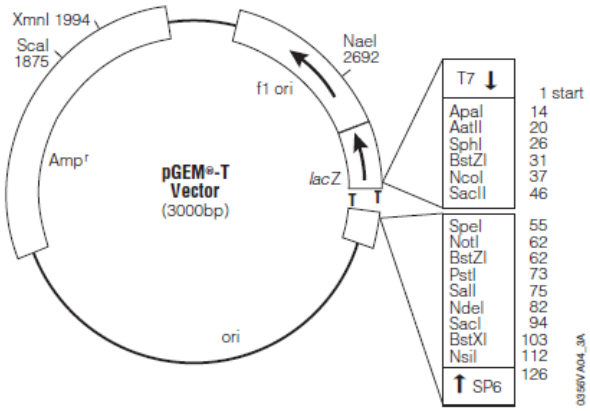

Figure 2.4: Map of the pGEM®-T cloning vector detailing the multiple cloning site (Promega technical manual).

The ligation mixture was transformed into competent *E. coli* JM 109 cells using the TransformAid™ Bacterial Transformation Kit, as per the manufacturer's instructions. The resulting *E. coli* JM 109 cells (50 µl) from the transformation mixture were plated onto pre-warmed 2 x YT plates [1.6% (w/v) tryptone, 1% (w/v) yeast extract, 0.5% (w/v) NaCl, 1% (w/v) bacteriological agar containing 50 µg/ml ampicillin, 20 µg/ml X-gal, 10 µg/ml IPTG] and incubated at 37°C for 16 h. Blue and white colonies should grow due to alpha complementation of the β-galactosidase gene of the pGEM®-T cloning vector. This is due to the disruption of the *lacZ* gene by the ligation of the *TcMCA5* insert into the pGEM®-T cloning vector (Fig. 2.4). Non-recombinant colonies were blue in colour since their *lacZ* gene was not disrupted, and thus could produce

β-galactosidase which was able to metabolise the X-gal synthetic substrate. Recombinant colonies were thus white in colour due to their inability to metabolise the synthetic substrate.

White colonies containing the recombinant pGEM®-T were selected and grown in 5 ml of 2 x YT liquid medium (containing 50 µg/ml ampicillin) at 37°C for 16 h with agitation. The plasmid DNA of the recombinant colonies was isolated using the GeneJet™ Plasmid Miniprep Kit according to the manufacturer's instructions. The isolated plasmid DNA was used as the template for a colony PCR using the previously described PCR amplification reaction conditions, with the exception that FIREpol® Taq polymerase was used instead of the High Fidelity taq polymerase. The colony PCR products (10 µl) and samples of the plasmid DNA (5 µl) were added to an equal volume of GLB and electrophoresed on a 1% (w/v) agarose gel, containing ethidium bromide (0.5 µg/ml), in TAE buffer.

The plasmid DNA of the positive clones was subjected to a small scale restriction digestion (10 µl) to confirm the correct size of the gene. Briefly, restriction digestion with EcoRI was carried out in its unique buffer at 37°C for 2 h with subsequent heat deactivation at 65°C for 15 min. The resulting reaction mixture was incubated with BamHI in its unique buffer at 37°C for 2 h and thereafter heat inactivated at 80°C for 20 min. The restriction digestion products (10 µl) resulting from the EcoRI and BamHI restriction digestions were added to an equal volume of GLB and analysed on a 1% (w/v) agarose gel, containing ethidium bromide (0.5 µg/ml), in TAE buffer. To confirm the orientation of the *TcMCA5* gene within the pGEM®-T vector, isolated plasmid DNA from the positive clones were subjected to a small scale restriction digestion with XhoI and NcoI. After confirmation of the amplified gene size by colony PCR, the plasmid DNA of each of the positive clones, which possessed the *TcMCA5* gene in the correct orientation, were sequenced at the Central Analytical Facility (CAF), Stellenbosch University.

2.2.5 Subcloning of the *TcMCA5* gene into the bacterial pET-28a expression vector

The recombinant *TcMCA5*-pGEMT plasmids were subjected to a restriction digestion (50 µl) with EcoRI in its unique buffer at 37°C for 4 h with subsequent heat deactivation at 65°C for 15 min. The resulting reaction mixture was incubated with BamHI in its unique buffer at 37°C for 4 h and thereafter heat inactivated at 80°C for 20 min. The restriction mixture (50 µl) was added to an equal volume of GLB and electrophoresed

on a 1% (w/v) agarose gel in TAE buffer, both containing crystal violet (10 µg/ml). Crystal violet was used to visualise the bands, instead of ethidium bromide, before excision (Rand, 1996). The use of ethidium bromide at this point in the cloning process would require visualisation using UV light which damages the DNA and in effect would result in reduced efficiency of the cloning process. The gel was viewed on a light box, the 1 600 bp product excised and subsequently purified using the E.Z.N.A® gel extraction kit as per the manufacturer's instructions.

The pET-28a, pET-32a and pGEX4T-1 expression vectors (Fig. 2.5) were each subjected to a restriction digestion (50 µl) with EcoRI in its unique buffer at 37°C for 4 h with the subsequent heat deactivation at 65°C for 15 min. The resulting reaction mixture was incubated with BamHI in its unique buffer at 37°C for 4 h and thereafter heat inactivated at 80°C for 20 min. Subsequently, 1 U of SAP was added and incubated at 37°C for 1 h to dephosphorylate the vector. A 3:1 ratio of vector to gene insert was incubated with 1 U of T4 DNA ligase at 37°C for 1 h followed by a further incubation step at RT for 16 h.

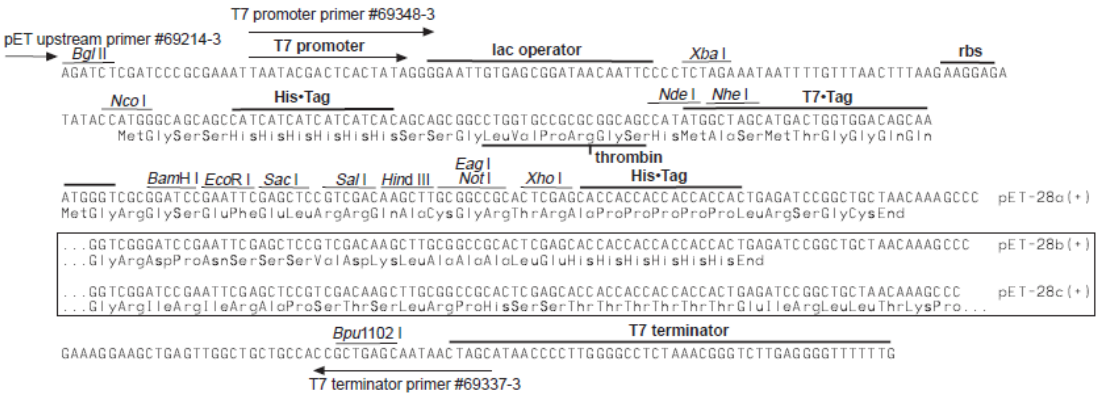

Figure 2.5: Map of the pET-28a expression vector detailing the multiple cloning site (Novagen technical manual).

The ligation mixture was transformed into competent *E. coli* BL21 (DE3) cells by $CaCl_2$ transformation (Cohen *et al.*, 1972; Sambrook *et al.*, 2001). Briefly, 10 ml of 2 x YT liquid medium was inoculated with a single *E. coli* BL21 (DE3) colony and subsequently grown at 37°C for 16 h with agitation. The overnight culture was diluted 1:100 with 90 ml of fresh 2 x YT liquid medium and grown at 37°C with agitation until an OD_{600} of 0.3 to 0.4 was reached. The cultures were transferred into ice cold, sterile centrifuge tubes and incubated on ice for 10 min. The cells were pelleted (4 500 *g*, 10 min, 4°C) and resuspended in ice cold, sterile $CaCl_2$ solution [60 mM $CaCl_2$, 10 mM HEPES, pH 7.0 (40 ml)]. The cell solution was pelleted again (4 500 *g*, 10 min, 4°C) and

resuspended in ice cold, sterile $CaCl_2$ solution (2 ml). The competent cells (20 µl) were incubated with the ligation mixture (1 µl) on ice for 30 min. Thereafter, cells were heat shocked at 42°C for 90 s and incubated on ice immediately for 2 min. The cells were added to pre-warmed super optimal catabolizer with catabolite repression (SOC) medium [2% (w/v) tryptone, 0.5% (w/v) yeast extract, 10 mM NaCl, 2.5 mM KCl, 10 mM $MgCl_2$, 10 mM $MgSO_4$, 20 mM glucose (80 µl)] and incubated at 37°C for 1 h with gentle agitation. The resulting cell mixture (100 µl) was plated onto two pre-warmed 2 x YT plates (containing 34 µg/ml kanamycin) and incubated at 37°C for 16 h.

Recombinant *TcMCA5*-pET28a colonies were grown in 5 ml of 2 x YT liquid medium (containing 34 µg/ml kanamycin) and grown at 37°C for 16 h with agitation. The plasmid DNA was isolated using the GeneJet™ Plasmid Miniprep Kit, as per the manufacturer's instructions and was used as the template for the colony PCR. Using the previously described PCR amplification reaction conditions, with the exception that FIREpol® Taq polymerase was used instead of the High Fidelity Taq polymerase, a colony PCR was performed. The colony PCR products (10 µl) along with samples of the plasmid DNA (5 µl) was added to an equal volume of GLB and electrophoresed on a 1% (w/v) agarose gel, containing ethidium bromide (0.5 µg/ml), in TAE buffer. The plasmid DNA of the positive clones was subjected to a small scale restriction digestion (10 µl) with EcoRI in its unique buffer at 37°C for 2 h with the subsequent heat deactivation at 65°C for 15 min. The resulting reaction mixture was incubated with BamHI in its unique buffer at 37°C for 2 h and thereafter heat inactivated at 80°C for 20 min. Restriction digestion products (10 µl) resulting from the EcoRI and BamHI restriction digestions were added to an equal volume of GLB and analysed on a 1% (w/v) agarose gel, containing ethidium bromide (0.5 µg/ml), in TAE buffer to confirm the correct size of the *TcMCA5* gene. After confirmation of amplified gene size, plasmid DNA of the positive clones was sequenced at the Central Analytical Facility (CAF), Stellenbosch University.

2.2.6 Recombinant expression of TcMCA5

The expression conditions were optimised by incubation at 37°C and 30°C with 0, 0.1, 0.3, 0.5, 0.7 and 1 mM IPTG induction over four hours. Single colonies of positively identified recombinant *TcMCA5*-pET28a BL21 (DE3) clones were used to inoculate 100 ml of terrific broth (TB) liquid medium [1.2% (w/v) tryptone, 2.4% (w/v) yeast extract, 0.4% (v/v) glycerol, 0.17 M KH_2PO_4, 0.72 M K_2HPO_4] or 10 ml of 2 x YT liquid medium, which both contained kanamycin (34 µg/ml). After incubation at 37°C for 16 h in baffled flasks, the 2 x YT culture was diluted 1:100 with 90 ml of fresh 2 x YT

liquid medium (containing 34 µg/ml kanamycin) and grown at 37°C in a baffled flask with agitation until an OD_{600} of 0.65 was reached. Expression was induced with IPTG (0.1 M), at a final concentration of 1 mM, at 37°C for 4 h with agitation. Kanamycin (34 µg/ml, 100 µl) was added at the start of induction as well as after 2 h. The cells from the IPTG expression as well as from the TB expression were pelleted by centrifugation (5 000 *g*, 10 min, 4°C), the pellets were resuspended in 1% (v/v) Triton X-100-PBS (2 ml), lysozyme added (1 mg/ml final concentration) and incubated at 37°C for 30 min. The cell suspension was frozen at -70°C for 1 h and subsequently thawed at RT. The cell suspensions were sonicated four times for 30 s each and the cellular debris was subsequently pelleted from the soluble protein lysate by centrifugation (5 000 *g*, 10 min, 4°C). The protein lysate was subsequently filtered through Whatman No. 1 filter paper and stored at -20°C.

Samples of the supernatant and the pellet containing the soluble and insoluble fractions respectively were electrophoresed on two 12.5% reducing SDS-PAGE gels (Laemmli, 1970) with one stained with Coomassie blue R-250 and the other transferred onto nitrocellulose using the semi dry blotter from Sigma with the transfer of proteins confirmed by staining with Ponceau S solution [0.1% (w/v) Ponceau S, 15% (v/v) acetic acid]. The unoccupied sites on the nitrocellulose membrane were blocked [5% (w/v) low fat milk powder in TBS (20 mM Tris-HCl buffer, 200 mM NaCl, pH 7.4)] at RT for 1 hr. The mouse anti-6xHis IgG primary antibody [1:1 000 diluted in 0.5% (w/v) BSA-PBS] was added and incubated at 4°C for 16 h. The blot was washed three times over 15 min with TBS and goat anti-mouse IgG HRPO conjugate [1:15 000 diluted in 0.5% (w/v) BSA-PBS] was subsequently added and incubated at RT for 1 h. The blot was washed three times over 15 min with TBS before the addition of 4-chloro-1-naphthol·H_2O_2 substrate [0.06% (w/v) 4-chloro-1-naphthol, 0.1% (v/v) methanol and 0.0015% (v/v) H_2O_2 in TBS]. The blot was allowed to develop in the dark. Additional western blots were performed using the anti-TcMCA5 IgY primary antibody [100 µg/ml diluted in 0.5% (w/v) BSA-PBS] with the rabbit anti-chicken IgY HRPO conjugate as secondary detection antibody. The Pierce™ ECL western blotting substrate was used and the blot was developed at RT for 2 min in the dark and subsequently transferred onto Kodak BioMax light film.

2.2.7 Solubilisation, refolding and purification of recombinant TcMCA5

When recombinant proteins are expressed within inclusion bodies, they are generally the predominant protein and are protected from degradation by the host's proteolytic

enzymes (Burgess, 2009). Solubilisation and refolding of the inclusion bodies was performed to regain complete renaturation and enzyme activity. This generally involves the solubilisation of the inclusion bodies using chaotropic agents such as guanidine hydrochloride and urea or non-chaotropic agents such as SDS and N-lauroylsarsocine sodium salt (sarkosyl) (Burgess, 2009). Thereafter the solubilised proteins are refolded by removing the excess denaturant in an optimised refolding buffer by dilution, dialysis or by chromatographic methods (Clark, 1998). The use of immobilised metal ion affinity chromatography (IMAC) in the form of a nickel chelate column allows for the gradual removal of the denaturant and the subsequent refolding of the immobilised recombinant protein (Petty, 2001). There are a variety of commercial screens that assist in the identification of suitable refolding buffers. Once refolded, the protein must undergo re-oxidation in order to allow for the formation of disulfide bonds in the correct conformation and is achieved by either the addition of 0.1 to 1 mM DTT in the inclusion body lysis buffer or within the refolding buffers (Burgess, 2009).

Two methods of solubilisation and refolding were performed, one using guanidine hydrochloride and urea (chaotropic), which was adapted from the protocol used by the Heyer Lab at the University of California, College of Biological Sciences (Personal communication), and the other using sarkosyl (non-chaotropic) which was adapted and modified from Schlager and co-workers (2012).

Urea solubilisation was performed after 4 h of induced expression at 37°C with IPTG (1 mM). The cells were pelleted by centrifugation (5 000 *g*, 10 min, 4°C), and to the pellet, buffer A [6 M guanidine-HCl, 0.1 M NaH_2PO_4, 0.01 M Tris-HCl buffer, pH 8.0 (5 ml for a 50 ml culture)] was added and stirred at RT for 2 h. The solubilised proteins were separated from the insoluble debris by centrifugation (10 000 *g*, 30 min, 4°C). Samples of the supernatant and the pellet containing the resolubilised protein lysate and insoluble fractions respectively were electrophoresed on a 12.5% reducing SDS-PAGE gel (Laemmli, 1970) and stained with Coomassie blue R-250.

Sarkosyl solubilisation was performed after 4 hr of induced expression at 37°C with IPTG (1 mM). The cells were pelleted by centrifugation (5 000 *g*, 10 min, 4°C), and to the pellet, lysis buffer (PCL) [8 mM Na_2HPO_4, 286 mM NaCl, 1.4 mM KH_2PO_4, 2.6 mM KCl, 1% (w/v) SDS, pH 7.4, 1 mM DTT (5 ml for a 50 ml culture)] was added. The resulting solution was sonicated twice over 4 min and subsequently incubated on ice for 30 min. The solubilised proteins were separated from the insoluble debris by centrifugation (10 000 *g*, 20 min, 4°C). Samples of the supernatant and the pellet containing the solubilised protein lysate and insoluble fractions respectively were

electrophoresed on a 12.5% reducing SDS-PAGE gel (Laemmli, 1970) and stained with Coomassie blue R-250.

The refolding of solubilised TcMCA5 is outlined below using the urea and sarkosyl methods. Buffers A, B, C and E were used for the urea method whilst the PCW and PCE buffers were used for the sarkosyl method.

His-select® nickel affinity resin (1 ml) was placed in a 10 ml chromatography column, washed with 2 column volumes of dH_2O and equilibrated with 10 column volumes of buffer A or 5 column volumes of wash buffer (PCW) [8 mM Na_2HPO_4, 286 mM NaCl, 1.4 mM KH_2PO_4, 2.6 mM KCl, 0.1% (w/v) sarkosyl, pH 7.4]. The solubilised protein lysate (5 ml) was incubated with the resin at 4°C for 3 h and mixed using an end-over-end rotator. The unbound proteins were collected and the resin was washed with 25 ml buffer B (8 M urea, 0.1 M NaH_2PO_4, 0.01 M Tris-HCl buffer, pH 8.0) and finally 25 ml buffer C (8 M urea, 0.1 M NaH_2PO_4, 0.01 M Tris-HCl buffer, pH 6.3). The column for the sarkosyl method was washed with 40 ml PCW buffer until an absorbance value at 280 nm of 0.02 was reached.

The bound proteins were eluted in 1 ml fractions with 10 ml buffer E (8 M urea, 0.1 M NaH_2PO_4, 0.01 M Tris-HCl buffer, pH 4.) or with 10 ml elution buffer (PCE) [8 mM Na_2HPO_4, 286 mM NaCl, 1.4 mM KH_2PO_4, 2.6 mM KCl, 0.1% (w/v) sarkosyl, 50 mM imidazole, pH 7.4]. The column was regenerated with 2 column volumes of dH_2O, 5 column volumes of 6 M guanidine hydrochloride, 3 column volumes of dH_2O, and 3 column volumes of equilibration buffer (50 mM NaH_2PO_4, 500 mM NaCl, 10 mM imidazole, pH 6.8) and stored in 30% (v/v) ethanol at 4°C. Samples of the unbound and the eluted fractions were electrophoresed on a 12.5% reducing SDS-PAGE gel (Laemmli, 1970) and stained with Coomassie blue R-250.

The fractions containing the enzyme were pooled and concentrated against polyethylene glycol (PEG) M_r 20 000 until the final volume was approximately 5 ml. Protein concentration was determined using the BCA™ protein assay kit. Purified samples (5 µl) were electrophoresed on a 12.5% reducing SDS-PAGE gel (Laemmli, 1970) and visualised using a silver stain (Blum *et al.*, 1987) to asses purity.

2.2.8 Enzymatic characterisation of recombinant TcMAC5

2.2.8.1 Activity assay

To quantify the hydrolysis of a fluorogenic peptide substrate by the purified recombinant TcMCA5, an AMC calibration curve was constructed. The AMC standards ranging from 5 to 15 000 nM (50 µl) were incubated with 50 µl MCA assay buffer (50 mM Tris-HCl buffer, 150 mM NaCl, 10 mM $CaCl_2$, pH 7.5, 5 mM DTT) at 37°C for 5 min and the fluorescence (Ex_{360nm} and Em_{460nm}) measured using a FLUORStar Optima Spectrophotometer from BMG Labtech (Offenburg, Germany) (Fig. 2.6). The slope of the calibration curve was used to determine the enzyme concentrations which gave rise to the fluorescence values obtained in the various enzymatic assays.

Samples of the eluted fractions from the on-column refolding and purification from both the sarkosyl and urea refolding methods (100 µl) were incubated with MCA buffer containing 10 µM Z-Gly-Gly-Arg-AMC substrate (100 µl) at 37°C for 10 min. Thereafter, the fluorescence (Ex_{360nm} and Em_{460nm}) was measured using a FLUORStar Optima Spectrophotometer.

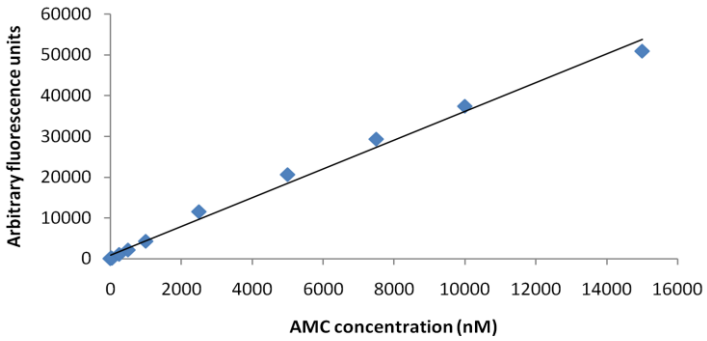

Figure 2.6: AMC standard curve showing the relationship between fluorescence and AMC concentration. AMC dilutions were incubated with MCA buffer at 37°C and the fluorescence measured (Ex_{360nm} Em_{460nm}). The equation of the trendline is given by y = 3.529x + 818.7 with a correlation coefficient of 0.992.

2.2.8.2 Gelatin containing SDS-PAGE for recombinant TcMCA5 activity visualisation

Samples of the eluted fractions from the on-column refolding and purification were electrophoresed on a 12.5% non-reducing SDS-PAGE gel containing 1% (w/v) gelatin and washed twice over 1 h with 2.5% (v/v) Triton X-100-PBS (50 ml) at RT to remove the excess SDS (Heussen and Dowdle, 1980). Fifty millilitres of MCA assay buffer or cysteine protease assay buffer [100 mM Na-acetate, 1 mM Na_2EDTA, 0.02% (m/v)

NaN_3, 1 µg/ml pepstatin, 40 mM cysteine, pH 5.0] was incubated with the gel at 37°C for 3 h and subsequently stained with 0.1% (w/v) amido black at RT for 1 h. Thereafter, the gel was destained against several changes of methanol: acetic acid: dH_2O (30: 10: 60).

2.2.9 Antibody preparation and ELISA optimisation

2.2.9.1 Preparation of immunogen, the immunisation of chickens and IgY isolation

Chickens were used to raise antibodies against the purified recombinant TcMAC5 protein. Two chickens were immunised intramuscularly on either side of the breast bone. The recombinant TcMCA5 protein (50 µg/ml, 1.5 ml) was added to an equal volume of Freund's complete adjuvant and triturated to form a stable water-in-oil emulsion prior to immunisation. Booster injections, using Freund's incomplete adjuvant, were given at weeks 2, 4 and 6. Eggs collected prior to immunisation served as the pre-immune control, and those collected throughout the immunisation schedule were stored at 4°C.

Chicken immunoglobulin (IgY) was isolated from the yolks of the eggs collected at each week as described by Goldring and Coetzer (2003). Briefly, the yolks were separated from the eggs whites and rinsed under running tap water. The yolk sac was punctured, the yolk collected and the volume determined. The yolk was mixed with two yolk volumes of IgY buffer [100 mM NaH_2PO_4, pH 7.6, 0.02% (w/v) NaN_3] and 3.5% (w/v) PEG 6 000 being subsequently added and dissolved with stirring. The resulting solution was centrifuged (4 420 *g*, 30 min, RT), and the supernatant filtered through adsorbent cotton wool. The final PEG concentration was increased to 12% (w/v) by the addition of 8.5% (w/v) PEG 6 000 and was once again dissolved by stirring. The resulting solution was centrifuged (12 000 *g*, 10 min, RT), and the resulting pellet dissolved in IgY buffer equal to the yolk volume. Finally, 12% (w/v) PEG 6 000 was added and dissolved with stirring. The resulting solution was centrifuged (12 000 *g*, 10 min, RT), and the resulting pellet was dissolved in final IgY buffer [100 mM NaH_2PO_4, pH 7.6, 0.1% (w/v) NaN_3] equal to a sixth of the yolk volume and stored at 4°C. The concentration of isolated IgY was determined spectrophotometrically at 280 nm using an extinction coefficient of $E_{280\ nm}^{1\ mg/ml} = 1.25$ (Goldring *et al.*, 2005).

2.2.9.2 ELISA evaluation of antibody production

The progress of IgY antibody production by chickens during the immunisation period against the TcMCA5 recombinant protein, was monitored by enzyme linked immunosorbent assay (ELISA). The wells of 96 well Nunc-Immuno™ Maxisorp ELISA plates were coated with recombinant TcMCA5 (1 µg/ml, 150 µl per well) in PBS (100 mM NaH_2PO_4, 100 mM Na_2HPO_4, 100 mM NaCl, pH 7.4) for 16 h at 4°C. The coating solution was discarded and the plates were blocked with blocking buffer [0.5% (w/v) BSA-PBS, 0.1% (v/v) Tween-20, 200 µl per well] to prevent the non-specific binding of antibodies, by incubation at 37°C for 1 h. The wells were washed three times with 0.1% (v/v) Tween-20-PBS using the BIOTEK® ELx50™ Microplate washer and was subsequently incubated with anti-TcMCA5 IgY primary antibody diluted in blocking buffer (100 µg/ml, 100 µl per well) at 37°C for 2 h. The wells were washed as before and the rabbit anti-chicken IgY HRPO conjugate diluted in blocking buffer (1:15 000, 100 µl per well) was added and incubated at 37°C for 1 h. The wells were washed as before and the ABTS substrate solution [0.05% (w/v) ABTS, 0.0015% (v/v) H_2O_2 in 0.15 M citrate-phosphate buffer, pH 5.0 (145 µl per well)] was subsequently added. The plate was incubated in the dark for 15 min prior to reading the absorbance at 405 nm using the FLUORStar Optima Spectrophotometer in 15 min intervals until absorbance values of above 1.0 were obtained.

2.2.10 Culture and western blot of procyclic *Trypanosoma congolense* (strain IL 3000) parasites

The *in vitro* culture of *T. congolense* procyclic form (PCF) parasites was performed as used by Eyford and co-workers (2011) and developed by Hirumi and Hirumi (1991). Briefly, 10 ml Eagle's minimum essential medium [EMEM base powder, 2 mM glutamine, 10 mM proline, 20% (v/v) heat inactivated foetal bovine serum] was used to culture the *T. congolense* PCF parasites at 27°C and 5% (v/v) CO_2 until the culture became slightly over grown.

Cultured *T. congolense* PCF parasites were pelleted by centrifugation (2 000 *g*, 10 min, RT), washed twice with PBS (100 mM Na_2HPO_4, 2 mM KH_2PO_4, 2.7 mM KCl, 137 mM NaCl, pH 7.2) and were subsequently resuspended in lysis buffer [20 mM Tris-HCl buffer, pH 7.2, 10 mM Na_2EDTA, 1% (v/v) Triton X-100, 10 µM E64 (140 µl)]. An equal volume of reducing treatment buffer was added to the parasites before boiling for 10 min. A total of 1 x 10^5 parasites were added to each lane (20 µl) and electrophoresed on a 12.5% reducing SDS-PAGE gel (Laemmli, 1970). The

trypanosomal lysate from the SDS-PAGE gel was transferred onto a nitrocellulose membrane using the semi dry blotter from Sigma and the western blot performed as per section 2.2.6.

2.3 Results

2.3.1 Cloning of *TcMCA5* gene into the pGEM-T® cloning vector

A single putative full length metacaspase gene (EMBL accession: CCC93200.1) was identified in chromosome 9 of *T. congolense* (strain IL 3000), namely *TcMCA5* and was 1 600 bp in length. Genomic DNA was successfully isolated from the PCF of *T. congolense* (strain IL 3 000) (Fig. 2.7, panel A) and was used as the template for PCR amplification of the *TcMCA5* gene using the specific primers designed for this purpose (Table 2.1). A High Fidelity PCR enzyme mix was used for the amplification comprising a combination of Taq DNA polymerase and a thermostable DNA polymerase with proofreading ability. These characteristics ensured that the exact sequence would be amplified from the genomic DNA as any transcription errors would result in inaccurate protein translation and thus incorrect protein folding in downstream experiments.

The PCR amplification resulted in a product of the expected size of 1 600 bp (Fig. 2.7, panel B). The PCR product was subsequently purified using the ZymoResearch Clean and Concentrator™ kit.

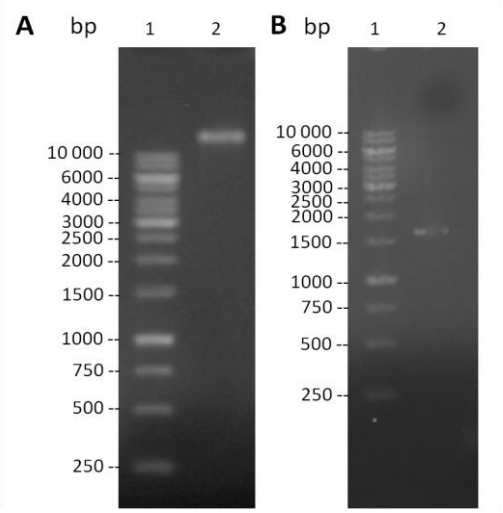

Figure 2.7: Analysis of the isolation of *T. congolense* (strain IL 3 000) genomic DNA and PCR amplification of the *TcMCA5* gene. Samples from the DNA extraction and PCR amplification were electrophoresed on a 1% (w/v) agarose gel containing 0.5 µg/ml ethidium bromide. **(A)** Lane 1: O'GeneRuler™; lane 2: *T. congolense* genomic DNA. **(B)** Lane 1: O'GeneRuler; lane 2: *TcMCA5* PCR product.

The ligation of the purified 1 600 bp *TcMCA5* PCR product into the pGEM®-T cloning vector was successful resulting in non-recombinant blue and recombinant white colonies due to blue/white screening. Plasmid DNA isolation of the recombinant white colonies was performed and subsequently used as the template for colony PCR to amplify the 1 600 bp *TcMCA5* gene.

Ten recombinant *TcMCA5*-pGEMT colonies were identified by the PCR amplification of a 1 600 bp product when the SP6 and T7 promoter vector primers were used (Fig. 2.8, panel A). The PCR amplification using the T7 promoter and the *TcMCA5* reverse primers resulted in the same ten colonies being identified as recombinant as confirmed by the presence of the 1 600 bp product (Fig. 2.8, panel B). The amplified PCR products from colonies 1, 3, 7, 12, 13 and 21 were at a much higher concentration than for those obtained from colonies 4, 5, 6 and 11. This was evident in both colony PCR reactions.

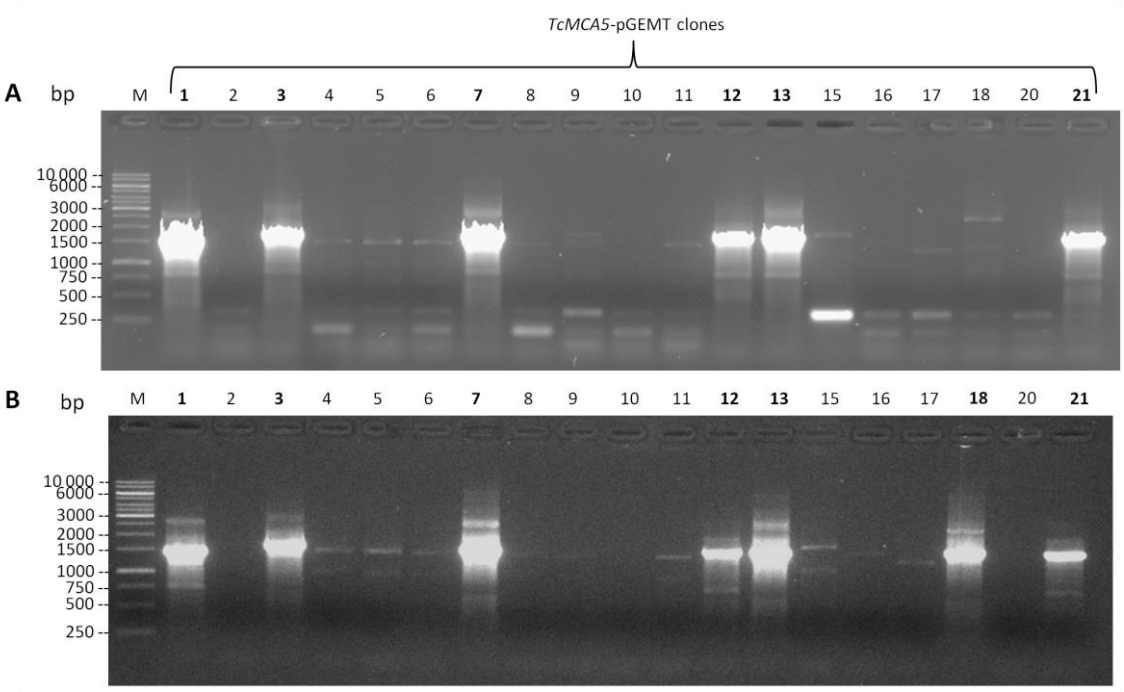

Figure 2.8: Screening for recombinant *TcMCA5* clones ligated into the pGEM®-T cloning vector from the isolated plasmid DNA, by PCR amplification. Following the transformation of *TcMCA5*-pGEMT ligation mixture into competent *E. coli* JM 109 cells, and the subsequent selection of white colonies, the isolated plasmid DNA was subjected to PCR using **(A)** the T7 promoter and SP6 promoter vector primers and **(B)** the T7 promoter vector and the *TcMCA5* reverse primers. Samples were electrophoresed on a 1% (w/v) agarose gel containing 0.5 µg/ml ethidium bromide. M: O'GeneRuler™.

After a small scale restriction digestion of the ten recombinant colonies using both BamHI and EcoRI, only two out of the eleven colonies, clones 7 and 13, yielded two

products at 1 600 and 3 000 bp which corresponded to the *TcMCA5* insert and the pGEM®-T cloning vector respectively (Fig. 2.9).

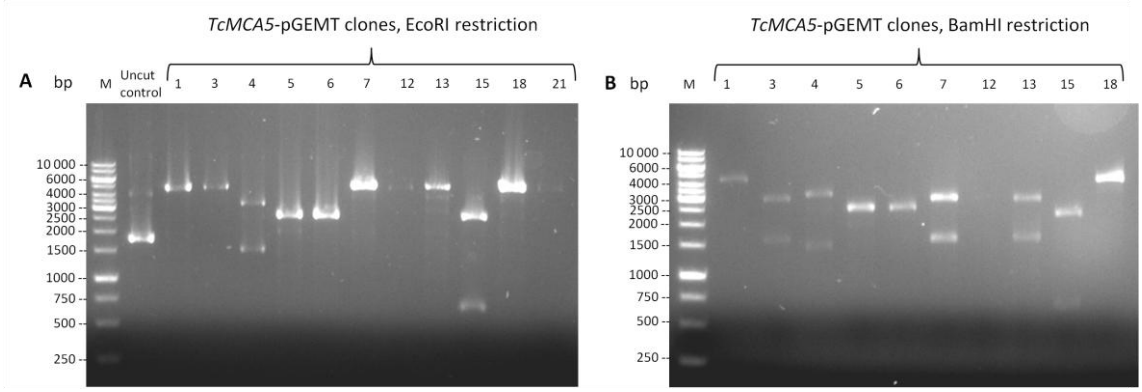

Figure 2.9: Analysis of the EcoRI and BamHI restriction digestion of the isolated plasmid DNA from recombinant *TcMCA5*-pGEMT clones by agarose gel electrophoresis. The isolated *TcMCA5*-pGEMT plasmid DNA of different recombinant colonies were subjected to **(A)** a 2 h restriction digestion with EcoRI at 37°C and thereafter, **(B)** a further 2 h restriction digestion with BamHI at 37°C. Samples were electrophoresed on a 1% (w/v) agarose gel containing 0.5 µg/ml ethidium bromide. M: O' GeneRuler™.

The orientations of the *TcMCA5* insert within the pGEM®-T cloning vector of these two positively identified recombinant clones were investigated by restriction digestion as outlined in Fig. 2.10. The double restriction digestion, using XhoI and NcoI, of the isolated plasmid DNA of *TcMCA5*-pGEMT clones 7 and 13, both yielded the required 984 and 3 620 bp products that were predicted. Samples of the plasmid DNA isolated from *TcMCA5*-pGEMT clones 7 and 13 were sequenced. The sequencing results confirmed that the *TcMCA5* gene had been successfully amplified from the trypanosomal genomic DNA and ligated into the pGEM®-T cloning vector for both recombinant clones. The recombinant *TcMCA5* sequence from each recombinant clone was identical to that retrieved from GeneBank® (TcIL3000.9.6120).

The clones were then annotated as M7 and M13, corresponding to the extracted plasmid DNA from the *TcMCA5*-pGEMT clones 7 and 13 respectively (Fig. 2.8).

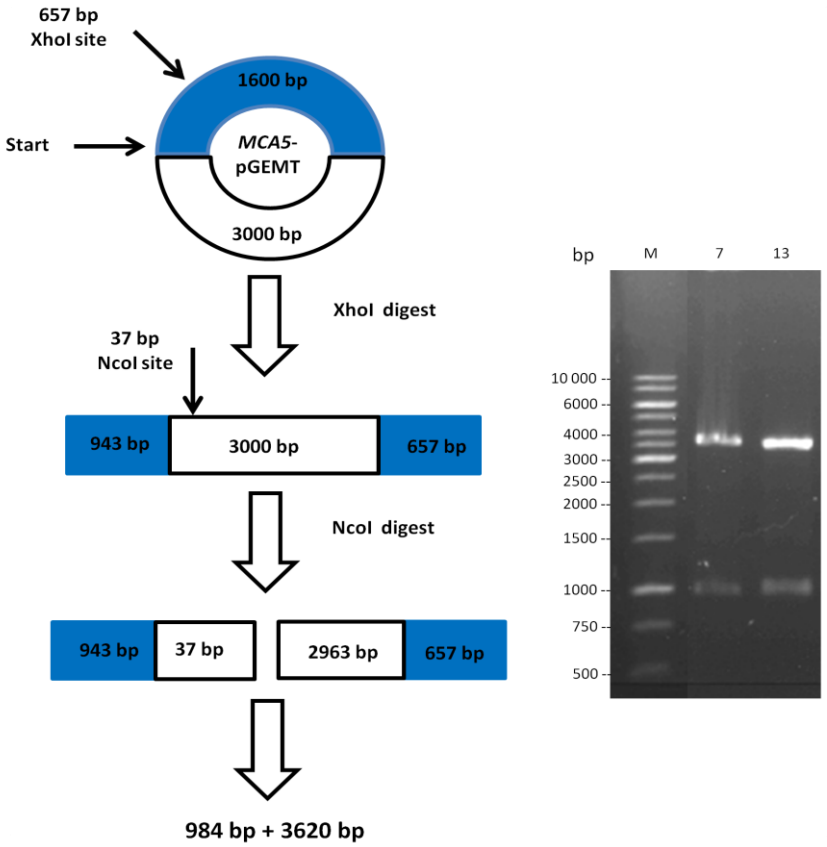

Figure 2.10: Schematic diagram of the recombinant *TcMCA5*-pGEMT vector and the results of different restriction digestions to confirm the correct orientation of the *TcMCA5* insert within the pGEM®-T cloning vector. The isolated *TcMCA5*-pGEMT plasmid DNA of clones 7 and 13 were subjected to a 2 h restriction digestion with XhoI at 37°C and thereafter a further 2 h digestion with NcoI at 37°C. Samples were electrophoresed on a 1% (w/v) agarose gel containing 0.5 µg/ml ethidium bromide. M: O' GeneRuler™.

2.3.2 Subcloning of the *TcMCA5* gene into the bacterial pET-28a expression vector

The isolated plasmid DNA from the two positive recombinant *TcMCA5*-pGEMT clones, M7 and M13, were subjected to a large scale restriction digestion with EcoRI and BamHI to obtain the insert for the subsequent ligation into an expression vector. As shown in Fig. 2.11, panel A, after the restriction digestion, two bands were produced at 1 600 bp and 3 000 bp which correspond to the *TcMCA5* insert and the pGEM®-T cloning vector respectively. The restriction mixture was subsequently electrophoresed on a 10 µg/ml crystal violet containing agarose gel and the 1 600 bp *TcMCA5* insert was excised and purified.

The purity, size and approximate concentrations of the isolated *TcMCA5* insert along with the previously digested and de-phosphorylated pET-28a, pET-32a and pGEX4T-1 expression vectors were determined from Fig. 2.11, panel B. Ligation mixtures of the *TcMCA5* insert with the various expression vectors were prepared, which included

expression vector re-ligation controls, and were subsequently transformed into *E. coli* BL21 (DE3) cells by $CaCl_2$ transformation. Recombinant colonies were only evident for the M7pET28, M13pET28 and M13pET32 ligations with each yielding at least 2 colony forming units.

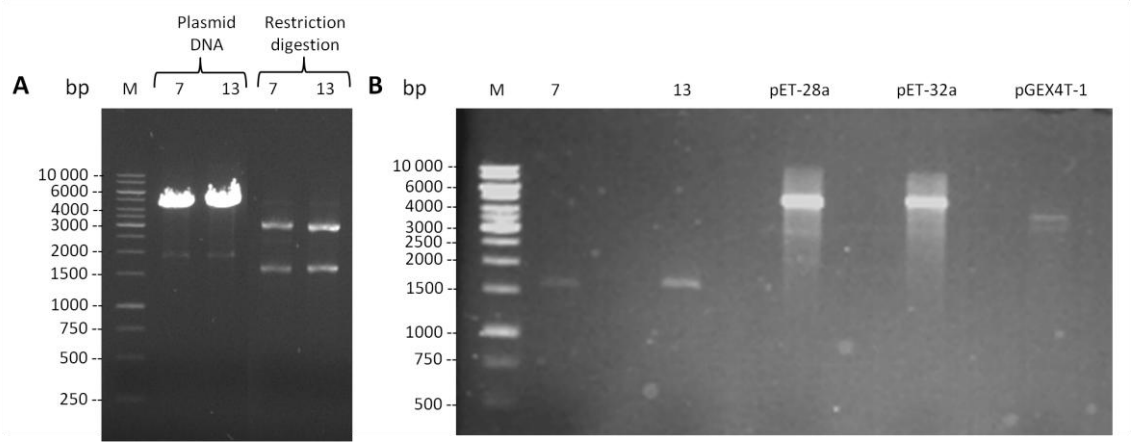

Figure 2.11: Gel extraction of the *TcMCA5* insert after the restriction digestion with EcoRI and BamHI of the positive recombinant *TcMCA5*-pGEMT clones 7 and 13. (A) After the restriction digestion of the plasmid DNA with BamHI and EcoRI for 2 h each at 37°C, the *TcMCA5* insert was visualised using 10 µg/ml crystal violet, excised from the 1% (w/v) agarose gel and **(B)** purified using the E.Z.N.A® gel extraction kit. Samples were electrophoresed on a 1% (w/v) agarose gel containing 0.5 µg/ml ethidium bromide. M: O'GeneRuler™.

The plasmid DNA of the resulting recombinant *TcMCA5*-pET28a and *TcMCA5*-pET32a clones was isolated and used as the template for colony PCR to amplify the 1 600 bp *TcMCA5* gene using the *TcMCA5* forward and reverse gene primers (Fig. 2.12, panel A) and the T7 promoter and termination vector primers (Fig. 2.12, panel B). When using the T7 promoter and termination vector primers, an extra 200 bp should be added onto the expected size of the *TcMCA5* product due to the amplification of the vector DNA on either side of the *TcMCA5* insert at the EcoRI and BamHI restriction sites (Fig 2.5). A band at approximately 1 800 bp is present for M7pET28a clones 1 to 3 and M13pET28a clone 1. When the plasmid DNA from the recombinant clones identified by the T7 vector primers, were amplified using the *TcMCA5* forward and reverse gene primers, a product of 1 600 bp was observed in each case. The PCR amplification products for the M13pET28a clone 1 and the M13pET32a clones 1 to 5 did not correspond to the expected sizes.

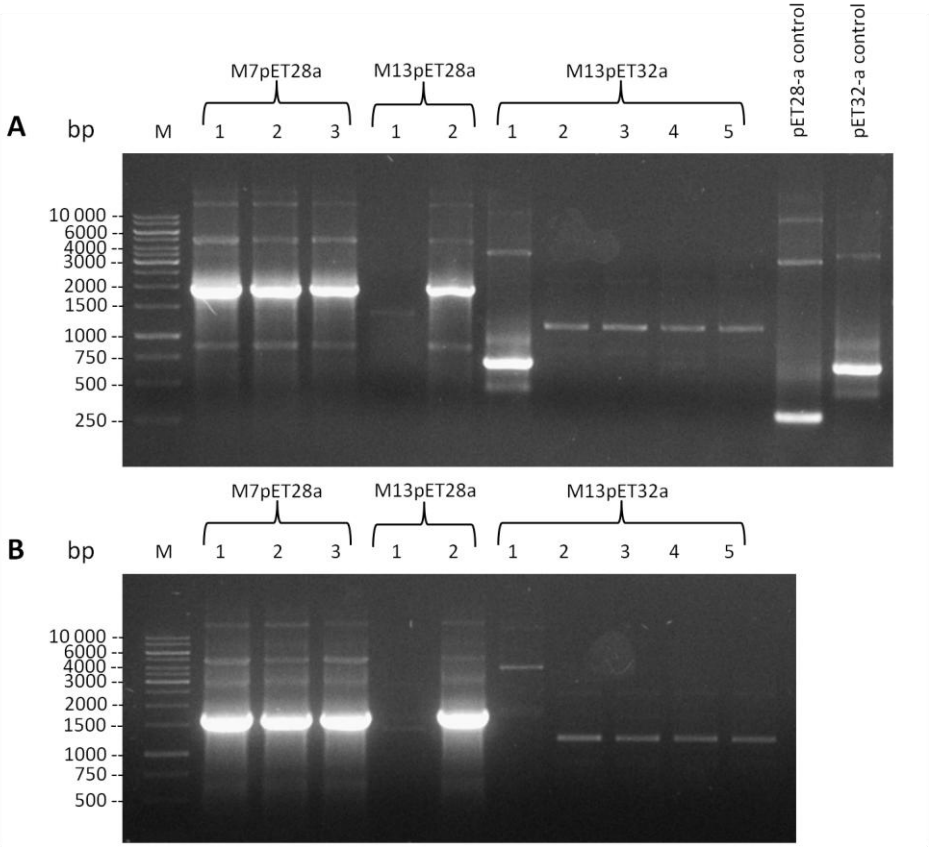

Figure 2.12: Screening for recombinant *TcMCA5* clones ligated into the pET-28a and pET-32a expression vectors, from the isolated plasmid DNA by PCR amplification. Following the transformation of the *TcMCA5*-pET28a and *TcMCA5*-pET32a ligation mixtures into *E. coli* BL21 (DE3) cells and the selection of colonies, the isolated plasmid DNA from each clone was subjected to PCR amplification using **(A)** the T7 promoter and terminator vector primers as well as **(B)** the *TcMCA5* forward and reverse primers. Samples were electrophoresed on a 1% (w/v) agarose gel containing 0.5 µg/ml ethidium bromide. M: O'GeneRuler™.

The plasmid DNA of M7pET28 clones 1 to 3 and M13pET28 clone 2 were sequenced using the *TcMCA5* forward and reverse as well as the T7 promoter and terminator primers. The sequencing results indicated that the recombinant clones all possessed the *TcMCA5* gene, identical to the sequence retrieved from GeneBank® (TcIL3000.9.6120).

2.3.3 Recombinant expression, solubilisation, refolding and purification of TcMCA5

The single putative full length metacaspase gene (UniProtKB ID: G0UUY6) identified in chromosome 9 of *T. congolense* strain IL 3000 (TcMCA5) codes for a protein of 533 amino acids in length with an expected molecular weight of 59 kDa and a pI of 8.42 as predicted by the Compute pI/Mw tool on the ExPASy server (Gasteiger *et al.*, 2005).

2.3.3.1 Expression optimisation of recombinant TcMCA5

The PROSO II sequence-based solubility prediction calculator predicted that TcMCA5 had a 92.5% chance of being insoluble when over-expressed in *E. coli* (Smialowski *et al.*, 2006). Protein solubility is determined by its primary structure (Smialowski *et al.*, 2006). It has been demonstrated that proteins which possess a higher percentage of aromatic amino acid residues and stretches of 20 or more hydrophobic amino acid residues, are more likely to be insoluble when over-expressed in *E. coli* (Christendat *et al.*, 2000). Research done by Bertone and co-workers (2001) indicated that proteins whose hydrophobic amino acid composition was greater than 16% were more likely to be insoluble. The TcMCA5 protein is comprised of 22.1% hydrophobic amino acids. In addition to the disordered C-terminal extension caused by the large amount turn forming Pro residues, it follows that TcMCA5 would be insoluble when over-expressed, based on the basic analysis of its primary structure.

Expression of the M7pET28a clones 1 to 3 and M13pET28a clone 2 was performed at 37°C, with and without IPTG induction. Following expression without IPTG induction, a prominent protein band at approximately 69.8 kDa was observed after staining with Coomassie blue R-250 (Fig. 2.13, panel A) and identified using the mouse anti-6xHis IgG HRPO and 4-chloro-1-naphthol·H_2O_2 detection system (Fig. 2.13, panel B) in the insoluble pellet fraction. Two additional prominent, lower molecular weight proteins at 41.4 and 37.3 kDa were present for each clone but were not detected in the western blot by the mouse anti-6xHis IgG HRPO conjugate (Fig. 2.13, panel B). Due to the fact that the lower molecular weight proteins from the recombinant TcMCA5 expression were not detected by the mouse anti-6xHis IgG HRPO conjugate this led to the conclusion that they might be the result of autocatalytic cleavage of the recombinant TcMCA5. The M7pET28 clone 2 was selected for large scale expression.

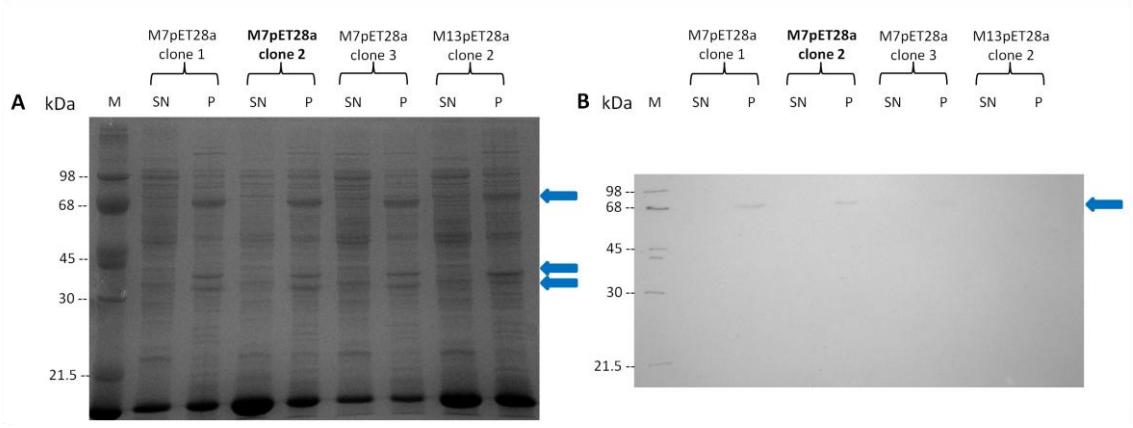

Figure 2.13: Analysis of recombinantly expressed TcMCA5 in pET-28a. Samples of the soluble and insoluble fractions of the expression of recombinant TcMCA5, from the M7pET28a clones 1 to 3 and M13pET28a clone 2, were electrophoresed on two 12.5% reducing SDS-PAGE gels with one **(A)** stained with Coomassie blue R-250 and the other **(B)** transferred onto nitrocellulose, blocked with 5% (w/v) milk-TBS and incubated with mouse anti-6xHis IgG [1:1 000 in 0.5% (w/v) BSA-PBS]. Goat anti-mouse IgG HRPO conjugate [1:12 000 in 0.5% (w/v) BSA-PBS] and 4-chloro-1-naphthol·H_2O_2 were used as the detection system.

Proteins expressed within inclusion bodies can vary from being completely misfolded to mostly native protein (Bowden *et al.*, 1991; Ventura and Villaverde, 2006). The presence of the two lower molecular weight proteins/cleavage products, lends to the fact that the expressed recombinant TcMCA5 may be in a partially native state and has retained some degree of activity. Moss and co-workers (2007) demonstrated that purified recombinant TbMCA2, which shares a 34% sequence similarity with TcMCA5, displayed 93, 91 and 70% inhibition by 100 µM leupeptin, antipain and N-tosyl-L-lysyl chloromethylketone (TLCK) respectively. When recombinant TcMCA5 expression by IPTG induction was carried out at 37°C in the presence of 100 µM leupeptin, antipain and TLCK, no inhibition of TcMCA5 autocatalytic activity was observed (results not shown).

Recombinant expression at lower temperatures is thought to allow for slower transcription and translation which would result in more time for the recombinant protein to refold into its enzymatically active form, resulting in lower levels of inclusion body formation (Vera *et al.*, 2006; Burgess, 2009). No expression of recombinant TcMCA5 was observed when incubated at 25, 15 or 4°C without IPTG induction (results not shown).

Consequently, expression of insoluble recombinant TcMCA5 was attempted at 37°C and 30°C with IPTG induction at various concentrations, the results of which are shown in Fig. 2.14, panel A and B respectively. Expression of 69.8 kDa recombinant TcMCA5,

as well as the two lower molecular weight proteins/cleavage products at approximately 41.4 and 37.3 kDa, was highest at 1 mM IPTG at 37°C when comparing induction at 1, 0.7, 0.5 and 0.3 mM IPTG at both temperatures. At 30°C (Fig. 2.14, panel B), the expression of recombinant TcMCA5 is significantly less than at 37°C (Fig. 2.14, panel A) with the lower molecular weight proteins/cleavage products still present. After the purification of recombinant TcMCA5, antibodies were raised in chickens and were used to determine if they would recognise the recombinantly expressed TcMCA5 in the 1 mM ITPG expression samples at 37°C in a western blot format (Fig. 2.15). In addition to the 69.8 kDa full length recombinant TcMCA5, the two lower molecular weight proteins/cleavage products at approximately 41.4 and 37.3 kDa were recognised by the chicken anti-TcMCA5 IgY. Due to the high concentration of primary antibody used, 100 µg/ml, additional bands were recognised.

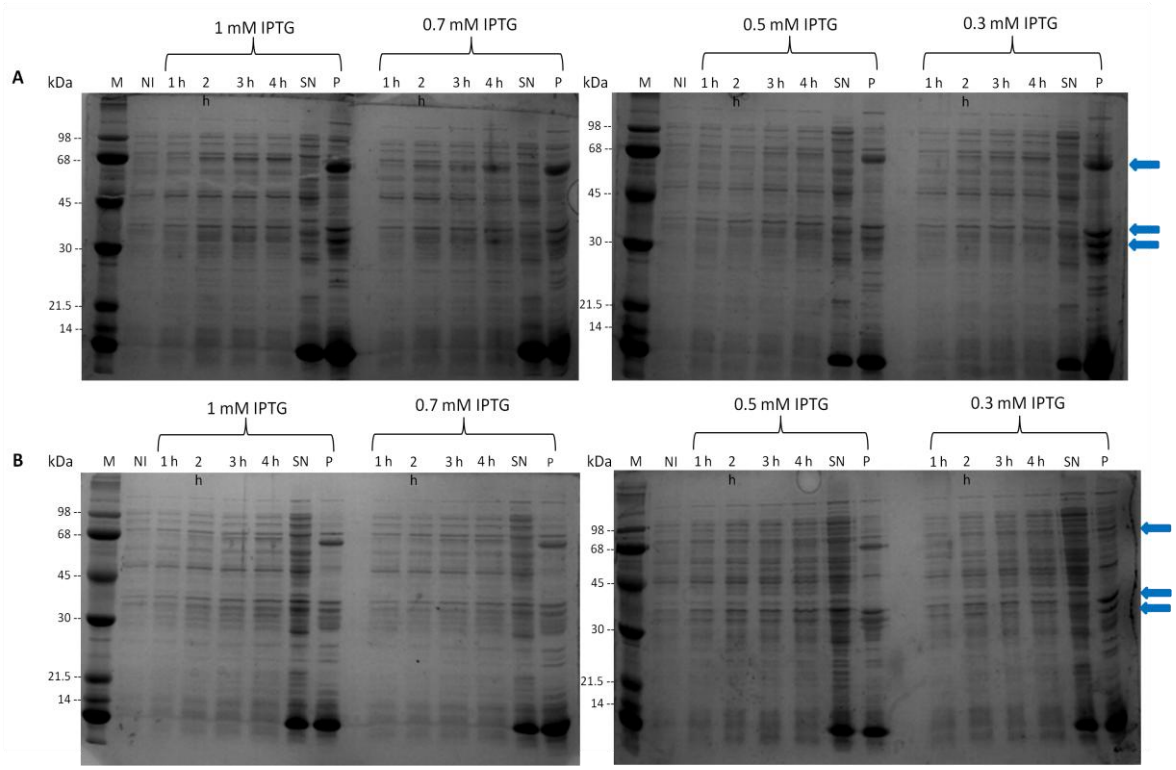

Figure 2.14: Expression by IPTG induction of recombinant TcMCA5 in pET-28a. Six different IPTG concentrations (1, 0.7, 0.5, 0.3, 0.1 and 0 mM) at temperatures **(A)** 37°C and **(B)** 30°C was employed in the optimisation of the expression of recombinant TcMCA5 in the pET-28a expression vector. Samples were electrophoresed on a 12.5% reducing SDS-PAGE gel and stained with Coomassie blue R-250. NI: non-induced control sample.

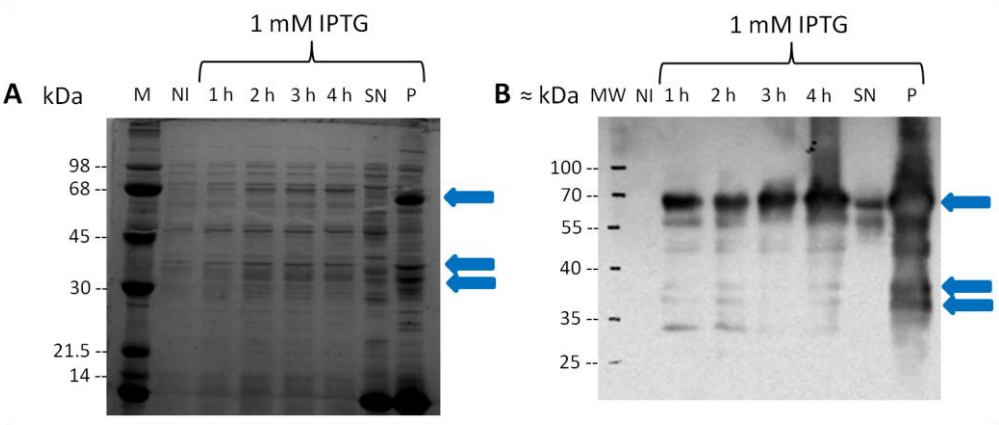

Figure 2.15: Western blot analysis of recombinantly expressed TcMCA5 in pET-28a. Expression samples from the expression of M7pET28a at 37°C, induced at 1 mM IPTG, were electrophoresed on two 12.5% reducing SDS-PAGE gels with one **(A)** stained with Coomassie blue R-250 and the other **(B)** transferred onto nitrocellulose, blocked with 5% (w/v) low fat milk-TBS and incubated with chicken anti-TcMCA5 IgY from chicken 1, week 7 [100 µg/ml in 0.5% (w/v) BSA-PBS]. Rabbit anti-chicken IgY HRPO conjugate [1:15 000 in 0.5% (w/v) BSA-PBS] and Pierce™ ECL western blotting substrate were used as the detection system. MW: PageRuler™ prestained protein marker. NI: non-induced control sample.

2.3.3.2 Solubilisation, refolding and purification of recombinantly expressed TcMCA5

Some degree of native conformation of the recombinant TcMCA5 protein is present within the inclusion bodies as is evident due to the products of autocatalytic cleavage/lower molecular weight proteins (Fig. 2.14 and 2.15). Solubilisation of the inclusion bodies using urea and sarkosyl methods was performed and the recombinantly expressed TcMCA5 was subsequently refolded and purified on a nickel chelate column. Refolding and purification using the urea method is shown in Fig. 2.16, panel A, where the eluted proteins were relatively pure with the two lower molecular weight proteins/cleavage products being eluted in fractions 2 to 5. A small amount of the N-terminal 6xHis tag remained attached to the lower molecular weight proteins/cleavage products as they are only eluted upon the application of the elution buffer after extensive washing of the nickel chelate resin. They were however not detected using the anti-6xHis IgG antibody in Fig. 2.13. The smearing observed in the samples from the wash steps was caused by the high concentrations of urea present in the samples.

Even after extensive washing of the nickel chelate resin after the unbound fraction had been collected, in the refolding and purification using the sarkosyl method, the first two eluted fractions contained large amounts of undesired bacterial host proteins including the two lower molecular weight proteins/cleavage products (Fig. 2.16, panel B). From

fractions 3 to 10, purified TcMCA5 was obtained along with low concentrations of the two lower molecular weight proteins/cleavage products.

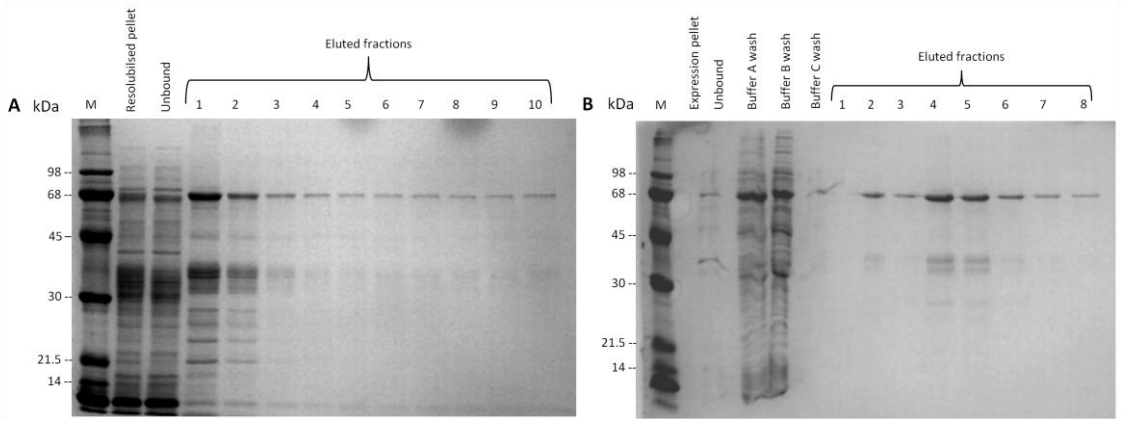

Figure 2.16: Nickel affinity on-column refolding and purification of solubilised recombinant TcMCA5 using sarkosyl and urea methods. Samples from the soluble and insoluble expression fractions as well as from the **(A)** sarkosyl method and the **(B)** urea method of on-column refolding and affinity purification were electrophoresed on a 12.5% reducing SDS-PAGE gel and stained with Coomassie blue R-250.

Comparing panels A and B in Fig. 2.16, solubilisation and on-column refolding using the urea and sarkosyl methods respectively, it is evident that in the presence of urea, recombinant TcMCA5 has less activity as visualised by the low concentration of the two lower molecular weight products/cleavage products. This could be due to the fact that the eluted fractions are still in 8 M urea and need to undergo a stepwise dialysis to remove the denaturant. In addition, there was less contamination by bacterial host proteins when using urea. Solubilisation and on-column refolding using sarkosyl resulted in significant amounts of pure recombinant TcMCA5 protein being eluted along with the lower molecular weight proteins/cleavage products. Bacterial host proteins were only eluted in fractions 1 and 2 and thereafter pure recombinant TcMCA5 was eluted which did not require dialysis prior to use in enzymatic assays.

2.3.4 Enzymatic characterisation of TcMCA5

2.3.4.1 Activity assay

Using the AMC standard curve (Fig. 2.6), the concentration of active recombinant TcMCA5 was determined (Table 2.2). The higher fluorescence values correspond to a higher concentration of active recombinant TcMCA5 which was able to hydrolyse the fluorogenic substrate (Fig. 2.17) with the fractions eluted from the sarkosyl method resulting in much higher fluorescence values when compared with those eluted using

the urea method. As seen in Table 2.2, the concentration of recombinant TcMCA5 in each eluted fraction was higher when using the sarkosyl method compared to that of the urea method. This is consistent with what was observed in Fig. 2.16, panels A and B, that although the intensities of the visualised bands are similar, the concentration of enzymatically active recombinant TcMCA5 is higher using the sarkosyl method. This might be due to the fact that the fractions eluted from the urea method are still in 8 M urea at a pH of 4.3.

Table 2.2: Concentrations of purified recombinant TcMCA5 after on-column refolding using sarkosyl and urea methods based on the hydrolysis of Z-Gly-Gly-Arg-AMC.

	Calculated concentration (nM)	
	Sarkosyl method	Urea method
Fraction 2	-	147.77
Fraction 3	2582.52	174.29
Fraction 4	6100.73	121.74
Fraction 5	5129.48	98.10
Fraction 6	3745.87	85.18
Fraction 7	2128.20	-
Fraction 8	1474.38	-

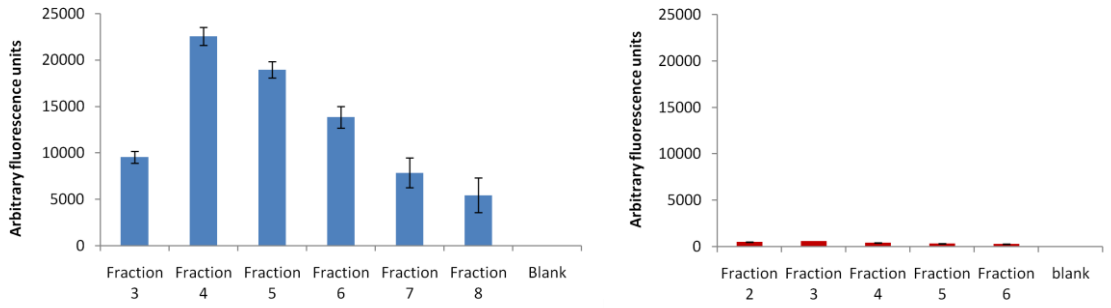

Figure 2.17: Sarkosyl and urea solubilised, refolded and purified recombinant TcMCA5 hydrolysis of Z-Gly-Gly-Arg-AMC. Samples of the on-column refolded and purified TcMCA5 eluted from the **(A)** sarkosyl and **(B)** urea methods were incubated with MCA assay buffer containing the fluorogenic substrate (20 µM) at 37°C for 10 min and the resulting fluorescence was measured at Ex_{360nm} and Em_{406nm}. The fluorescence readings represent the average of triplicate experiments and are plotted as arbitrary fluorescence units.

2.3.4.2 Gelatin containing SDS-PAGE

Enzymatic activity can be visualised using a gelatin containing SDS-PAGE gel, also known as a zymogram (Heussen and Dowdle, 1980). Gelatin is the most commonly used substrate for peptidases and activity is evident as clear bands against the amido black stained background (Manchenko, 2003). Samples from the on-column refolding

and purification fractions, using both the urea and sarkosyl methods, of recombinant TcMCA5 were analysed on a gelatin containing SDS-PAGE gel. A positive control in the form of papain was included in each zymogram. Since TcMCA5 is a cysteine peptidase, a cysteine peptidase activity buffer was used as well as a previously described MCA assay buffer (Moss *et al.*, 2007). No TcMCA5 proteolytic activity was seen in either of the assay buffers; however papain remained active in both buffers (results not shown).

In order to increase the sensitivity of detection, a longer period of incubation in assay buffer was performed (Lantz and Ciborowski, 1994). This, however, made no difference as there was still no evidence of proteolytic activity for TcMCA5, and in addition a high level of diffusion was observed for the papain control (Fig. 2.18).

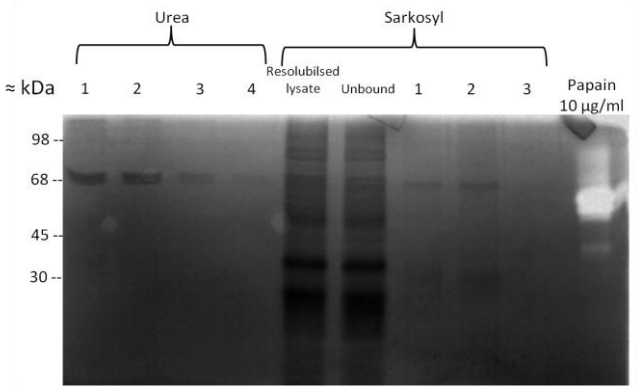

Figure 2.18: Gelatin-containing 12.5% non-reducing SDS-PAGE gel to demonstrate proteolytic activity of recombinantly expressed, solubilised, refolded and purified TcMCA5 using longer incubation times. Samples from the fractions eluted using the urea and sarkosyl solubilisation and on-column refolding methods were electrophoresed on a 12.5% non-reducing SDS-PAGE gel containing 0.1% (w/v) gelatin. After incubation in MCA buffer at 37°C for 16 h, the gel was stained with amido black. Papain (10 µg/ml) was included as a positive control. Note that kDa values of the molecular weight marker are approximate under non-reducing conditions.

2.3.4.3 Autocatalytic processing of purified recombinant TcMCA5

Moss and co-workers (2007) showed that TbMCA2 was dependent on Ca^{2+} ions for autocatalytic cleavage. Since solubilisation and on-column refolding of recombinant TcMCA5 using urea yielded a lower concentration of lower molecular weight proteins/cleavage products, if Ca^{2+} is required for autocatalytic activity, incubation with Ca^{2+} should result in a higher concentration of the cleavage products. This, however, is not the case for the fractions eluted using the urea method (Fig. 2.19), where no additional cleavage products were visualised. The presence of a high concentration of urea in the fractions obtained from the urea method might be preventing any

measurable enzyme activity. The eluted fractions three and four from the sarkosyl method showed an increase in the number of lower molecular weight proteins/cleavage products (Fig. 2.19) when compared to the fractions shown in Fig. 2.16, panel B.

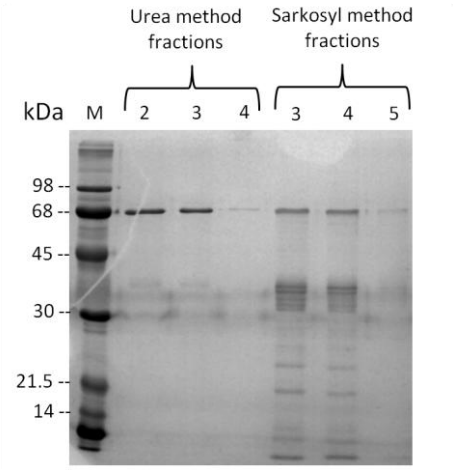

Figure 2.19: Analysis of $CaCl_2$ induced autocatalytic cleavage of recombinant TcMCA5. After on-column refolding and purification by urea and sarkosyl methods, samples of the eluted fractions were incubated with 0.1 M $CaCl_2$ at 37°C for 30 min before being electrophoresed on a 12.5% reducing SDS-PAGE gel and stained with Coomassie blue R-250.

2.3.5 Evaluation of anti-TcMCA5 antibody production by ELISA

The anti-TcMCA5 IgY antibodies isolated from a single egg from each week during the immunisation period were used for an initial ELISA to determine when the production of anti-TcMCA5 IgY antibodies peaked. From Fig. 2.20, it is evident that chicken 1 had produced significant amounts of antibodies from weeks 3 to 5 and from weeks 7 to 11. Chicken 2 had also produced significant amounts of antibodies from weeks 4 to 8, with antibody production dropping substantially at week 9 with production picking up slightly until and including week 11.

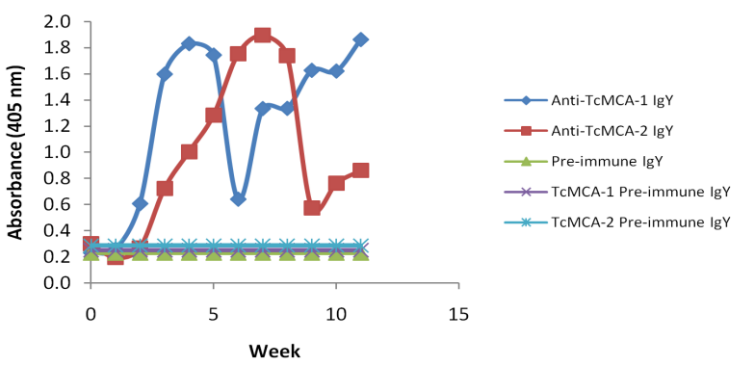

Figure 2.20: ELISA of anti-TcMCA5 IgY antibodies isolated from the egg yolks of immunised chickens. ELISA plates were coated with TcMCA5 (1 µg/ml in PBS, pH 7.4), blocked with 0.5% (w/v) BSA-PBS, 0.1% (v/v) Tween-20 and incubated with anti-TcMCA5 IgY from chickens 1 and 2, weeks 1 to 11 (100 µg/ml). Rabbit anti-chicken IgY HRPO secondary antibody (1:15 000) and ABTS·H_2O_2 were used as the detection system. The absorbance readings at 405 nm represent the average of duplicate experiments after 15 min development.

A checkerboard ELISA was performed to obtain the optimal coating and anti-TcMCA5 IgY antibody concentrations. A no coat control was included for each concentration to allow for the determination of corrected absorbance values and to account for any background interference which may have occurred. From Fig. 2.21, it can be seen that at a TcMCA5 coating concentration of 2.5 µg/ml in PBS and 2.5 µg/ml anti-TcMCA5 IgY from chicken 2, week 7, the highest corrected absorbance value at 405 nm was obtained.

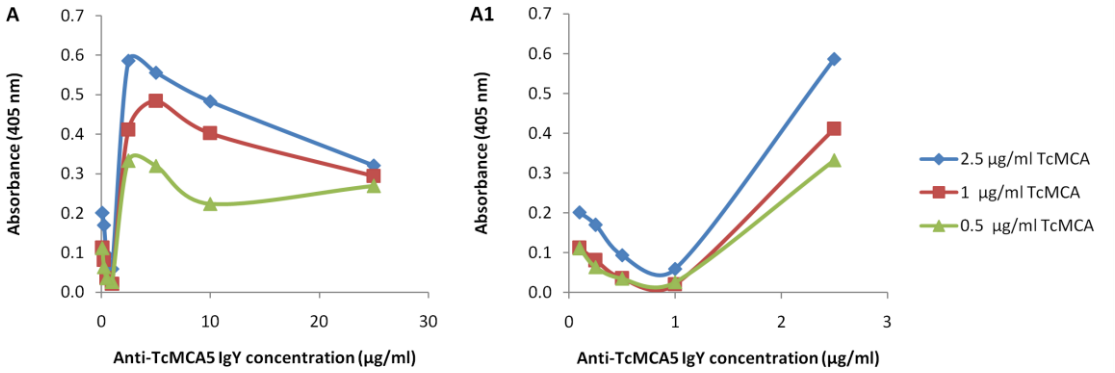

Figure 2.21: Checkerboard ELISA of TcMCA5 coating and anti-TcMCA5 IgY antibody concentrations. ELISA plates were coated with TcMCA5 (2.5, 1 and 0.5 µg/ml in PBS, pH 7.4), blocked with 0.5% (w/v) BSA-PBS, 0.1% (v/v) Tween-20 and incubated with anti-TcMCA5 IgY from chicken 2, week 7 (25, 10, 5, 2.5, 1, 0.5, 0.25 and 0.1 µg/). Rabbit anti-chicken IgY HRPO secondary antibody (1:15 000) and ABTS·H_2O_2 were used as the detection system. The absorbance readings at 405 nm represent the average of duplicate experiments after 45 min development. Panel A1 is the expanded view of the 0.1 to 1 µg/ml anti-TcMCA5 IgY concentrations.

2.3.6 Western blot of cultured *Trypanosoma congolense* (strain IL 3000) procyclic parasite lysate with anti-TcMCA5 IgY antibodies

A western blot was performed using *T. congolense* (strain IL 3000) PCF parasite lysates in order to determine whether or not the anti-TcMCA5 IgY antibodies recognised the native TcMCA5 antigen in the procyclic life stage of the parasite (Fig. 2.22). The anti-TcMCA5 IgY antibodies identified two protein bands at approximately 70 and 40 kDa which correspond favourably to the recombinantly expressed TcMCA5 and its cleavage products, 69.8, 41.4 and 37.3 kDa. An additional band at approximately 26 kDa was detected in panel B.

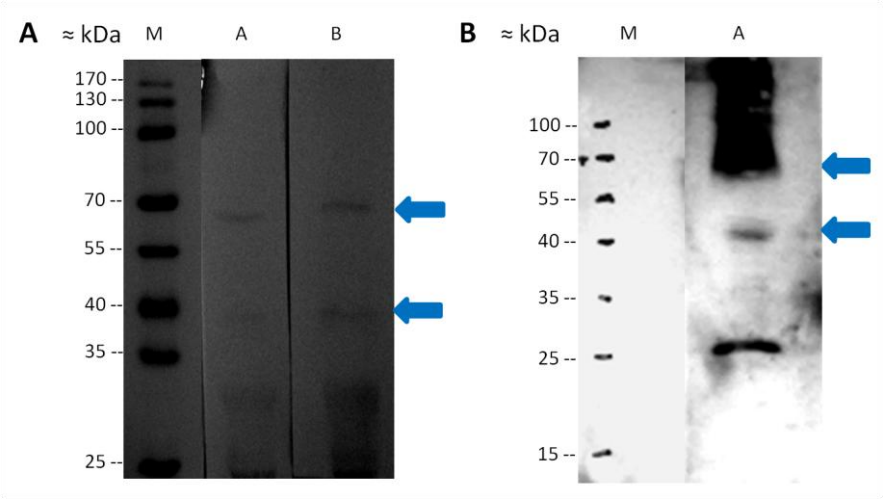

Figure 2.22: Western blot of procyclic *Trypanosoma congolense* parasite lysate to determine the ability of anti-TcMCA5 IgY antibodies to recognise the native TcMCA5 antigen within the parasite. Parasite lysate was electrophoresed on a 12.5% reducing SDS-PAGE gel and blotted onto a nitrocellulose membrane and blocked with 5% (w/v) low fat milk powder-TBS. The blots were incubated with (A) anti-TcMCA5 IgY from chicken 1, week 7 and (B) anti-TcMCA5 IgY from chicken 1, week 8 (100 µg/ml) followed by rabbit anti-chicken IgY HRPO (1:15 000). The bands were developed with **(A)** 4-chloro-1-naphthol·H_2O_2 substrate and **(B)** Pierce™ ECL western blotting substrate. M: PageRuler™ prestained protein marker.

2.3.6.1 Three dimensional structure prediction of TcMCA5

To date, no three dimensional structure of an MCA5 enzyme has been solved. Only six metacaspase structures have been solved to date, two YCA1 enzymes, from *S. cervisiae,* and four TbMCA2 enzymes, from *T. b. brucei*, the details of which are given in Table 2.3.

Table 2.3: The Protein Databank details of the three dimensional structures of metacaspases which have been solved.

PDB identifier	Protein	Ligand	Resolution (Å)
4AF8	TbMCA2	NaCl	1.4
4AFP	TbMCA2	Samarium $^{3+}$	2.1
4AFR	TbMCA2 (C213A mutant)	-	1.6
4AFV	TbMCA2	$CaCl_2$	1.5
4F6O	YCA1	1,1-diphenylethanol	1.68
4F6P	YCA1 (C276A mutant)	1,1-diphenylethanol	1.62

To predict the structure of TcMCA5, its protein sequence, together with the 3D structure TbMCA2 template from the Protein Database (4AF8), was entered into the EsyPred 3D prediction software (Lambert *et al.*, 2002; Gasteiger *et al.*, 2005). TcMCA5 shares only 34% sequence identity with TbMCA2 due to the fact that TcMCA5 possesses a Pro rich, C-terminal domain, the gene of which has a high GC content and is predicted to form general loops. The predicted structure does, however, possess the caspase-haemogloublin fold (Fig. 2.23) which is characteristic of the family C14 of the CD clan of cysteine proteases and is shared by the eukaryotic caspases (Taylor-Brown and Hurd, 2013).

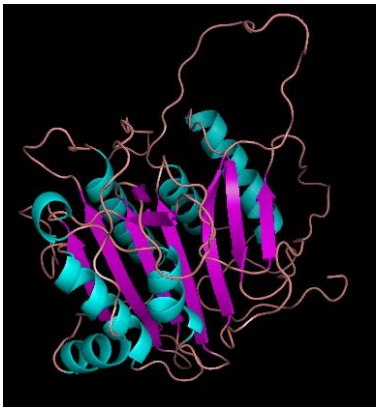

Figure 2.23: Three dimensional structure of TcMCA5 as predicted by EsyPred 3D. By using 4AF8, Chain A from TbMCA2, as the template, the tertiary structure of TcMCA5 was predicted.

2.4 Discussion

New targets for chemotherapies and diagnostics need to be identified due to the process of antigenic variation displayed by trypanosomal parasites which negate any progress towards a vaccine (Barry and McCulloch, 2001). Numerous protozoan proteases have been identified as virulence factors and are thus targets for such studies (Mottram *et al.*, 2004). In 2000, the metacaspases were discovered and are part of the C14 family of cysteine proteases, in which eukaryotic caspases are found

(Uren *et al.*, 2000). Many studies into the metacaspases' possible role in PCD (Bozhkov *et al.*, 2010; Coll *et al.*, 2010) and cell cycle progression in *T. b. brucei* and *L. major* (Helms *et al.*, 2006; Ambit *et al.*, 2008) have been made. There are still many questions as to their mechanism of action and their importance to the parasite's survival. Due to the fact that TbMCA2, -3 and -5 have been identified as viable drug targets (Mottram *et al.*, 2003) and taking into account the central role that LmMCA5 (Lee *et al.*, 2007) and TcrMCA5 (Kosec *et al.*, 2006b) play in the epimastigote form when undergoing PCD, it follows that the metacaspase 5 gene from *T. congolense* (strain IL 3000) might also be a viable target for drug and diagnostics development.

Since the development of recombinant DNA technology whereby large amounts of proteins can be recombinantly expressed, various virulence factors have been characterised enzymatically and their 3D structures solved. With this data, their functionality within the parasite can be determined and their interactions with possible drug candidates investigated. In 2003, over 90% of all the three-dimensional structures submitted to the protein data bank were expressed in bacterial systems using the pET expression system which utilises the T7 promoter (Sørensen and Mortensen, 2005). Due to the simplicity, rapid growth to high densities, low cost and genetics which have been well studied along with the variety of plasmid vectors that can be used, *E. coli* is the host strain of choice for recombinant cloning and expression (Sørensen and Mortensen, 2005). Since TcMCA5 is a protease, the *E. coli* BL21 (DE3) strain was used for cloning and expression as it is deficient in both Lon and OmpT proteases that could degrade the recombinantly expressed protein. In addition, expression within the BL21 (DE3) strain is regulated by the T7 promoter and thus allows for the use of pET expression vectors which require a T7 promoter for expression (Sørensen and Mortensen, 2005).

The cloning and recombinant expression of TcMCA5 in *E. coli* BL21 (DE3) cells under the control of the T7 promoter found in the pET-28a expression vector was successful. Due to its Pro, Glu and Tyr rich C-terminal extension, TcMCA5 was recombinantly expressed within insoluble inclusion bodies. However, analysis of expression showed the presence of two lower molecular weight proteins/cleavage products at 41.4 and 37.3 kDa along with the full length TcMCA5 which was 10 kDa larger than the expected size of 59 kDa. The rabbit anti-6xHis IgG antibodies only identified the full length TcMCA5 whilst the chicken anti-TcMCA5 IgY antibodies identified the full length TcMCA5 as well as the lower molecular weight proteins/cleavage products.

Caspases are synthesised as inactive zymogens and require autocatalytic processing at specific Asp residues to form the active multi-subunit protease (Mottram *et al.*, 2003). The predicted Asp residues needed for autocatalytic cleavage are not present in metacaspases when their sequences were aligned to those of the caspases, thus it cannot be said with certainty that metacaspases are processed in a similar way (Mottram *et al.*, 2003).

González and co-workers (2007) performed a western blot using rabbit anti-LmMCA antibodies against stationary phase *L. major* promastigotes and LmMCA in yeast, which were devoid of YCA1. Three bands were obtained; one which corresponded to the full length LmMCA and the two lower bands were thought to be the result of LmMCA autocatalytic cleavage (Gonzáles *et al.*, 2007). Despite the fact that inhibitors, leupeptin, antipain and TLCK, were added to the culture medium, the lower molecular weight proteins/cleavage products were still produced. This lends credence to the suggestion that the recombinant TcMCA5 was still in a relatively native form within the inclusion bodies and would be responsible for autocatalytic processing. Autocatalytic processing has been reported for LmMCA (Gonzáles *et al.*, 2007), however TbMCA2 and -3 as well as TcrMCA3 and -5 do not require autocatalytic processing to be proteolytically active (Kosec *et al.*, 2006b; Moss *et al.*, 2007).

Leibly and co-workers (2012) hypothesised that a number of expressed 'insoluble' proteins are not present in the inclusion bodies but rather as protein aggregates. They suggested that by the adjusting of the pH, ionic strength and additives present, the composition of cell lysis buffer might be the key to allow the protein to be soluble (Leibly *et al.*, 2012). However, by the PROSO II prediction, and taking into account the primary amino acid sequence, TcMCA5 is definitely insoluble (Smialowski *et al.*, 2006). Since TcrMCA3 and -5 share a 48 and 62% identity with TcMCA5 respectively, it is not surprising that during recombinant expression, TcrMCA3 and -5 were expressed within insoluble inclusion bodies (Kosec *et al.*, 2006b).

The expression of soluble recombinant proteins has been found to be aided by the use of fusion tags such as maltose-binding protein (MBP) and GST (Esposito and Chatterjee, 2006), co-expression with molecular chaperones (Schileker *et al.*, 2002), the addition of various stabilizing small molecule additives (Leibly *et al.*, 2012) and a decrease in expression temperature (Burgess, 2009). Despite numerous attempts, the *TcMCA5* insert was only successfully ligated into the pET-28a and pET-32a vectors. A range of temperatures from 37°C to 4°C were tested in an attempt to recombinantly express TcMCA5 as a soluble protein without success below 30°C.

The recombinantly expressed TcMCA5 was successfully solubilised and refolded using chaotropic (urea) and non-chaotropic (sarkosyl) methods during IMAC purification. Recombinant TcrMCA3 and -5 were solubilised using a chaotropic method (urea) as per Middleberg (2002) and were successfully refolded using IMAC purification (Kosec *et al.*, 2006b).

The sarkosyl method of solubilisation and refolding was adapted from Schlager and co-workers (2012). They developed a method whereby inclusion bodies were solubilised by SDS, the excess of which was precipitated using cloud point extraction by cooling, and was removed from the solubilised protein by centrifugation. Cloud point extraction is a common technique used in the purification of membrane proteins (Arnold and Linke, 2007). The remaining wash and elution buffers contained a low concentration of sarkosyl, 0.1% (w/v), to maintain the protein's solubility during the refolding procedure using IMAC. The use of the sarkosyl method of solubilisation, refolding and purification of the recombinant TcMCA5 resulted in the highest yield of pure and enzymatically active protein.

According to Burgess (2009) it has been found that most proteins refold at a pH between 8 and 8.5, but the pH at which protein is refolded is best at one pH unit above or below the protein's pI. The buffers used in the sarkosyl method all had a pH of 7.4 which is within one unit of the pI of TcMCA5 which is 8.2 as suggested by Burgess (2009).

The elution of refolded and purified recombinant TcMCA5 in the urea method was based on a decrease in pH and not an increase in imidazole concentration as used in the sarkosyl method. The lysis buffer (buffer A) and refolding buffer (buffer B) had a pH of 8.0, with the second refolding buffer (buffer C) and the elution buffer (buffer E) having pH values of 6.3 and 4.3, respectively. The pI of TcMCA5 is 8.2 and thus the pH of the second wash buffer, and most importantly the elution buffer, is four pH units below its pI. This fact, in addition with the high concentration of urea present in the elution buffer, can account for the low proteolytic activity of TcMCA5 which was observed.

Machado and co-workers (2013) found that full length recombinant TbMCA2 has a pH optimum of 7.7. Optimal native metacaspase activity, from *L. donovani* anexic amastigotes and promastigotes, was measured in a buffer with a pH of 7.5, whilst activity was measured between pH 6.5 to 9, with little activity below pH 6 and none at a pH of 4 (Lee *et al.*, 2007). This explains the high activity obtained in the fractions from

refolding and purification using the sarkosyl method compared to that resulting from the urea method.

When incubated with calcium, the recombinant TcMCA5 purified using the sarkosyl method, underwent further processing as seen with TbMCA2 (Moss *et al.*, 2007). It has been observed that in the presence of calcium, using far-UV circular dichorism, reversible structural changes occurred in recombinant TbMCA2 (Machado *et al.*, 2013).

Metacaspases are monomeric and possess the caspase/haemoglobinase fold (Aravind and Koonin, 2002). The three dimensional structure of TbMCA2 shows an eight-stranded β-sheet which is comprised of six parallel and two anti-parallel strands which differs from the caspase's six-stranded β-sheet which requires activation by dimerisation. The two extra strands in the metacaspase's β-sheet prevent the dimerisation process and is thus structurally different to caspases, yet another good reason for it being an attractive drug target and diagnostic antigen (Machado *et al.*, 2013).

Antibodies against the recombinant metacaspases from *T. cruzi*, TcrMCA3 and -5 were raised in mice and were successfully used to detect the expression of the proteases in each of the life cycles (Kosec *et al.*, 2006b). An ideal diagnostic antigen should be expressed in the mammalian infective BSF parasite. Due to lack of *T. congolense* BSF parasite stocks, *T. congolense* PCF parasites were used to successfully confirm the presence of native TcMCA5 within the parasite. Since native TcMCA5 was identified within the lysates of PCF *T. congolense* parasites using anti-TcMCA5 IgY antibodies, it can no longer be termed a putative protein as defined in the TriTryp database.

The diagnostic potential of TcMCA5 still needs to be verified by making use of *T. congolense* infected and non-infected serum samples. The diagnostic potential of several previously identified virulence factors from *T. congolense* and *T. vivax* will be tested on the recombinantly expressed and purified antigens.

CHAPTER 3

EXPRESSION, PURIFICATION AND ANTIBODY PRODUCTION OF KNOWN VIRULENCE FACTORS OF *TRYPANOSOMA CONGOLENSE* AND *TRYPANOSOMA VIVAX*

3.1 Introduction

The tsetse transmitted *T. congolense* and *T. vivax* are the causative agents for animal trypanosomiasis in Africa (Authié, 1994). This livestock disease has a direct impact on farmers as well as an indirect impact on the African economy (Févre *et al.*, 2008). The currently available trypanocides have been in use for over 50 years with no new trypanocidal chemotherapeutic compounds being introduced in the last 30 years (Barrett, 2010). These protozoan parasites are able to evade the immune system of the mammalian host by a process of VSG switching which makes the development of an anti-trypanosomal vaccine against the parasite itself improbable (Barry and McCulloch, 2001). In light of this, an anti-disease vaccine strategy has been pursued to control the pathogenesis within the mammalian host by identifying virulence factors, some of which are peptidases, and could be used as vaccines (Antoine-Moussiaux *et al.*, 2009).

Many parasite peptidases have been identified as having either chemotherapeutic or vaccine potential (McKerrow *et al.*, 1999; Selzer *et al.*, 1999). Cysteine peptidases have been implicated in immunoevasion, virulence, cellular invasion as well as enzyme activation (Sajid and McKerrow, 2002). Other peptidase families, notably serine peptidases, have also been implicated in the pathogenesis of AAT (Rosenthal, 1999).

When first described in *T. b. brucei*, the serine peptidase OPB, was shown to degrade neurotensin and atrial natruiretic factor (ANF) (Troeberg *et al.*, 1996). The OPB enzyme is released into the mammalian host's bloodstream and is able to retain its catalytic activity in the bloodstream as it is unaffected by the plasma peptidase inhibitors (Troeberg *et al.*, 1996; Morty *et al.*, 2001). Following parasite lysis, it has been shown that the catalytic activity of OPB is responsible for the disruption of the endocrine system and might be the cause of hypervolemia in early AT infections due to the reduction of plasma ANF levels (Anosa and Isoun, 1976; Soudan *et al.*, 1993). The involvement of OPB in cell invasion in *T. cruzi* infections has been demonstrated by the activation of a Ca^{2+} signalling mechanism (Burleigh *et al.*, 1997). Thus OPB is considered a virulence factor in the disease progression of AT (Morty *et al.*, 2005; Motta *et al.*, 2012).

Cysteine peptidases have been implicated in the pathogenesis associated with *T. cruzi* and *Leishmania* spp. infections (McKerrow *et al.*, 2006) and as such have been identified as anti-disease vaccine candidates and targets for the development of chemotherapies (Caffrey *et al.*, 2000; Lalmanach *et al.*, 2002). Due to their sensitivity to plasma peptidase inhibitors such as α-macroglobulin and cystatins, the *in vivo* activity of the cysteine peptidases in the bloodstream still requires verification (Troeberg *et al.*, 1996). A *T. b. brucei* PGP type I has been shown to be catalytically active *in vivo* within the bloodstream, is insensitive to plasma cysteine peptidase inhibitors and was proposed as a virulence factor (Morty *et al.*, 2006).

Pyroglutamyl peptidase type I functions to hydrolytically remove the L-pGlu residues from bioactive peptides and hormones (Atkinson *et al.*, 2009) and is thought to be involved in the regulation of the endocrine system as well as the metabolism in mammals (Cummins and O'Connor, 1998). The L-pGlu residues, formed by the cyclisation of an N-terminal Gln residue, are found at the end of many bioactive peptides and hormones and function to regulate their specific activities as well as to offer a degree of protection from aminopeptidase degradation (Cummins and O'Connor, 1998; Barrett and Rawlings, 2004; Atkinson *et al.*, 2009). Since TbPGP has been proposed as a virulence factor (Morty *et al.*, 2006), Kosec and co-workers (2006a) have proposed TcrPGP, which has a high sequence identitiy to TbPGP, to be a virulence factor. If found to be expressed in the mammalian infective BSF, TcrPGP might be important to the pathogenesis of Chagas disease (Kosec *et al.*, 2006a) (Fig. 1.14). It has since been demonstrated that TcPGP, is expressed in the mammalian infective *T. congolense* BSF and thus considered as an important virulence factor in AAT (Mucache, 2012).

Numerous parasite cysteine peptidases are synthesised as pro-enzymes containing a prodomain followed by the catalytic domain and in some cases followed by a C-terminal extension (Sajid and McKerrow, 2002). Many cysteine peptidases are unusually immunogenic and as such have potential for use as serodiagnostic tools for various diseases (Sajid and McKerrow, 2002). The C1 family of the CA clan is the most studied family of the cysteine peptidases of which some have been considered as targets for the development of chemotherapeutic drugs (Atkinson *et al.*, 2009) such as cruzain, also known as cruzipain (McKerrow *et al.*, 2006) and *Plasmodium* derived falcipains (Rosenthal, 2004).

It has been demonstrated that the activity of cruzipain, the major CATL lysosomal peptidase found in *T. cruzi*, is implicated in the occurrence of plasma leakage within

post-capillary venules and may play a role in the process of cell invasion by the recruitment of macrophages (Chagas *et al.*, 1997; Cabrera *et al.*, 2009).

Congopain, the major CATL peptidase in *T. congolense* was found to be expressed in the mammalian infective BSF (Authié *et al.*, 1992), was fully characterised and termed an immunodominant antigen by Chagas and co-workers (1997). N'Dama cattle are able to limit parasitaemia of the invading trypanosomes and their induced pathology and were thus termed trypanotolerant (Authié, 1994). It was found that during the course of trypanosomal infections in N'Dama cattle, anti-congopain IgG antibodies were elicited in high concentrations (Authié *et al.*, 1993b). It was hypothesised by Authié and co-workers (1994) that immune responses directed towards congopain were a contributing factor in the mechanisms of trypanotolerance. It has since been shown that anti-congopain IgG antibodies are able to completely inhibit the enzymatic activity of congopain (Authié *et al.*, 2001). Doyle and co-workers (2007) demonstrated that by the inhibition of cruzipain, *T. cruzi* infected immunodeficient mice were able to recover from infection. Upon the deletion of both CATL genes in *L. mexicana*, a significant reduction in virulence was observed accompanied by a change in immune response to a Th1 response from that of a Th2 (Alexander *et al.*, 1998). Congopain has been implicated in immunosupression, the development of anaemia (Authié *et al.*, 2001) and plays a key role in the occurrence of trypanotolerance (Authié *et al.*, 1993a). It has thus been termed a virulence factor in *T. congolense* infections (Authié *et al.*, 2001).

Since congopain has been demonstrated to be immunogenic in cattle (Lalmanach *et al.*, 2002), it follows that rhodesian, the congopain homologue in *T. b. rhodesiense*, has been identified as a possible diagnostic antigen (Manful *et al.*, 2010). By that reasoning, vivapain, the congopain homologue in *T. vivax*, too should be considered as a possible diagnostic antigen. Antibodies against vivapain were raised in chickens and mice, and were able to detect vivapain in parasite lysates, confirming the potential of vivapain as a diagnostic antigen (Vather, 2010).

These virulence factors, present in the mammalian infective BSF, have application in the development of serodiagnostic tests. Due to the toxic nature of the currently used trypanocides along with the non-specific symptoms of AT infection, correct diagnosis and subsequent treatment is vital in the control of the disease (Chappuis *et al.*, 2005a). The widely used CATT is based on the detection of anti-trypanosomal antibodies by immobilised Coomassie blue stained trypanosomes of a defined VAT according to the infecting species (Magnus *et al.*, 1978). The use of the CATT is suited to active case

finding but antibody detection ELISAs are not, due to the requirement of sophisticated equipment and the expertise needed to perform them (Chappuis *et al.*, 2005a). The antibody detection ELISAs do, however, have application in surveillance of AT as well as in the initial phases of the development of lateral-flow tests (Chappuis *et al.*, 2005a).

The indirect and inhibition antibody detection ELISAs are the most widely used formats where IgG antibodies elicited against specific antigens are detected. The inhibition antibody detection ELISA measures the decrease in binding of the experimentally produced antibodies (anti-antigen antibodies) to the immobilised antigen due to the presence of antibodies in the infected test sera (Fig. 4.1). Infected sera should contain antibodies against the various immunodominant antigens whilst non-infected sera should not. The antibodies present in the infected sera, specific for the coated antigen, will bind to the antigen and as a result the anti-antigen antibodies will not be able to bind. Subsequently, the HRPO conjugated antibody will be unable to bind and thus no or a reduced signal will result upon the addition of the chromogenic substrate. Due to the lack of trypanosomal antibodies in non-infected sera, the anti-antigen antibodies will be able to bind to the immobilised antigen followed by binding of the HRPO conjugated detection antibody resulting in an increase of absorbance upon the addition of the chromogenic substrate. The indirect antibody detection ELISA detects the presence or absence of anti-antigen antibodies in the sera with the use of a species specific HRPO conjugated detection antibody.

Previously identified virulence factors, oligopeptidase B from *T. congolense* and *T. vivax* (TcOPB and TvOPB), pyroglutamyl peptidase from *T. congolense* (TcPGP), cathepsin L-like peptidases (CATL), full length congopain ($TcCATL_{FL}$), and the catalytic domains of congopain (TcCATL) from *T. congolense* and vivapain (TvCATL) from *T. vivax* have been shown to be expressed in the mammalian infective BSF and thus are potential diagnostic antigens. The antigens were recombinantly expressed, purified and antibodies were raised against each in chickens. Antibodies were also raised against an 18-mer N-terminal peptide of TcCATL (Fig.1.13) for the use in the inhibition antibody detection ELISA format. These antibodies along with their respective antigens were used in checkerboard ELISA optimisations prior to further optimisations using *T. congolense* and *T. vivax* infected and non-infected sera for the development of antibody detection ELISAs for the serodiagnosis of AAT.

3.2 Materials and methods

3.2.1 Materials

Molecular biology: As outlined in section 2.2.1. Tetracycline, yeast nitrogen base without amino acids (YNB) and biotin were purchased from Sigma (St. Louis, MO, USA) and Whatman No. 4 filter paper from Whatman International Ltd (UK).

Full length oligopeptidase B from *T. congolense* in pET-28a (TcOPB) (Bizaaré, 2008), full length oligopeptidase B from *T. vivax* in pGEX4T-1 (TvOPB) (Huson, 2006), pyroglutamyl peptidase from *T. congolense* in pGEX4T-1 (TcPGP) (Mucache, 2012), catalytic domain of vivapain from *T. vivax* in pPIC9 (TvCATL) (Vather, 2010), full length congopain from *T. congolense* in pPIC9 ($TcCATL_{FL}$) and the catalytic domain of congopain from *T. congolense* in pPIC9 (TcCATL) (Pillay, 2010) were all sourced from work previously done in our laboratory.

Purification and quantification of recombinant proteins: As outlined in section 2.2.1. Glutathione agarose and blue dextran (200 kDa) were purchased from Sigma (St. Louis, MO, USA), thrombin from Novagen (Darmstadt, Germany) and tertiary-butanol from Merck (Darmstadt, Germany). The ÄKTApurifier® along with the HiPrep™ 16/16 Sephacryl™ S200 HR column and HiPrep™ 16/16 Sephacryl™ S300 HR column were purchased from GE Healthcare (Uppsala, Sweden). The sheep IgG was isolated previously in our laboratory.

Chicken IgY preparation and ELISA: As outlined in section 2.2.1. The 18-mer N-terminal peptide of TcCATL was synthesised by GL Biochem (Shanghai). Sephadex G-10 and G-25 and sodium hydroborocyanide were purchased from Sigma (St. Louis, MO. USA), Aminolink® and SulfoLink® matrix from Pierce (Rockford, IL, USA) and ABTS from Roche (Mannheim, Germany).

Antibodies: As per section 2.2.1.

3.2.2 Calibration of HiPrep™ 16/16 Sephacryl™ S200 HR and S300 HR Molecular exclusion resins using the ÄKTApurifier®

Molecular exclusion chromatography (MEC) was performed using a HiPrep™ 16/16 Sephacryl™ S200 HR resin and a HiPrep™ 16/16 Sephacryl™ S300 HR resin (16 x 600 mm) with the ÄKTApurifier®. The S200 HR resin has a fractionation range of 5 to 250 kDa, whilst the S300 HR resin has a fractionation range of 1 to 150 kDa. The resins were equilibrated with 60 ml ultra pure H_2O (UPH_2O) at 1 ml/min and thereafter,

with 180 ml MEC buffer (50 mM NaH_2PO_4, 300 mM NaCl, pH 8.0) at 1 ml/min. The resin was subsequently calibrated with a calibration solution [5 mg each of blue dextran (200 kDa), sheep IgG (130 kDa), bovine serum albumin (BSA, 68 kDa), ovalbumin (45 kDa) and myoglobin (14 kDa) in MEC buffer (2 ml)]. The resin was eluted at 0.08 kPa with a flow rate of 0.5 ml/min, with 1 ml fractions collected and the absorbance being recorded at 280 nm. The resins were regenerated with 60 ml of a NaOH solution (0.2 M) and re-equilibrated with 180 ml MEC buffer. The Fischer plots were constructed for the protein calibration solution whereby the log of the respective molecular weights were related to their respective elution volumes for the S300 (Fig. 3.1) and the S200 (Fig. 3.2) HR molecular exclusion resins. The elution volume (V_e) or retention volume of blue dextran was taken as the void volume (V_0) of the column.

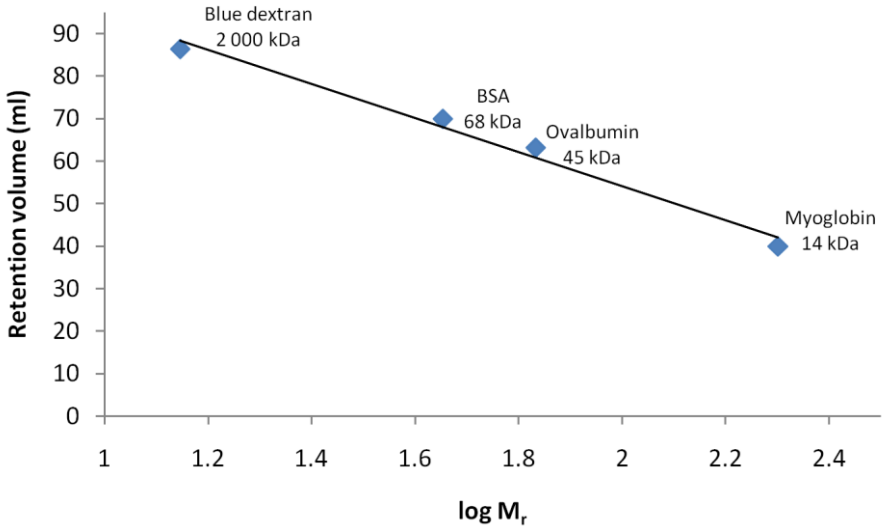

Figure 3.1: Calibration curve of a HiPrep™ 16/16 Sephacryl™ S300 HR molecular exclusion resin. A HiPrep™ 16/16 Sephacryl™ S300 HR resin (16 x 600 mm, flow rate of 0.5 min/min, 0.08MPa) was calibrated with a calibration solution in MEC buffer (50 mM NaH_2PO_4, 300 mM NaCl, pH 8.0). Fractions were monitored by recording the absorbance at 280 nm and the resulting relative mobility of the component protein plotted against the log of the respective molecular weights. The equation of the trendline is given by y = - 40.03x + 134.2, with a correlation coefficient of 0.984.

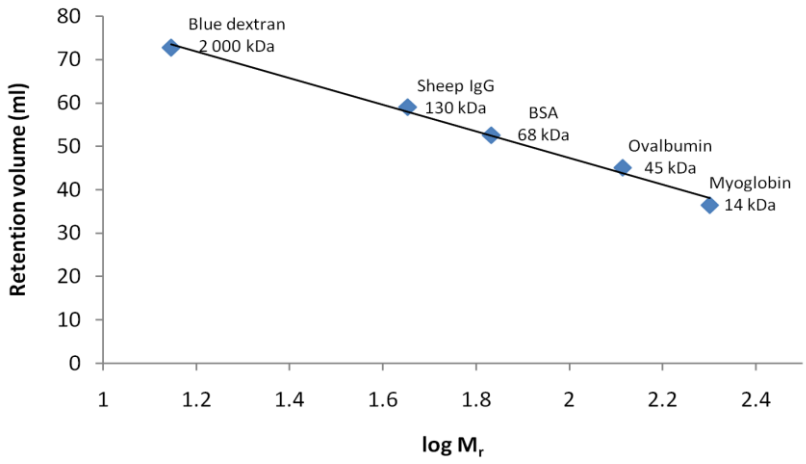

Figure 3.2: Calibration curve of a HiPrep™ 16/16 Sephacryl™ S200 HR molecular exclusion resin. A HiPrep™ 16/16 Sephacryl™ S200 HR resin (16 x 600 mm, flow rate of 0.5 min/min, 0.08 MPa), was calibrated with a calibration solution in MEC buffer (50 mM NaH_2PO_4, 300 mM NaCl, pH 8.0). Fractions were monitored by recording the absorbance at 280 nm and the resulting relative mobility of the component protein plotted against the log of the respective molecular weights. The equation of the trendline is given by y = - 30.71x + 108.7, with a correlation coefficient of 0.991.

3.2.3 Recombinant expression and purification of full length oligopeptidase B from *T. congolense,* (TcOPB)

TcOPB has been previously cloned into the pET28-a bacterial expression vector and transformed into BL21 (DE3) *E. coli* cells by Lorelle Bizaaré (2008). One litre of 2 x YT liquid medium [1.6% (w/v) tryptone, 1% (w/v) yeast extract, 0.5% (w/v) NaCl containing 34 µg/ml kanamycin] was inoculated with a single recombinant pET-28a BL21 (DE3) colony. After incubation 37°C for 16 h in baffled flasks, the cells were pelleted by centrifugation (4 000 *g*, 10 min, 4°C). The pellet was resuspended in 1% (v/v) Triton X-100-PBS (20 ml), lysozyme added (1 mg/ml final concentration) and incubated at 37°C for 30 min. The cell suspension was frozen at -70°C for 1 h and subsequently thawed at RT. The cell suspension was sonicated four times for each 30 s respectively and the cellular debris was subsequently pelleted from the soluble protein lysate by centrifugation (5 000 *g*, 10 min, 4°C). The protein lysate was filtered through Whatman No. 1 filter paper and stored at -20°C. Samples of the supernatant and the pellet containing the soluble and insoluble fractions respectively were analysed by a 12.5% reducing SDS-PAGE gel (Laemmli, 1970) and stained with Coomassie blue R-250 (as per section 2.2.6).

His-select® nickel affinity resin (1 ml) was placed in a 10 ml chromatography column, washed with 2 column volumes of dH_2O and equilibrated with 5 column volumes of equilibration buffer (50 mM NaH_2PO_4, 0.5 M NaCl, 10 mM imidazole, pH 6.8).

Expression lysate (9 ml) was incubated with the resin for 4°C for 3 h and mixed using an end-over-end rotator. The unbound proteins were collected and the resin washed with 40 ml equilibration buffer until an absorbance value at 280 nm of 0.02 was reached. The bound proteins were eluted in 1 ml fractions with 15 ml elution buffer (50 mM NaH_2PO_4, 0.3 M NaCl, 50 mM imidazole, pH 8.0). The resin was regenerated with 2 column volumes of dH_2O, 5 column volumes of 6 M guanidine hydrochloride, 3 column volumes of dH_2O, and 3 column volumes of equilibration buffer and stored in 30% (v/v) ethanol at 4°C. Samples of the unbound and the eluted fractions were electrophoresed on a 12.5% reducing SDS-PAGE gel (Laemmli, 1970) and stained with Coomassie blue R-250 (as per section 2.2.7).

The fractions containing the purified TcOPB enzyme were pooled and dialysed against 3 changes of MEC buffer (50 mM NaH_2PO_4, 300 mM NaCl, pH 8.0) at 4°C and was subsequently concentrated against polyethylene glycol (PEG) M_r 20 000.

Molecular exclusion chromatography (MEC) was performed using a HiPrep™ 16/16 Sephacryl™ S300 HR resin (16 x 600 mm) with the ÄKTApurifier®. After equilibration with 180 ml MEC buffer, the protein sample (2 ml) was loaded onto the column. The resin was eluted at 0.08 kPa with a flow rate of 0.5 ml/min, with 1 ml fractions collected and the absorbance recorded at 280 nm. Samples at the corresponding elution volume of TcOPB were analysed by 12.5% reducing SDS-PAGE gel (Laemmli, 1970) and visualised using a silver stain (Blum *et al.*, 1987). The resin was regenerated with 60 ml of a NaOH solution (0.2 M) and re-equilibrated with 180 ml MEC buffer.

The TcOPB containing fractions from the MEC purification were pooled and dialysed against 3 changes of 50 mM phosphate buffer, pH 7.2 at 4°C. The dialysed sample was concentrated using an Amicon® Ultra-15 centrifugal concentrator according to the manufacturer's instructions. The final concentration of TcOPB was determined using the BCA™ protein assay kit as per manufacturer's instructions (as per section 2.2.3).

3.2.4 Recombinant expression and purification of full length oligopeptidase B from *T. vivax,* (TvOPB), and pyroglutamyl peptidase from *T. congolense,* (TcPGP)

Both TcPGP and TvOPB were all previously cloned into pGEX4T-1 bacterial expression vectors and transformed into BL21 (DE3) *E. coli* cells by Laura Huson (2006) and Hérmogénes Mucache (2012) respectively. One hundred ml of 2 x YT liquid medium (containing 50 µg/ml ampicillin) was inoculated with a single recombinant pGEX4T-1 BL21 (DE3) colony and incubated at 37°C for 16 h in baffled flasks. The

overnight culture was diluted 1:100 with 900 ml fresh 2 x YT medium (containing 50 µg/ml ampicillin) and grown at 37°C in baffled flasks with agitation until an OD_{600} of 0.7 was reached. Expression was induced with IPTG (0.1 M) at a final concentration of 0.3 mM, at 37°C for 2 h with agitation. Ampicillin (50 µg/ml, 1 ml) was added at the start of induction as well as 2 h thereafter. The cells were pelleted by centrifugation (2 000 *g*, 10 min, 4°C) and resuspended in 1% (v/v) Triton X-100-PBS (20 ml). Lysozyme was added (1 mg/ml final concentration) and incubated at 37°C for 30 min. The cell suspension was frozen at -70°C for 1 h and subsequently thawed at RT. The cell suspension was sonicated four times for each 30 s respectively and the cellular debris was subsequently pelleted from the soluble protein lysate by centrifugation (5 000 *g*, 10 min, 4°C). The protein lysate was filtered through Whatman No. 1 filter paper and stored at -20°C. Samples of the supernatant and the pellet containing the soluble and insoluble fractions respectively were analysed by 12.5% reducing SDS-PAGE (Laemmli, 1970) and stained with Coomassie blue R-250 (as per section 2.2.6).

Glutathione agarose resin (1 ml) was placed in a 10 ml chromatography column, washed and equilibrated with 1% (v/v) Triton X-100-PBS (20 ml). Expression lysate (9 ml) was added to the resin and mixed at 4°C for 3 h using an end-over-end rotator. The unbound proteins were collected and the resin washed with 1% (v/v) Triton X-100-PBS (50 ml) until an absorbance value at 280 nm of 0.02 was reached. The resin was subsequently equilibrated with 20 ml thrombin cleavage buffer (20 mM Tris-HCl buffer, 150 mM NaCl, 2.5 mM $CaCl_2$, pH 8.4) and resuspended in 0.8 ml thrombin cleavage buffer to which thrombin was added (2 U). The resin was mixed at 4°C for 16 h using an end-over-end rotator. Cleaved recombinant protein was eluted in 1 ml fractions with 9 ml thrombin cleavage buffer and the bound GST and uncleaved GST fusion protein being eluted with 10 ml reduced glutathione (10 mM in 50 mM Tris-HCl buffer, pH 8.0). The resin was regenerated with 5 column volumes of sodium borate buffer (200 mM in 500 mM NaCl, pH 8.0), 5 column volumes of sodium acetate buffer (100 mM in 500 mM NaCl, pH 4.0), 5 column volumes of dH_2O and stored in 30% (v/v) ethanol at 4°C. Samples of each fraction were analysed by 12.5% reducing SDS-PAGE (Laemmli, 1970) and stained with Coomassie blue R-250 (as per section 2.2.7).

The fractions containing the enzyme were pooled and dialysed against 3 changes of dialysis buffer (50 mM phosphate buffer, pH 7.2) at 4°C and subsequently concentrated

against PEG 20 000. Protein concentration was determined using the BCA™ protein assay kit (as per section 2.2.3).

3.2.5 Recombinant expression and purification of the catalytic domain of vivapain from *T. vivax,* (TvCATL), full length congopain, ($TcCATL_{FL}$), and the catalytic domain of congopain, (TcCATL), from *T. congolense*

Pichia pastoris is a methylotropic yeast which has been utilised for high levels of expression of recombinant proteins which is regulated by the alcohol oxidase promoter (AOX, EC 1.1.3.13) (Cregg and Madden, 1988; Cereghino *et al.*, 2002). TvCATL (catalytic domain of vivapain), $TcCATL_{FL}$ (full length congopain) and TcCATL (catalytic domain of congopain) have all be previously cloned into pPIC 9 yeast expression vectors and transformed into GS115 yeast cells by Perina Vather (2010), and Davita Pillay (2010) respectively. These constructs were expressed and purified in the same manner unless otherwise specified.

Glycerol stocks of TvCATL, $TcCATL_{FL}$ and TcCATL were streaked onto individual yeast extract peptone dextrose plates (YPD) [1% (w/v) yeast extract, 2% (w/v) peptone, 2% (w/v) dextrose, 1% (w/v) bacteriological agar containing 10 µg/ml tetracycline] and incubated at 30°C for 3 days. Fifty millilitres of YPD liquid medium [1% (w/v) yeast extract, 2% (w/v) peptone, 2% (w/v) dextrose containing 10 µg/ml tetracycline] was inoculated with a single colony and grown in baffled flasks at 30°C for 2 days with agitation. The YPD culture was added to 450 ml buffered media glycerol yeast (BMGY) [1% (w/v) yeast extract, 2% (w/v) peptone, 100 mM potassium phosphate buffer, pH 6.5, 1.34% (w/v) yeast nitrogen base without amino acids (YNB) containing 10 µg/ml tetracycline and 50 µg/ml ampicillin] and was subsequently grown at 30°C for a further 3 days with agitation. The yeast cells were pelleted by centrifugation (2 000 *g*, 10 min, 4°C) and resuspended in 500 ml buffered minimal media (BMM) [100 mM potassium phosphate buffer, pH 6.5, 1.34% (w/v) YNB, 0.0004% (w/v) biotin, 0.5% (v/v) methanol containing 10 µg/ml tetracycline and 50 µg/ml ampicillin]. The resulting cell suspension was transferred into baffled culture flasks and covered with 3 layers of sterile cheesecloth to facilitate aeration. Expression of each of the recombinant proteins occurred over 7 days at 30°C with agitation and the addition of 0.5% (v/v) methanol every 24 h.

The yeast cells were pelleted (2 000 *g*, 10 min, 4°C) and the supernatants, containing the expressed proteins, collected. Three phase partitioning (TPP), developed by Pike and Dennison (1989), was implemented as an initial concentration step whereby the

recombinantly expressed protein is precipitated using ammonium sulfate and tertiary-butanol. As a result, the tertiary-butanol increases the buoyancy of the precipitated protein which is found above the denser aqueous phase. Briefly, the yeast supernatant (500 ml) was filtered through Whatman No. 4 filter paper to which tertiary-butanol was added to a final concentration of 30% (v/v). Ammonium sulfate was added to a final concentration of 30% (w/v) and stirred until completely dissolved. A final concentration of 40% (w/v) ammonium sulfate was required for TvCATL. The resulting mixture was centrifuged (6 000 *g*, 10 min, 4°C) in a spin out rotor to achieve three separate phases. The upper tertiary-butanol and lower aqueous phases were removed leaving the protein precipitate. The protein precipitate was dissolved in the least volume of dialysis buffer and dialysed against 3 changes of dialysis buffer at 4°C and was subsequently concentrated against PEG 20 000.

Molecular exclusion chromatography (MEC) was performed using a HiPrep™ 16/16 Sephacryl™ S200 HR and S 300 HR resins (16 x 600 mm), where specified, with the ÄKTApurifier®. After equilibration with 180 ml MEC buffer, the protein sample (2 ml) was loaded onto the column. The resin was eluted at 0.08 kPa with a flow rate of 0.5 ml/min, with 1 ml fractions collected and the absorbance recorded at 280 nm. Samples at the corresponding elution volume of the protein loaded, were analysed by 12.5% reducing SDS-PAGE (Laemmli, 1970) and visualised using a silver stain (Blum *et al.*, 1987). The resin was regenerated with a 60 ml NaOH solution (0.2 M) and re-equilibrated with 180 ml MEC buffer.

The protein containing fractions from the MEC purification were pooled and dialysed against 3 changes of dialysis buffer, at 4°C and subsequently concentrated using Amicon® Ultra-15 centrifugal concentrators according to the manufacturer's instructions. Protein concentration was determined using the BCA™ protein assay kit (as per section 2.2.3).

3.2.6 Antibody production and ELISA optimisation

3.2.6.1 Coupling of the TcCATL N-terminal peptide to rabbit albumin via MBS

The TcCATL N-terminal peptide (4 mg) was dissolved in DMSO (150 µl) and reducing buffer [100 mM Tris-HCl buffer, pH 8.0, 10 mM Na_2EDTA, 1% (w/v) SDS (350 µl)] was subsequently added. After the addition of DTT (10 mM, 500 µl), the mixture was incubated at 37°C for 1.5 h. The reduced peptide was separated from DTT using a

Sephadex G-10 column (15 x 110 mm, 0.6 ml/min), previously equilibrated with 50 ml MEC buffer [100 mM sodium phosphate buffer, pH 7.0, 0.02% (w/v) NaN_3]. The column was eluted with 25 ml MEC buffer at a flow rate of 0.6 ml/min with 0.5 ml fractions being collected. A sample of each fraction (10 µl) was tested with 10 µl of Ellman's reagent (10 mg Ellman's reagent [5,5'-Dithio-*bis*-(2-nitrobenzoic acid)] in 2.5 ml Ellman's reagent buffer [100 mM Tris-HCl buffer, pH 8.0, 10 mM Na_2EDTA, 1% (m/v) SDS]) with the first fractions to give a yellow reaction, i.e. the reduced peptide, being subsequently pooled (Kitagawa and Aikawa, 1976).

Rabbit albumin (2.794 mg) was dissolved in PBS (895 µl) to which MBS (102 µl) was subsequently added resulting in a 40:1 rabbit albumin to MBS molar ratio. The resulting solution was stirred at RT for 30 min. The MBS-rabbit albumin solution was loaded onto a Sephadex G-25 resin (15 x 130 mm) previously equilibrated with 50 ml chromatography buffer (100 mM NaH_2PO_4, pH 7.0). The resin was eluted at a flow rate of 10 ml/min and 1 ml fractions were collected. Elution was monitored by measuring the absorbance at 280 nm, with the activated rabbit albumin carrier being eluted in the first peak. The reduced peptide and activated rabbit albumin carrier fractions were combined and stirred at RT for 3 h. The solution was divided into four equal aliquots and stored at -20°C until immunisation.

3.2.6.2 Preparation of immunogen for the immunisation of chickens and IgY isolation from the egg yolk

As outlined in section 2.2.9.1, chickens were used to raise antibodies against the purified recombinant proteins, TcOPB, TvOPB, TcPGP, TvCATL, $TcCATL_{FL}$ and TcCATL. In addition to the recombinant proteins, the rabbit albumin coupled TcCATL N-terminal peptide was also used to raise antibodies. Three chickens for each of the recombinant proteins and two chickens for the TcCATL N-terminal peptide were immunised intramuscularly on either side of the breast bone. Each of the recombinant proteins (50 µg/ml, 1.5 ml) and the conjugated TcCATL N-terminal peptide (1.1 ml) were added to an equal volume of Freund's adjuvant and triturated to form a stable oil-in-water emulsion prior to immunisation.

3.2.6.3 ELISA evaluation of antibody production

The protocol was as outlined in section 2.2.9.2. Two buffers were used as the antigen coating diluent; PBS (100 mM Na_2HPO_4, 2 mM KH_2PO_4, 2.7 mM KCl and 137 mM NaCl, pH 7.4) and carbonate coating buffer (CCB) (50 mM carbonate buffer, pH 9.6).

3.2.7 Affinity purification of isolated IgY antibodies

3.2.7.1 Coupling of TcCATL N-terminal peptide to SulfoLink®

The TcCATL N-terminal peptide (5 mg) was dissolved in DMSO (100 µl) and 400 µl SulfoLink coupling buffer (50 mM Tris-HCl buffer, 5 mM Na_2EDTA, pH 8.5) was added. After the addition of DTT (10 mM, 500 µl), the mixture was incubated at 37°C for 1.5 h. The reduced peptide was separated from DTT using a Sephadex G-10 column (15 x 110 mm), previously equilibrated with 50 ml MEC buffer (as per section 3.2.6.1). The column was eluted with 25 ml MEC buffer at a flow rate of 0.6 ml/min and 0.5 ml fractions collected. A sample of each fraction (10 µl) was tested with 10 µl Ellman's reagent [10 mg Ellman's reagent in 2.5 ml Ellman's reagent buffer [100 mM Tris-HCl buffer, pH 8.0, 10 mM Na_2EDTA, 1% (w/v) SDS)] with the first fractions to give a yellow reaction, i.e. reduced peptide, being pooled.

SulfoLink® resin (1 ml) was placed in a 10 ml chromatography column and equilibrated with 6 column volumes of general buffer to which the reduced peptide was added. The resin was mixed for 15 min at RT using an end-over-end rotator. The resin was washed with 16 column volumes of wash buffer (1 M NaCl) followed by 2 column volumes of IgY buffer and stored at 4°C until use.

3.2.7.2 Coupling of $TcCATL_{FL}$ to AminoLink®

Purified $TcCATL_{FL}$ was coupled to AminoLink® coupling gel for the affinity purification of antibodies produced against the recombinant protein. AminoLink® coupling gel (1 ml) was placed in a 10 ml chromatography column and equilibrated with 6 column volumes of Aminolink coupling buffer [100 mM NaH_2PO_4, 0.05% (w/v) NaN_3, pH 7.4]. Purified $TcCATL_{FL}$ (5 mg/ml, 1 ml) was diluted in coupling buffer (3 ml) and, along with 5 M $NaCNBH_3$ in 1 M NaOH (50 µl), was added to the resin. The resin was mixed for 2 h at RT using an end-over-end rotator and allowed to settle for 16 h at 4°C. The unbound fraction was collected, the column was washed with 4 ml coupling buffer and subsequently with 4 ml quenching buffer (1 M Tris-HCl buffer, pH 7.4). To the resin, 2 ml quenching buffer and 5 M $NaCNBH_3$ in 1 M NaOH (50 µl) was added and mixed for 2 h at RT using an end over end rotator. The resin was subsequently washed with 25 ml wash buffer, until the absorbance at 280 nm reached baseline, followed by 6 ml IgY buffer and stored at 4°C until use.

The isolated IgY antibodies, from section 3.2.6.2, were pooled and filtered through Whatman No. 1 filter paper. The affinity columns were equilibrated with 5 column

volumes of wash buffer [100 mM NaH_2PO_4, 0.05% (w/v) NaN_3, pH 6.5] and each pool cycled through the column for 16 h at RT at a flow rate of 0.6 ml/min. The unbound IgY was collected and the resin was subsequently washed with 10 column volumes of wash buffer until an absorbance value at 280 nm of 0.02 was obtained. The bound IgY, specific to the antigen in question, was eluted with elution buffer [100 mM glycine-HCl, 0.02% (w/v) NaN_3, pH 2.8] and 900 µl fractions collected into microcentrifuge tubes containing 100 µl neutralisation buffer [1 M NaH_2PO_4, 0.02% (w/v) NaN_3, pH 8.5] and each was immediately mixed by inversion. Elution of the specific antibodies was monitored spectrophotometrically at 280 nm using 900 µl of elution buffer and 100 µl neutralisation buffer as the blank. The affinity purified IgY-containing fractions were pooled, with 10% (w/v) NaN_3 being subsequently added to a final concentration of 0.1% (w/v) before storing at 4°C. The affinity columns were regenerated using 12 column volumes of wash buffer and stored at 4°C until use.

3.2.8 Western blot of recombinantly purified proteins with their respective IgY antibodies raised in chickens

Western blotting was performed as outlined in section 2.2.6 using the Pierce™ ECL western blotting substrate.

3.3 Results

3.3.1 Recombinant expression and purification of full length oligopeptidase B from *T. congolense,* (TcOPB)

The expression of recombinant TcOPB at 80 kDa was achieved as seen in Fig. 3.3, panel A. The expression lysates were subjected to nickel chelate affinity chromatography using the 6xHis fusion tag which was introduced to TcOPB by the pET-28a expression vector (Fig. 3.3, panel B). Purification was successful, however lower molecular weight contaminating proteins were present in the eluted fractions and needed to be removed by molecular exclusion chromatography.

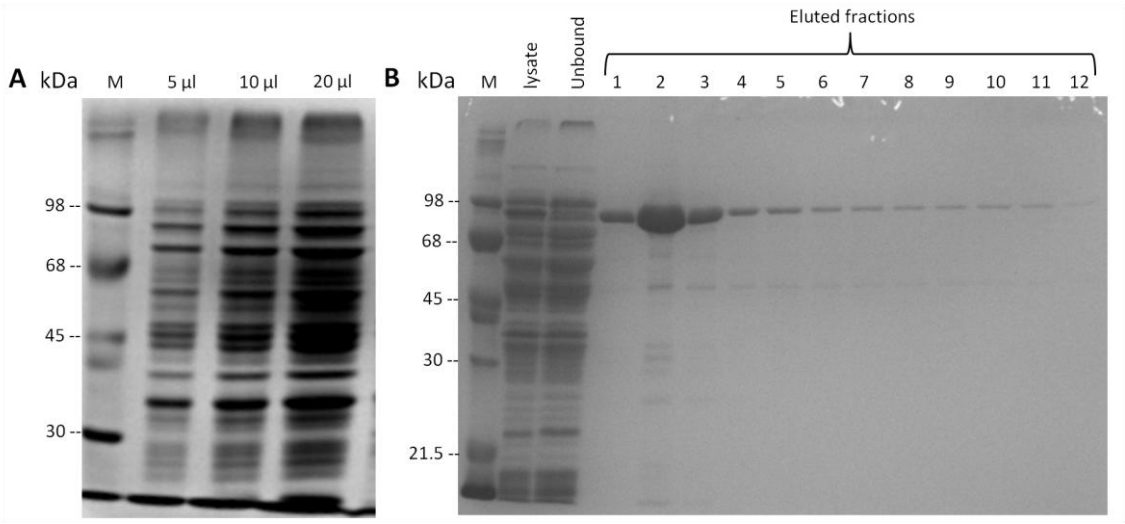

Figure 3.3: Analysis of recombinantly expressed and affinity purified TcOPB. (A) Samples from the expression lysate were analysed by a 10% reducing SDS-PAGE gel. **(B)** Samples from the His-select® nickel affinity purification of TcOPB were analysed by a 12.5% reducing SDS-PAGE gel. Proteins were stained with Coomassie blue R-250.

According to the calibration curve for the S300 HR molecular exclusion resin (Fig. 3.1), TcOPB was predicted to have a retention volume of approximately 59 ml. Three peaks, with retention volumes of 40.48 and 54.23 and 64.28 ml, were the result of the molecular exclusion of TcOPB (Fig. 3.4, panel A), of which the second peak at a retention volume of 54.23 ml contained TcOPB, fractions 47 to 62 (Fig. 3.4, panel B). This compared favourably with the predicted retention volume. Along with TcOPB, the elution of higher and lower molecular weight contaminating proteins were attributed to the peak at 40.48 and 64.28 ml before and after the elution of TcOPB respectively. The higher molecular weight contaminating proteins were not visible after affinity purification (Fig. 3.3, panel B). Fractions 47 to 62 (Fig. 3.4, panel B), containing the purified TcOPB, were pooled, concentrated and used for antibody production.

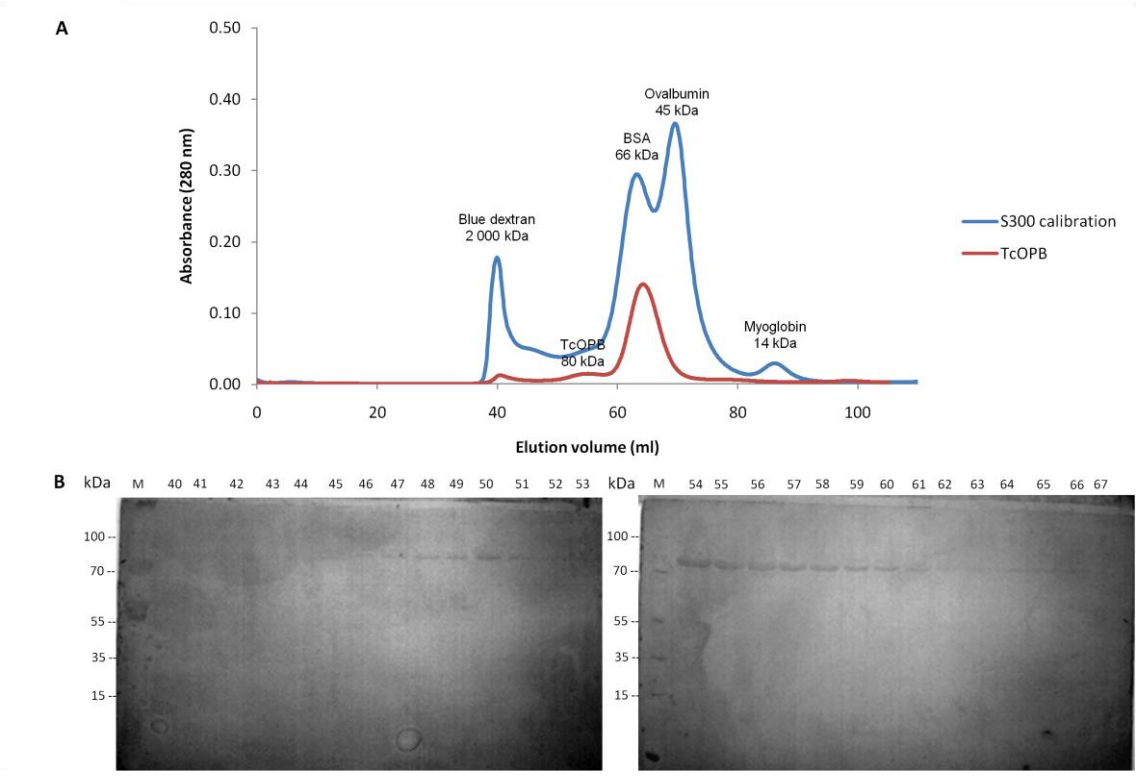

Figure 3.4: Purification of recombinant TcOPB using a HiPrep™ 16/16 Sephacryl™ S300 HR molecular exclusion resin. (A) Elution profile of TcOPB on a HiPrep™ 16/16 Sephacryl™ S300 HR resin (16 x 600 mm, flow rate 0.5 min/min, 0.08 MPa), previously equilibrated with MEC buffer (50 mM NaH_2PO_4, 300 mM NaCl, pH 8.0) and eluted using MEC buffer. Elution of fractions was monitored by recording the absorbance at 280 nm. **(B)** Samples of the eluted fractions were analysed by a 12.5% reducing SDS-PAGE gel. Proteins were visualised using silver staining. M: PageRuler™ Plus Prestained protein marker.

3.3.2 Recombinant expression and purification of full length oligopeptidase B from *T. vivax*, (TvOPB), and pyroglutamyl peptidase from *T. congolense*, (TcPGP)

3.3.2.1 Full length oligopeptidase B from *T. vivax,* (TvOPB)

The expression of recombinant TvOPB with the glutathione S-transferase (GST) fusion tag at 106 kDa was achieved as seen in Fig. 3.5, panel A. The expression lysates were subjected to glutathione agarose based affinity chromatography making use of the GST fusion tag which was introduced to TvOPB by the pGEX4T-1 expression vector. Purification was successful with cleaved TvOPB being eluted at 80 kDa in fractions 1 to 8, along with uncleaved TvOPB fusion protein, cleaved TvOPB and cleaved GST at 105, 80 and 25 kDa, respectively, in the reduced glutathione fractions (Fig. 3.5, panel B). An increased concentration of thrombin and an increased number of fractions collected before reduced glutathione elution commenced would have resulted in a

higher yield of pure cleaved TvOPB. The purified TvOPB in fractions 1 to 8 were pooled, concentrated and used for antibody production.

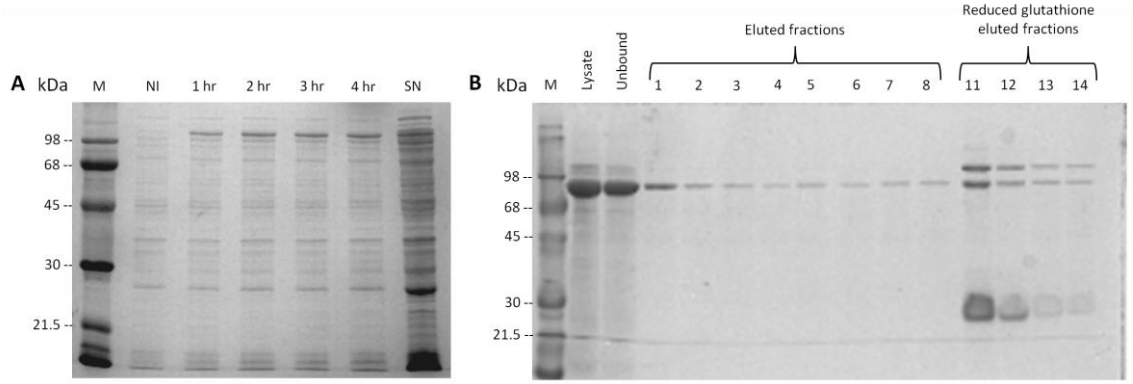

Figure 3.5: Analysis of recombinantly expressed TvOPB by IPTG induction and the subsequent affinity purification. (A) Samples of the expression of TvOPB by IPTG induction were analysed by a 10% reducing SDS-PAGE gel. **(B)** Samples of the glutathione S-transferase affinity chromatography purification of expression supernatants were analysed by a 12.5% reducing SDS-PAGE gel. Proteins were stained with Coomassie blue R-250. Ni: non-induced control sample.

3.3.2.2 Pyroglutamyl peptidase from *T. congolense*, (TcPGP)

The expression of recombinant TcPGP with the GST fusion tag at 51 kDa was achieved as is shown in Fig. 3.6, panel A. The expression lysates were subjected to glutathione agarose based affinity chromatography making use of the GST fusion tag, introduced to the TcPGP protein by the pGEX4T-1 expression vector. Purification was successful, with pure cleaved TcPGP at 28 kDa eluting in fractions 1 to 10, and the uncleaved TcPGP fusion protein and cleaved GST at 53 and 25 kDa, respectively, in the reduced glutathione fractions (Fig. 3.6, panel B). The purified TcPGP in fractions 1 to 10 were pooled, concentrated and used for antibody production.

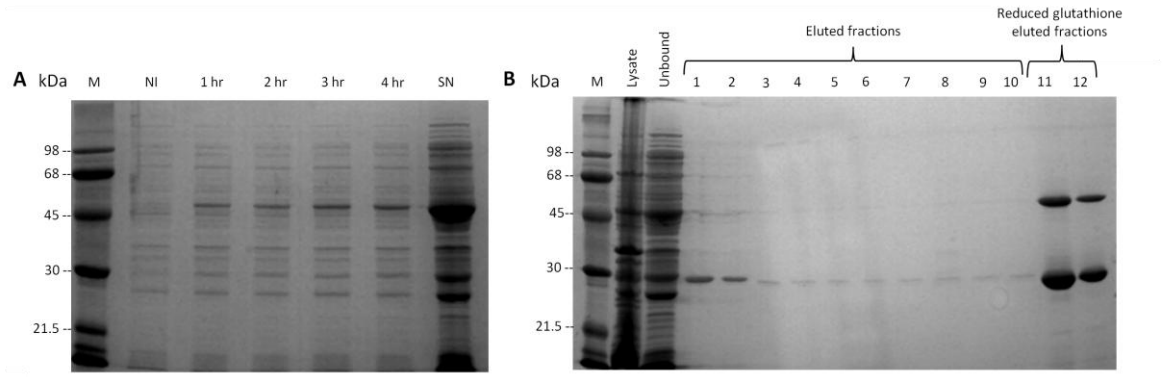

Figure 3.6: Analysis of recombinantly expressed TcPGP by IPTG induction and the subsequent affinity purification. (A) Samples of the expression of TcPGP by IPTG induction were analysed by a 10% reducing SDS-PAGE gel. **(B)** Samples of the glutathione S-transferase affinity chromatography purification of expression supernatants were analysed by a 12.5% reducing SDS-PAGE gel. Proteins were stained with Coomassie blue R-250. Non-induced control sample.

3.3.3 Recombinant expression and purification of the catalytic domain of vivapain from *T. vivax,* (TvCATL), full length congopain, ($TcCATL_{FL}$), and the catalytic domain of congopain, (TcCATL), from *T. congolense*

3.3.3.1 Catalytic domain of vivapain from *T. vivax,* (TvCATL)

The expression of recombinant TvCATL, in its glycosylated and non-glycosylated forms, at 29 and 33 kDa was achieved as seen in Fig. 3.7, panel A. The expression supernatants were subsequently subjected to TPP purification. Purification was successful with two bands at 29 and 33 kDa being visualised (Fig. 3.7, panel B). The protein sample after TPP was diluted in a larger volume of dialysis buffer than what was needed and resulted in a very dilute sample. Due to the high dilution of the protein sample after TPP, any higher or lower molecular weight contaminating proteins were not visible and thus required further purification by MEC (Fig. 3.8).

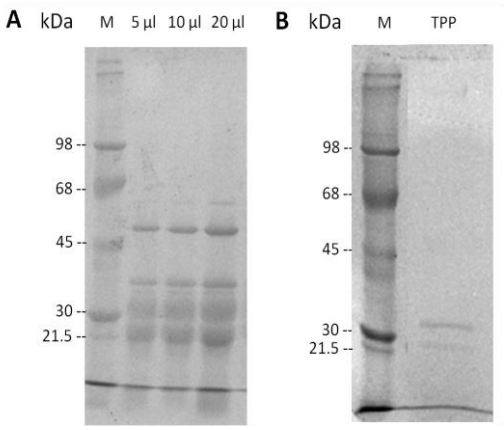

Figure 3.7: Analysis of the expression of recombinant TvCATL in *Pichia pastoris* and purification on a 12.5% reducing SDS-PAGE gel. (A) Expression of TvCATL after 7 days in BMM. **(B)** The expression supernatant was subjected to TPP with 40% (w/v) ammonium sulfate to purify TvCATL. Proteins were stained with Coomassie blue R-250.

TvCATL is glycosylated in the yeast system and thus two peaks following purification by MEC should be expected (Vather, 2010; Jackson, 2011). According to the calibration curve for the S200 HR molecular exclusion resin (Fig. 3.2), TvCATL was predicted to have retention volumes of approximately 65.9 and 63.98 ml for the 29 and 33 kDa TvCATL proteins respectively. Three peaks with retention volumes of 35.82, 59.13 and 72.05 ml were the result of the molecular exclusion of TvCATL (Fig. 3.8, panel A). As shown in Fig. 3.8, panel B, pure glycosylated and de-glycosylated TvCATL were eluted around a retention volume of 72.13 ml in fractions 64 to 85 and required no further purification. The peaks at the retention volumes of 35.82 and 59.13 ml were attributed to higher molecular weight contaminating proteins. Fractions 65 to 85 containing purified glycosylated and non-glycosylated TvCATL were pooled, dialysed and used for antibody production.

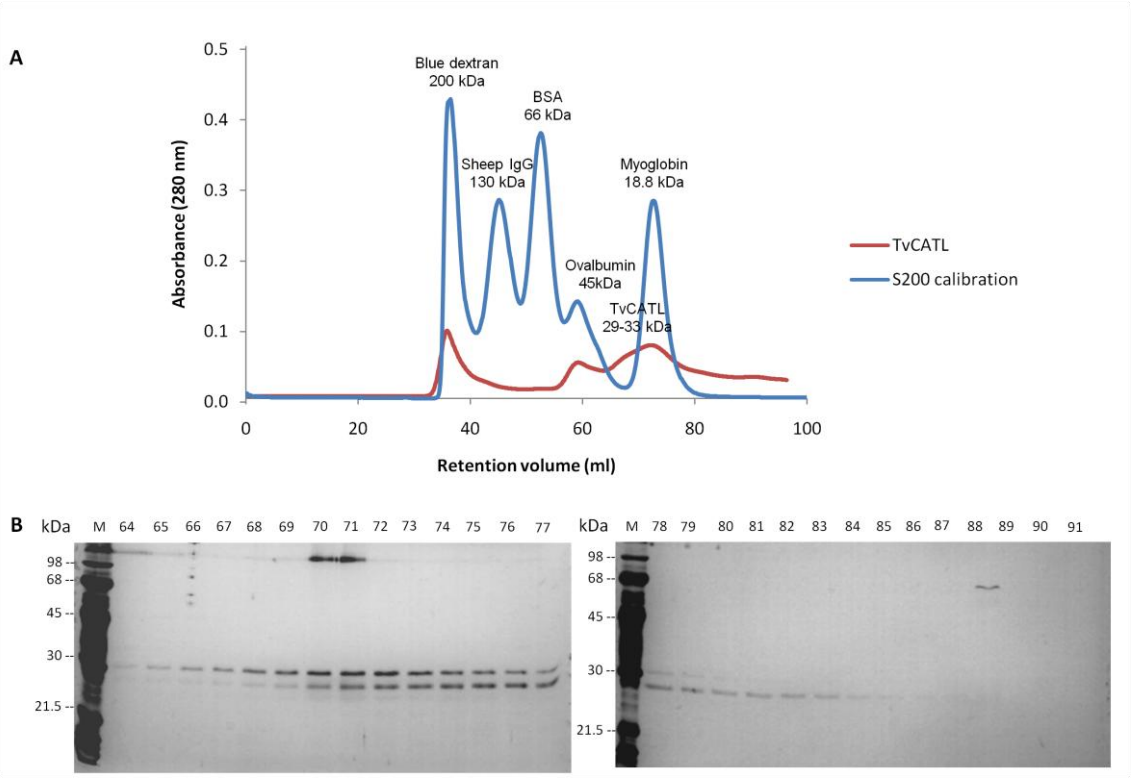

Figure 3.8: Purification of recombinant TvCATL using a HiPrep™ 16/16 Sephacryl™ S200 HR molecular exclusion resin. (A) Elution profile of TvCATL on a HiPrep™ 16/16 Sephacryl™ S200 HR resin (16 x 600 mm, flow rate 0.5 min/min, 0.08MPa), previously equilibrated with MEC buffer (50 mM NaH_2PO_4, 300 mM NaCl, pH 8.0) and eluted using MEC buffer. Fractions were monitored by recording the absorbance at 280 nm. **(B)** Samples of the eluted fractions were analysed by a 12.5% reducing SDS-PAGE gel. Proteins were visualised using silver staining.

3.3.3.2 Full length congopain from *T. congolense*, ($TcCATL_{FL}$)

The expression of recombinant $TcCATL_{FL}$ at 40 kDa was achieved as shown in Fig. 3.9, panel A, and the expression supernatants subjected to TPP purification. Purification was successful, yielding a high concentration of $TcCATL_{FL}$ at 40 kDa along with lower and higher molecular weight contaminating proteins which required further purification by MEC (Fig. 3.9, panel B).

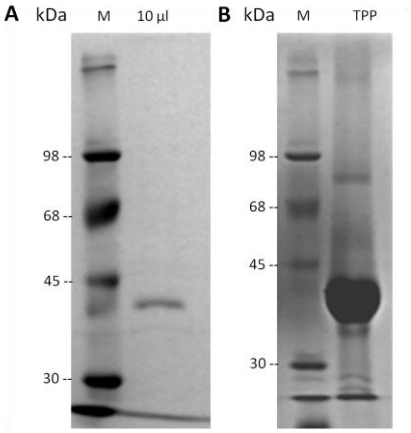

Figure 3.9: Analysis of the expression of recombinant $TcCATL_{FL}$ in *Pichia pastoris* and purification on a 10% reducing SDS-PAGE gel. (A) Expression of $TcCATL_{FL}$ after 7 days in BMM. **(B)** The expression supernatant was subjected to TPP with 30% (w/v) ammonium sulfate to purify $TcCATL_{FL}$. Proteins were stained with Coomassie blue R-250.

According to the calibration curve for the S200 HR molecular exclusion resin (Fig. 3.2), $TcCATL_{FL}$ was predicted to have a retention volume of approximately 61.1 ml. Three peaks with retention volumes of 36.41, 50.50 and 61.90 ml were the result of the MEC of $TcCATL_{FL}$ (Fig. 3.10, panel A). From Fig. 3.10, panel B, $TcCATL_{FL}$ is present in fractions 60 to 96. A protein of a lower molecular weight than $TcCATL_{FL}$ was present in fractions 65 to 72 along with $TcCATL_{FL}$. High levels of $TcCATL_{FL}$ expression was achieved using the *Pichia pastoris* system and thus was present throughout the collected fractions during MEC along with a lower molecular weight protein eluted in fractions 65 to 72. Thus, one peak could not be accurately chosen to represent the retention volume of $TcCATL_{FL}$, however the last peak at 61.90 ml compares favourably to the predicted elution volume of $TcCATL_{FL}$. Fractions 65 to 72 underwent further MEC purification to remove the lower molecular weight protein from $TcCATL_{FL}$. Fractions 58 to 81 and 91 to 97 containing pure $TcCATL_{FL}$ were pooled, dialysed and used for antibody production.

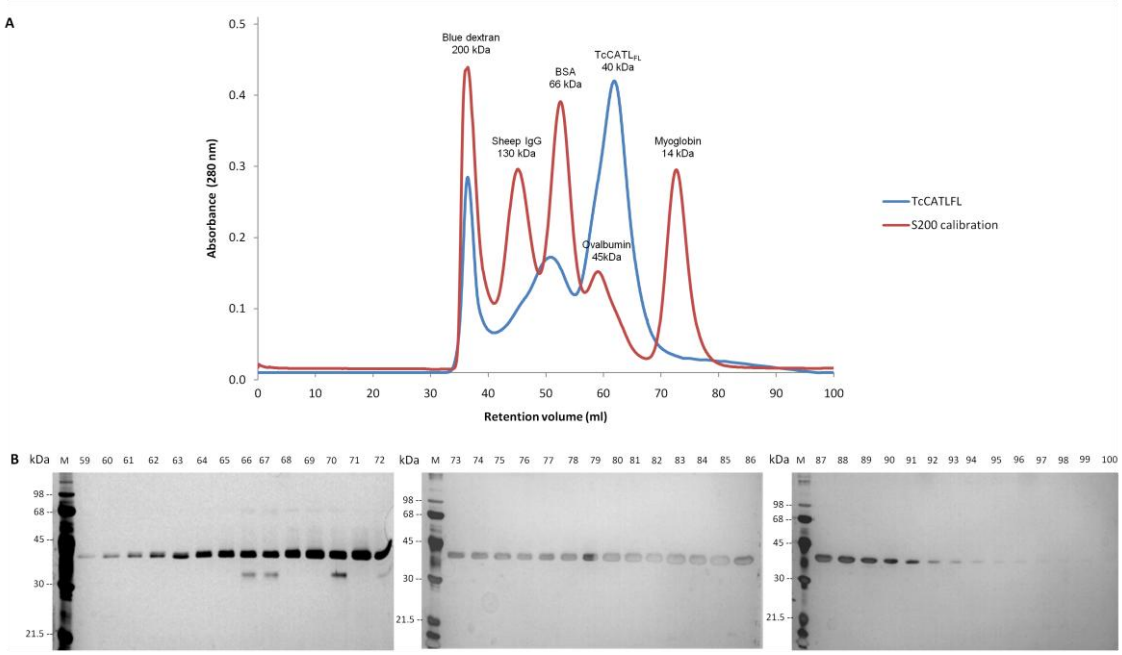

Figure 3.10: Purification of recombinant TcCATL$_{FL}$ using a HiPrep™ 16/16 Sephacryl™ S200 HR molecular exclusion resin. (A) Elution profile of TcCATL$_{FL}$ on a HiPrep™ 16/16 Sephacryl™ S200 HR resin (16 x 600 mm, flow rate 0.5 min/min, 0.08 MPa), previously equilibrated with MEC buffer (50 mM NaH_2PO_4, 300 mM NaCl, pH 8.0) and eluted using MEC buffer. Fractions were monitored by recording the absorbance at 280 nm. **(B)** Samples of the eluted fractions were analysed by a 12.5% reducing SDS-PAGE gel. Proteins were visualised using silver staining.

3.3.3.3 Catalytic domain of congopain from *T. congolense*, (TcCATL)

The expression of recombinant TcCATL at 27 kDa was achieved as seen in Fig. 3.11, panel A, and the expression supernatants subjected to TPP purification. Purification was successful, yielding a high concentration of TcCATL at 27 kDa along with higher molecular weight contaminating proteins which required further purification by MEC (Fig. 3.11, panel B).

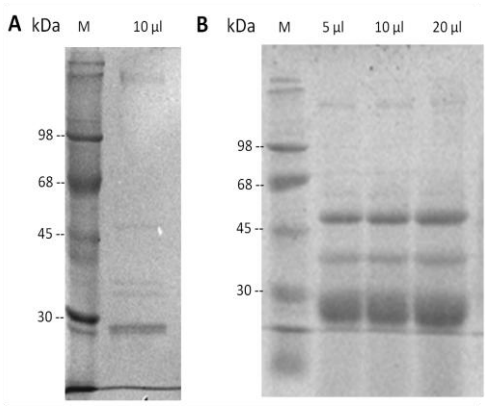

Figure 3.11: Analysis of the expression of recombinant TcCATL in *Pichia pastoris* and purification on a 10% reducing SDS-PAGE gel. (A) Expression of TcCATL after 7 days in BMM. **(B)** The expression supernatant was subjected to TPP with 30% (w/v) ammonium sulfate to purify TcCATL. Proteins were stained with Coomassie blue R-250.

According to the calibration curve for the S200 HR molecular exclusion resin (Fig. 3.2), TcCATL was predicted to have a retention volume of approximately 66.99 ml. Two peaks with retention volumes of 35.99 and 68.61 ml were present following the molecular exclusion of TcCATL (Fig. 3.12, panel A). Pure TcCATL, present in fractions 64 to 76, had a retention volume of 68.61 ml and compared favourably with the predicted value (Fig. 3.12, panel B). The peak with a retention volume of 36.32 ml was attributed to the higher molecular weight contaminating proteins as seen in Fig. 3.11, panel B. Fractions 64 to 76 containing pure TcCATL were pooled, dialysed and used for antibody production.

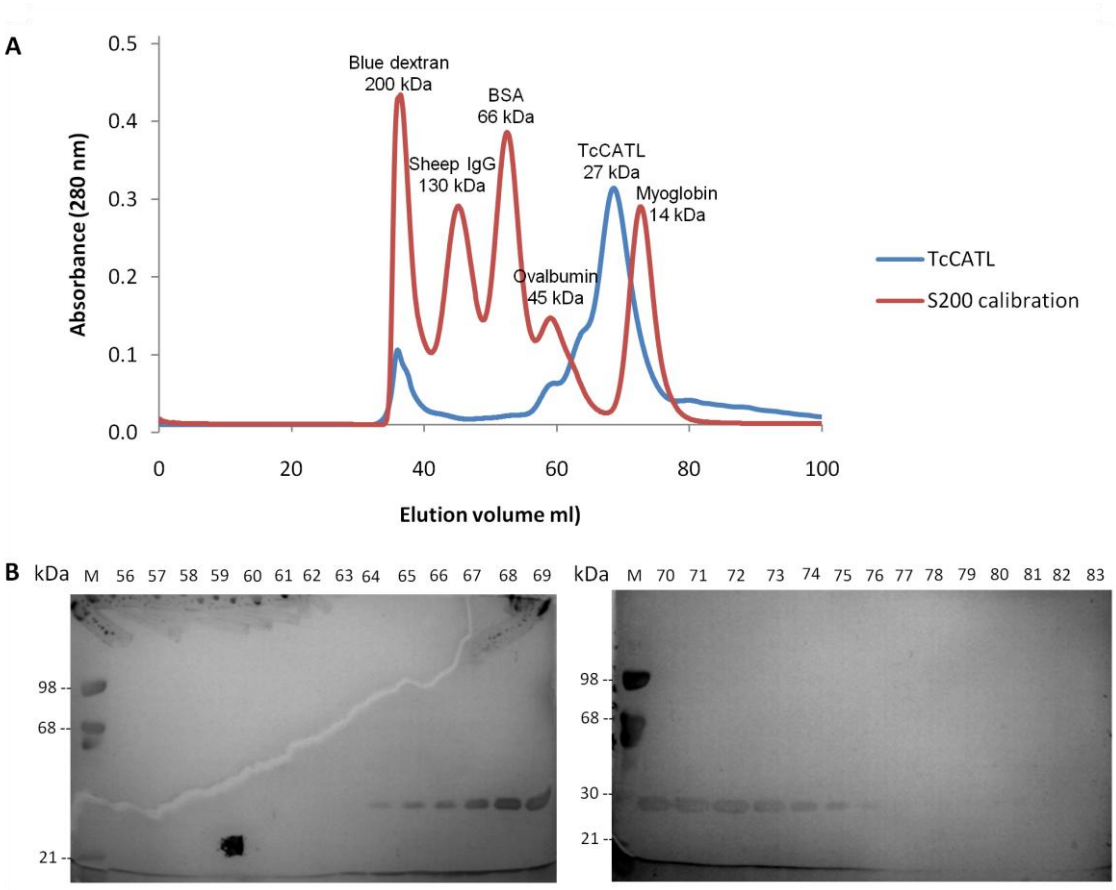

Figure 3.12: Purification of recombinant TcCATL using a HiPrep™ 16/16 Sephacryl™ S200 HR molecular exclusion resin. (A) Elution profile of TcCATL on a HiPrep™ 16/16 Sephacryl™ S200 HR resin (16 x 600 mm, flow rate 0.5 min/min, 0.08 MPa), previously equilibrated with MEC buffer (50 mM NaH_2PO_4, 300 mM NaCl, pH 8.0) and eluted using MEC buffer. Fractions were monitored by recording the absorbance at 280 nm. **(B)** Samples of the eluted fractions were analysed by a 12.5% reducing SDS-PAGE gel. Proteins were visualised using silver staining.

3.3.4 Antibody preparation and ELISA optimisation for TcOPB

The anti-TcOPB IgY antibodies were isolated from a single egg collected from each week during the immunisation period and subsequently used in an initial ELISA to determine when the production of antibodies was highest. From Fig. 3.13, it is evident that chickens 1, 2 and 3 were producing signification amounts of IgY from weeks 4 to 10.

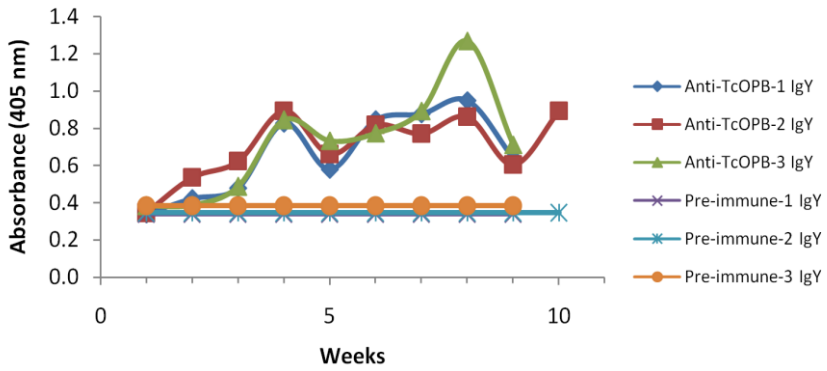

Figure 3.13: ELISA of anti-TcOPB IgY antibodies isolated from the egg yolks of immunised chickens. ELISA plates were coated with TcOPB (1 µg/ml in PBS, pH 7.4), blocked with 0.5% (w/v) BSA-PBS and incubated with anti-TcOPB IgY from chickens 1 to 3, weeks 1 to 10 (100 µg/ml). Rabbit anti-chicken IgY HRPO secondary antibody (1:20 000) and ABTS·H_2O_2 were used as the detection system. The absorbance readings at 405 nm represent the average of duplicate experiments after 15 min development.

A checkerboard ELISA was employed for the optimisation of the TcOPB coating and the anti-TcOPB IgY concentrations as described by Crowther (2000). A no coat control was included for each of the samples to account for any background interference which may have occurred. The anti-TcOPB IgY antibody from chicken 1 at week 7 gave the best mid range absorbance at 405 nm and was used in the checkerboard ELISA. As shown in Fig. 3.14, coating with 0.1 and 0.05 µg/ml TcOPB and using 10 µg/ml anti-TcOPB IgY as the primary antibody, gave the highest corrected absorbance readings at 405 nm. Using these concentrations, the effect of different blocking buffers was investigated.

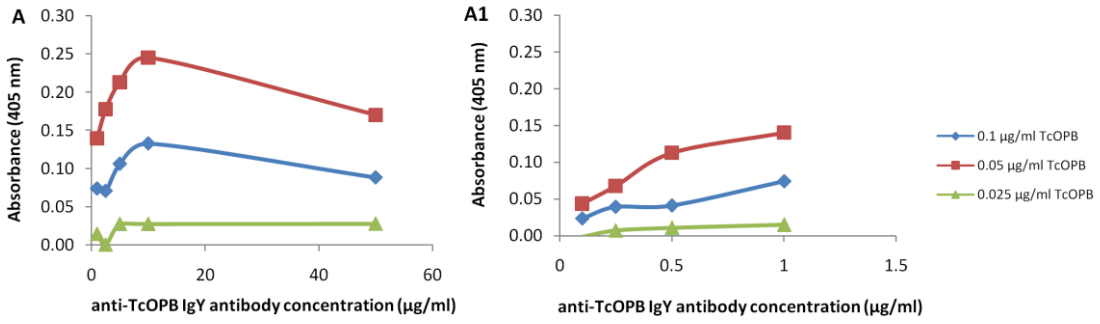

Figure 3.14: Checkerboard ELISA of TcOPB coating and anti-TcOPB IgY antibody concentrations. ELISA plates were coated with TcOPB (0.1, 0.05 and 0.025 µg/ml in PBS, pH 7.4), blocked with 0.5% (w/v) BSA-PBS and incubated with anti-TcOPB IgY from chicken 1, week 7 (50, 10, 5, 2.5, 1, 0.5, 0.25 and 0.1 µg/). Rabbit anti-chicken IgY HRPO secondary antibody (1:20 000) and ABTS·H_2O_2 were used as the detection system. The absorbance readings at 405 nm represent the average of duplicate experiments after 60 min development. Panel A1 is the expanded view of the 0.1 to 1 µg/ml anti-TcOPB IgY concentrations.

A variety of blocking buffers have been reported for ELISA diagnostics, 1% (w/v) casein-PBS (Tran *et al.*, 2009), 0.5% (v/v) mouse serum-PBS (Eisler *et al.*, 1998), 5% (w/v) skim milk powder-PBS, 0.1% (v/v) Tween-20 (OIE, 2013) to name but a few. Thus four different blocking buffers were tested: (A) 0.5% (w/v) BSA-PBS, (B) 0.5% (w/v) BSA-PBS, 0.1% (v/v) Tween-20, (C) 0.2% (w/v) BSA-PBS, 0.05% (v/v) Tween-20 and (D) 1% (v/v) horse serum-PBS. The blocking step is essential to prevent any non-specific binding of the subsequent reagents to the unoccupied hydrophobic sites in the plate well. Detergents and proteins may be used in combination for this purpose as both have their unique advantages and disadvantages (KPL, 2013). A no coat control was included for each of the samples to account for any background interference which may have occurred. From Fig. 3.15, the trends in the corrected absorbance values were similar for panels B and C with low values being obtained in panel D. Using 0.5% (w/v) BSA-PBS, 0.1% (v/v) Tween-20 as the blocking buffer (Fig. 3.15, panel B), higher corrected absorbance values at 405 nm were obtained at 1 µg/ml anti-TcOPB IgY antibody than that obtained when 0.5% (w/v) BSA-PBS was used (Fig 3.15, panel A). Since low concentrations of primary antibody are used for ELISAs, it follows that blocking with 0.5% (w/v) BSA-PBS, 0.1% (v/v) Tween-20 is optimal and was chosen as the standardised blocking reagent amongst the different ELISA antigens.

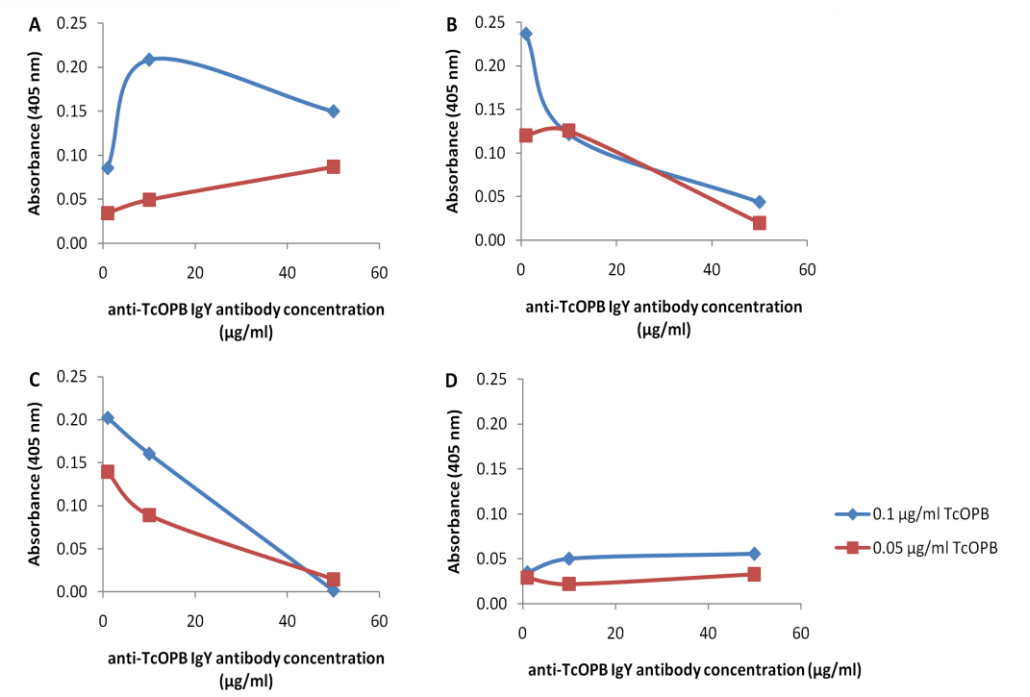

Figure 3.15: Checkerboard ELISA of TcOPB and anti-TcOPB IgY antibody concentrations using different blocking agents. ELISA plates were coated with TcOPB (0.1 and 0.05 µg/ml in PBS, pH 7.4) and blocked with **(A)** 0.5% (w/v) BSA-PBS, **(B)** 0.5% (w/v) BSA-PBS, 0.1% (v/v) Tween-20, **(C)** 0.2% (w/v) BSA-PBS, 0.05% (v/v) Tween-20 and **(D)** 1% (v/v) horse serum-PBS. Anti-TcOPB IgY from chicken 1, week 7 (50, 10 and 1 µg/ml) were subsequently added. Rabbit anti-chicken IgY HRPO secondary antibody (1:10 000) and ABTS·H_2O_2 were used as the detection system. The absorbance readings at 405 nm represent the average of duplicate experiments after 60 min development.

A checkerboard ELISA was repeated using higher TcOPB coating concentrations along with the new blocking buffer, 0.5% (w/v) BSA-PBS, 0.1% (v/v) Tween-20. A no coat control was included for each of the samples to account for any background interference which may have occurred. The results were compared to those shown in Fig. 3.14, at 60 min of development, in which 0.5% (w/v) BSA-PBS was used as the blocking buffer. From Fig. 3.16 below, it was evident that the new blocking buffer resulted in higher corrected absorbance values at 405 nm, when comparing the 0.1 µg/ml TcOPB coating, at an anti-TcOPB IgY antibody concentration of 1 µg/ml, from an absorbance value of 0.07 to > 0.1. It was thus determined that coating with TcOPB at 1 µg/ml in PBS, blocking with 0.5% (w/v) BSA-PBS, 0.1% (v/v) Tween-20 and anti-TcOPB IgY at 1 µg/ml were the optimal conditions for future inhibition and indirect ELISA formats.

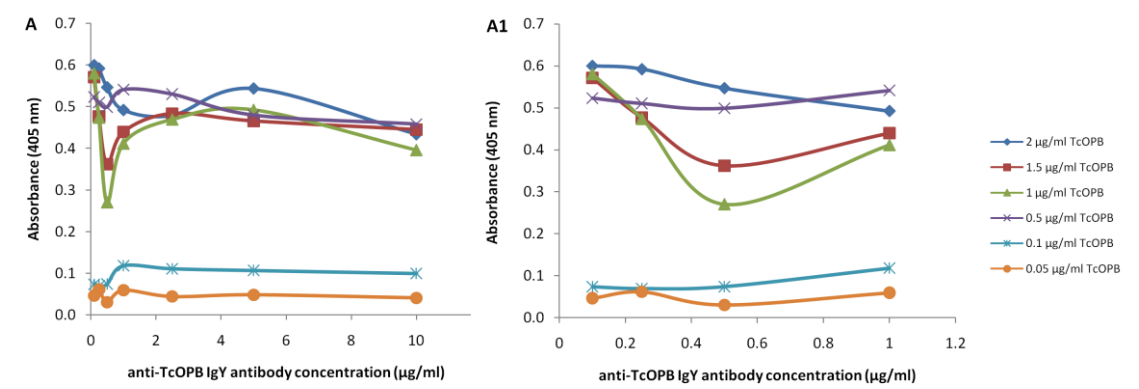

Figure 3.16: Checkerboard ELISA of a range of TcOPB coating and anti-TcOPB IgY antibody concentrations. ELISA plates were coated with TcOPB (2, 1.5, 1, 0.5, 0.1 and 0.05 µg/ml in PBS, pH 7.4), blocked with 0.5% (w/v) BSA-PBS, 0.1% (v/v) Tween-20 and incubated with anti-TcOPB IgY from chicken 1, week 7 (10, 5, 2.5, 1, 0.5, 0.25 and 0.1 µg/ml). Rabbit anti-chicken IgY HRPO secondary antibody (1:15 000) and ABTS·H_2O_2 were used as the detection system. The absorbance readings at 405 nm represent the average of duplicate experiments after 60 min development. Panel A1 is the expanded view of the 0.1 to 1 µg/ml anti-TcOPB IgY concentrations.

3.3.5 Antibody preparation and ELISA optimisation for TvOPB

The anti-TvOPB IgY antibodies were isolated from a single egg collected from each week during the immunisation period and subsequently used in an initial ELISA to determine when the production of antibodies was highest. The pre-immune IgY antibodies were abnormally high, more so from that isolated from chicken 2 (Fig. 3.17). The production of anti-TvOPB IgY antibodies fluctuated between weeks 1 to 11 for all three chickens. Most initial ELISAs take 15 min of development to achieve absorbance values at 405 nm of 1.0 and above due to the high concentration of coating antigen and primary antibody. The results shown in Fig. 3.17 were obtained after 45 min of development and the highest absorbance value at 405 nm was just under 0.7.

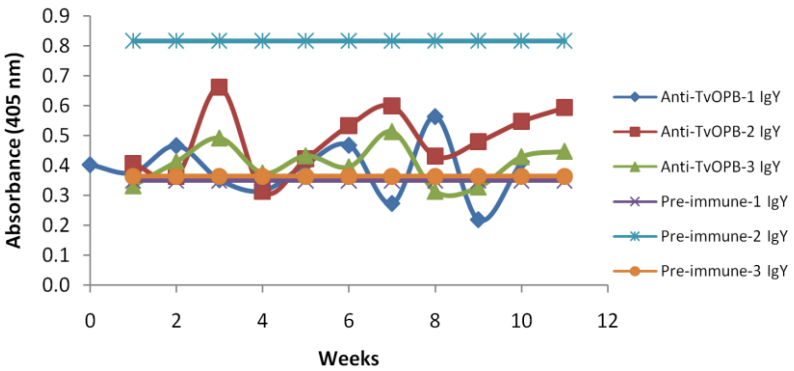

Figure 3.17: ELISA of anti-TvOPB IgY antibodies isolated from the egg yolks of immunised chickens. ELISA plates were coated with TvOPB (1 µg/ml in PBS, pH 7.4), blocked with 0.5% (w/v) BSA-PBS and incubated with anti-TvOPB IgY from chickens 1 to 3, weeks 1 to 11 (100 µg/). Rabbit anti-chicken IgY HRPO secondary antibody (1:20 000) and ABTS·H_2O_2 were used as the detection system. The absorbance readings at 405 nm represent the average of duplicate experiments after 45 min development.

Due to the poor results for the antibody production of anti-TvOPB IgY seen in Fig. 3.17, the ELISA was repeated using a higher TvOPB coating concentration of 5 µg/ml in carbonate coating buffer, pH 9.6 (CCB), instead of PBS. This change in coating conditions resulted in a marked increase in the absorbance values at 405 nm especially for the antibodies produced by chicken 2 and in a shorter development time (Fig. 3.18). It appeared that chicken 1 produced less anti-TvOPB IgY antibodies when compared to chickens 2 and 3, with the absorbance values at 405 nm being less than those obtained from the pre-immune IgY antibodies, which were still abnormally high.

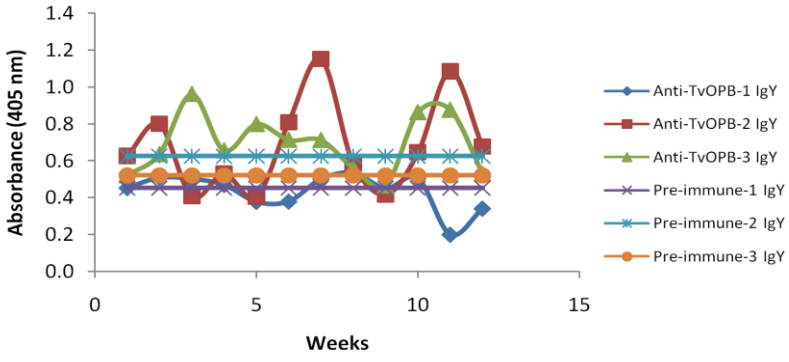

Figure 3.18: ELISA of anti-TvOPB IgY antibodies isolated from the egg yolks of immunised chickens using a different coating diluent. ELISA plates were coated with TvOPB (5 µg/ml in CCB, pH 9.6), blocked with 0.5% (w/v) BSA-PBS and incubated with anti-TvOPB IgY from chickens 1 to 3, weeks 1 to 12 (100 µg/ml). Rabbit anti-chicken IgY HRPO secondary antibody (1:20 000) and ABTS·H_2O_2 were used as the detection system. The absorbance readings at 405 nm represent the average of duplicate experiments after 15 min development.

Further optimisation of the TvOPB coating conditions needed to be performed. Using anti-TvOPB IgY antibodies from chicken 3, weeks 6 and 10, which gave reasonable absorbance values and were mid range between those from chicken 3 and chicken 2, as seen in Fig. 3.18, an optimisation ELISA was performed. From Fig. 3.19, coating at 5 µg/ml TvOPB in CCB, pH 9.6, gave the highest absorbance values at 405 nm after 45 min of development for the anti-TvOPB IgY weeks 6 and 10, but also for its pre-immune IgY. This highlighted the need to obtain a new pre-immune IgY.

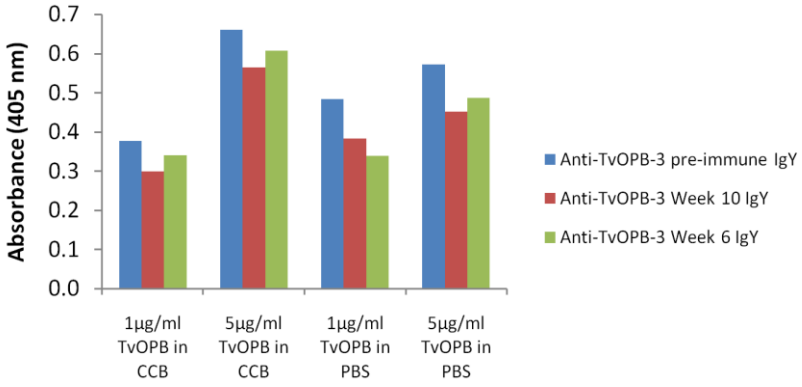

Figure 3.19: Optimisation of ELISA of TvOPB coating concentrations with anti-TvOPB IgY antibodies. ELISA plates were coated with TvOPB (5 and 1 µg/ml in PBS, pH 7.4 and CCB, pH 9.6), blocked with 0.5% (w/v) BSA-PBS and incubated with anti-TvOPB IgY from chicken 3, pre-immune and weeks 6 and 10 (100 µg/ml). Rabbit anti-chicken IgY HRPO secondary antibody (1:20 000) and ABTS·H_2O_2 were used as the detection system. The absorbance readings at 405 nm represent the average of duplicate experiments after 45 min development.

Using the TvOPB coating conditions determined from Fig. 3.19, the concentration of the secondary detection antibody, rabbit anti-chicken IgY HRPO conjugate, was optimised. Anti-TvOPB IgY was isolated from each of the weeks from all three chickens and along with 1:15 000 and 1:20 000 dilutions of the secondary antibody, were used to confirm the trend in antibody production as seen in Fig. 3.17.

With a 1:20 000 dilution of the secondary rabbit anti-chicken IgY HRPO conjugate (Fig. 3.20, panel A), lower absorbance values at 405 nm were obtained when compared to those resulting from the 1:15 000 dilution of the secondary antibody (Fig. 3.20, panel B). Furthermore, the 1:15 000 secondary antibody dilution diminished the intensity of the fluctuations between each week as compared to those seen when a 1:20 000 dilution was used. In addition, when comparing the trend of antibody production for each chicken shown in Fig. 3.20 to those seen in Fig. 3.18, chicken 3 now seemed to have produced the least amount of anti-TvOPB IgY antibodies instead of chicken 1.

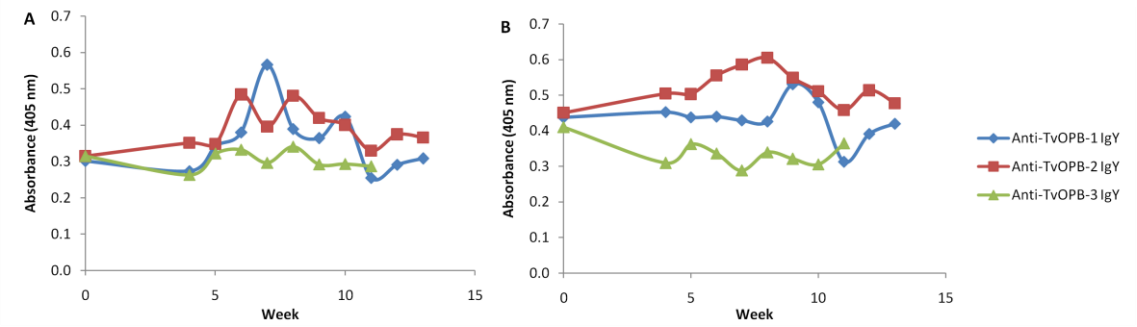

Figure 3.20: Optimisation of secondary antibody in the ELISA of TvOPB against anti-TvOPB IgY antibodies. ELISA plates were coated with TvOPB (5 µg/ml in CCB, pH 9.6), blocked with 0.5% (w/v) BSA-PBS and incubated with anti-TvOPB IgY from chickens 1 to 3, weeks 4 to 14 (100 µg/ml). Rabbit anti-chicken IgY HRPO secondary antibody (1:20 000 and 1:15 000) and ABTS·H_2O_2 were used as the detection system. The absorbance readings at 405 nm represent the average of duplicate experiments after 45 min development. Panel A depicts the 1:15 000 dilution whilst panel B depicts the 1:20 000 dilution.

From the previous optimisation ELISAs, the optimal TvOPB coating concentration, diluent and secondary detection antibody concentration had been determined. Using the anti-TvOPB IgY from chicken 2, week 8, which gave the highest absorbance value at 405 nm with a 1:15 000 secondary antibody dilution, a checkerboard ELISA was performed for further optimisation. A no coat control was included for each of the samples to account for any background interference which may have occurred. The corrected absorbance values at 405 nm were below 0.1 after 45 min of development; however the highest corrected absorbance values at 405 nm and thus optimal conditions for future inhibition and indirect ELISA formats were found at a coating concentration of 1 µg/ml TvOPB and between 1 and 5 µg/ml anti-TvOPB IgY antibodies (Fig. 3.21).

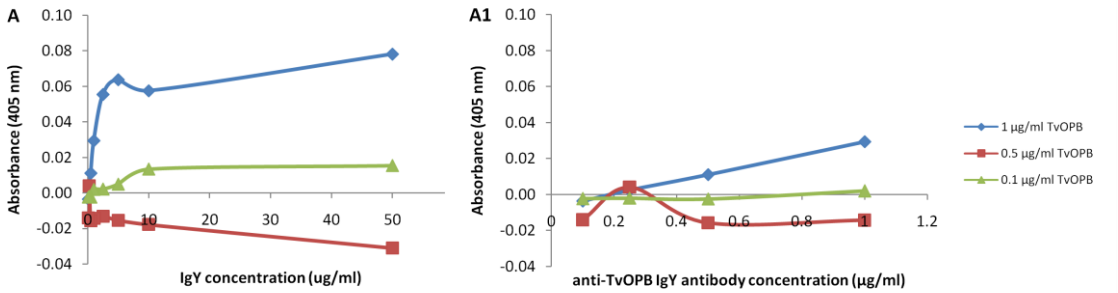

Figure 3.21: Checkerboard ELISA of TvOPB coating and anti-TvOPB IgY antibody concentrations. ELISA plates were coated with TvOPB (1, 0.5 and 0.1 µg/ml in CCB, pH 9.6), blocked with 0.5% (w/v) BSA-PBS and incubated with anti-TvOPB IgY from chicken 2, week 8 (50, 10, 5, 2.5, 1, 0.5, 0.25 and 0.1 µg/ml). Rabbit anti-chicken IgY HRPO secondary antibody (1:15 000) and ABTS·H_2O_2 were used as the detection system. The absorbance readings at 405 nm represent the average of duplicate experiments after 45 min development. Panel A1 is the expanded view of the 0.1 to 1 µg/ml anti-TvOPB IgY concentrations.

Investigation into the optimisation of the blocking step was performed using four different blocking agents: (A) 0.5% (w/v) BSA-PBS, (B) 0.5% (w/v) BSA-PBS, 0.1% (v/v) Tween-20, (C) 0.2% (w/v) BSA-PBS, 0.05% (v/v) Tween-20 and (D) 1% (v/v) horse serum-PBS. A no coat control was included for each of the samples to account for any background interference which may have occurred. From Fig. 3.22, no significant difference was evident in panels A to C, with panel D showing the same trend but at lower corrected absorbance values at 405 nm. In order to standardise the blocking reagent amongst the different ELISA antigens, the 0.5% (w/v) BSA-PBS, 0.1% (v/v) Tween-20 was chosen as the optimum blocking buffer as was the case for the TcOPB antigen.

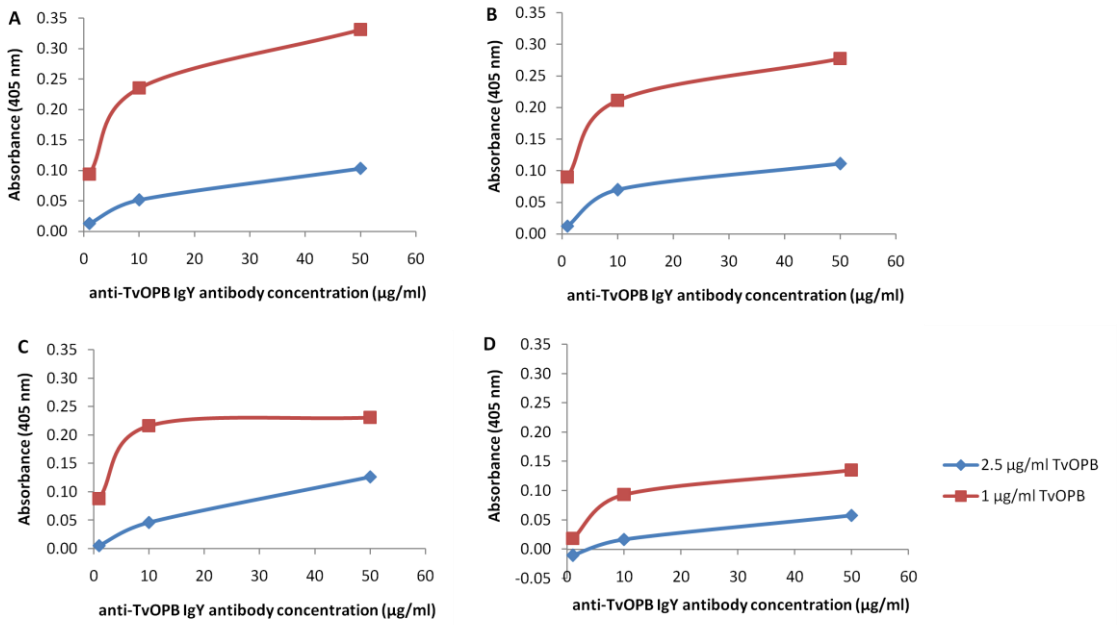

Figure 3.22: Checkerboard ELISA of TvOPB and anti-TvOPB IgY antibody titrations using different blocking agents. ELISA plates were coated with TvOPB (2.5 and 1 µg/ml in CCB, pH 9.6) and blocked with **(A)** 0.5% (w/v) BSA-PBS, **(B)** 0.5% (w/v) BSA-PBS, 0.1% (v/v) Tween-20, **(C)** 0.2% (w/v) BSA-PBS, 0.05% (v/v) Tween-20 and **(D)** 1% (v/v) horse serum-PBS. Anti-TvOPB IgY from chicken 2, week 8 (50, 10 and 1 µg/ml) were subsequently added. Rabbit anti-chicken IgY HRPO secondary antibody (1:15 000) and ABTS·H_2O_2 were used as the detection system. The absorbance readings at 405 nm represent the average of duplicate experiments after 60 min development.

A new pre-immune IgY antibody was isolated from an egg from a non-immunised chicken and used in a checkerboard ELISA together with the previously optimised TvOPB ELISA conditions. A no coat control was included for each of the samples to account for any background interference which may have occurred. Even with an increased coating concentration of 6 µg/ml TvOPB, Fig. 3.23, panel A, showed low to negative corrected absorbance values at 405 nm. Low absorbance values at 405 nm,

which were not corrected, were still evident after 60 min of development (Fig. 3.23, panel B).

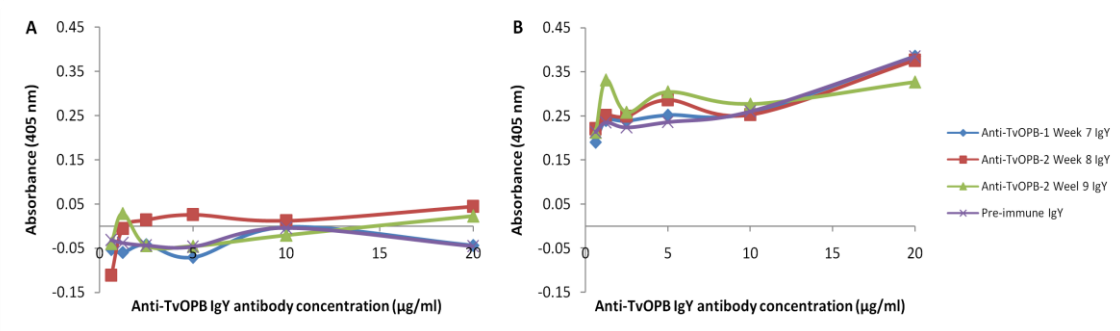

Figure 3.23: Checkerboard ELISA of TvOPB and different anti-TvOPB IgY antibody concentrations. ELISA plates were coated with TvOPB (6 µg/ml in CCB, pH 9.6), blocked with 0.5% (w/v) BSA-PBS, 0.1% (v/v) Tween-20 and incubated with anti-TvOPB IgY from chicken 1, week 7 and chicken 2, weeks 8 and 9 (20, 10, 5, 2.5, 1.25 and 0.625 µg/ml). Rabbit anti-chicken IgY HRPO secondary antibody (1:15 000) and ABTS·H_2O_2 were used as the detection system. The absorbance readings at 405 nm represent the average of duplicate experiments after 60 min development. Panel A shows where the no coat control was subtracted from the absorbance readings and panel B shows were the no coat control was ignored.

From the poor ELISA results obtained even after extensive optimisation steps, it was thought that the amount of antigen used for immunisation, 50 µg/immunisation, was not sufficient to elicit an immune response in the chicken. A new immunisation schedule was implemented using 50 and 100 µg/immunisation antigen per chicken.

Anti-TvOPB IgY antibodies were isolated from a single egg from each chicken at each week during the new immunisation schedule and used in an ELISA shown in Fig. 3.24. A no coat control was included for each of the samples to account for any background interference which may have occurred. In Fig. 3.24 the production of anti-TvOPB IgY production in chickens 1 and 2 is depicted, of which both were immunised with 50 µg/immunisation TvOPB. The corrected (Panel A) and non corrected (Panel B) absorbance values at 405 nm of the anti-TvOPB IgY from each of the weeks were lower than that of the new pre-immune IgY antibody, only chicken 2 had a single corrected absorbance value at 405 nm at week 9 which was above the pre-immune IgY antibody (Panel B). Panels C and D from Fig. 3.24, depict the anti-TvOPB IgY production in chickens 3 and 4, which were both immunised with 100 µg/immunisation TvOPB. These chickens seem to have elicited a higher response than that seen in chickens 1 and 2, with chicken 3 producing the highest amount of anti-TvOPB IgY from weeks 4 to 10, even after the absorbance values at 405 nm had been corrected (Panel C). In addition, the antibodies from chicken 3, weeks 3 to 10 were the only

weeks which the corrected absorbance values at 405 nm were higher than those of the pre-immune IgY antibody.

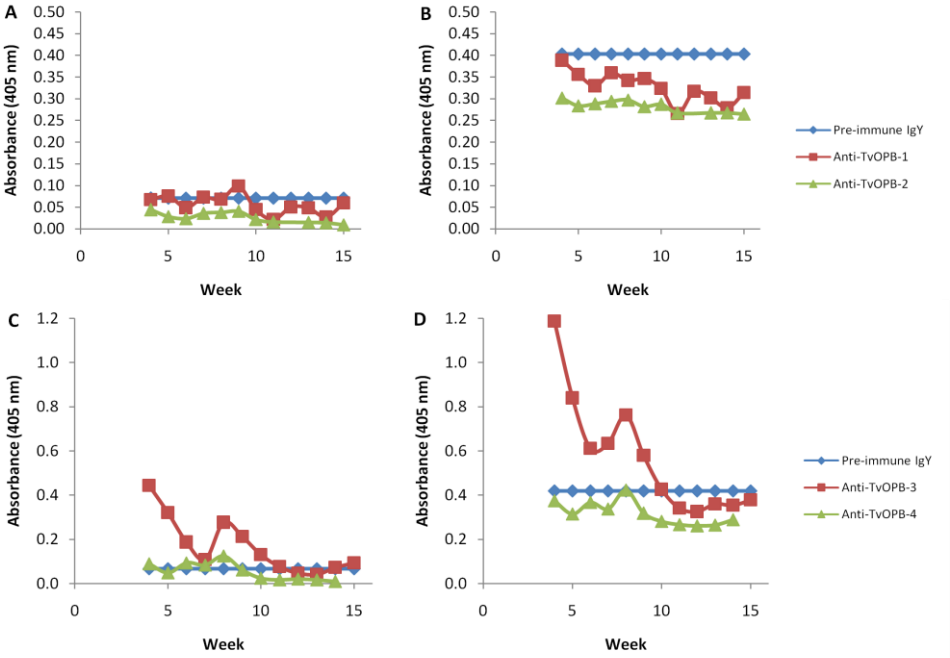

Figure 3.24: ELISA of anti-TvOPB IgY antibodies isolated from the egg yolks of chickens immunised with 50 and 100 µg/immunisation of TvOPB. ELISA plates were coated with TvOPB (2.5 µg/ml in CCB, pH 9.6), blocked with 0.5% (w/v) BSA-PBS, 0.1% (v/v) Tween-20 and incubated with anti-TvOPB IgY from **(A and B)** chickens 1 and 2 immunised with 50 µg/immunisation and **(C and D)** chickens 3 and 4 immunised with 100 µg/immunisation, weeks 1 to 15. Rabbit anti-chicken IgY HRPO secondary antibody (1:30 000) and ABTS·H_2O_2 were used as the detection system. The absorbance readings at 405 nm represent the average of duplicate experiments after 60 min development. Panels A and C show where the no coat control was subtracted from the absorbance readings. Panels B and D show were the no coat control was ignored.

3.3.6 Antibody preparation and ELISA optimisation for TcPGP

The anti-TcPGP IgY antibodies were isolated from a single egg from each week during the immunisation period and subsequently used in an initial ELISA to determine when the production of antibodies peaked. From Fig. 3.25, it is evident that there was significant production of anti-TcPGP IgY antibodies from weeks 3 to 16, except for week 12 from chicken 1, with absorbance values at 405 nm above those of the pre-immune IgY antibody.

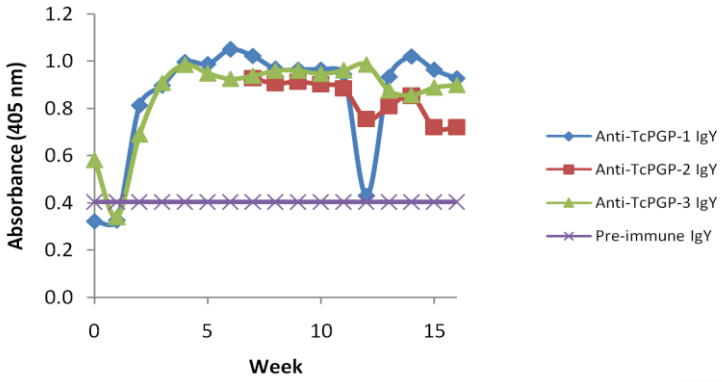

Figure 3.25: ELISA of anti-TcPGP IgY antibodies isolated from the egg yolks of immunised chickens. ELISA plates were coated with TcPGP (1 µg/ml in PBS, pH 7.4), blocked with 0.5% (w/v) BSA-PBS and incubated with anti-TcPGP IgY from chickens 1 to 3, weeks 1 to 16 (100 µg/ml). Rabbit anti-chicken IgY HRPO secondary antibody (1:20 000) and ABTS·H_2O_2 were used as the detection system. The absorbance readings at 405 nm represent the average of duplicate experiments after 15 min development.

The results from the checkerboard ELISA to find the optimal TcPGP coating and anti-TcPGP IgY concentrations for further inhibition and indirect ELISAs formats is shown in Fig. 3.26. A no coat control was included for each of the samples to account for any background interference which may have occurred. From Fig. 3.26, the highest corrected absorbance value at 405 nm was at a TcPGP coating concentration of 2.5 µg/ml in PBS with anti-TcPGP IgY at 5 µg/ml.

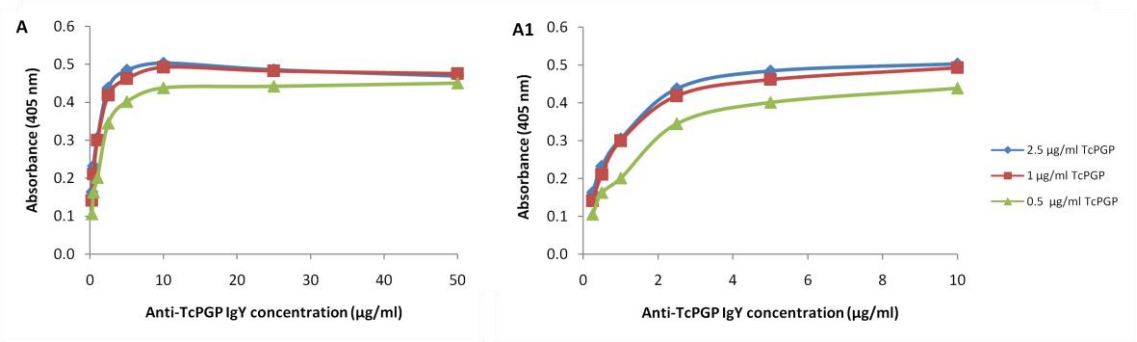

Figure 3.26: Checkerboard ELISA of TcPGP coating and anti-TcPGP IgY antibody concentrations. ELISA plates were coated with TcPGP (2.5, 1 and 0.5 µg/ml in PBS, pH 7.4), blocked with 0.5% (w/v) BSA-PBS, 0.1% (v/v) Tween 20 and incubated with anti-TcPGP IgY from chicken 3, weeks 6 to 8 pool (50, 25, 10, 5, 2.5, 1, 0.5, 0.25 µg/ml). Rabbit anti-chicken IgY HRPO secondary antibody (1:15 000) and ABTS·H_2O_2 were used as the detection system. The absorbance readings at 405 nm represent the average of duplicate experiments after 45 min development. Panel A1 is the expanded in view of the 0.1 to 10 µg/ml anti-TcPGP IgY concentrations.

3.3.7 Antibody preparation and ELISA optimisation for TvCATL

The anti-TvCATL IgY antibodies were isolated from a single egg from each week during the immunisation period and tested in an initial ELISA to determine when the production of antibodies peaked. From Fig. 3.27 it can be seen that significant amounts of anti-TvCATL IgY antibodies were produced throughout the immunisation period with most having absorbance values at 405 nm above that of the pre-immune IgY antibody.

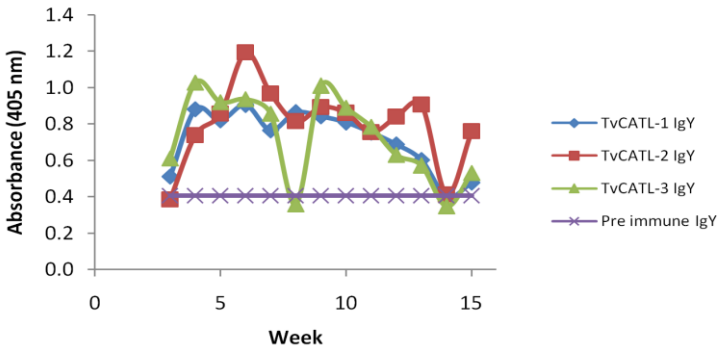

Figure 3.27: ELISA of anti-TvCATL IgY antibodies isolated from the egg yolks of immunised chickens. ELISA plates were coated with TvCATL (1 µg/ml in PBS, pH 7.4), blocked with 0.5% (w/v) BSA-PBS and incubated with anti-TvCATL IgY from chickens 1 to 3, weeks 1 to 16 (100 µg/ml). Rabbit anti-chicken IgY HRPO secondary antibody (1:15 000) and ABTS·H_2O_2 were used as the detection system. The absorbance readings at 405 nm represent the average of duplicate experiments after 45 min development.

A checkerboard ELISA was performed using different TvCATL coating concentrations and anti-TvCATL IgY antibody concentrations from chicken 2, week 6 which gave the highest absorbance value at 405 nm shown in Fig. 3.27. A no coat control was included for each of the samples to account for any background interference which may have occurred. Low corrected absorbance values at 405 nm were observed after 45 min of development, the highest of which occurred at 0.5 µg/ml TvCATL in PBS and 2.5 µg/ml anti-TvCATL IgY antibody (Fig. 3.28).

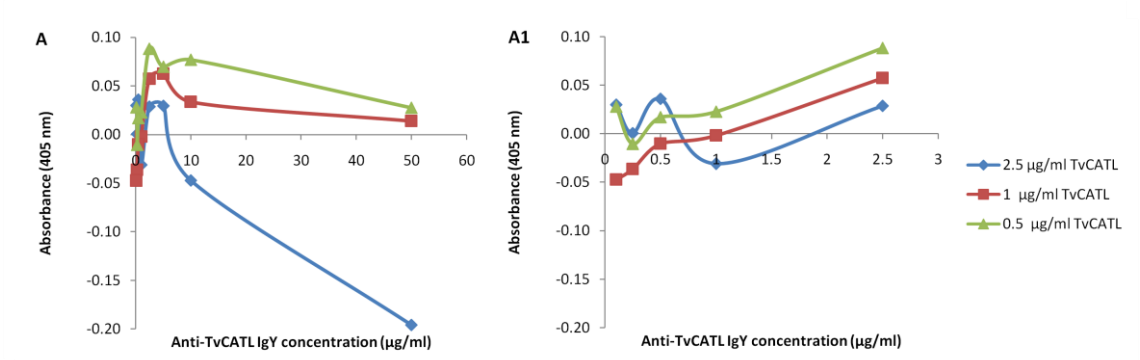

Figure 3.28: Checkerboard ELISA of TvCATL coating and anti-TvCATL IgY antibody concentrations. ELISA plates were coated with TvCATL (2.5, 1 and 0.5 µg/ml in PBS, pH 7.4), blocked with 0.5% (w/v) BSA-PBS, 0.1% (v/v) Tween 20 and incubated with anti-TcPGP IgY from chicken 2, week 6 (50, 10, 5, 2.5, 1, 0.5, 0.25 µg/ml). Rabbit anti-chicken IgY HRPO secondary antibody (1:15 000) and ABTS·H_2O_2 were used as the detection system. The absorbance readings at 405 nm represent the average of duplicate experiments after 45 min development. Panel A1 is the expanded in view of the 0.1 to 2.5 µg/ml anti-TvCATL IgY concentrations.

Further optimisation of the TvCATL checkerboard ELISA was conducted, using different TvCATL coating concentrations and diluents, PBS and CCB, pH 9.6, as well as anti-TvCATL IgY concentrations. A no coat control was included for each of the samples to account for any background interference which may occur. The corrected absorbance values at 405 nm for the TvCATL diluted in CCB were low when compared to those diluted in PBS (Fig. 3.29). The highest corrected absorbance value at 405 nm was obtained at 0.5 µg/ml TvCATL in PBS and 2.5 µg/ml anti-TvCATL IgY. This compares favourably with the result shown in Fig. 3.28 and was found to be the optimal conditions for future inhibition and indirect TvCATL ELISA formats.

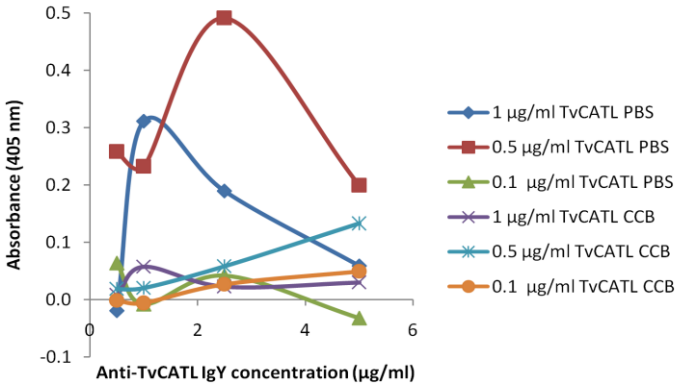

Figure 3.29: Checkerboard ELISA of TvCATL coating, dilution buffers and anti-TvCATL IgY antibody concentrations. ELISA plates were coated with TvCATL (1, 0.5 and 0.1 µg/ml in PBS, pH 7.4 and CCB, pH 9.6), blocked with 0.5% (w/v) BSA-PBS, 0.1% (v/v) Tween-20 and incubated with anti-TvCATL IgY anti-TvCATL IgY from chicken 2, week 6 (5, 2.5, 1 and 0.5 µg/ml). Rabbit anti-chicken IgY HRPO secondary antibody (1:15 000) and ABTS·H_2O_2 were used as the detection system. The absorbance readings at 405 nm represent the average of duplicate experiments after 45 min development.

3.3.8 Antibody preparation and ELISA optimisation for $TcCATL_{FL}$

The anti-$TcCATL_{FL}$ IgY antibodies were isolated from a single egg from each week during the immunisation period and subsequently used in an initial ELISA to determine when the production of antibodies was highest. Throughout the immunisation period, the laying of eggs was sporadic. From Fig. 3.30, it can be seen that the pre-immune IgY absorbance values at 405 nm are abnormally high, more so the anti-$TcCATL_{FL}$ IgY from chicken 2, as was the case for the anti-TvOPB IgY. Taking into account the pre-immune IgY, chickens 1 and 3 started producing anti-$TcCATL_{FL}$ IgY antibodies from week 3 onwards. The anti-$TcCATL_{FL}$ IgY was isolated from each week to determine whether or not the production of anti-$TcCATL_{FL}$ IgY antibodies followed the same trend as seen in Fig. 3.30, with the new pre-immune IgY antibody being used instead.

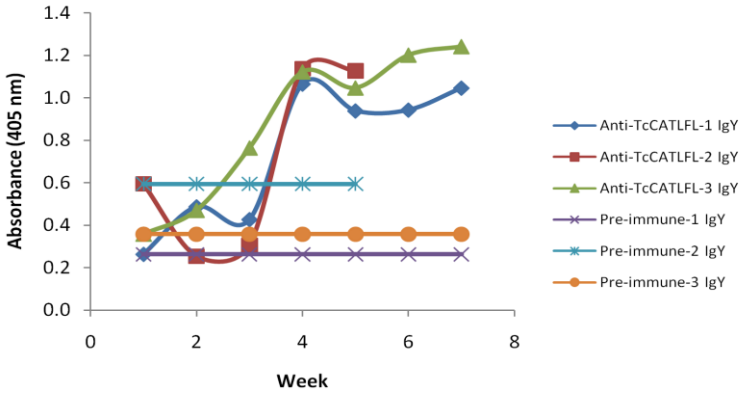

Figure 3.30: ELISA of anti-$TcCATL_{FL}$ IgY antibodies isolated from the egg yolks of immunised chickens. ELISA plates were coated with $TcCATL_{FL}$ (1 µg/ml in PBS, pH 7.4), blocked with 0.5% (w/v) BSA PBS and incubated with anti-$TcCATL_{FL}$ IgY from chickens 1 to 3, weeks 1 to 10 (100 µg/ml). Rabbit anti-chicken IgY HRPO secondary antibody (1:20 000) and ABTS·H_2O_2 were used as the detection system. The absorbance readings at 405 nm represent the average of duplicate experiments after 30 min development.

A checkerboard ELISA to optimise the $TcCATL_{FL}$ coating and the anti-$TcCATL_{FL}$ IgY antibody concentrations was performed. A no coat control was included for each of the samples to account for any background interference which may have occurred. Anti-$TcCATL_{FL}$ IgY from chicken 3, week 8 was chosen as the best mid-range antibody which gave a high absorbance value at 405 nm (results not shown). From Fig. 3.31, the highest corrected absorbance values at 405 nm and thus the optimal conditions for further inhibition and indirect ELISAs formats were at 0.05 µg/ml $TcCATL_{FL}$ in PBS and anti-$TcCATL_{FL}$ IgY at 10 µg/ml.

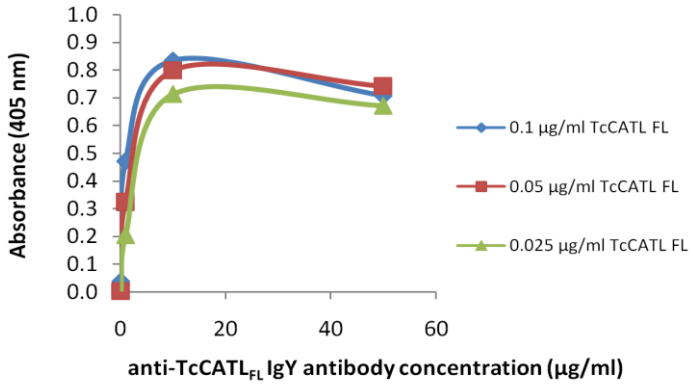

Figure 3.31: Checkerboard ELISA of TcCATL$_{FL}$ coating and anti-TcCATL$_{FL}$ IgY antibody concentrations. ELISA plates were coated with TcCATL$_{FL}$ (0.1, 0.05 and 0.025 µg/ml in PBS, pH 7.4), blocked with 0.5% (w/v) BSA-PBS and incubated with anti-TcCATL$_{FL}$ IgY from chicken 3, week 8 (50, 10 and 0.1 µg/ml). Rabbit anti-chicken IgY HRPO secondary antibody (1:20 000) and ABTS·H_2O_2 were used as the detection system. The absorbance readings at 405 nm represent the average of duplicate experiments after 45 min development.

Since the expression of TcCATL$_{FL}$ yielded high concentrations of recombinant protein and was easily purified, TcCATL$_{FL}$ was coupled to AminoLink® resin to allow for the affinity purification of the anti-TcCATL$_{FL}$ IgY antibodies. The antibodies from chicken 3, week 6 were passed over the affinity column and the eluted fractions 1 to 5, with high absorbance values at 280 nm, were pooled (Fig. 3.32).

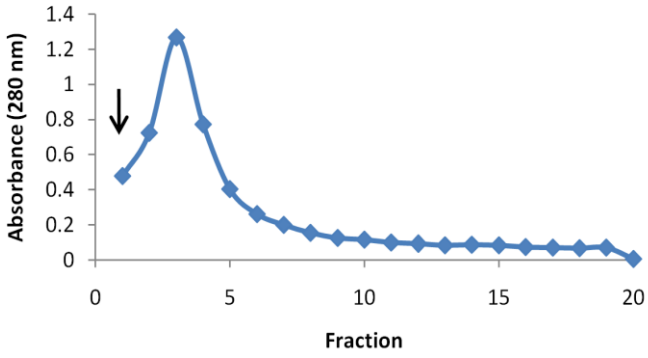

Figure 3.32: Affinity purification of anti-TcCATL$_{FL}$ IgY. Elution profile of anti-TcCATL$_{FL}$ antibodies after purification using the TcCATL$_{FL}$-Aminolink® resin. Elution buffer, pH 2.8, was applied at ↓.

A checkerboard ELISA to optimise the TcCATL$_{FL}$ coating and the affinity purified anti-TcCATL$_{FL}$ IgY antibody concentrations was subsequently performed. A no coat control was included for each of the samples to account for any background interference which may have occurred. From Fig. 3.33, it was seen that the highest corrected absorbance value at 405 nm, and thus the optimal conditions for future inhibition and indirect

ELISAs was obtained at 0.05 µg/ml $TcCATL_{FL}$ in PBS, and affinity purified anti-$TcCATL_{FL}$ IgY at 0.05 µg/ml.

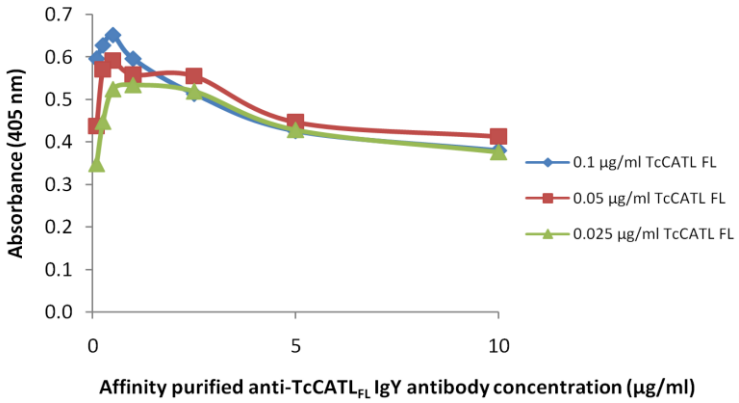

Figure 3.33: Checkerboard ELISA of $TcCATL_{FL}$ coating and affinity purified anti-$TcCATL_{FL}$ IgY antibody concentrations. ELISA plates were coated with $TcCATL_{FL}$ (0.1, 0.05 and 0.025 µg/ml in PBS, pH 7.4), blocked with 0.5% (w/v) BSA-PBS and incubated with affinity purified anti-$TcCATL_{FL}$ IgY from chicken 3, week 6 (10, 5, 2.5, 1, 0.5, 0.25 and 0.1 µg/ml). Rabbit anti-chicken IgY HRPO secondary antibody (1:20 000) and ABTS·H_2O_2 were used as the detection system. The absorbance readings at 405 nm represent the average of duplicate experiments after 60 min development.

3.3.9 Antibody preparation and ELISA optimisation for TcCATL

The anti-TcCATL IgY antibodies were isolated from a single egg from each week during the immunisation period and subsequently used in an initial ELISA to determine when the production of antibodies was highest. From Fig. 3.34, it was seen that the pre-immune IgY antibody absorbance values were abnormally high, as was the case for those of TvOPB and $TcCATL_{FL}$. Taking into account the pre-immune IgY, chickens 1 and 2 started producing anti-TcCATL IgY antibodies from week 4. Chicken 3 did not lay eggs from weeks 3 to 9 so we can only assume that the IgY production trend observed in the other two chickens applies.

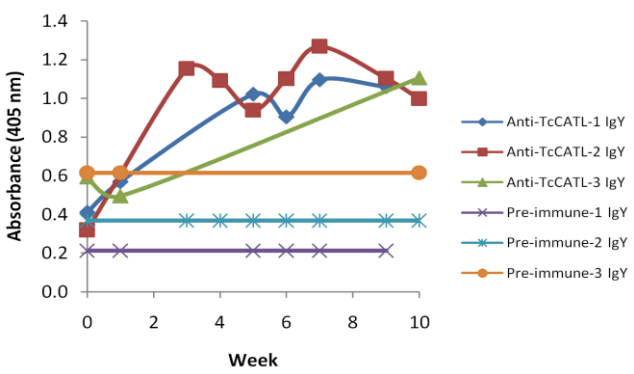

Figure 3.34: ELISA of anti-TcCATL IgY antibodies isolated from the egg yolks of immunised chickens. ELISA plates were coated with TcCATL (1 µg/ml in PBS, pH 7.4), blocked with 0.5% (w/v) BSA-PBS and incubated with anti-TcCATL IgY from chickens 1 to 3, weeks 1 to 10 (100 µg/ml). Rabbit anti-chicken IgY HRPO secondary antibody (1:20 000) and ABTS·H_2O_2 were used as the detection system. The absorbance readings at 405 nm represent the average of duplicate experiments after 30 min development.

A checkerboard ELISA to optimise the TcCATL coating and the anti-TcCATL IgY antibody concentrations was performed. A no coat control was included for each of the samples to account for any background interference which may have occurred. Anti-TcCATL IgY from all the eggs laid by chicken 3, week 11 was chosen as it gave the highest absorbance value at 405 nm (result not shown). The highest corrected absorbance value at 405 nm, and thus the optimal conditions for future inhibition and indirect ELISAs was obtained at 0.1 µg/ml TcCATL in PBS, and anti-$TcCATL_{FL}$ IgY at 10 µg/ml (Fig. 3.35).

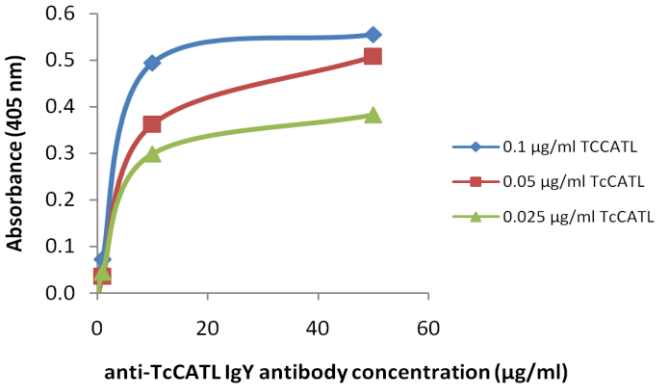

Figure 3.35: Checkerboard ELISA of TcCATL coating and anti-TcCATL IgY antibody concentrations. ELISA plates were coated with TcCATL (0.1, 0.05 and 0.01 µg/ml in PBS, pH 7.4), blocked with 0.5% (w/v) BSA-PBS and incubated with anti-TcCATL IgY from chicken 3, week 11 (50, 10 and 0.1 µg/ml). Rabbit anti-chicken IgY HRPO secondary antibody (1:20 000) and ABTS·H_2O_2 were used as the detection system. The absorbance readings at 405 nm represent the average of duplicate experiments after 45 min development.

3.3.10 Antibody preparation and ELISA optimisation for TcCATL N-terminal peptide

The anti-TcCATL N-terminal peptide IgY antibodies isolated from a single egg from each week were used in an initial ELISA to determine at which weeks the production of antibodies was highest. From Fig. 3.36, it was seen that antibody production in chicken 1 peaked from weeks 5 to 16 and in chicken 2 from weeks 4 to 10.

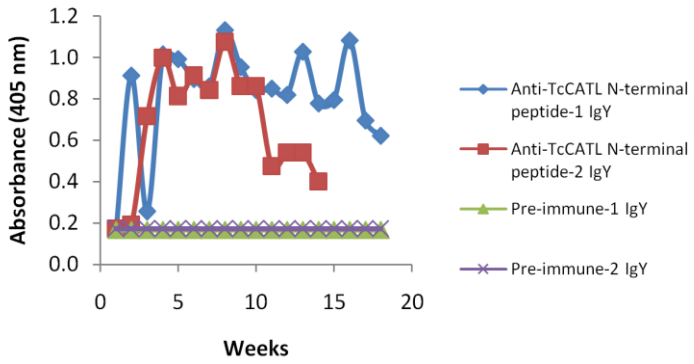

Figure 3.36: ELISA of anti-TcCATL N-terminal peptide IgY antibodies isolated from the egg yolks of immunised chickens. ELISA plates were coated with peptide (1 µg/ml in PBS, pH 7.4), blocked with 0.5% (w/v) BSA-PBS and incubated with anti-TcCATL N-terminal peptide IgY from chickens 1 and 2, weeks 1 to 16 (100 µg/ml). Rabbit anti-chicken IgY HRPO secondary antibody (1:20 000) and ABTS·H_2O_2 were used as the detection system. The absorbance readings at 405 nm represent the average of duplicate experiments after 30 min development.

The TcCATL N-terminal peptide was coupled to SulfoLink® resin and used to affinity purify selected anti-TcCATL N-terminal peptide IgY antibodies from weeks with high absorbance values at 280 nm (Fig. 3.37).

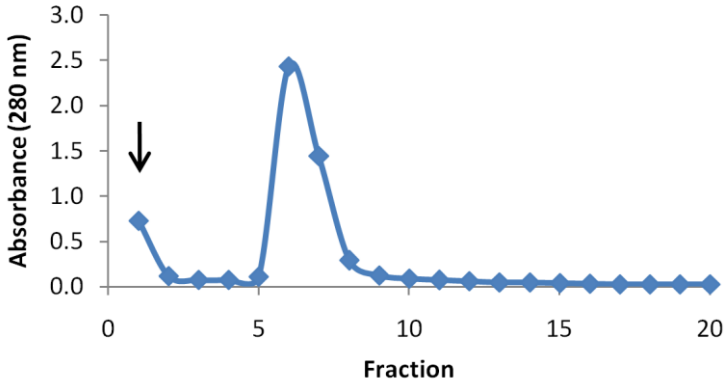

Figure 3.37: Affinity purification of anti-TcCATL N-terminal peptide IgY antibodies. Elution profile of anti-TcCATL N-terminal peptide IgY antibodies after purification using the Aminolink®-TcCATL N-terminal peptide resin. Elution buffer, pH 2.8, was applied at ↓.

Five affinity purifications of the anti-TcCATL N-terminal peptide IgY antibodies from various weeks was conducted and those with similarly high absorbance values at 280 nm pooled into three separate pools. Each of the affinity purified anti-TcCATL N-terminal peptide IgY pools were used in a checkerboard ELISA against TcCATL. A no coat control was included for each of the samples to account for any background interference which may have occurred. From Fig. 3.38, panel A, pool 1 gave the highest corrected absorbance values at 405 nm at a TcCATL coating concentration of 0.1 µg/ml in PBS and 2.5 µg/ml affinity purified anti-TcCATL N-terminal peptide IgY. The next highest corrected absorbance values at 405 nm were from pool 2 at a TcCATL coating concentration of 0.1 µg/ml in PBS and 5 µg/ml affinity purified anti-TcCATL N-terminal peptide IgY (Fig. 3.38, panel B). After 60 min of development, the corrected absorbance values at 405 nm for pool 3 were low (Fig. 3.38, panel C).

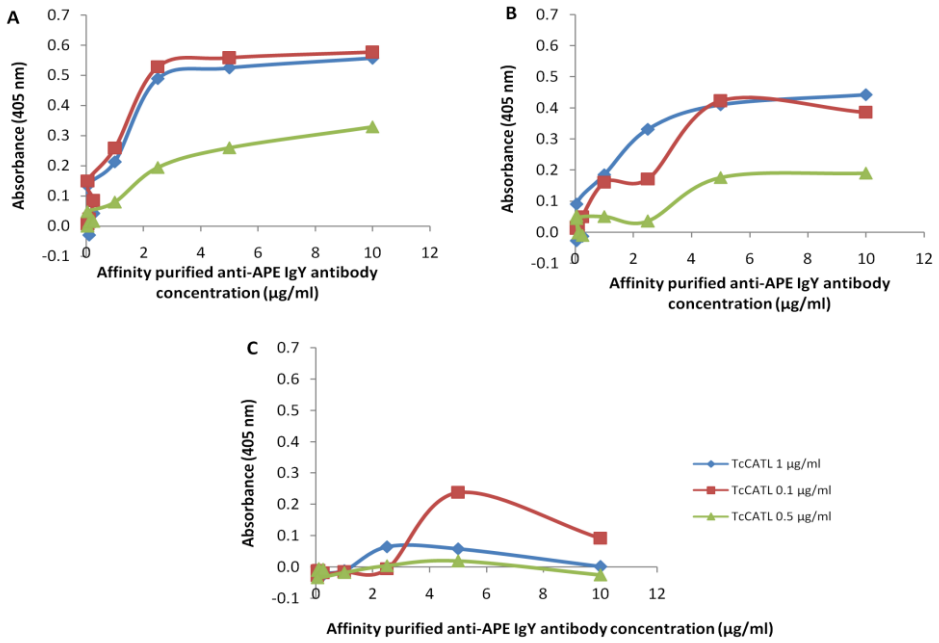

Figure 3.38: Checkerboard ELISA of affinity purified anti-TcCATL N-terminal peptide IgY antibodies against the TcCATL antigen. ELISA plates were coated with TcCATL (1, 0.1 and 0.5 µg/ml in PBS, pH 7.4), blocked with 0.5% (w/v) BSA-PBS and incubated with affinity purified anti-TcCATL N-terminal peptide IgY primary antibodies from **(A)** pool 1, **(B)** pool 2 and **(C)** pool 3 (10, 5, 2.5, 1, 0.5, 0.25, 0.1 and 0.05 µg/ml). Rabbit anti-chicken IgY HRPO secondary antibody (1:20 000) and ABTS·H_2O_2 were used as the detection system. The absorbance readings at 405 nm represent the average of duplicate experiments after 60 min development.

After the optimisation ELISAs, the best performing antibodies from each immunisation for each antigen was identified and subsequently used to confirm their identification of the antigen in a western blot format (Fig. 3.39). It was observed that the affinity purified anti-$TcCATL_{FL}$ IgY antibodies from chicken 3, week 6 recognised two bands at

approximately 35 and 37 kDa, which corresponds favourably to the 40 kDa sized $TcCATL_{FL}$. Dark smudges were visible in the $TcCATL_{FL}$ lane A which might have been due the movement of the nitrocellulose when placed onto the Kodak BioMax light film and to a longer than necessary exposure time. The anti-TcCATL IgY antibodies from chicken 3, week 11 recognised two bands at approximately 25 and 35 kDa, which corresponds favourably to the 27 kDa sized TcCATL. The band at 35 kDa might be caused due to the fact that the anti-TcCATL IgY antibodies had not been affinity purified. The anti-TcCATL N-terminal peptide IgY antibodies from pool 1, recognised a single band at approximately 25 kDa, which corresponds favourably to the 27 kDa sized TcCATL. This confirms that the band at 35 kDa was due to the purity of the antibodies as the same antigen stock was used for both anti-TcCATL IgY antibodies. The anti-TcPGP IgY antibodies from chicken 3, pool 6 to 8, recognised a single band at approximately 25 kDa which corresponds favourably to the 28 kDa sized TcPGP. The anti-TcOPB IgY antibodies from chicken 1, week 7, recognised a single band at approximately 77 kDa which corresponds favourably with the 80 kDa sized TcOPB.

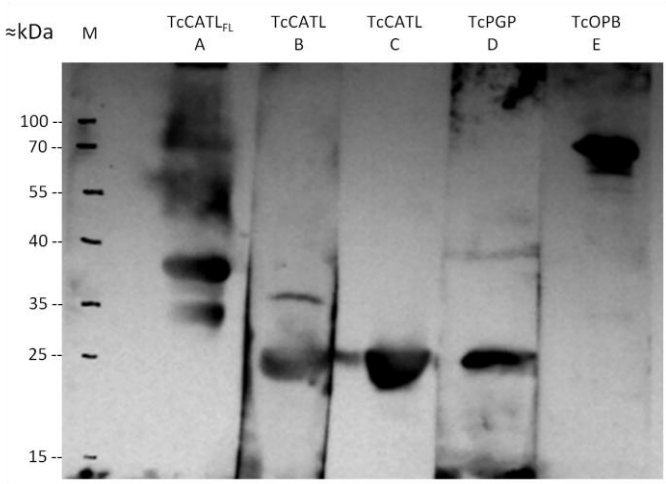

Figure 3.39: Western blot of the purified recombinant antigens from *Trypanosoma congolense* with their best raised IgY antibody. Recombinant protein (250 µg/ml) was electrophoresed on a 12.5% reducing SDS-PAGE gel, blotted onto nitrocellulose and incubated with (A) affinity purified anti-$TcCATL_{FL}$ IgY from chicken 3, week 6, (B) anti-TcCATL IgY from chicken 3, week 11, (C) affinity purified anti-TcCATL N-terminal peptide IgY from pool 1, (D) anti-TcPGP IgY from chicken 3, weeks 6 to 8, and (E) anti-TcOPB IgY from chicken 3, week 10 (100 µg/ml in 0.5% BSA-PBS). Rabbit anti-chicken IgY-HRPO conjugate (1:15 000 in 0.5% (w/v) BSA-PBS) and Pierce™ ECL western blotting substrate were used as the detection system. M: PageRuler™ prestained protein marker.

The optimum antigen and primary antibody concentrations determined for each antigen for the use in inhibition and indirect antibody detection ELISAs are found in Table 3.1.

Table 3.1: Optimised antigen coating and primary IgY antibody concentrations for future inhibition and indirect ELISA formats.

Antigen	Antigen concentration (µg/ml)	Primary antibody	Primary antibody concentration (µg/ml)
TcOPB	1	Anti-TcOPB IgY from chicken 3, week 10	1
TcPGP	1	Anti-TcPGP IgY from chicken 3, weeks 6 to 8	5
$TcCATL_{FL}$	0.05	Affinity purified anti-$TcCATL_{FL}$ IgY from chicken 3, week 6	0.5
TcCATL	2	-	-

3.4 Discussion

Protozoan peptidases have been shown to be key virulence factors as they play essential roles in the parasite and parasite-host interactions (Sajid and McKerrow, 2002; Antoine-Moussiaux *et al.*, 2009; Atkinson *et al.*, 2009). By targeting the virulence factors rather than the parasite, an anti-disease strategy can be designed. In addition to being targets for the development of chemotherapeutic drugs, the virulence factors may have diagnostic potential. Immunodominant antigens, HSP70/BiP (Bossard *et al.*, 2010), ISG75 (Tran *et al.*, 2009) and VSG RoTat 1.2 (Verloo *et al.*, 2001) have been used in the development of antibody detection ELISAs for the serodiagnosis of various AAT infective species. The TbMCA2, -3 and -5 (Helms *et al.*, 2006), TbMCA4 (Proto *et al.*, 2011) CATL and CATB (Mendoza-Palomares *et al.*, 2008), OPB (Coetzer *et al.*, 2008) and the inhibitor of cysteine peptidase (ICP) (Santos *et al.*, 2007) have all been termed virulence factors which have potential as diagnostic antigens.

The objective of the work described in this chapter was to recombinantly express and purify the trypanosomal antigens OPB, PGP and CATL from *T. congolense* and *T. vivax*. Antibodies against these antigens were subsequently rasied in chickens and together, each antigen and their corresponding antibodies were used to optimise ELISAs. These ELISAs would form the basis of the antibody detection ELISAs developed for each antigen as described in the next chapter.

Recombinant OPB from *T. congolense* (TcOPB) was successfully expressed as an 80 kDa 6xHis tag fusion protein using the pET expression system and was purified using IMAC. This corresponds favourably with what was reported by Bizaaré (2008). The pET expression system utilises the T7 promoter which necessitates the use of *E. coli* BL21 (DE3) strain in which expression is regulated by the T7 promoter and in addition, is deficient in both Lon and OmpT proteases that could degrade the expressed foreign protein (Sørensen and Mortensen, 2005). The expression of TcOPB

was leaky, and as a result further purification of the 80 kDa recombinant protein by MEC was required after IMAC purification to remove the lower molecular weight contaminating proteins.

Recombinant OPB from *T. vivax* (TvOPB) and PGP from *T. congolense* (TcPGP) were successfully expressed (80 and 28 kDa, respectively) as GST fusion proteins in the pGEX expression system and purified using GST affinity chromatography after the on-column thrombin cleavage of the GST tag. This corresponds to that reported by Huson (2006) and Mucache (2012) respectively. The pGEX expression system makes use of a *Tac* promoter and requires IPTG for the induction of expression allowing it to be used in any *E. coli* strain (JM109 or BL21) (Sørensen and Mortensen, 2005). The *E. coli* BL21 (DE3) strain was used due to their deficiency in Lon and OmpT proteases (Sørensen and Mortensen, 2005).

Recombinantly expressed and purified TcOPB and TvOPB were found to be monomeric, 80 kDa in size as confirmed by their relative mobility on a Coomassie blue R-250 stained SDS-PAGE gel, and in the case of TcOPB, the MEC S-300 calibration curve. The existence of TcrOPB as a dimer was demonstrated by Motta and co-workers (2012) as two bands were observed at 120 and 80 kDa on a Coomassie blue R-250 stained SDS-PAGE gel with elution of the purified TcrOPB occurring at 189 kDa from a MEC Superdex-200 column. It has been demonstrated that TbOPB exists as a dimer by the analysis of its 3D structure (Canning *et al.*, 2013). However, no such studies have been done for the OPB of *T. congolense* and *T. vivax*. The OPB from *L. major* has been shown to be monomeric (McLuskey *et al.*, 2010).

Mammalian PGPs exist as monomers ranging from 22 to 60 kDa in size (Busby Jr. *et al.*, 1982; Mantle *et al.*, 1990) whilst bacterial PGPs exist as multimers with an average subunit size of 25 kDa (Cummins and O'Connor, 1998). This corresponds favourably to the 28 kDa recombinantly expressed TcPGP after on-column thrombin cleavage of the GST tag.

The CATL enzyme from *T. b. rhodesiense*, rhodesian (Caffrey *et al.*, 2001), and the CATB enzyme from *T. congolense* (Mendoza-Palomares *et al.*, 2008) and from *L. major* (Chan *et al.*, 1999) along with multiple isoforms of CATB from *Trichobilharzia regent* (Dvorák *et al.*, 2005) have been successfully expressed using the *Pichia pastoris* expression system. After the expression of TvCATL, $TcCATL_{FL}$ and TcCATL using the *Pichia pastoris* expression system and the pPic9 vector, purification thereof was performed by TPP followed by MEC since the pPic9 vector lacks an affinity tag.

Recombinant TvCATL was expressed at 29 and 33 kDa as reported previously by Vather (2010).

Active vivapain, TvCATL, comprised of its propeptide and catalytic domain, was not activated by a decrease in pH to 4.2 prior to TPP, thus resulting in two molecular forms of TvCATL, the 33 kDa glycosylated pro-enzyme form and the non-glycosylated 29 kDa catalytically active form (Vather, 2010). Glycosylated proteins are predicted to have a higher retention time compared to that of non-glycosylated proteins according to the quantitative structure-property relationship (QSPR) model (Granér, 2005). The 33 kDa glycosylated and 29 kDa non-glycosylated TvCATL were predicted to have retention volumes of 65.9 and 63.98 ml respectively. After MEC purification using the S300 HR column, TvCATL was found to have a retention volume of 72.05 ml approximately similar to that of the calibration protein, myoglobin (18.8 kDa) which correlates well with the QSPR model. In theory, TvCATL should have a retention volume approximately similar to that of the calibration protein, ovalbumin (45 kDa). Thus MEC purification of a mixture of glycosylated and non-glycosylated proteins revealed that the actual difference in molecular weight and retention volume was larger than that was calculated from the MEC calibration curve (Granér, 2005). This trend has not been reported by Vather (2010) nor Jackson (2011) as their elution profiles of TvCATL was accompanied by the hydrolysis of a fluorescence labelled peptide by TvCATL in each fraction instead of the elution profile of the protein calibration solution.

The inactive full length congopain, $TcCATL_{FL}$, was unable to proteolytically cleave itself and thus the 40 kDa sized recombinant protein which was obtained after expression and MEC purification corresponded to that reported by Pillay (2010). The active congopain, TcCATL, comprised of its propeptide and catalytic domain, is not a glycosylated protein and was expressed with a molecular weight of 27 kDa which corresponded to that reported by Pillay (2010). It is thought that the propeptide plays a key role in protein folding as well as the resulting secretion of the CATL enzymes (Vernet *et al.*, 1990).

Antibodies were produced in chickens against the purified antigens for use in the inhibition ELISA format for the antibody detection of *T. congolense* and *T. vivax* infections. Antibodies were also produced against an 18-mer N-terminal TcCATL peptide for the development of a serodiagnostic antibody detection ELISA.

Antibodies were successfully raised in chickens against each recombinantly produced antigen as well as the TcCATL N-terminal peptide and were able to detect their

respective recombinant proteins in both the ELISA and in western blot format, with the exception of TvOPB. After an immunisation schedule of 50 µg/immunisation and 100 µg/immunisation, low yields of anti-TvOPB IgY antibodies were obtained and this led to the conclusion that the TvOPB antigen was poorly immunogenic.

Each antigen and their respective antibody pair were subjected to numerous checkerboard titrations to determine their optimal concentrations along with the antigen diluent, blocking buffer composition and secondary antibody concentration. This was done prior to the checkerboard ELISAs using the experimentally infected and non-infected cattle sera as the amount of serum in the available samples was limited. The best ELISA results for the TvOPB antigen was obtained using CCB as the diluent rather than PBS which was suitable for the other antigens. Initially, 0.5% (w/v) BSA-PBS was used as the blocking buffer, however, after a number of ELISA optimisations for each antigen, it was discovered that blocking with 0.5% (w/v) BSA-PBS containing 0.1% (v/v) Tween-20 was more efficient, resulting in effective blocking of the unoccupied sites in the wells of the ELISA plates.

In the next chapter, results of studies to determine the diagnostic potential of TcOPB, TvOPB, TcPGP, $TcCATL_{FL}$, TcCATL and TvCATL, in two antibody detection ELISA formats, an inhibition and indirect format will be described. This was performed by ELISA optimisations of the inhibition and indirect formats using the ELISA parameters for each recombinantly expressed and purified virulence factor antigen, reported in the present chapter, along with experimentally infected and non-infected sera. Results of the verification of each of the antigen's diagnostic ability by the use of the *T. congolense* and *T. vivax* blinded serum panels will be described.

CHAPTER 4

INDIRECT AND INHIBITION ELISA FOR THE DETECTION OF *TRYPANOSOMA CONGOLENSE* AND *TRYPANOSOMA VIVAX*

4.1 Introduction

The simplest technique for the diagnosis of AAT is by direct microscopic examination of the blood on prepared slides (Nantulya, 1990). These parasitological techniques are quick, easy and a large number of samples can be screened, but are, however, characterised by a low sensitivity due to fluctuating levels of parasitaemia (Chappuis *et al.*, 2005a). These techniques can be improved by the concentration of parasites before microscropic examination by using the microhaemocrit centrifugation test (mHCT) (Woo, 1970), buffy coat method (BCM) (Murray *et al.*, 1977), the quantitative buffy coat (QBC) (Levine *et al.*, 1989) or the mini-anion-exchange centrifugation technique (mAECT) (Lumsden *et al.*, 1979). The use of the mAECT has been established for the diagnosis of *T. b. gambiense* infections but is yet to be established for the diagnosis of AAT infections (Chappuis *et al.*, 2005a).

The detection of anti-trypanosomal antibodies and antigens released by the dying parasites is the most commonly used method for the diagnosis of HAT and AAT (Nantulya, 1990). The CATT/*T. b. gambiense*, LATEX/*T. b. gambiense*, IFA, TL along with the antibody and antigen detection ELISAs are all used to varying degrees for the diagnosis of HAT (Chappuis *et al.*, 2005a). Due to the simplicity, low cost and rapid results, the CATT and LATEX tests are used in active case finding. Due to the requirement of trained personnel and the use of advanced equipment, the IFA, TL and ELISA tests are not used in active case finding, but rather are performed in laboratories. In addition, the results of the IFA and TL tests are somewhat subjective and coupled with variation in the levels of parasitaemia are characterised by varying degrees of sensitivity (Chappuis *et al.*, 2005a).

The control and diagnosis of AAT, caused by *T. b. brucei, T. congolense* and *T. vivax* in livestock, is achieved by the use of the ELISA together with parasitological techniques (Luckins, 1992). The antibody detection ELISA, using whole parasite lysates, is able to measure the levels of whole anti-trypanosomal antibodies in the blood or serum, negating the problem posed by low levels of parasitaemia, thus making it an ideal method for surveillance and epidemiological studies (Machila *et al.*, 2001; Van den Bossche *et al.*, 2004) when accompanied with strict standardisation and

quantification (Rebeski *et al.*, 1999c). Commercial ELISA kits for the diagnosis of HAT uses the same antigens as the LATEX/*T. b. gambiense* but are fixed on a microtitre plate instead (Hasker *et al.*, 2012) and for AAT, denatured *T. congolense* and *T. vivax* parasite lysate (Rebeski *et al.*, 1999a; Rebeski *et al.*, 1999b).

The antigen detection ELISAs make use of monoclonal antibodies which are used to detect trypanosomal antigens in serum samples and are available for the diagnosis of HAT and *T. b. brucei*, *T. congolense* and *T. vivax* AAT infections (Nantulya and Lindqvist, 1989; Rebeski *et al.*, 1999c). Antibody detection ELISAs make use of trypanosomal lysate as the antigen which are obtained from parasites which have been propagated in rats or *in vitro* cultures to detect circulating anti-trypanosomal antibodies in serum samples (Greiner *et al.*, 1997; Hopkins *et al.*, 1998). Antibody detection ELISAs can be performed in either indirect or inhibition formats as outlined in Fig.4.1. Many antibody detection ELISAs for the diagnosis of HAT have been developed and evaluated in active case findings, however very few have been developed for the diagnosis of AAT. An ELISA based on the VSG from the *T. evansi* RoTat 1.2 clone has been successfully evaluated (Verloo *et al.*, 2000) and the use of solublised whole *T. evansi* lysate in an antibody detection ELISA format has been recommended by the OIE (2013).

Since lateral flow tests are quick, easy to use and require neither training nor sophisticated equipment, they are ideal for active case finding in rural settings. However, no such diagnostic lateral flow tests exist for AAT (Büscher *et al.*, 2013; Sullivan *et al.*, 2013). The use of the ELISA as a diagnostic tool may be the stepping stone for the development of lateral flow tests. A recent development for the serological diagnosis of *T. b. gambiense* has resulted in the SD BIOLINE HAT, HAT SERO K-SeT and HAT SeroStrip which are currently being evaluated in the Democratic Republic of the Congo (Büscher *et al.*, 2013).

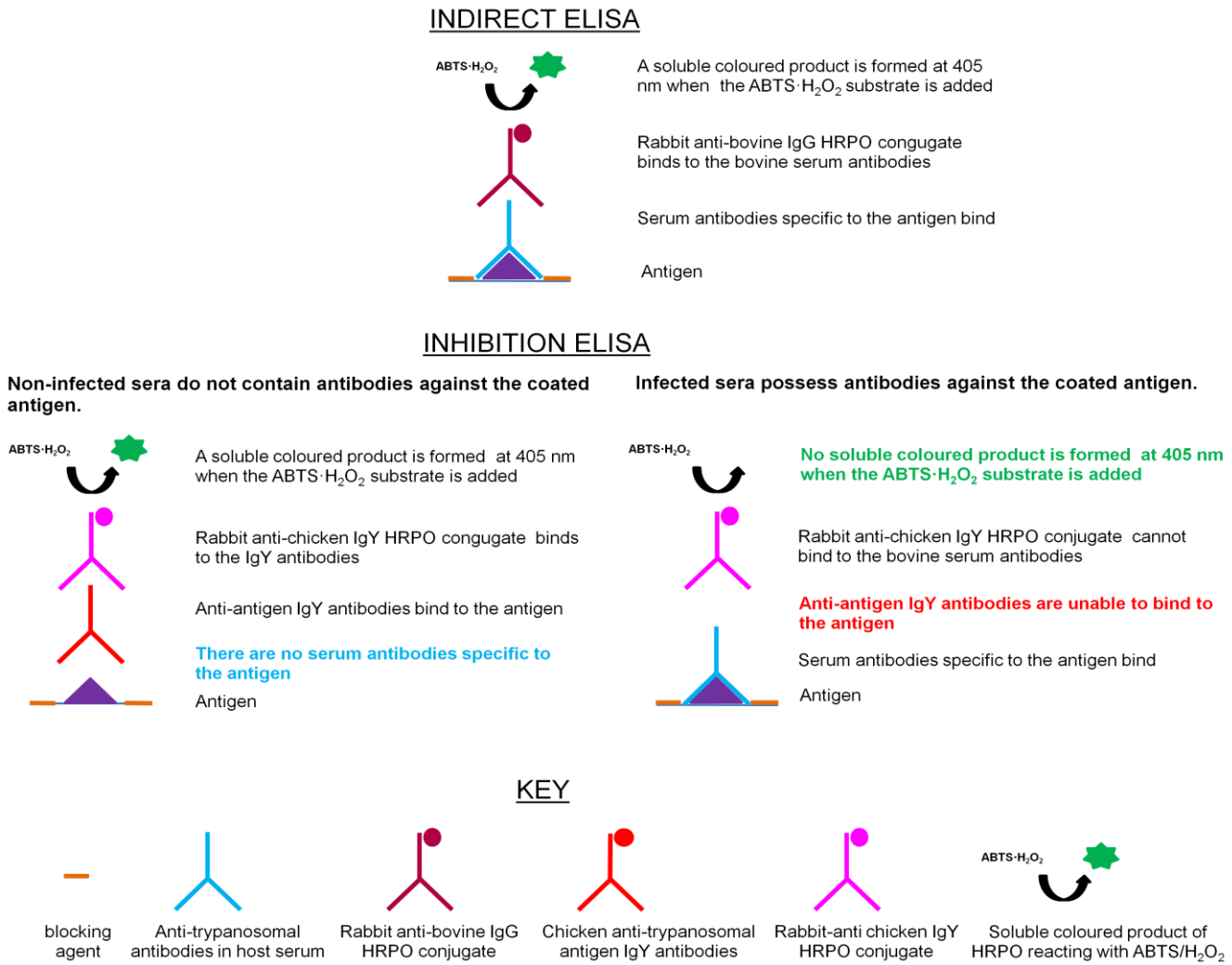

Figure 4.1: Comparison of the antibody interactions in the indirect and inhibition format of an antibody detection ELISA.

Since the serological tests currently in use require trypanosomal parasites grown in culture as the antigen, inconsistent results are obtained. As a result of the danger posed by the culturing of human infective BSF parasites in the case of *T. b. gambiense* and *T. b. rhodesiense*, the use of antigens produced using recombinant technology presents an attractive alternative. The antigens chosen for this purpose should be virulence factors which are expressed in the BSF. Recombinant antigens can be expressed and purified in large concentrations with little safety risk. Various researchers have tested the ability of a variety of recombinantly expressed antigens as diagnostic tools in the ELISA format. Tran and co-workers (2009) researched the suitability of ISG75 in an antibody detection ELISA for the diagnosis of surra in camels which yielded a sensitivity of 94.6% (95% CI: 87.8 to 98.2%) and compared favourably to the sensitivities obtained using the commercially available diagnostic kits. Using a *T. vivax* flagellar-associated protein, GM6, Pillay and co-workers (2013) investigated the diagnostic potential of the antigen for the diagnosis of *T. vivax* infections which yielded sensitivities of 91.5% (95% CI: 83.2 to 99.5) and 91.3% (95% CI: 78.9 to 93.1) for sera samples obtained from two locations in East and West Africa.

Due to the need for the development of AAT diagnostics, the application of several antigens in an antibody detection ELISA was investigated. Previously identified virulence factors: cathepsin L-like peptidases, full length congopain ($TcCATL_{FL}$) and the catalytic domain of congopain (TcCATL) from *T. congolense*, the catalytic domain of vivapain (TvCATL) from *T. vivax*, oligopeptidase B from *T. congolense* and *T. vivax* (TcOPB and TvOPB) and pyroglutamyl peptidase from *T. congolense* (TcPGP) were thought to be possible diagnostic antigens. These antigens' applicability towards the development of a pan-*Trypanozoon* lateral flow diagnostic tool was investigated. These antigens, which had been recombinantly expressed, purified and antibodies raised against, were used for the optimisation of antibody detection ELISAs. Their ability to successfully discriminate between infected and non-infected cattle using serum samples in a blinded serum panel of *T. congolense* and *T. vivax* experimentaly infected cattle, using the inhibition and indirect antibody detection ELISA formats was evaluated, with receiver-operating characteristic (ROC) analysis indicating their respective diagnostic potential.

4.2 Materials and methods

4.2.1 Materials

Sera: Sera from infected and non-infected cattle were obtained from ClinVet International (PTY) LTD, Bloemfontein, South Africa and were annotated as infected and non-infected sera for simplicity.

Primary chicken IgY production and ELISA: Chicken antibodies were produced as outlined in sections 2.2.1 and 3.2.6, and called primary antibodies. The ABTS tablets and buffer were purchased from Roche (Mannheim, Germany) and the BIOTEK® ELx800™ absorbance microplate reader from BioTek Instruments Inc. (United States).

Enzyme-labelled antibodies: The rabbit anti-chicken IgY HRPO (A9046) and the rabbit anti-bovine IgG HRPO (A8917) conjugates were purchased from Sigma (St. Louis, MO, USA).

Western blot: BioTrace™ nitrocellulose membrane was purchased from PALL Corp (Ann Arbor, USA), the semi dry blotter, 4-cholor-1-naphthol and Kodak BioMax light film were from Sigma (St. Louis, MO, USA), the PageRuler™ prestained protein ladder and Pierce™ ECL western blotting substrate were from Pierce (Rockford, IL, USA).

4.2.2 Inhibition antibody detection ELISA

An inhibition antibody detection ELISA detects antibodies in the serum of an infected animal by the decrease in absorbance values. Once the host has been infected by a trypanosome species, the host's immune system will elicit an immune response to the various antigens which are released by the parasite or as a by-product of parasite lysis. These anti-trypansomal antibodies present in the serum will bind to the antigens coated onto the ELISA plates and as a result, the IgY antibodies, produced in chickens against the antigen, will be unable to bind (Fig. 4.1). Subsequently, the rabbit anti-chicken IgY HRPO conjugate will not be bound and the addition of the ABTS·H_2O_2 substrate will not form a coloured product, thus a decrease in absorbance is observed. Non-infected hosts would not have generated anti-trypanosomal antibodies which allows for the primary IgY antibodies to bind to the coated antigen. The HRPO conjugated secondary antibodies would subsequently bind and result in a coloured product upon the addition of the ABTS·H_2O_2 substrate, resulting in an increase in absorbance (Fig. 4.1).

Purified recombinant protein, expressed and purified as described in section 3, diluted in PBS (100 mM NaCl, 100 mM NaH_2PO_4, 100 mM Na_2HPO_4, pH 7.4) or carbonate

coating buffer (CCB) (50 mM carbonate buffer, pH 9.6) (100 µl per well) was used to coat the wells of 96-well Nunc-Immuno™ Maxisorp ELISA plates for 16 h at 4°C. Control wells not coated with antigen (no coat control) were included for each sample and were left empty. The coating solution was discarded and the plates were blocked with blocking buffer [0.5% (w/v) BSA-PBS, 0.1% (v/v) Tween-20 (200 µl per well)], to prevent the non-specific binding of antibodies, by incubation at 37°C for 1 h. Sera, diluted with blocking buffer (1:10 or 1:100, 100 µl per well), were added to both the antigen and the no coat control wells, and incubated at 37°C for 1 h. Each serum sample was tested in triplicate and, in addition, a no serum control was included in quadruplicate on each plate. The wells were washed three times with 0.1% (v/v) Tween-20-PBS using a BIOTEK® ELx50™ Microplate washer after which the primary antibodies, diluted with blocking buffer (100 µl per well), were added and incubated at 37°C for 1 h. The wells were washed as before, and the rabbit anti-chicken IgY HRPO conjugate in blocking buffer (1: 30 000, 100 µl per well), was added and incubated at 37°C for 1 h. The wells were washed as before and the Roche ABTS substrate solution [50 mg ABTS tablet, 50 ml ABTS buffer (phosphate-citrate-sodium perborate solution, pH 4.6) (100 µl per well)] was subsequently added. The plate was incubated in the dark for 15 min prior to measuring the absorbance at 405 nm using a FLUORStar Optima spectrophotometer in 15 min intervals for 75 min. The absorbance values at 405 nm for the blinded serum panels were measured using a BIOTEK® ELx800™ absorbance microplate reader in combination with the Gen5™ software.

After the ELISA optimisation for each antigen, a known positive/infected control serum, 151 (+28), was included in triplicate on each plate for the *T. congolense* blinded serum panel.

4.2.2.1 Sensitivity and specificity calculations for the inhibition antibody detection ELISA

The mean of the triplicate absorbance values at 405 nm for the no coat control wells were subtracted from those of the corresponding antigen coated wells to yield the corrected absorbance values at 405 nm. The percentage inhibition for each sample was calculated according to the following equation (Bossard *et al.*, 2010):

$$\text{Percentage inhibition } (\%) = \frac{A_{405\ nm}(\text{no serum control}) - A_{405\ nm}(\text{serum})}{A_{405\ nm}(\text{no serum control})} \times 100\ \%$$

The mean, standard deviation (SD) and the three cut-off values were calculated using the percentage inhibition values from the panel of known negative sera along with the serum samples which were tested. The cut-off values for each of the antigens was calculated by the addition of one, two and three SDs to the mean percentage inhibition from the panel of known negative sera.

Based on the cut-off values, the percentage inhibition of each serum sample was used to predict their infection status, which was subsequently compared to the actual infection status. The sensitivity and specificity of the inhibition ELISA for each antigen was determined at each cut-off value.

The specificity of an ELISA is its ability to correctly identify non-infected serum samples by the generation of percentage inhibition values which are below that of the calculated cut-off values. The sensitivity of an ELISA is its ability to correctly identify infected samples by yielding of percentage inhibition values which are above that of the calculated cut-off values.

4.2.3 Indirect antibody detection ELISA

An indirect antibody detection ELISA detects antibodies in the serum of an infected animal by the increase in absorbance values. Since the indirect ELISA format does not make use of a primary antibody, any anti-trypanosomal antibodies present in the bovine serum which are bound to the coated antigen, will be bound directly by the rabbit anti-bovine IgG HRPO conjugate. Once the ABTS·H_2O_2 substrate has been added, a direct relationship between the formation of the coloured product and the presence of the antigen specific anti-trypanosomal antibodies is observed. Serum from non-infected hosts, which have not generated anti-trypanosomal antigen antibodies, will not bind to the coated antigen and as a result the HRPO conjugated secondary antibodies will not bind and a decrease in absorbance is observed (Fig. 4.1).

Purified recombinant protein, produced as described in chapter 3 (sections 3.2.3 - 3.2.5), diluted in PBS, pH 7.4, or CCB, pH 9.6 (100 µl per well), was used to coat the wells of 96-well Nunc-Immuno™ Maxisorp ELISA plates for 16 h at 4°C. Control wells not coated with antigen (no coat control) were included for each sample and were left empty The coating solution was discarded and the plates were blocked with blocking buffer [0.5 % (w/v) BSA-PBS, 0.1% (v/v) Tween-20 (200 µl per well)] to prevent the non-specific binding of antibodies, by incubation at 37°C for 1 h. Sera, diluted with blocking buffer (1:10 or 1:100, 100 µl per well), were added to both the antigen and no-coat control wells, and incubated at 37°C for 2 h. Each serum sample

was tested in triplicate and, in addition, a no serum control was included in quadruplicate on each plate. The wells were washed three times with 0.1% (v/v) Tween-20-PBS using a BIOTEK® ELx50™ Microplate washer after which the rabbit anti-bovine IgG HRPO conjugate, diluted in blocking buffer (100 µl per well), was added and incubated at 37°C for 1 h. The wells were washed as before and the Roche ABTS substrate solution [50 mg ABTS tablet, 50 ml ABTS buffer (phosphate-citrate-sodium perborate solution, pH 4.6) (100 µl per well)] was subsequently added. The plate was incubated in the dark for 10 min prior to measuring the absorbance at 405 nm using a FLUORStar Optima spectrophotometer in 10 min intervals for 60 min. The absorbance values at 405 nm for the blinded serum panels were measured using a BIOTEK® ELx800™ absorbance microplate reader in combination with the Gen5™ software.

After the ELISA optimisation for each antigen, a known negative/non-infected serum, 151 (-7), and a known positive/infected serum, 151 (+28) control were included in triplicate on each plate for the *T. congolense* blinded serum panel. For the *T. vivax* blinded serum panel a known negative serum, 152 (-7), and a known positive serum control, 315 (+28) and 321 (+28) for TvCATL and TvOPB respectively, were included in triplicate on each plate.

4.2.3.1 Sensitivity and specificity calculations for the indirect antibody detection ELISA

The mean of the triplicate absorbance values at 405 nm for the no coat control wells were subtracted from those of the corresponding antigen coated wells to yield the corrected absorbance values at 405 nm. These values were divided by the mean of the triplicate absorbance values at 405 nm of the known positive control serum. The percentage positivity values were calculated according to the following equation (Bossard *et al.*, 2010):

$$\text{Percentage positivity (\%)} = \frac{A_{405\,nm}\ (\text{serum})}{A_{405\,nm}(\text{known positive control serum})} \times 100\ \%$$

The mean, SD and the three cut-off values were calculated using the percentage positivity values from the panel of known negative sera along with the serum samples which were tested. The cut-off value for each of the antigens was calculated by the

addition of one, two and three SDs to the mean percentage positivity from the panel of known negative sera.

Based on the cut-off values, the percentage positivity of each serum sample was used to predict their infection status, which was subsequently compared to the actual infection status. The sensitivity and specificity of the indirect ELISA for each antigen was determined at each cut-off value.

4.2.4 Receiver-operating characteristic (ROC) analysis of the diagnostic potential of the tested antigens

The receiver operating characteristic (ROC) curves were generated using GraphPad Prism version 6.00 for Windows, GraphPad Software, La Jolla California USA, www.graphpad.com.

To determine the accuracy or diagnostic performance of each tested antigen, ROC analysis was performed for each of the ELISA formats for each antigen's ability to discriminate between infected and non-infected serum samples (Zweig and Campbell, 1993). The calculated sensitivity and 100%-specificity were plotted together, the best combination of which was visualised for each antigen used in each ELISA format (Greiner *et al.*, 1995). The closer the ROC curve approached the upper left hand side of the graph, the better the sensitivity, specificity and thus overall accuracy of the test (Zweig and Campbell, 1993).

An area under curve (AUC) value is generated along with a p value, the standard error of the AUC as well as the 95% upper and lower confidence intervals (CI). The AUC is an indication of the ability of the diagnostic test to discriminate between infected and non-infected serum samples. The higher the AUC value, the better the discrimination. The p value is the probability of obtaining a large difference in values when the test is repeated, that the measured values were obtained by chance, i.e. the test is unable to discriminate between infected and non-infected serum samples (Metz, 2006).

To measure the overall effectiveness of each antigen using each ELISA format (Zweig and Campbell, 1993), the Youden index (*J*) was calculated as according to the following equation:

$$J = \text{maximum}\{\text{sensitivity} + \text{specificity}\} - 1$$

The Youden index is the measure of the maximum vertical line between the ROC curve and the diagonal chance line, where AUC equals 0.5 (Schisterman *et al.*, 2005). The closer the ROC curve tends to 1, the more effective the diagnostic test is (Schisterman *et al.*, 2005).

4.3 Results

The inhibition and indirect ELISAs were optimised for blocking buffer, coating antigen concentration and diluents as well as primary and secondary antibody concentrations as shown in subsequent sections. The serum samples used were annotated according to that outlined in appendix B. The serum samples used for optimisation were from cattle infected with parasites (positive sera), whilst negative sera were from the cattle prior to infection.

Limits for the upper and lower values for percentage inhibition and percentage positivity were 0 to 100%. The calculated values above and below these limits were modified accordingly. The absorbance graphs for the corresponding percentage inhibition or percentage positivity are found in appendix C.

4.3.1 Optimisation of inhibition and indirect TcOPB ELISA with *Trypanosoma congolense* infected and non-infected bovine sera

4.3.1.1 Inhibition TcOPB ELISA

Using the optimised TcOPB coating at 1 µg/ml in PBS and 1 µg/ml anti-TcOPB IgY primary antibody from chicken 3, week 10 as described in section 3.3.4, a trial inhibition ELISA was performed using infected and non-infected serum samples Corrected absorbance values at 405 nm for the non-infected serum samples were found to be slightly higher than those for the infected serum samples (Appendix C, Fig. C.1). Measurable percentage inhibition values were only obtained for one infected serum sample, 18 (+7), and one non-infected serum sample, 164 (-7) (Fig. 4.2). Ideally, percentage inhibition values should be higher for infected serum samples than for non-infected serum samples. The serum samples used yielded high percentage inhibition values for the infected and low values for the non-infected serum samples against the antigens in this study.

It was thus decided that the optimal conditions for the TcOPB inhibition ELISA format for the blinded serum panel was found to be coating with TcOPB at 1 µg/ml in PBS,

blocking with 0.5% (w/v) BSA-PBS, 0.1% Tween-20, using anti-TcOPB IgY from chicken 3, week 10 and the rabbit-chicken IgY HRPO conjugate secondary antibody at a 1:15 000 dilution.

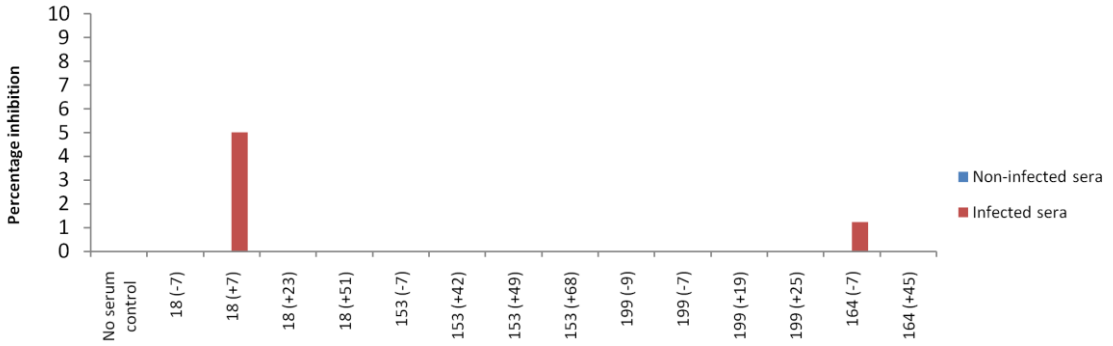

Figure 4.2: Inhibition ELISA using TcOPB and anti-TcOPB IgY antibodies against infected and non-infected sera. ELISA plates were coated with TcOPB (1 µg/ml in PBS, pH 7.4), blocked with 0.5% (w/v) BSA-PBS, 0.1% (v/v) Tween-20 and incubated with sera (1:10 dilution). Thereafter anti-TcOPB IgY from chicken 3, week 10 (1 µg/ml) was added. Rabbit anti-chicken IgY HRPO secondary antibody (1:15 000) and ABTS·H_2O_2 were used as the detection system. The absorbance readings at 405 nm represent the average of triplicate experiments after 30 min development. Each plate had a no serum control in quadruplicate.

4.3.1.2 Indirect TcOPB ELISA

Due to the poor results obtained in the inhibition ELISA format, the applicability of indirect ELISA format to the TcOPB antigen was investigated. Since the indirect ELISA format does not make use of a primary antibody, the optimal TcOPB coating concentration and rabbit anti-bovine IgG HRPO conjugate secondary antibody dilution was determined using one infected, 208 (+19), and one non-infected, 208 (-10), serum sample in an indirect checkerboard ELISA. From Fig. 4.3, after 60 min of development, the corrected and non-corrected absorbance values at 405 nm for the non-infected serum samples were higher than those of the infected samples for both secondary antibody dilutions. The exceptions to which occured at 5 µg/ml TcOPB coating and 1:10 000 secondary antibody dilution for the corrected absorbance values at 405 nm (Fig. 4.3, Panel A). For the non-corrected absorbance values at 405 nm, exceptions occurred at 8 µg/ml TcOPB coating and 1:5 000 dilution of rabbit anti-bovine IgG HRPO conjugate secondary antibody (Fig. 4.3, Panel B).

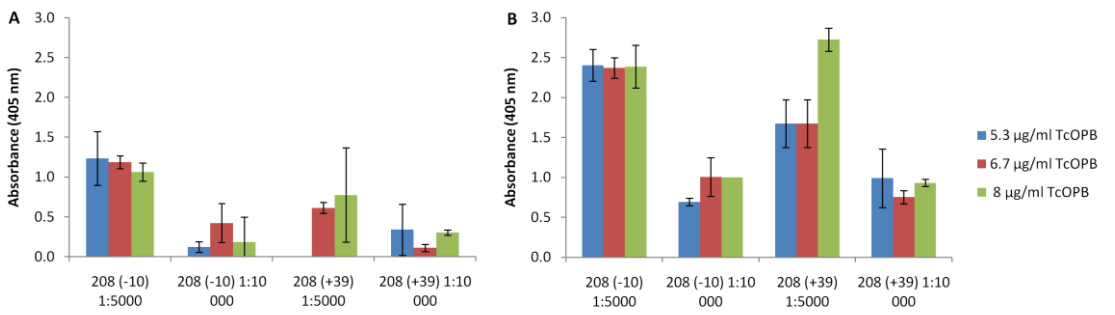

Figure 4.3: Indirect checkerboard ELISA using different TcOPB concentrations against an infected and a non-infected serum sample. ELISA plates were coated with TcOPB (5.3, 6.7 and 8 µg/ml in PBS, pH 7.4), blocked with 0.5% (w/v) BSA-PBS, 0.1% (v/v) Tween-20 and incubated with sera (1:10 dilution). Rabbit anti-bovine IgG HRPO secondary antibody (1:10 000) and ABTS·H_2O_2 were used as the detection system. The absorbance readings at 405 nm represent the average of triplicate experiments after 60 min development. Each plate had a no serum control in quadruplicate. Panel A shows where the no coat control was subtracted from the absorbance values and panel B shows where the no coat control was ignored.

In addition to the effect of different blocking buffers, the effect of the TcOPB coating diluent was investigated. Two diluents, PBS, pH 7.4, and carbonate coating buffer (CCB), pH 9.6, along with two blocking buffers, 0.5% (w/v) BSA-PBS, 0.1% (v/v) Tween-20 (BPT) and 1% (v/v) horse serum-PBS (HSP) were used. These variables were tested using one infected, 201 (+7), and one non-infected, 215 (-8), serum sample. The corrected absorbance values at 405 nm of the non-infected serum sample were slightly lower than that of the infected serum sample with the trend being similar for each of the conditions (Fig. 4.4). Coating with 2 µg/ml TcOPB in PBS and CCB, and blocking with BPT and HSP yielded higher corrected absorbance values at 405 nm for the infected serum sample than the non-infected serum, with the highest being recorded at 5 µg/ml TcOPB in PBS, using the BPT blocking buffer.

The optimal conditions for the TcOPB indirect ELISA format for the blinded serum panel was found to be coating with TcOPB at 5 µg/ml in PBS, blocking with BPT and using the rabbit anti-bovine IgG HRPO conjugate secondary antibody at a 1:10 000 dilution.

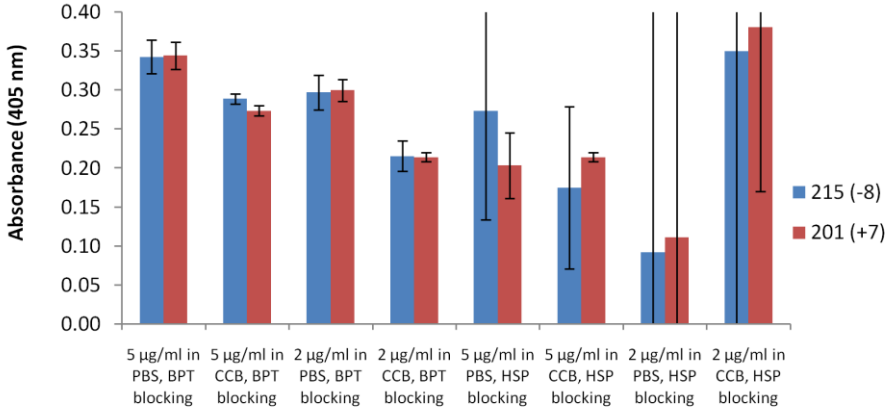

Figure 4.4: Indirect TcOPB ELISA comparing different TcOPB coating concentrations, dilution buffers and blocking buffers with infected and non-infected serum samples. ELISA plates were coated with TcOPB (5 and 2 µg/ml in PBS, pH 7.4 and CCB, pH 9.6), blocked with 0.5% (w/v) BSA-PBS, 0.1% (v/v) Tween-20 (BPT) and 1% horse serum-PBS (HSP) and incubated with sera (1:10 dilution). Rabbit anti-bovine IgG HRPO secondary antibody (1:10 000) and ABTS·H_2O_2 were used as the detection system. The absorbance readings at 405 nm represent the average of triplicate experiments after 30 min development. Each plate had a no serum control in quadruplicate.

4.3.2 Optimisation of inhibition and indirect TcPGP ELISA with *Trypanosoma congolense* infected and non-infected bovine sera

4.3.2.1 Inhibition TcPGP ELISA

Using the optimised TcPGP coating of 1 µg/ml in PBS and 5 µg/ml anti-TcPGP IgY from chicken 3, weeks 6 to 8 pool as described in section 3.3.6, a trial inhibition ELISA was performed with infected and non-infected serum samples. Corrected absorbance values at 405 nm for the non-infected serum samples were found to be slightly higher than those of the infected serum samples (Appendix C, Fig. C.2). When the percentage inhibition values were calculated, it was evident that the TcPGP inhibition ELISA was able to differentiate between non-infected and infected sera as the infected serum samples had higher percentage inhibition values than those for the non-infected serum samples, with the exception of serum 152 (-7) (Fig. 4.5).

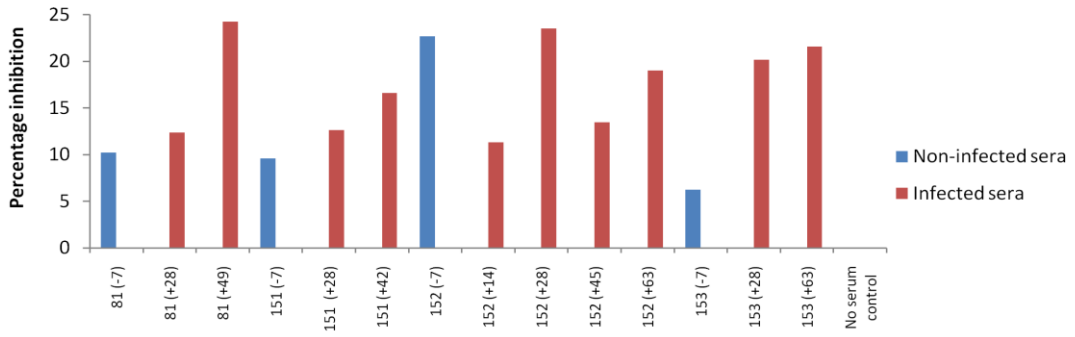

Figure 4.5: Inhibition TcPGP ELISA and anti-TcPGP IgY antibodies with infected and non-infected sera. ELISA plates were coated with TcPGP (1 µg/ml in PBS, pH 7.4), blocked with 0.5% (w/v) BSA-PBS, 0.1% (v/v) Tween-20 and incubated with sera (1:10 dilution). Thereafter anti-TcPGP IgY from chicken 3, weeks 6 to 8 pool (5 µg/ml) was added. Rabbit anti-chicken IgY HRPO secondary antibody (1:15 000) and ABTS·H_2O_2 were used as the detection system. The absorbance readings at 405 nm represent the average of triplicate experiments after 60 min development. Each plate had a no serum control in quadruplicate.

The optimisation of the anti-TcPGP IgY concentration using infected and non-infected serum samples in an inhibition ELISA format is shown in Fig. 4.6. The corrected absorbance values at 405 nm were higher at 5 µg/ml than at 2 µg/ml anti-TcPGP IgY, but were both high for the no serum control (Appendix C, Fig. C.3). Higher corrected absorbance values at 405 nm were measured for the non-infected serum samples than those measured for the infected serum samples (Appendix C, Fig. C.3). Upon the calculation of the percentage inhibition values, higher values were obtained for the infected serum samples than for the non-infected serum samples when 2 µg/ml of anti-TcPGP IgY was used compared to when 5 µg/ml anti-TcPGP IgY was used.

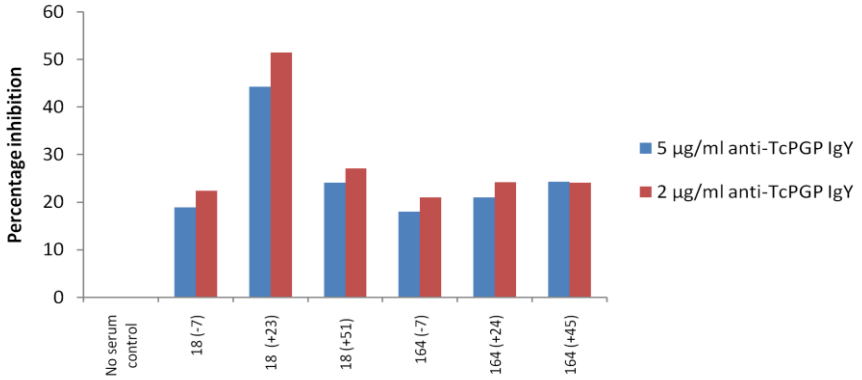

Figure 4.6: Inhibition TcPGP ELISA comparing anti-TcPGP IgY antibody concentrations with infected and non-infected sera. ELISA plates were coated with TcPGP (1 µg/ml in PBS, pH 7.4), blocked with 0.5% (w/v) BSA-PBS, 0.1% (v/v) Tween-20 and incubated with sera (1:10 dilution). Thereafter anti-TcPGP IgY from chicken 3, weeks 6 to 8 pool (5 and 2 µg/ml) was added. Rabbit anti-chicken IgY HRPO secondary antibody (1:15 000) and ABTS·H_2O_2 were used as the detection system. The absorbance readings at 405 nm represent the average of triplicate experiments after 60 min development. Each plate had a no serum control in quadruplicate.

Using the anti-TcPGP IgY primary antibody at 2 and 5 µg/ml, a panel of 49 known non-infected serum samples were tested to determine a cut-off value for the TcPGP inhibition ELISA. The corrected absorbance values at 405 nm were higher when using 5 µg/ml anti-TcPGP IgY compared to those at 2 µg/ml (Appendix C, Fig. C.4). From Fig. 4.7, the percentage inhibiton values at 2 µg/ml of anti-TcPGP IgY primary antibody were higher and were able to detect more serum samples than when the 5 µg/ml anti-TcPGP IgY primary antibody was used.

The optimal conditions for the TcPGP inhibition ELISA format for the blinded serum panel was found to be coating with TcPGP at 1 µg/ml in PBS, blocking with BPT, using anti-TcPGP IgY from chicken 3, weeks 6 to 8 pool at 2 µg/ml and rabbit-chicken IgY HRPO conjugate secondary antibody at a 1:15 000 dilution.

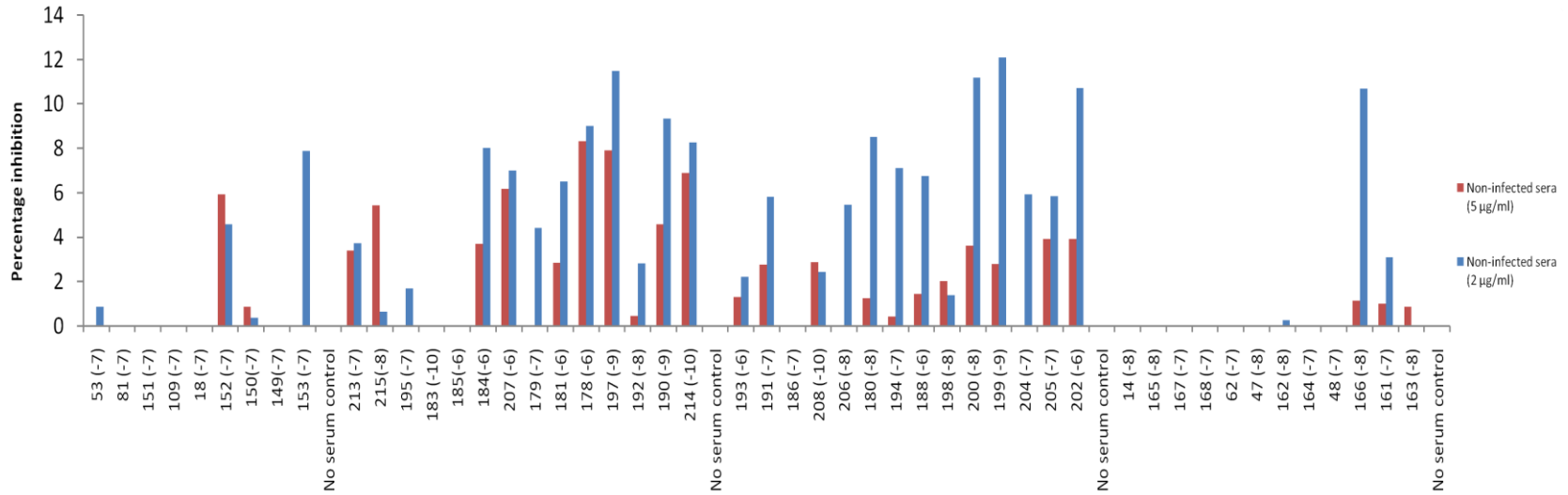

Figure 4.7: Inhibition TcPGP ELISA with non-infected sera to obtain a cut-off value. ELISA plates were coated with TcPGP (1 µg/ml in PBS, pH 7.4), blocked with 0.5% (w/v) BSA-PBS, 0.1% (v/v) Tween-20 and incubated with sera (1:10 dilution). Thereafter anti-TcPGP IgY from chicken 3, weeks 6 to 8 pool (5 and 2 µg/ml) was added. Rabbit anti-chicken IgY HRPO secondary antibody (1:15 000) and ABTS·H_2O_2 were used as the detection system. The absorbance readings at 405 nm represent the average of triplicate experiments after 60 min development. Each plate had a no serum control in quadruplicate.

4.3.2.2 Indirect TcPGP ELISA

Since the indirect ELISA format does not make use of a primary antibody, the optimal TcPGP coating concentration, diluent and blocking buffer were determined using one infected, 151 (+28), and one non-infected, 151 (-7), serum sample. Two diluents, PBS, pH 7.4 and CCB, pH 9.6, along with two blocking buffers, BPT and HSP were tested. After 20 min of development the corrected absorbance values at 405 nm were higher for the infected serum sample than those for the non-infected serum sample at each condition. Similar corrected absorbance values at 405 nm and discrimination between infected and non-infected serum samples were achieved using 2 and 5 µg/ml TcPGP in PBS and BPT as the blocking buffer (Fig. 4.8). The ideal conditions would be where the least amount of antigen yields the highest absorbance values, thus coating at 2 µg/ml was preferable over 5 µg/ml.

The optimal conditions for the TcPGP indirect ELISA format for the blinded serum panel was found to be coating with TcPGP at 2 µg/ml in PBS, using BPT as the blocking buffer and the rabbit anti-bovine IgG HRPO conjugate secondary antibody at a 1:10 000 dilution.

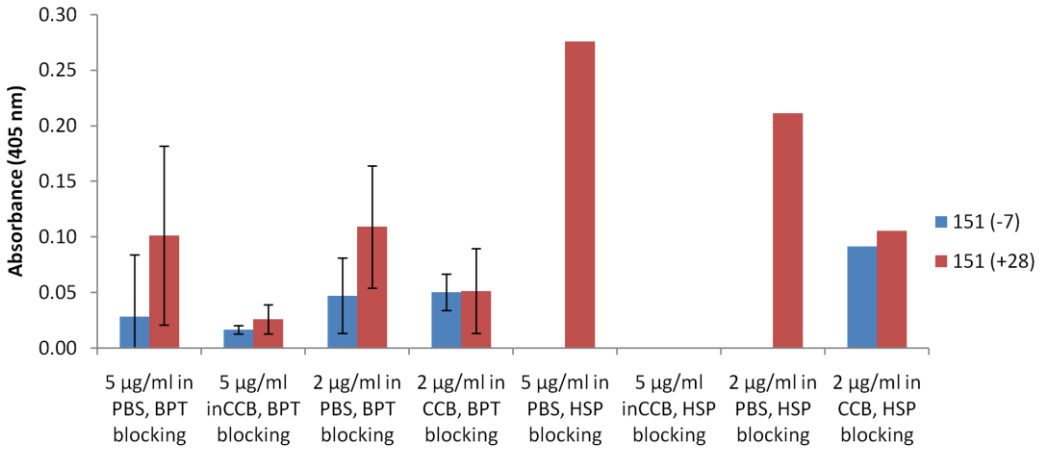

Figure 4.8: Checkerboard indirect TcPGP ELISA using different blocking buffers and coating conditions with an infected and a non-infected serum sample. ELISA plates were coated with TcPGP (5 and 2 µg/ml in PBS, pH 7.4 and CCB, pH 9.6), blocked with **(A)** 0.5% (w/v) BSA-PBS, 0.1% (v/v) Tween-20 (BPT) and **(B)** 1% (v/v) horse serum-PBS (HSP) and incubated with sera (1:10 dilution). Rabbit anti-bovine IgG HRPO secondary antibody (1:10 000) and ABTS·H_2O_2 were used as the detection system. The absorbance readings at 405 nm represent the average of triplicate experiments after 20 min development. Each plate had a no serum control in quadruplicate.

4.3.3 Optimisation of inhibition and indirect $TcCATL_{FL}$ ELISA with *Trypanosoma congolense* infected and non-infected bovine sera

4.3.3.1 Inhibition $TcCATL_{FL}$ ELISA

Using the optimised $TcCATL_{FL}$ coating of 0.05 µg/ml in PBS and 0.5 µg/ml affinity purified anti-$TcCATL_{FL}$ IgY from chicken 3, week 6 as described in section 3.3.8, a trial inhibition ELISA was performed with infected and non-infected serum samples. The corrected absorbance values at 405 nm were slightly higher for the non-infected serum samples than for the infected serum samples (Appendix C, Fig. C.5). Upon the calculation of the percentage inhibition values, with the exception of sera 48, 163, 190 and 200, the $TcCATL_{FL}$ inhibition ELISA was able to discriminate between infected and non-infected serum samples (Fig. 4.9).

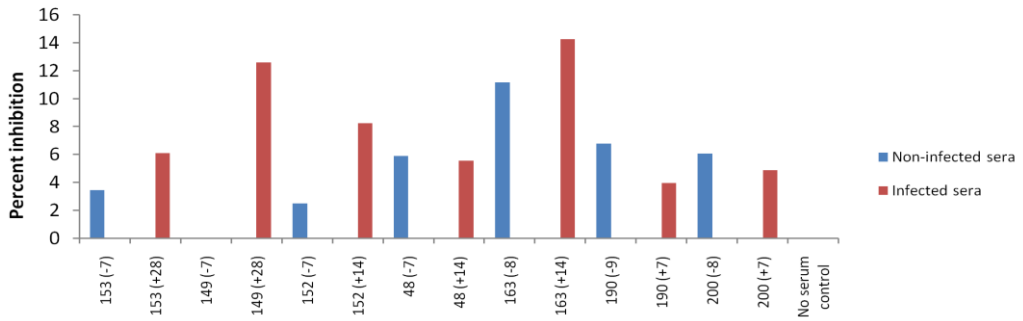

Figure 4.9: Inhibition $TcCATL_{FL}$ ELISA using affinity purified anti-$TcCATL_{FL}$ IgY antibodies with infected and non-infected sera. ELISA plates were coated with $TcCATL_{FL}$ (0.05 µg/ml in PBS, pH 7.4), blocked with 0.5% (w/v) BSA-PBS and incubated with sera (1:10 dilution). Thereafter affinity purified anti-$TcCATL_{FL}$ IgY from chicken 3, week 6 (0.5 µg/ml) was added. Rabbit anti-chicken IgY HRPO secondary antibody (1:20 000) and ABTS·H_2O_2 were used as the detection system. The absorbance readings at 405 nm represent the average of triplicate experiments after 60 min development. Each plate had a no serum control in quadruplicate.

The results presented in Fig. 4.9 confirmed that the optimised $TcCATL_{FL}$ coating and anti-$TcCATL_{FL}$ IgY concentrations were suitable for the inhibition ELISA format and were used to test 82 infected and 29 non-infected serum samples. The corrected absorbance values at 405 nm are found in Appendix C, Fig. C.6. With the exception of the non-infected serum samples 48, 81, 151, 178, 179, 181, 186, 193, 197 and 214 which gave abnormally high percentage inhibition values, the percentage inhibition for the infected sera samples were higher than those for their respective non-infected serum samples (Fig. 4.10).

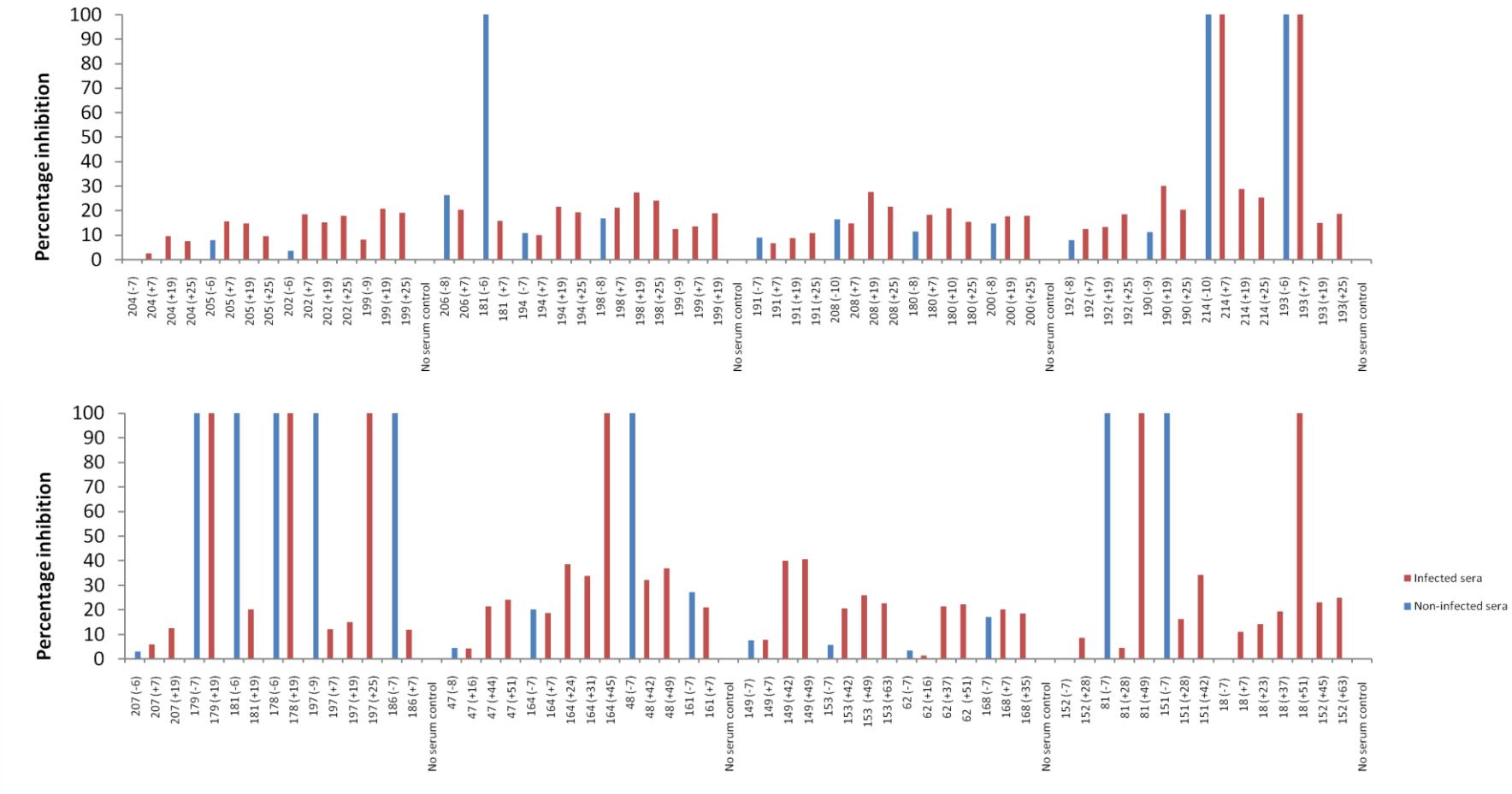

Figure 4.10: Mass inhibition TcCATL$_{FL}$ ELISA using affinity purified anti-TcCATL$_{FL}$ IgY antibodies with infected and non-infected sera. ELISA plates were coated with TcCATL$_{FL}$ (0.05 µg/ml in PBS, pH 7.4), blocked with 0.5% (w/v) BSA-PBS and incubated with sera (1:10 dilution). Thereafter affinity purified anti-TcCATL$_{FL}$ IgY primary antibodies from chicken 3, week 6 (0.5 µg/ml) were added. Rabbit anti-chicken IgY HRPO secondary antibody (1:15 000) and ABTS·H_2O_2 were used as the detection system. The absorbance readings at 405 nm represent the average of triplicate experiments after 60 min development. Each plate had a no serum control in quadruplicate.

Following the abnormally high percentage inhibition results for some of the non-infected sera seen in Fig. 4.10, non-specific binding might have been the cause. Optimisation of the blocking buffer was performed by testing the four different buffers against non-infected and infected serum samples from the same test animal , 149 (-7), 149 (+42) and 149 (+49) using: 0.5% (w/v) BSA-PBS (BP); 0.5% (w/v) BSA-PBS, 0.1% (v/v) Tween-20 (BPT); 0.2% (w/v) BSA-PBS, 0.05% (v/v) Tween-20 (BPTT) and 1% (v/v) horse serum-PBS (HSP).

The corrected absorbance values at 405 nm for the non-infected serum samples were lower than those for the infected serum samples, with infected serum 149 (+49) having almost the same values as the no serum control (Appendix C, Fig. C.7). This trend was evident with each blocking buffer. Using the BPT blocking buffer, the highest corrected absorbance values at 405 nm were obtained, followed by BP, HSP and BPTT. Seen in Fig. 4.11, all four blocking buffers resulted in percentage inhibition values which are higher for the non-infected serum samples than for the infected serum samples. The BPT buffer, however, resulted in the smallest difference in percentage inhibition values between the non-infected and the infected serum samples and was the most suitable buffer to use in further optimisation of the $TcCATL_{FL}$ inhibition ELISA.

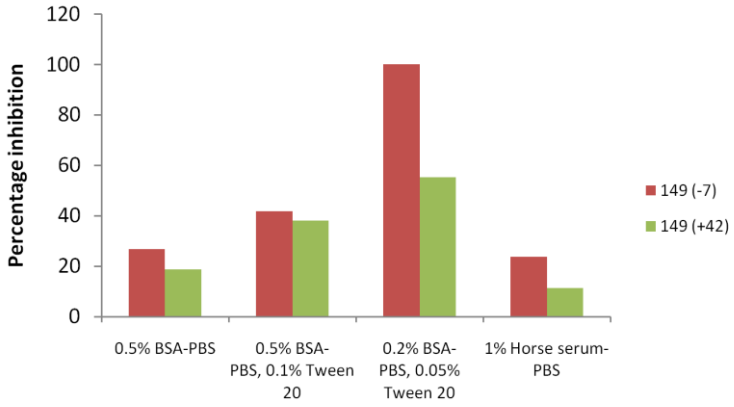

Figure 4.11: Inhibition $TcCATL_{FL}$ ELISA using affinity purified anti-$TcCATL_{FL}$ IgY antibodies in different blocking buffers with infected and non-infected sera. ELISA plates were coated with $TcCATL_{FL}$ (0.05 µg/ml in PBS, pH 7.4), blocked with **(A)** 0.5% (w/v) BSA-PBS, **(B)** 0.5% (w/v) BSA-PBS, 0.1% (v/v) Tween-20, **(C)** 0.2% (w/v) BSA-PBS, 0.05% (v/v) Tween-20 and **(D)** 1% (v/v) horse serum-PBS and incubated with sera (1:10 dilution). Thereafter affinity purified anti-$TcCATL_{FL}$ IgY from chicken 3, week 6 (0.5 µg/ml) was added. Rabbit anti-chicken IgY HRPO secondary antibody (1:15 000) and ABTS·H_2O_2 were used as the detection system. The absorbance readings at 405 nm represent the average of triplicate experiments after 60 min development. Each plate had a no serum control in quadruplicate.

Along with the new BPT blocking buffer, the ability of the crude and affinity purified anti-$TcCATL_{FL}$ antibodies to discriminate between infected and non-infected serum

samples was compared. The crude anti-TcCATL$_{FL}$ IgY antibodies resulted in higher corrected absorbance values at 405 nm than those for the affinity purified anti-TcCATL$_{FL}$ IgY but followed the same trend (Appendix C. Fig. C.8). The affinity purified anti-TcCATL$_{FL}$ IgY yielded lower percentage inhibtion values for the non-infected serum samples along with higher values for the infected samples when compared to that obtained with the crude anti-TcCATL$_{FL}$ IgY (Fig. 4.12). This was expected as the crude anti-TcCATL$_{FL}$ IgY antibodies were able to react with other proteins which may have been present in the serum, resulting in higher absorbance values and subsequently higher percentage inhibition values.

The optimal conditions for the TcCATL$_{FL}$ inhibition ELISA format for the blinded serum panel was found to be coating with TcCATL$_{FL}$ at 0.05 µg/ml in PBS, blocking with BPT, using affinity purified anti-TcTcCATL$_{FL}$ IgY from chicken 3, week 8 pool at 0.1 µg/ml and rabbit-chicken IgY HRPO conjugate secondary antibody at a 1:15 000 dilution.

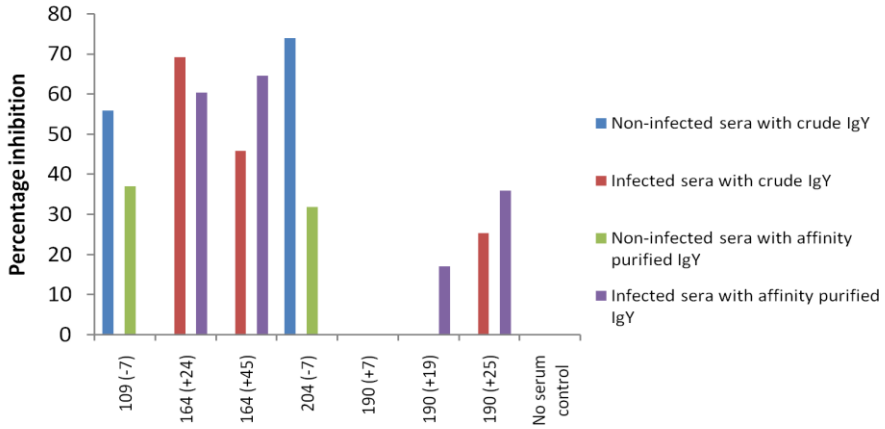

Figure 4.12: Inhibition TcCATL$_{FL}$ ELISA using crude and affinity purified anti-TcCATL$_{FL}$ IgY antibodies with infected and non-infected sera. ELISA plates were coated with TcCATL$_{FL}$ (0.05 µg/ml in PBS, pH 7.4), blocked with 0.5% (w/v) BSA-PBS, 0.1% (v/v) Tween-20 and incubated with sera (1:10 dilution). Thereafter affinity purified anti-TcCATL$_{FL}$ IgY primary from chicken 3, week 6 (0.1 µg/ml) and crude anti-TcCATL$_{FL}$ IgY from chicken 3, week 8 (10 µg/ml) were added. Rabbit anti-chicken IgY HRPO secondary antibody (1:15 000) and ABTS·H_2O_2 were used as the detection system. The absorbance readings at 405 nm represent the average of triplicate experiments after 45 min development. Each plate had a no serum control in quadruplicate.

4.3.3.2 Indirect TcCATL$_{FL}$ ELISA

Since the indirect ELISA format does not make use of a primary antibody, the optimal TcCATL$_{FL}$ coating concentration, diluent and blocking buffer were determined using one non-infected, 152 (-7), and one infected, 153 (+28), serum sample. Two diluents, PBS, pH 7.4 and CCB, pH 9.6, along with two blocking buffers, BPT and HSP were

tested. From Fig. 4.13, it was evident that coating with 2 µg/ml $TcCATL_{FL}$ in PBS and CCB as well as 5 µg/ml $TcCATL_{FL}$ in PBS and blocking with BPT gave the highest corrected absorbance values at 405 nm. Using these conditions, the corrected absorbance values at 405 nm were higher for the infected serum sample than for the non-infected serum sample and were comparable for each coating and blocking condition. The ideal conditions would be where the least amount of antigen yields the highest absorbance values, thus coating at 2 µg/ml was preferable over 5 µg/ml.

The optimial conditions for the $TcCATL_{FL}$ indirect ELISA format for the blinded serum panel was found to be coating with $TcCATL_{FL}$ at 2 µg/ml in PBS, using BPT as the blocking buffer and the rabbit anti-bovine IgG HRPO conjugate secondary antibody at a 1:10 000 dilution.

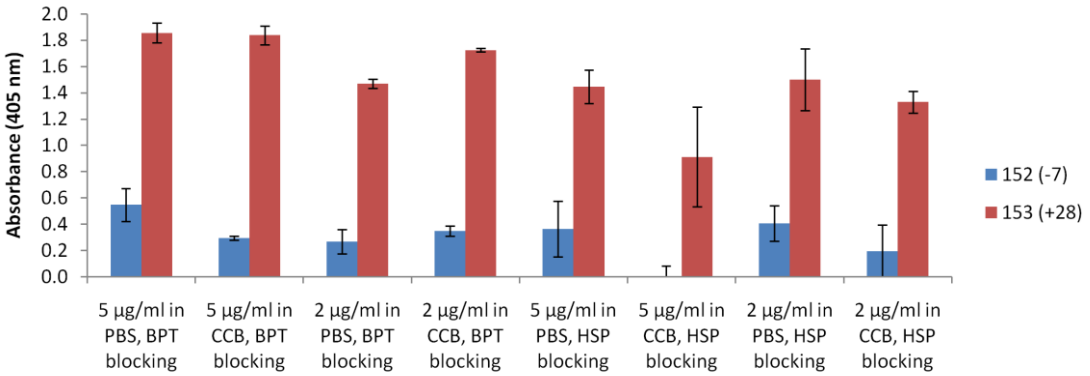

Figure 4.13: Indirect $TcCATL_{FL}$ ELISA using different blocking buffers and coating conditions with infected and non-infected sera. ELISA plates were coated with $TcCATL_{FL}$ (5 and 2 µg/ml in PBS, pH 7.4 and CCB, pH 9.6), blocked with 0.5% (w/v) BSA-PBS, 0.1% (v/v) Tween-20 (BPT) or 1% (v/v) horse serum-PBS (HSP) and incubated with sera (1:10 dilution). Rabbit anti-bovine IgG HRPO secondary antibody (1:10 000) and ABTS·H_2O_2 were used as the detection system. The absorbance readings at 405 nm represent the average of triplicate experiments after 20 min development. Each plate had a no serum control in quadruplicate.

4.3.4 Optimisation of inhibition and indirect TcCATL ELISA with *Trypanosoma congolense* infected and non-infected bovine sera

4.3.4.1 Inhibition TcCATL ELISA

Using the optimised TcCATL coating of 0.1 µg/ml in PBS and using 2.5 µg/ml anti-TcCATL IgY primary antibodies from chicken 3, week 11 or affinity purified anti-TcCATL N-terminal peptide IgY from pool 1 as described in section 3.3.9, trial

inhibition TcCATL ELISAs were performed with infected and non-infected serum samples.

The affinity purified anti-TcCATL N-terminal peptide IgY from pool 1 had lower corrected absorbance values at 405 nm when compared to those obtained using crude anti-TcCATL IgY from chicken 3, week 11 (Appendix C, Fig. C.9). However, when using the affinity purified anti-TcCATL N-terminal peptide IgY, the corrected absorbance values at 405 nm were higher for the infected serum samples than for the non infected serum samples. Upon the calculation of the percentage inhibition values, the non-infected serum samples had higher values than those of the infected serum samples. A single exception was found for infected serum 190 (+7) when the crude anti-TcCATL IgY antibody was used (Fig. 4.14).

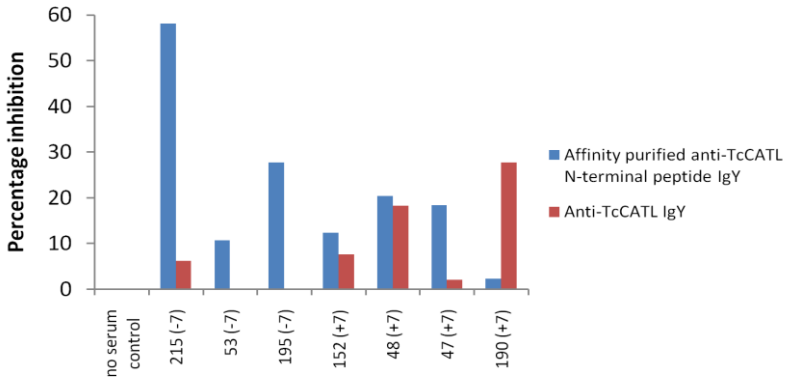

Figure 4.14: Inhibition TcCATL ELISA using anti-TcCATL and affinity purified anti-TcCATL N-terminal peptide IgY antibodies with infected and non-infected sera. ELISA plates were coated with TcCATL (0.1 µg/ml in PBS, pH 7.4), blocked with 0.5% (w/v) BSA-PBS and incubated with sera (1:10 dilution). Thereafter anti-TcCATL IgY from chicken 3, week 11 and affinity purified anti-TcCATL N-terminal peptide IgY from pool 1 (2.5 µg/ml) were added. Rabbit anti-chicken IgY HRPO secondary antibody (1:20 000) and ABTS·H_2O_2 were used as the detection system. The absorbance readings at 405 nm represent the average of triplicate experiments after 60 min development. Each plate had a no serum control in quadruplicate.

As a result of the low level of inhibition obtained with the anti-TcCATL N-terminal peptide IgY antibodies in the inhibition TcCATL ELISA, it was decided not to pursue the use of this particular antigen in the inhibition ELISA format with the panel of blinded serum samples.

4.3.4.2 Indirect TcCATL ELISA

Since the indirect ELISA format does not make use of a primary antibody, the optimal TcCATL coating concentration, diluent and blocking buffer was determined using one

infected, 151 (+28), and one non-infected, 151 (-7), serum samples. Two diluents, PBS, pH 7.4 and CCB, pH 9.6, along with two blocking buffers, BPT and HSP were tested. Seen in Fig. 4.15, the corrected absorbance values at 405 nm for the non-infected serum samples were higher than those for the infected serum samples at each of the conditions tested. The difference in the corrected absorbance values at 405 nm between the infected and non-infected serum samples were less when using the BPT blocking buffer compared to when the HSP blocking buffer was used. The ideal conditions would be where the least amount of antigen yields the highest absorbance values, thus coating at 2 µg/ml was preferable over 5 µg/ml.

The optimal conditions for the $TcCATL_{FL}$ indirect ELISA format for the panel of blinded serum samples was found to be coating with TcCATL at 2 µg/ml in PBS, using BPT as the blocking buffer and the rabbit anti-bovine IgG HRPO conjugate secondary antibody at a 1:10 000 dilution.

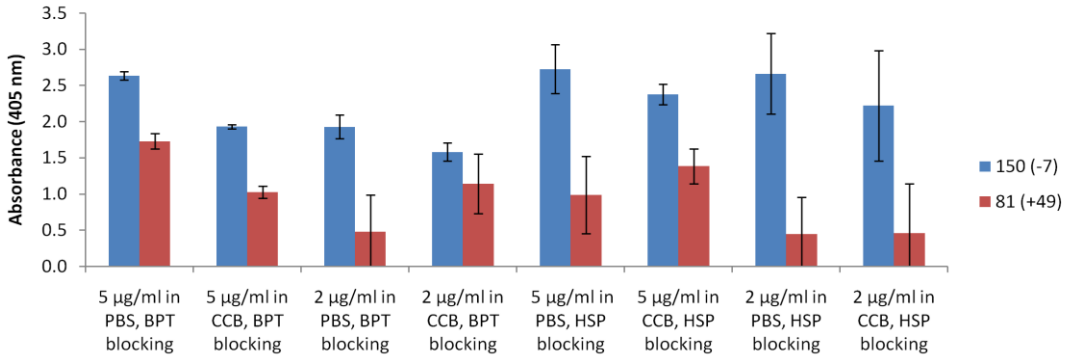

Figure 4.15: Indirect TcCATL ELISA comparing different TcCATL coating concentrations, buffers and blocking buffers with infected and non-infected sera. ELISA plates were coated with TcCATL (2 µg/ml in PBS, pH 7.4 and CCB, pH 9.6), blocked with 0.5% (w/v) BSA-PBS, 0.1% (v/v) Tween-20 (BPT) or 1% (v/v) horse serum-PBS (HSP) and incubated with sera (1:10 dilution). Rabbit anti-bovine IgG HRPO secondary antibody (1:10 000) and ABTS·H_2O_2 were used as the detection system. The absorbance readings at 405 nm represent the average of triplicate experiments after 30 min development. Each plate had a no serum control in quadruplicate.

4.3.5 Optimisation of indirect TvCATL ELISA with *Trypanosoma vivax* infected and non-infected bovine sera

Optimisation of indirect TvCATL ELISAs were only performed after the blinded serum panel using *T. congolense* infected serum samples as the experimental *T. vivax* infections were conducted later. The results of *T. congolense* blinded serum panel (Section 4.3.7), indicated that the indirect ELISA format yielded better specificity and

sensitivity for the tested antigens. Thus the *T. vivax* blinded serum panel was only conducted using the TvCATL and TvOPB antigens in the indirect ELISA format.

Using the optimised TvCATL coating of 0.5 µg/ml TvCATL in PBS, described in section 3.3.7, an indirect checkerboard ELISA trial was performed. The TvCATL indirect ELISA was optimised using one known non-infected serum sample along with three known infected serum samples and tested at three different coating concentrations along with four different dilutions of the rabbit anti-bovine IgG HRPO conjugate secondary antibody. The serum samples were used at a 1:100 dilution compared to the previous *T. congolense* blinded serum panel in the inhibition and indirect ELISA formats in which a 1:10 dilution was used.

Each of the three known infected serum samples were assigned a parasitaemia score of 6, which is the highest intensity of infection quantified (Woo, 1970), and were named P1, 2 and 3, samples 315 (+28), 263 (+28) and 321 (+28) respectively. From Fig. 4.16, although the corrected absorbance values at 405 nm were low, the highest corrected absorbance value at 405 nm was obtained for P1 at a secondary antibody dilution of 1:5 000 and TvCATL coating of 0.5 µg/ml in PBS. The P1 serum would be used as the known positive serum control which would be used to calculate the percentage positivity.

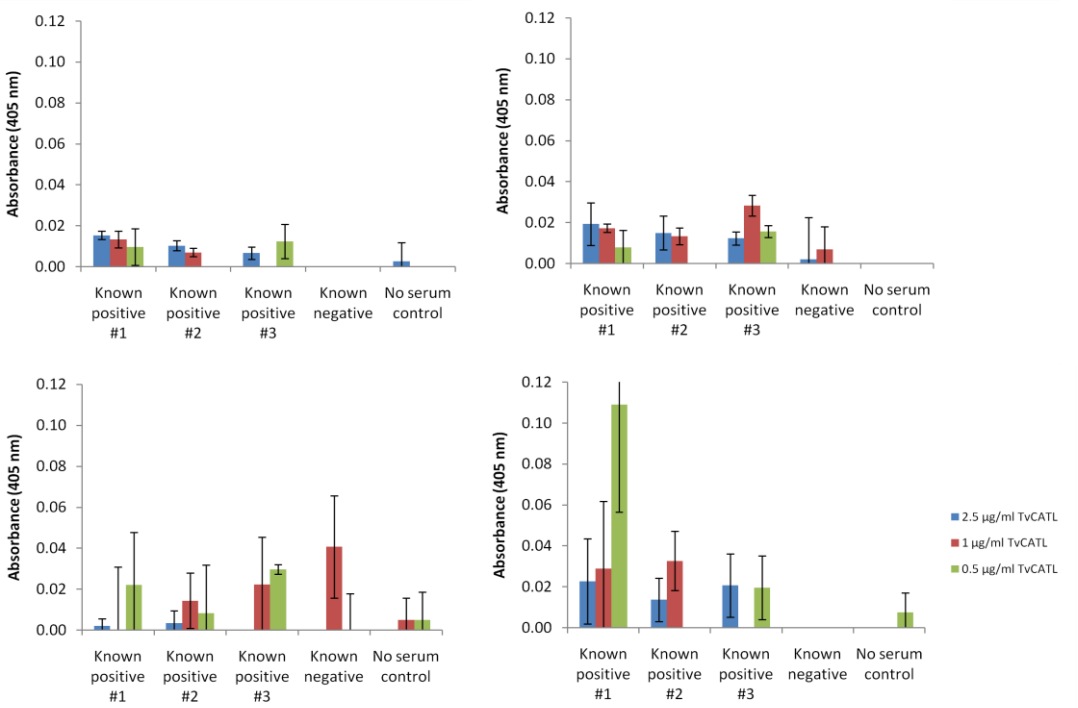

Figure 4.16: Indirect TvCATL ELISA using known infected and non-infected sera. ELISA plates were coated with TvCATL (2.5, 1 and 0.5 µg/ml in PBS, pH 7.4), blocked with 0.5% (w/v) BSA-PBS, 0.1% (v/v) Tween-20 and incubated with sera (1:100 dilution). Rabbit anti-bovine IgG HRPO secondary antibody [**(A)** 1:15 000, **(B)** 1:10 000, **(C)** 1:7 500 and **(D)** 1:5 000] and ABTS·H_2O_2 were used as the detection system. The absorbance readings at 405 nm represent the average of triplicate experiments after 30 min development. Each plate had a no serum control in quadruplicate.

4.3.6 Optimisation of indirect TvOPB ELISA with *Trypanosoma vivax* infected and non-infected bovine sera

Using the optimised TvOPB coating of 5 µg/ml in CCB, pH 9.6, described in section 3.3.5, an indirect checkerboard ELISA trial was performed. The TvOPB indirect ELISA was optimised using one known non-infected serum sample along with three known infected serum samples and tested at three different coating concentrations along with four different dilutions of the rabbit anti-bovine IgG HRPO conjugate secondary antibody. The serum samples were used at a 1:100 dilution compared to the previous *T. congolense* blinded serum panel in the inhibition and indirect ELISA in which a 1:10 dilution was used.

Each of the three known infected serum samples were assigned a parasitaemia score of 6, which is the highest intensity of infection quantified (Woo, 1970), and were named P1, 2 and 3, samples 315 (+28), 263 (+28) and 321 (+28) respectively. From Fig. 4.17, although the corrected absorbance values at 405 nm were low, the highest corrected absorbance value at 405 nm was obtained for P3 at a secondary antibody dilution of

1:15 000 and TvOPB coating at 5 µg/ml in CCB. The P3 serum would be used as the known positive serum control which would be used to calculate the percentage positivity.

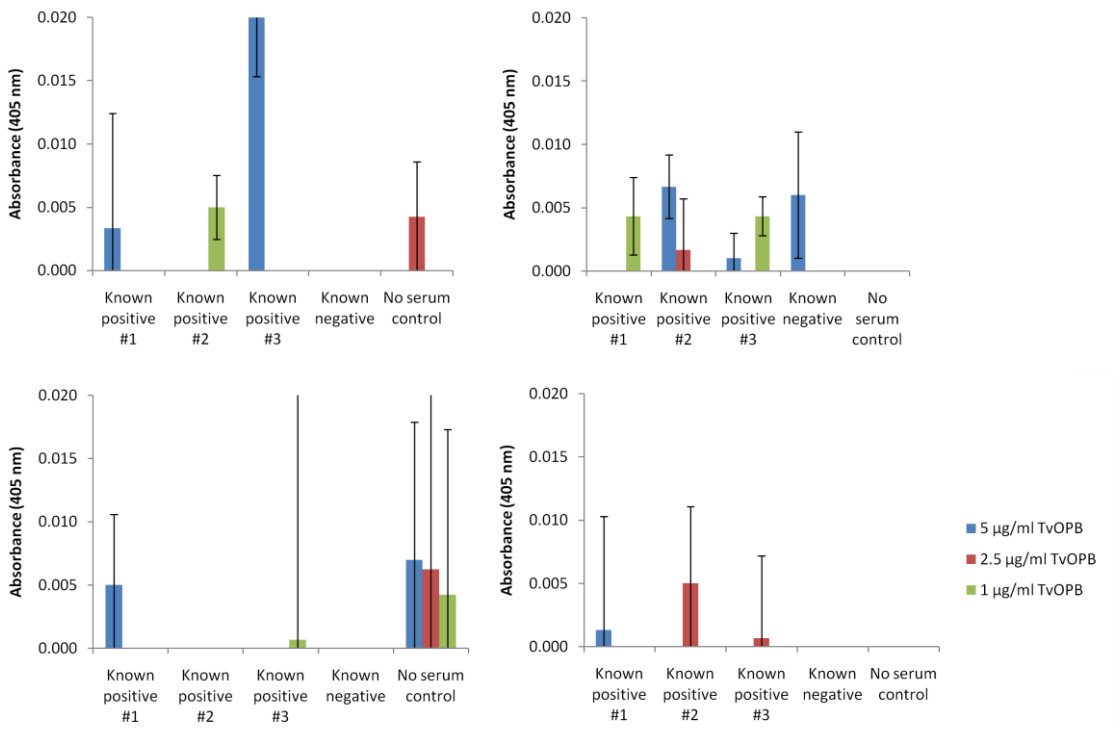

Figure 4.17: Indirect TvOPB ELISA using known infected and non-infected sera. ELISA plates were coated with TvOPB (5, 2.5 and 1 µg/ml in CCB, pH 9.6), blocked with 0.5% (w/v) BSA-PBS, 0.1% (v/v) Tween-20 and incubated with sera (1:100 dilution). Rabbit anti-bovine IgG HRPO secondary antibody [**(A)** 1:15 000, **(B)** 1:10 000, **(C)** 1:7 500 and **(D)** 1:5 000] and ABTS·H_2O_2 were used as the detection system. The absorbance readings at 405 nm represent the average of triplicate experiments after 30 min development. Each plate had a no serum control in quadruplicate.

4.3.7 *Trypanosoma congolense* blinded serum panel using the inhibition and indirect ELISA formats with the TcOPB, TcPGP, $TcCATL_{FL}$ and TcCATL antigens

The optimised antigen coating concentrations, the respective primary antibody concentration and the secondary antibody dilution for each antigen for each ELISA format is given in Table 4.1. The testing of the *T. congolense* blinded serum panel using the TcCATL antigen was only attempted using the indirect ELISA format due to the poor results obtained in the optimisations of the inhibition ELISA format for this antigen. The *T. congolense* blinded serum panel was tested at 1:10 dilution.

Table 4.1: Summary of optimised conditions for the testing of the *T. congolense* blinded serum panel using the inhibition and indirect ELISA formats.

ELISA format	Antigen	Antigen concentration in PBS (µg/ml)	Primary antibody	Primary antibody concentration (µg/ml)	Secondary HRPO conjugate antibody dilution
Inhibition	TcOPB	1	Anti-TcOPB IgY from chicken 3, week 10	1	Rabbit anti-chicken IgY 1:30 000
	TcPGP	1	Anti-TcPGP IgY from chicken 3, weeks 6 to 8	2	
	$TcCATL_{FL}$	2	Affinity purified anti-$TcCATL_{FL}$ IgY from chicken 3, week 6	0.5	
Indirect	TcOPB	5	-	-	Rabbit anti-bovine IgG 1:10 000
	TcPGP	5	-	-	
	$TcCATL_{FL}$	2	-	-	
	TcCATL	2	-	-	

The corrected absorbance values at 405 nm were used to calculate the percentage inhibition and percentage positivity for each of the serum samples of the blinded serum panel along with the panel of known negative/non-infected serum samples, in the inhibition and indirect ELISA formats respectively. This allowed for the determination of cut-off values and the subsequent prediction of the infection status of each of the samples.

After the panel was unblinded, the sensitivity and specificity of each antigen in each of the ELISA formats were calculated. The blinded panel consisted of 77 samples of which 39 were positive and the remaining 38 were negative.

Table 4.2: The decision matrix to determine the specificity and sensitivity of a diagnostic test. Adapted from Park and co-workers (2004).

	True disease status		
Test result	Positive	Negative	
Positive	TP	FP	
Negative	FN	TN	
Total	P	N	P + N

*TP, true positive; FP, false positive; FN, false negative and TN, true negative.

Using the decision matrix from Table 4.2, the infection status predictions from each antigen in each ELISA format was used to generate Table 4.3. From the data in Table 4.3, the sensitivity, specificity, accuracy, positive predictive value (PPV) and negative predictive values (NPV) for each antigen and each ELISA format were

calculated (Tables 4.4 and 4.5). Accuracy is defined as the probability that the test yields a correct result, sensitivity as the probability that a true infection will test positive, specificity as the probability that a true non-infected case will test negative, 100%-specificity as the probability that a true negative will test positive, the PPV as the probability that an animal giving a positive test will truly be infected and the NPV as the probability that an animal giving a negative test will truly be disease free. Using the annotations in Table 4.2, accuracy was calculated by (TP + TN)/(P+N), sensitivity by TP/P, specificity by TN/N, 100%-specificity by FP/N, PPV by TP/(TP+FP) and NPV by TN/(TN + FN). Thus the ideal diagnostic test would have high accuracy, sensitivity, specificity, PPV and NPV values along with a low 100%-specificity value.

At some of the cut-off values for each antigen tested in the inhibition and indirect ELISA formats (Table 4.4 and 4.5 respectively), higher or lower values for the above-mentioned parameters were obtained and thus the best combination thereof was selected and highlighted.

Table 4.3: Scores from the *T. congolense* blinded serum panel using the inhibition and indirect ELISA formats at the second cut-off[a].

ELISA result	Number of serum samples with predicted infection statuses													
	Inhibition						Indirect							
	TcOPB		TcPGP		$TcCATL_{FL}$		TcOPB		TcPGP		$TcCATL_{FL}$		TcCATL	
	Positive	Negative	Positive	Negative	Positive	Negative	Positive	Negative	Positive	Negative	Positive	Negative	Positive	Negative
Positive	0	0	9	3	30	10	16	8	1	1	39	6	38	5
Negative	39	38	28	37	13	24	23	30	38	37	1	31	1	33

[a] n = 77.

Table 4.4: Calculated specificity and sensitivity values for the *T. congolense* blinded serum panel using the inhibition ELISA format.

Antigen		Cut-off (%)	Specificity (%)	100-specificity (%)	NPV (%)	Sensitivity (%)	PPV (%)	Accuracy (%)
TcOPB[a]	Mean + 1SD	51.72	100.00	5.26	50.67	0.00	9.41	49.35
	Mean + 2SD	133.7	100.00	0.00	50.67	0.00	ND	49.35
	Mean + 3SD	215.67	100.00	0.00	50.67	0.00	ND	49.35
TcPGP[b]	Mean + 1SD	20.4	73.68	26.32	57.14	46.15	31.53	59.74
	Mean + 2SD	29.27	92.11	7.89	56.92	23.08	12.18	57.14
	Mean + 3SD	38.13	94.74	5.26	56.94	7.69	8.46	50.65
$TcCATL_{FL}$[a]	Mean + 1SD	13.82	47.37	52.63	64.29	74.36	45.02	61.04
	Mean + 2SD	22.13	63.16	26.32	64.86	76.92	28.86	70.13
	Mean + 3SD	30.22	76.32	23.68	67.44	64.10	25.99	70.13

[a] cut-off values at 30 min development.
[b] cut-off values at 45 min development.
ND: not determined

Table 4.5: Calculated specificity and sensitivity values for the *T. congolense* blinded serum panel using the indirect ELISA format.

Antigen		Cut-off (%)	Specificity (%)	100-specificity (%)	NPV (%)	Sensitivity (%)	PPV (%)	Accuracy (%)
TcOPB[a]	Mean + 1SD	16.25	42.11	57.89	55.17	66.67	51.20	54.55
	Mean + 2SD	22.21	78.95	21.05	56.60	41.03	27.11	59.74
	Mean + 3SD	28.18	89.47	13.16	54.84	25.64	19.35	57.14
TcPGP[a]	Mean + 1SD	28.68	81.58	15.79	49.21	20.51	24.29	50.65
	Mean + 2SD	64.46	97.37	2.63	49.33	2.56	5.06	49.35
	Mean + 3SD	100.2	100.00	0.00	49.35	0.00	ND	49.35
$TcCATL_{FL}$[a]	Mean + 1SD	33.86	68.42	28.95	92.86	97.44	23.77	83.12
	Mean + 2SD	49.50	81.58	15.79	96.88	100.00	14.01	90.91
	Mean + 3SD	65.15	89.47	10.53	91.89	92.31	10.28	90.91
TcCATL[a]	Mean + 1SD	18.33	73.68	26.32	96.55	97.44	21.42	85.71
	Mean + 2SD	26.19	86.84	13.16	97.06	97.44	11.94	92.21
	Mean + 3SD	34.07	89.47	7.89	97.14	100.00	7.52	94.81

[a] cut-off values at 30 min development.
ND: not determined

Using the TcOPB antigen in the inhibition ELISA format resulted in very high cut-off values (51.72 to 200.67%), large degrees of standard deviation, and 100% sensitivity at a cost of 0% specificity. This indicates that the test was unable to discriminate between infected and non-infected serum samples as shown by an accuracy of 49.35%, i.e. the diagnosis was made by chance.

Diagnosis of *T. congolense* infection using the indirect TcOB ELISA showed higher specificity (78.95%), PPV (51.20%) and accuracy values at the second cut-off. The values for sensitivity (66.67%) and PPV (51.20%) were higher at the first cut-off. A large difference in the PPV and 100%-specificity values existed between the first and second cut-offs, and together with the other parameters, a definite choice in cut-off could not be made.

The inhibition TcPGP ELISA gave a higher specificity (92.11%) at the second cut-off when compared to that obtained at the first cut-off (73.68%). However, the 100%-specificity, sensitivity, PPV and accuracy values at the first cut-off were higher than at the second cut-off, both of which shared the same NPV value. Upon comparison of the results, the second cut-off might be better than the first as for a small difference in accuracy (59 to 57%), a lower 100%-specificity value (7 to 26%) was achieved which led to a smaller probability that a truly non-infected serum sample will test positive.

The use of the TcPGP antigen in the indirect ELISA format resulted in high cut-off values with large degrees of standard deviation. With high specificity values (81.58 to 100%), low sensitivity values (0 to 20.51%), average NPV values (49.21 to 49.35% and accuracy values between 49.35 and 50.65%, the use of the TcPGP antigen in this ELISA format was unable to effectively discriminate between infected and non-infected serum samples.

The inhibition $TcCATL_{FL}$ ELISA, despite some values being higher or lower at the first and third cut-off values, the best combination was obtained at the second cut-off. At this cut-off, the test was characterised by a good accuracy of 70.13%, along with good sensitivity, specificity and NPV values of 76.92, 63.16 and 64.86% respectively. The ability of the $TcCATL_{FL}$ antigen in this ELISA format was able to discriminate between infected and non-infected serum samples.

The use of the indirect $TcCATL_{FL}$ ELISA for the diagnosis of *T. congolense* infections resulted in high specificity (81.53%), NPV (96.88%), sensitivity (100 %) and accuracy (90.91%) values at the second cut-off. When considering the high NPV value (96.88%)

along with the low PPV value (14.01%), this indicates that the test was more likely to correctly distinguish the non-infected serum samples from infected samples. A low 100%-specificity value of 15.79% along with the above parameters proves that the $TcCATL_{FL}$ antigen in this ELISA format was able to discriminate between infected and non-infected serum samples, more so in the indirect format than the inhibition format.

The indirect TcCATL ELISA, despite some values being higher or lower at the first and third cut-off values, gave the best combination at the second cut-off. Characterised by high specificity (86.84%), sensitivity (97.44%), NPV (97.06%), a low 100%-specificity (13.16%) and an overall accuracy of 92.21% at the second cut-off, the TcCATL antigen used in this ELISA format was able to discriminate between infected and non-infected serum samples, more so for the non-infected serum samples due to the low PPV value (11.94%).

In Tables 4.4 and 4.5 only three cut-off values were used. The use of ROC curves enabled the visualisation of a large number of sensitivity and specificity combinations at different cut-off values which allowed for a more accurate choice of the optimal cut-off value. The calculated percentage inhibition and percentage positivity values from the inhibition and indirect ELISA formats respectively, testing the *T. congolense* blinded serum panel, were used to generate the ROC curves using GraphPad Prism version 6.00 for Windows software (Fig. 4.18).

The ROC analysis of the *T. congolense* blinded serum panel in the inhibition and indirect ELISA formats for each of the antigens used is shown in Fig. 4.18 from which the sensitivity and specificity were determined. The ROC curve is characterised by its AUC and P values, the closer the AUC tends to one and the smaller the P value. This is an indication of the ability of each antigen in each ELISA format to discriminate between infected and non-infected serum samples.

High P values (0.2078 to 0.4896), AUC values close to 0.5 and low Youden indices (0.2208 to 0.2922) were obtained for the TcPGP antigen in both the inhibition and indirect ELISA formats as well as for the TcOPB antigen in the inhibition format which confirmed that these tests were unable to discriminate between infected and non-infected serum samples (Table 4.6). This indicated that these antigens have little diagnostic potential in the ELISA format. Low P (<0.0001 to 0.000249) and high AUC values (0.7785 to 0.8084) along with high Youden indices (0.4979 to 0.5642) were obtained for both the TcOPB and TcCATL antigens in the indirect ELISA format as well as for the $TcCATL_{FL}$ antigen in both the inhibition and indirect ELISA formats. This

confirms that these antigens in the respective ELISA formats have diagnostic potential as they were able to discriminate between infected and non-infected serum samples (Table 4.6).

When comparing the cut-off values from Tables 4.4 and 4.5 with those calculated from the ROC curves (Table 4.6), lower values were obtained using the ROC evaluation. The sensitivity and specificity values for both analyses were within the same range, and it was determined that the first cut-off was optimal for the TcCATL antigen in the indirect ELISA format reported in Table 4.5 as they were closer to that obtained from the ROC analysis.

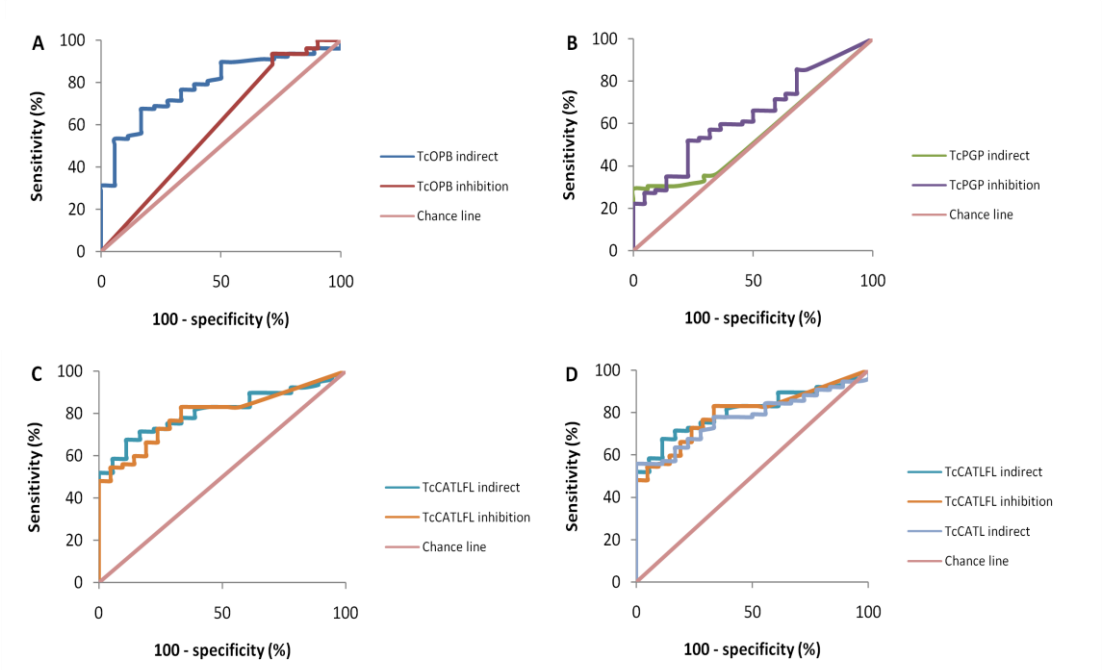

Figure 4.18: ROC analysis of the inhibition and indirect ELISA formats using the TcOPB, TcPGP, $TcCATL_{FL}$ and TcCATL antigens for the detection of *T.congolense* infections in cattle. The ROC curves for the specified antigens in both the inhibition and indirect ELISA formats are shown in: panel **(A)** TcOPB, **(B)** TcPGP, **(C)** $TcCATL_{FL}$ and **(D)** TcCATL compared to $TcCATL_{FL}$.

Table 4.6: ROC-based indices of diagnostic accuracy of the inhibition and indirect ELISA formats, testing different antigens with the *T. congolense* blinded serum panel.

	Inhibition			Indirect			
	TcOPB	TcPGP	$TcCATL_{FL}$	TcOPB	TcPGP	$TcCATL_{FL}$	TcCATL
AUC	0.5900	0.6417	0.7968	0.7872	0.5536	0.8084	0.7785
Standard Error	0.07529	0.06165	0.0459	0.05218	0.06816	0.04486	0.04749
95 % CI	0.4424 to 0.7376	0.5208 to 0.7625	0.7069 to 0.8868	0.6849 to 0.9984	0.4200 to 0.6872	0.7205 to 0.8964	0.6854 to 0.8716
P value	0.2078	0.4344	<0.0001	0.00016	0.4896	<0.0001	0.000249

Table 4.7: Optimal sensitivity and specificity of the selected antigens which were used to test the *T. congolense* blinded serum panel in the inhibition and indirect ELISA formats.

	Inhibition			Indirect			
	TcOPB	TcPGP	$TcCATL_{FL}$	TcOPB	TcPGP	$TcCATL_{FL}$	TcCATL
Cut-off (%)	28.77	16.93	20.43	14.75	26.71	27.10	25.50
Sensitivity (%)	93.51	51.95	54.55	67.53	29.11	67.53	55.84
95 % CI (%)	85.49 to 97.86	40.26 to 63.48	42.79 to 65.94	55.90 to 77.77	19.43 to 40.42	55.90 to 77.77	44.07 to 67.16
Specificity (%)	28.57	77.27	95.24	83.33	94.12	88.89	94.44
95 % CI (%)	11.28 to 52.18	54.63 to 92.18	76.18 to 99.88	58.58 to 96.42	71.31 to 99.85	65.29 to 98.62	72.71 to 99.86
Youden Index	0.2208	0.2922	0.4979	0.5086	0.2911	0.5642	0.5028

4.3.8 *Trypanosoma vivax* blinded serum panel using the indirect ELISA format with the TvCATL and TvOPB antigens

The optimised antigen coating concentrations and the secondary antibody dilution for each tested antigen in the indirect ELISA format are given in Table 4.8. The serum samples which comprised the blinded serum panel were tested at 1:100 and 1:10 dilutions.

Table 4.8: Summary of conditions for the testing of the *T. vivax* blinded serum panel using the indirect ELISA format.

Antigen	Antigen concentration and diluent (µg/ml)	Rabbit anti-bovine IgG HRPO conjugate secondary antibody dilution	Known positive serum control
TvCATL	0.5 in PBS	1:5 000	P1, 315 (+28)
TvOPB	5 in CCB	1:15 000	P3, 321 (+28)

Fourteen randomly selected serum samples from the blinded serum panel were tested at 1:100 and 1:10 dilutions and the resulting corrected absorbance values at 405 nm and percentage positivity values were compared. Higher corrected absorbance values at 405 nm were obtained for the 1:10 diluted serum samples, with the exception of serum samples 76 and 90, with the known positive serum sample having the highest corrected absorbance at 405 nm when diluted 1:10 instead of 1:100 (Appendix C, Fig. C.10). Using a 1:100 serum dilution resulted in higher percentage positivity for the fourteen selected serum samples, except for serum 83, compared to those obtained at a 1:10 serum dilution (Fig.4.19).

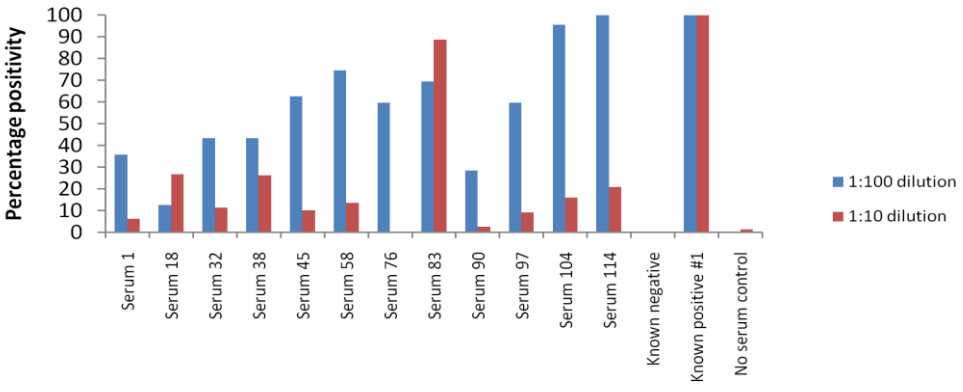

Figure 4.19: Comparison of serum dilutions in the indirect TvCATL ELISA testing a selection of serum samples from the *T. vivax* blinded serum panel. ELISA plates were coated with TcCATL (0.5 µg/ml in PBS, pH 7.4), blocked with 0.5% (w/v) BSA-PBS, 0.1% (v/v) Tween-20 and incubated with sera (1:100 and 1:10 dilutions). Rabbit anti-bovine IgG HRPO secondary antibody (1:5 000) and ABTS·H_2O_2 were used as the detection system. The absorbance readings at 405 nm represent the average of triplicate experiments at 30 min development. Each plate had a no serum control in quadruplicate.

The corrected absorbance values at 405 nm obtained were used to calculate the percentage positivity for each of the serum samples comprising the *T. vivax* blinded serum panel along with the panel of known non-infected serum samples which were tested in the indirect ELISA format. This allowed for the determination of three cut-off values and the subsequent prediction of the infection status of each of the *T. vivax* blinded panel tested serum samples.

After the panel was unblinded, the sensitivity and specificity of each antigen in the indirect ELISA format was calculated. The blinded panel consisted of 72 samples of which 31 were positive and the remaining 41 were negative.

The decision matrix outlined in Table 4.2 was used to predict the infection status of each of the tested serum samples (Table 4.9). From the data in Table 4.9, the sensitivity, specificity, accuracy, PPV, NPV and 100%-specificity values for each antigen at each serum dilution were calculated (Table 4.10). At some of the cut-off values for each antigen tested in the indirect ELISA format at the different serum dilutions (Table 4.10), higher or lower values for the above-mentioned parameters were obtained and thus the best combination thereof was selected and highlighted.

Table 4.9: Scores from the *T. vivax* blinded serum panel using the indirect ELISA format at the third cut-off[a].

ELISA result	Number of serum samples with predicted infection statuses							
	TvOPB (1:10)		TvOPB (1:100)		TvCATL (1:10)		TvCATL (1:100)	
	Positive	Negative	Positive	Negative	Positive	Negative	Positive	Negative
Positive	0	0	3	7	10	21	18	7
Negative	31	41	25	37	1	40	13	34

[a] *n* = 72.

Table 4.10: Calculated specificity and sensitivity values for the *T. vivax* blinded serum panel using the indirect ELISA format[a].

Antigen (serum dilution)		Cut-off (%)	Specificity (%)	100-specificity (%)	NPV (%)	Sensitivity (%)	PPV (%)	Accuracy (%)
TvOPB (1:10)	Mean + 1SD	97.69	100.00	0.00	56.94	0.00	ND	56.94
	Mean + 2SD	142.32	100.00	0.00	56.94	0.00	ND	56.94
	Mean + 3SD	186.94	100.00	0.00	56.94	0.00	ND	56.94
TvOPB (1:100)	Mean + 1SD	43.65	80.49	18.42	56.9	22.58	50	55.56
	Mean + 2SD	58.45	82.93	15.79	53.97	9.68	33.33	51.39
	Mean + 3SD	73.24	90.24	10.53	56.92	9.68	42.86	55.56
TvCATL (1:10)	Mean + 1SD	14.43	80.49	21.05	67.35	48.39	65.22	66.67
	Mean + 2SD	19.66	92.68	7.89	64.41	32.26	76.92	66.67
	Mean + 3SD	24.9	97.56	2.63	65.57	32.26	90.91	69.44
TvCATL (1:100)	Mean + 1SD	36.83	17.07	89.47	53.85	80.65	42.37	44.44
	Mean + 2SD	51.73	46.34	57.89	73.08	77.42	52.17	59.72
	Mean + 3SD	66.63	82.93	18.42	72.34	58.06	72.00	72.22

[a] cut-off values at 40 min development.
ND: not determined

Using the TvOPB antigen in the indirect ELISA format testing the serum panel at a 1:10 dilution, high cut-off values (97.69 to 186.94%) with large standard deviations were obtained thus discrimination could not be made between infected and non-infected serum samples at any of the cut-offs. This might have been caused by the low absorbance values at 405 nm even before they were corrected for the no-coat control, and as a result when the percentage positivity was calculated, large values were obtained of which many had to be adjusted to fall between the 0 to 100% limits.

Diagnosis of *T. vivax* infections using the indirect TvOPB ELISA showed that at a 1:100 serum dilution, high specificity (90.24%) with a low sensitivity (9.68%) was obtained at the third cut-off. The accuracy, PPV and NPV values were average (55.56, 42.86 and 56.92% respectively) with a low 100%-specificity value (10.53%) indicating the TvOPB antigen in this ELISA format, using a 1:100 serum dilution, was more able to correctly diagnose the non-infected rather than the infected serum samples due to the low sensitivity and PPV values.

Using the TvCATL antigen in the indirect ELISA format testing the serum panel at a 1:10 serum dilution, high specificity (97.56%), PPV (90.91%) and accuracy (69.44%) values were obtained at the third cut-off with slightly higher NPV and sensitivity values at the second cut-off. A low 100%-specificity value of 2.62% along with the above parameters proves that the $TcCATL_{FL}$ antigen in this ELISA format was able to discriminate between infected and non-infected serum samples, more so for the non-infected samples due to the low sensitivity (32.26%) despite the high PPV value of 90.91%.

The indirect TvCATL ELISA of the serum panel using a 1:100 serum dilution resulted in high specificity (82.93%), NPV (73.34%), PPV (72.00%) and accuracy (72.22%) values at the third cut-off. A low 100%-specificity (18.42%) and an average sensitivity (55.06%) along with the above parameters proves that the $TcCATL_{FL}$ antigen in this ELISA format was able to discriminate between infected and non-infected serum samples, more so for the non-infected serum samples. Using a 1:100 serum dilution along with the TvCATL antigen in an indirect ELISA format yielded higher sensitivity, accuracy and NPV values than when a 1:10 serum dilution was used. Despite the increased 100%-specificity and decreased PPV values, testing the serum at a 1:100 dilution led to better overall results.

The ROC analysis of the *T. vivax* blinded serum panel in the indirect ELISA format for each of the antigens used is shown in Fig. 4.20 from which the sensitivity and

specificity for each antigen at each serum dilution was determined The percentage positivity values from the TvCATL antigens were used to generate the ROC curves. The non-corrected absorbance values at 405 nmn were used to create the ROC curves for the TvOPB antigen due to the low non-corrected absorbance values at 405 nm and their resulting high percentage positivity values.

Along with high P values (0.0671 to 0.7740), AUC values close to 0.5 were obtained for the TvCATL antigen using a 1:10 serum dilution and for the TvOPB antigen using a 1:100 serum dilution in the indirect ELISA format. Despite the high Youden index obtained for the TvOPB antigen (0.5167), these values confirm that these tests were unable to discriminate between infected and non-infected serum samples and thus have very little diagnostic potential (Table 4.11). However, low P (<0.0001 to 0.0009148) and high AUC values (0.7345 to 0.8813) along with high Youden indices (0.5745 and 0.6768) were obtained for the TvCATL antigen using a 1:100 serum dilution and for the TvOPB antigen using a 1:10 serum dilution respectively in the indirect ELISA format. This confirms that these tests were able to discriminate between infected and non-infected serum samples and thus have promising diagnostic potential (Table 4.11).

When comparing the cut-off, specificity and sensitivity values calculated in Table 4.10 with those calculated from the ROC analysis (Table 4.11), the values for the TvCATL antigen at both serum dilutions were favourable and all within approximately 12 units of each. Due to the fact that the absorbance values were used instead of the percentage positivity values to create the ROC curves for the TvOPB antigen, the results are only a guideline since using the absorbance values the calculation of the serum sample's percentage positivity was not made with respect to the known infected serum control. When comparing the TvOPB ELISA results in Table 4.10 to those obtained in the ROC analysis (Table 4.12) when the serum was tested at a 1:10 dilution a large difference is obtained. Thus the diagnostic potential of the TvOPB antigen in the indirect ELISA format using a 1:10 serum dilution cannot be confirmed.

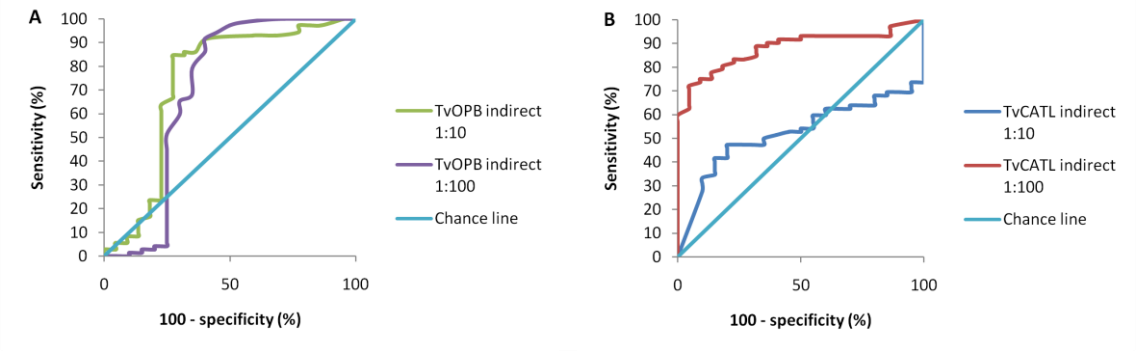

Figure 4.20: ROC analysis of the indirect antibody detection ELISA format using the TvOPB and TvCATL antigens for the detection of *T. vivax* infections in cattle. The ROC curves for the specified antigens in the indirect ELISA format at a 1:10 and 1:100 serum dilutions are shown in: panel **(A)** TvOPB antigen using the non-corrected absorbance values at 405 nm and **(B)** TvCATL antigen using the percentage positivity values.

Table 4.11: ROC-based indices of diagnostic accuracy of the indirect antibody detection ELISA, testing different antigens against the *T. vivax* blinded serum panel.

	Indirect (serum dilution)			
	TvOPB (1:10)[a]	TvOPB (1:100)[a]	TvCATL (1:10)	TvCATL (1:100)
AUC	0.7345	0.6690	0.5240	0.8813
Standard Error	0.07674	0.0924	0.06042	0.03473
95 % CI	0.5841 to 0.8850	0.5177 to 0.8802	0.4055 to 0.6424	0.8132 to 0.9494
P value	0.000915	0.00671	0.7440	<0.0001

[a] based on the non-corrected absorbance values at 405 nm.

Table 4.12: Optimal sensitivity and specificity of the selected antigens, from the ROC analysis, which were used to test the *T. vivax* blinded serum panel in the indirect antibody detection ELISA format.

	Indirect (serum dilution)			
	TvOPB (1:10)	TvOPB (1:100)	TvCATL (1:10)	TvCATL (1:100)
Cut-off (%)	> 0.1015	> 0.0825	< 4.300	> 49.06
Sensitivity (%)	84.72	91.67	41.67	72.22
95 % CI (%)	74.31 to 92.12	82.74 to 96.88	30.15 to 53.89	60.41 to 82.14
Specificity (%)	72.73	60.00	85	95.45
95 % CI (%)	49.78 to 89.27	36.05 to 80.88	62.11 to 96.79	77.16 to 99.88
Youden index	0.5745	0.5167	0.2667	0.6767

4.4 Discussion

After the optimisation of the inhibition and indirect antibody detection ELISAs, using the TcOPB, TcPGP, $TcCATL_{FL}$, TcCATL, TvOPB and TvCATL antigens, their diagnostic potential was evaluated using blinded panels of sera from cattle experimentally infected with *T. congolense* and *T. vivax* respectively.

The commercially available diagnostic tests as well as research into the development of new diagnostic tests make use of a wide range of serum dilutions from 1:40 in an antibody detection inhibition ELSA (Bossard *et al.*, 2010), 1:100 in an antibody detection indirect ELISA (Pillay *et al.*, 2013) to 1:400 in an antibody detection indirect ELISA (Tran *et al.*, 2009). During ELISA optimisations, it was found that using a 1:10 and a 1:100 serum dilution yielded comparable results; thus the *T. congolense* blinded serum panel was tested using a 1:10 serum dilution. The use of the $TcCATL_{FL}$ and TcCATL antigens in the inhibition and indirect ELISA formats were characterised by good sensitivity and specificity and according to the ROC analyses show good diagnostic potential when using a 1:10 serum dilution. The indirect ELISA format yielded the best results at the second cut-off where the $TcCATL_{FL}$and TcCATL antigens were characterised by a 100 and 97.44% sensitivity, 81.58 and 86.84 % specificity, 90.91 and 92.21% accuracy, and 0.8084 and 0.7785 AUC respectively. The use of the $TcCATL_{FL}$ antigen in the inhibition ELISA format yielded the next best results with a 76.92% sensivity, 63.16% specificity, 70.13% accuracy and a 0.7968 AUC.

The testing of the TvCATL and TvOPB antigens in the indirect ELISA format using the *T. vivax* blinded serum panel was performed after the *T. congolense* blinded serum panel. The TvCATL and TvOPB antigens were used to test *T. vivax* blinded serum panel using a serum dilution of 1:10 and 1:100. The TvCATL antigen yielded the best diagnostic performance at a 1:100 serum dilution, with a sensitivity of 58.06%, specificity of 82.93%, accuracy of 72.22% at the third cut-off along with a 0.8813 AUC was achieved. Despite that, the *T. congolense* antigens in both ELISA formats generally had higher specificities and NPV values than PPV values, thus they were more likely to correctly diagnose non-infected rather than infected serum samples. Indirect antibody detection ELISAs for the diagnosis of *T. congolense* and *T. vivax* have been developed by FAO/IAEA whereby ELISA plates are precoated with denatured parasite lysates (Rebeski *et al.*, 1999a; Rebeski *et al.*, 1999b). The performance of the above-mentioned antibody detection ELISAs correlated well with that obtained using the BCM and when used in parallel were characterised by 82.5%

sensitivity and a 88.7% specificity (Magona *et al.*, 2002). Low sensitivity and high specificity values were obtained for the diagnosis of bovine trypanosomiasis when tested against experimentally infected cattle with *T. congolense* and *T. vivax* (Eisler *et al.*, 1998). This follows the trend that is reported by the International Office of Epizootics (OIE) (2013).

Further diagnostic testing needs to be carried out to determine possible cross-reactivity with other bovine parasitic pathogens, which exist within the tsetse belt (*Anaplasma* spp., *Babesia* spp*., T. theileria*), serum from cattle naturally infected with *T. congolense* and *T. vivax* using the $TcCATL_{FL}$, TcCATL and TvCATL antigens being the next step towards the evaluation of their diagnostic potential. In this context, it was interesting to note that when testing the diagnostic potential of another recombinant *T. vivax* antigen, GM6, against experimentally infected and naturally infected cattle, it was found that the sensitivity varied from 91.4% (95% CI: 91.3 to 91.6%) and 91.5% (95% CI: 83.2 to 99.5%) respectively (Pillay *et al.*, 2013).

Since the $TcCATL_{FL}$ and TvCATL antigens share a 57% similarity and TcCATL being the catalytic domain of $TcCATL_{FL}$, it follows that they should display similar diagnostic potentials. Both the $TcCATL_{FL}$ and TcCATL antigens performed better in the indirect ELISA format than in the inhibition format. This was the basis of the decision to test the *T. vivax* antigens in the indirect ELISA format only.

Despite the indirect ELISA requiring one less step than the inhibition format, the detection of the IgG in the test sera and the diagnosis requires the comparison of the results to that of a known strong positive control serum which was included in the test (Rebeski *et al.*, 1999c). This known positive control serum is required to be determined for each antigen and each ELISA format to be tested. The inhibition ELISA on the other hand requires the generation of antibodies against each of the antigens which is time consuming. However, the results from the inhibition ELISA are calculated based on a no serum control which requires no optimisation (Section 4.2.2.1). The main advantage of the inhibition ELISA format is that the anti-trypansomal antibodies from a variety of livestock species are detectable using one set of ELISA reagents, whereas in the indirect ELISA format, species specific antibodies are required. The indirect ELISA format is only able to detect either IgG or IgM depending on the secondary antibody utilised whereas the inhibition ELISA format allows for the simultaneous detection of IgM and IgG.

In order to verify the diagnostic potential of any antigen, it is required that a comparison be made to existing commercial diagnostic ELISAs or serodiagnostic tests. The results from an ELISA using the ISG75 antigen for the diagnosis of surra in camels caused by *T. evansi* infection were compared to the ELISA/*T. evansi* (RoTat 1.2), CATT/*T. evansi* and TL assay and were found to correspond almost exactly (Tran *et al.*, 2009). In most commercial ELISAs the parasite lysate is used as the antigen. Pillay and co-workers (2013) demonstrated that the use of the *T. vivax* GM6 antigen in an antibody detection indirect ELISA resulted in a higher sensitivity than what was obtained using the the *T. vivax* parasite lysate as the antigen.

A lateral flow immunoassay detects specific antibodies in the serum or blood of an individual, the presence of which is indicated by a colour change on an adsorbent nitrocellulose strip (Bell and Peeling, 2006; Posthuma-Trumpie *et al.*, 2009). The format of the lateral flow test is comparable to that of the ELISA but simpler to use, results are quickly obtained and requires very little training of personell (Chappuis *et al.*, 2005a; Posthuma-Trumpie *et al.*, 2009). It follows that antigens which performed well in the antibody detection ELISAs against the blinded panel of serum samples, have the potential to be used in a lateral flow immunoassay format.

CHAPTER 5

GENERAL DISCUSSION

African trypanosomiasis (AT) is a devastating disease affecting both humans (HAT) and animals (AAT) in central Africa. Annually, US $4.5 billion is lost as both a direct and indirect consequence of AT (Swallow, 2000; Antoine-Moussiaux *et al.*, 2009). The protozoan parasitic trypanosomes undergo a dual life cycle in the mammalian host and the tsetse fly (*Glossina* spp.) vector (Kuzoe, 1993; Steverding, 2008). As a result of the process of antigenic variation displayed by the parasites, the development of a vaccine is very unlikely. In order to control AT, accurate diagnosis and subsequent treatment of infected patients and animals are required in order to reduce disease incidence (Simarro *et al.*, 2010; Bouyer *et al.*, 2013). The correct diagnosis of AT together with the identification of the infecting species, and disease staging, particularly in HAT cases, are important factors when selecting a suitable trypanocide.

Suitable diagnostic antigens and potential virulence factors, which can be used in the development of serodiagnostic tests, are identified by proteomic and pathogeno-proteomic studies (Hölzmuller *et al.*, 2008; Manful *et al.*, 2010; Eyford *et al.*, 2013). In order for an antigen to be considered for diagnostic purposes, the antigen needs to be expressed in the mammalian infective BSF parasites and at high levels to facilitate detection or be immunogenic to elicit antibodies in the mammalian host that can be detected. Most diagnostic tests make use of immobilised parasite lysates which are subject to batch-to-batch variations and in addition, pose a high risk to personnel when culturing. The use of recombinant antigens is an attractive alternative as high concentrations of recombinant protein can be expressed and purified reproducibly, at low cost and risk to personnel.

Many virulence factors are peptidases and immunodominant antigens (Antoine-Moussiaux *et al.*, 2009). Various cysteine peptidases have been implicated in the pathogenesis of kinetoplastid parasites (Caffrey *et al.*, 2011). For example, in *T. cruzi*, *T. b. brucei, T. congolense* and *Leishmania* spp., the calpain-like peptidases (Hertz-Fowler *et al.*, 2001; Mottram *et al.*, 2004; Alvarez *et al.*, 2011), metacaspases (MCA) (Lee *et al.*, 2007; Proto *et al.*, 2011; Laverrière *et al.*, 2012), pyroglutamyl peptidase (PGP) (Morty *et al.*, 2006; Mucache, 2012) and cathepsin L-like (CATL) cysteine peptidases (Sakanaria *et al.*, 1997; Steverding *et al.*, 2012) have each been identified as virulence factors. The serine peptidases, prolyl oligopeptidase (POP) and oligopeptidase B (OPB) from *T. cruzi*, *T. b. brucei* and *Leishmania* spp. (Swenerton *et*

al., 2011; Kangethe *et al.*, 2012; Motta *et al.*, 2012) together with the metalloprotease, GP63 (LaCount *et al.*, 2003; Oliver *et al.*, 2012) have been recognised as contributing factors to the virulence displayed by these parasites (dos Santos *et al.*, 2013).

The objective of this study was to evaluate the diagnostic potential of previously described virulence factors and immunodominant antigens, OPB, PGP and CATL from the main causative agents of AAT, *T. congolense* and *T. vivax*, in an antibody detection ELISA format. Furthermore, the putative MCA5, from *T. congolense* was cloned and recombinantly expressed for future investigation of its potential as a diagnostic or chemotherapeutic target.

The metacaspases from kinetoplastid parasites have been implicated in caspase-like cell death in *L. major* (Gonzáles *et al.*, 2007; Zalila *et al.*, 2011)*, T. b. brucei* (Szallies *et al.*, 2002; Helms *et al.*, 2006; Proto *et al.*, 2011) and *T. cruzi* (Kosec *et al.*, 2006b; Laverrière *et al.*, 2012) but have yet to be studied in *T. congolense* and *T. vivax*. The *TcMCA5* gene was cloned and recombinantly expressed with a 6xHis tag, within inclusion bodies, using the *E. coli* expression system, with a molecular weight of 69.8 kDa, along with the simultaneous expression of two lower molecular weight proteins of 41.4 and 37.3 kDa. The MCA3 and -5 of *T. cruzi* were reported to be expressed within inclusion bodies (Kosec *et al.*, 2006b). Solubilisation of recombinant TcMCA5 was achieved by using a method reported by Schlager and co-workers (2012) involving SDS and sarkosyl (N-lauroylsarsocine sodium salt). Cloud point extraction was used to solubilise the recombinant TcMCA5 which involves cooling, whereby excess SDS was precipitated and subsequently removed from the solubilised protein by centrifugation. The enzyme appeared to undergo autocatalytic processing, as revealed by two lower molecular weight proteins, which corresponded to similar processing demonstrated by native MCA5 from *L. major* (Gonzáles *et al.*, 2007; Lee *et al.*, 2007). Resolubilisation, refolding and purification using nickel affinity chromatography was successful and the active recombinant protein along with two lower molecular weight proteins were used to successfully raise antibodies in chickens with high titres. In an ELISA format, the anti-TcMCA5 IgY antibodies recognised the recombinant TcMCA5 antigen and the coating and primary antibody concentrations were optimised using checkerboard ELISAs as devised by Crowther (2000). Native TcMCA5 as well as the autocatalytic products were detected in western blots of *T. congolense* (strain IL 3000) procyclic form (PCF) lysate using the chicken anti-TcMCA5 IgY antibodies. Due to their potential involvement in cell death (Lee *et al.*, 2007; Zalila *et al.*, 2011) and differentiation (Ambit *et al.*, 2008) it is a possibility that the

MCAs have diagnostic potential. Further research using sera from experimentally infected cattle is required to corroborate this.

During the course of AT infection, disruption of the mammalian host's endocrine system is common (Tizard *et al.*, 1978; Brandenberger *et al.*, 1996). It was found that in the serum of infected rats, the degradation of peptide hormones followed an unusual pattern (Tetaert *et al.*, 1993). This phenomenon has since been attributed to OPB, as it is only able to cleave small peptides such as neuropeptides and hormones, which are no larger than 30 amino acid residues, C-terminal to basic residues (Polgár, 2002; Coetzer *et al.*, 2008). The absence of a signal peptide supports the fact that OPB is released into the host's bloodstream during parasite lysis where it is able to retain its catalytic activity (Morty *et al.*, 2001). The activity of OPB extends to cellular invasion, in the case of *T. cruzi,* whereby a Ca^{2+} signalling mechanism is activated and the peptidase is thus considered a virulence factor (Burleigh *et al.*, 1997).

Similar to OPB, PGP is catalytically active in the mammalian bloodstream as described for homologues from *T. b. brucei* and *T. congolense* (Morty *et al.*, 2006; Mucache, 2012). Due to the hydrolytic cleavage of the L-pGlu residues, which function to protect neuropeptides and hormones, protozoan PGP has been implicated in the disruption of the endocrine system during infection (Barrett and Rawlings, 2004; Atkinson *et al.*, 2009). Previously cloned 6xHis tagged TcOPB and glutathione-S-transferase (GST) tagged TvOPB and TcPGP were recombinantly expressed using the *E. coli* expression system and successfully purified by nickel- and GST- affinity chromatography respectively. Recombinant TcOPB was expressed and purified as an 80 kDa protein (Bizaaré, 2008). The recombinant TvOPB was expressed as a 106 kDa GST fusion protein and after cleavage with thrombin, was purified as an 80 kDa protein (Huson, 2006). The GST fusion protein, TcPGP was recombinantly expressed with a molecular weight of 53 kDa and was purified as a 28 kDa protein after thrombin cleavage of the GST tag which corresponds with what was reported by Mucache (2012). The successful purification of each antigen allowed for the immunisation of chickens which yielded high antibody titres during the course of the immunisation schedule with the exception of TvOPB. Despite a new immunisation schedule with a higher concentration of TvOPB being administered, low titres of anti-TvOPB IgY antibodies were obtained. Checkerboard ELISAs were successfully conducted and the optimal coating and antibody concentrations were determined for each antigen.

Congopain, (TcCATL), the immunodominant CATL peptidase from *T. congolense*, has been considered a virulence factor (Authié *et al.*, 2001) due to its possible involvement in the occurrence of trypanotolerance (Authié *et al.*, 1993a), the development of anaemia and the suppression of the immune system during infection (Authié, 1994). It is hypothesised that cruzipain (TcrCATL), the major lysosomal peptidase from *T. cruzi*, plays a role in cell differentiation since when overexpressed, *T. cruzi* epimastogotes displayed enhanced differentiation into MCF parasites (Bonaldo *et al.*, 1991; Tomas *et al.*, 1997). Vivapain (TvCATL), the congopain homologue in *T. vivax*, has previously been demonstrated to elicit an immune response in mice and may also have diagnostic potential (Vather, 2010).

The full length inactive congopain ($TcCATL_{FL}$), as well as active TcCATL and TvCATL, each comprising the catalytic domain and the propeptide of the peptidases, were recombinantly expressed using the *Pichia pastoris* expression system. The recombinant CATL antigens were successfully expressed with the $TcCATL_{FL}$ antigen (40 kDa), the TcCATL antigen (27 kDa) and the TvCATL antigen (29 and 33 kDa) which agreed with what had been previously reported by Pillay (2010) and Vather (2010), respectively. Thereafter, the antigens were purified using three phase partitioning (TPP), followed by molecular exclusion chromatography (MEC). The MEC purification of TvCATL, a glycosylated protein, resulted in a larger retention volume than expected due to its glycosylated nature. This observation was supported by the quantitative structure-property relationships (QSPR) theory as developed by Granér (2005). The purified recombinant CATL antigens as well as a peptide corresponding to the 18-mer N-treminal residues of TcCATL were used to raise antibodies in chickens and high titres of antibodies resulted after four immunisations with 50 µg/ml protein per immunisation. The anti-$TcCATL_{FL}$ and anti-TcCATL N-terminal peptide IgY antibodies were affinity purified and were used together with the anti-TvCATL IgY antibodies to successfully optimise the ELISA coating and antibody concentrations using a checkerboard methodology as devised by Crowther (2000).

After the ELISA optimisations for each of the OPB, PGP and CATL antigens, together with their respective IgY antibodies, the antigens were ready to be evaluated for their intended use, as diagnostic antigens in the antibody detection inhibition and indirect ELISA formats using experimentally *T. congolense* and *T. vivax* infected cattle sera.

Accurate diagnostics is crucial due to the adverse side effects of the trypanocidal drugs currently in use (Kinabo, 1993; Brun *et al.*, 2011) and to gain control of the insect

vector reservoir (Simarro *et al.*, 2010). Confirmation of infection requires the use of diagnostic assays due to the generalised symptoms of both HAT and AAT (Taylor and Authié, 2004; Chappuis *et al.*, 2005a), the toxicity of the trypanocides and, in addition, to prevent the development of trypanocide resistance (Geerts *et al.*, 2001; Delespaux *et al.*, 2002). In HAT cases, disease staging is imperative for the accurate prescription of curative trypanocides. During the early stage, and in cases of acute infections, high levels of parasitaemia are characteristic which makes parasitological detection of the parasites simpler and more reliable (Chappuis *et al.*, 2005a). This, however, is complicated in cases of low parasitaemia, and in chronic infections, whereby the parasitological techniques must be modified by prior concentration of the serum, blood or CSF sample before the detection of parasites can be made (Woo, 1970). The amplification of pan-*Trypanozoon* sequences by PCR is more sensitive than parasitological techniques but due to low levels of parasitaemia, false negative results may be observed and would still require parasitological confirmation (Tiberti *et al.*, 2013).

Trypanosomal infections cause specific IgM and IgG antibody responses (Sacks and Askonas, 1980; Pépin and Donelson, 2006) and several antibody detection assays have been developed for field use in active case finding and for laboratory use. The most applicable diagnostic tests to date are the immunofluorescent assay (IFA), the enzyme-linked immunosorbent assay (ELISA) and the card agglutination test (CATT) of which only the CATT is suitable for field use (Chappuis *et al.*, 2005a). The CATT/*T. b. gambiense* is based on the agglutination of immobilised *T. b. gambiense* parasites of a specified variant antigen type (VAT) by the anti-trypanosomal antibodies in the sample (Magnus *et al.*, 1978), and characterised by a 87 to 98% sensitivity (Truc *et al.*, 2002; Robays *et al.*, 2004). The LATEX/*T. b. gambiense* is an alternative to the CATT where the use of three purified VATs, LiTat 1.3, 1.5 and 1.6, coupled to suspended latex particles result in a higher specificity (96 to 99%) and a lower sensitivity (71 to 100%) compared to the CATT/*T. b. gambiense* (Jamonneau *et al.*, 2000; Penchenier *et al.*, 2000; Truc *et al.*, 2002). The CATT, however, is not considered as a diagnostic standard (Chappuis *et al.*, 2005a) where cross-reactivity with other pathogens present in the active foci decreases the accuracy of these diagnostic tests (Noireau *et al.*, 1988; Deborggraeve and Büscher, 2010). In addition, the diagnostic tools based on antibody detection cannot distinguish between active and cured HAT as anti-trypansomal antibodies can persist in the host for two to three years after cure (Lejon *et al.*, 2010). It has been noted that in animals, anti-trypanosomal

antibodies may persist for several months to a year after successful treatment and in the absence of tsetse challenge (Van den Bossche *et al.*, 2000a).

The use of ELISA methods in the serodiagnosis of AT requires extensive standardisation of antigens and antibodies and can be used to test serum, CSF or blood impregnated filter paper eluates (Lejon *et al.*, 1998). Two ELISA formats are currently implemented in the serodiagnosis of AT: the antigen detection ELISA where circulating antigens released by trypanosomes are detected using monoclonal antibodies (Nantulya, 1990; Eisler *et al.*, 1998) and the antibody detection ELISA where anti-trypanosomal antibodies are detected using trypanosomal lysate (Luckins, 1997). The inhibition antibody detection ELISA detects antibodies in the serum of an infected host by the decrease in absorbance values whilst the indirect antibody detection ELISA detects antibodies in the serum of an infected host by the increase in absorbance values (Fig. 4.1).

The serodiagnosis of *T. b. gambiense* infections using the antibody detection ELISA utilises the LiTat 1.3, 1.5 and 1.6 antigens which are immobilised onto a microtitre plate (Hasker *et al.*, 2012). The sensitivity of the ELISA/*T. b. gambiense* varies from 82.8 to 100% with specificity varying from 94.7 to 100% (Nantulya and Doua, 1992; Hasker *et al.*, 2012). Despite desirable performances, the ELISA/*T. b. gambiense* is time consuming, requires specific training and is expensive, thus the ELISA is more suited to disease surveillance as it can process numerous samples at a time and blood impregnated filter paper, collected in remote areas, can be used (Chappuis *et al.*, 2005a).

Identification of infected individuals and the subsequent treatment is vital to the control of AT, thus diagnostic tests need to be accurate, easy to use and cost efficient (Chappuis *et al.*, 2005a). The development of AAT diagnostics are based on the successes of established HAT diagnostics and the developments of novel HAT diagnostics. This was the case for the CATT/*T. evansi* (Zweygarth *et al.*, 1984; Songa *et al.*, 1987) which was based on the previously introduced CATT/*T. b gambiense* (Magnus *et al.*, 1978). The advances in ELISA serodiagnostics for HAT should be considered when potential AAT diagnostic antigens are chosen and the subsequent interpretation of the acquired results.

A lateral flow test would be the ideal format for initial serodiagnosis as it requires no expertise, no electricity, provides rapid results and can be used in rural settings during active case finding (Posthuma-Trumpie *et al.*, 2009). Currently under evaluation in the

Democratic Republic of the Congo for the diagnosis of *T. b. gambiense* infections (Büscher *et al.*, 2013) are the newly developed lateral flow serodiagnostic tools, the HAT SERO K-SeT, the HAT SeroStrip rapid test as well as the SD BIOLINE HAT (http://www.finddiagnostics.org/media/press/121206.html, accessed 7/06/2013).

Since the invariant surface glycoproteins (ISGs) are conserved amongst the *Trypanozoon* species, these have been extensively studied. Recently Tran and co-workers (2009) proposed the use of the ISG75 antigen in the development of a pan-*Trypanozoon* diagnostic test. The recombinant ISG75 antigen was used in an indirect antibody detection ELISA format against *T. b. gambiense* infected and non-infected sera. High sensitivity (95%) and specificity (93%) were obtained along with an area under curve AUC of 0.81 after receiver-operating characteristic (ROC) analysis (Sullivan *et al.*, 2013). When used in a lateral flow format against the same sera, the AUC increased to 0.99 for the recombinant ISG75 with a 88% sensitivity and a 93% specificity when analysed visually and a 100% sensitivity and 93% specificity when analysed using the Camag scanner (Sullivan *et al.*, 2013). This compared favourably with the performance of the CATT/*T. b. gambiense* which has a 87 to 98% sensitivity and 93 to 93% specificity (Truc *et al.*, 2002).

Similarly to the use of ISG65 for the detection of *T. b. gambiense* infections (Sullivan *et al.*, 2013), the recombinant extracellular domain of ISG75 from *T. b. gambiense* LiTat 1.3 was used in an indirect antibody detection ELISA for the diagnosis of *T. evansi* infections which causes surra in camels (Tran *et al.*, 2009). The performance of the ELISA/ISG75 was compared to the currently used *T. evansi* serodiagnostic tools, the ELISA/*T. evansi* using the RoTat 1.2 VAT, the CATT/*T. evansi* and the TL assay (Tran *et al.*, 2009). Both the ELISA/ISG75 and the ELISA/*T. evansi* were characterised by a 94.6% sensitivity and a 98.9% specificity (Tran *et al.*, 2009). This study demonstrated the suitability of ISG75 as a diagnostic antigen as well as the comparability of the results obtained using the parasite lysates to that of the recombinant antigen.

A *T. congolense* orthologue of the *T. b. brucei* ISG, based on the domain structures, was identified on the surface of the MCF and bloodstream form (BSF) *T. congolense* parasites and named Tc38630 (Eyford *et al.*, 2011). Based on the previous successes of the use of recombinant ISGs for the diagnosis of *T. b. gambiense* and *T. evansi* infections, the diagnostic potential of the Tc38630 protein was evaluated. Using an indirect antibody detection ELISA, with sera from experimentally infected mice, the diagnostic performance of the recombinant Tc38630 was compared to that of PCF

T. congolense parasite lysate (Mochabo *et al.*, 2013). It was found that the Tc38630 antigen was able to detect antibodies earlier than the parasite lysate (Mochabo *et al.*, 2013). Due to the favourable performance in the antigen detection ELISA, it was concluded that the Tc38630 protein was a promising diagnostic antigen for the diagnosis of AAT (Mochabo *et al.*, 2013).

The recombinantly expressed and purified antigens (TcOPB, TvOPB, TcPGP, $TcCATL_{FL}$, TcCATL and TvCATL) were used with sera from catlle experimentally infected with either *T. congolense or T. vivax* in the optimisation of the inhibition and indirect antibody detection ELISAs. The IgY antibodies, produced as described in chapter 3, were only utilised in the inhibition antibody detection ELISA format. Using a blinded *T. congolense* and *T. vivax* serum panel, the applicability of each of the antigens in the inhibition and indirect antibody detection ELISA format was determined and their performances were subjected to ROC analysis.

The most promising results were obtained in the indirect antibody detection ELISA using the CATL antigens. The $TcCATL_{FL}$ antigen correctly identified 39/39 infected and 31/38 non-infected serum samples and the TcCATL antigen correctly identified 38/39 infected and 33/38 non-infected serum samples, both at the second cut-off using a 1:10 serum dilution. The TvCATL antigen, using a 1:100 serum dilution, correctly identified 18/31 infected and 34/41 non-infected serum samples at the third cut-off.

Analysis of the ROC curves generated from the blinded serum panels characterised the $TcCATL_{FL}$ antigen with a 67.53% (95% CI: 55.9 to 77.77%) sensitivity, a 88.89% (95% CI: 65.29 to 98.62%) specificity at a cut-off of 27.10%. The TcCATL antigen was characterised by a 55.84% (95% CI: 44.07 to 67.16%) sensitivity, a 94.44% (95% CI: 72.71 to 99.86%) specificity at a cut-off of 25.50% and finally the TvCATL antigen by a 72.22% (95% CI: 66.41 to 82.14%) sensitivity and a 95.45% (95% CI: 77.16 to 99.88%) specificity at a cut-off of 49.06%. The closer the AUC and Youden indices tend to 1, the more effective the diagnostic test (Schisterman *et al.*, 2005). The following AUC and the Youden indices were calculated for the CATL antigens respectively from the ROC curves: $TcCATL_{FL}$ with 0.8084 and 0.5642, TcCATL with 0.7785 and 0.5028 and TvCATL with 0.8813 and 0.6767. Despite average Youden indices, the high AUC values for the CATL antigens are strong indicators of their diagnostic potential.

The sensitivity of the CATL antigens (55.84 to 72.22%) in the indirect antibody detection ELISA, from the blinded serum panels, was lower than that for the HAT ELISA serodiagnosis of *T. b. gambiense* using ISG65, 95% an 93% respectively

(Sullivan *et al.*, 2013) and the VSG LiTat 1.5 peptide, 89.2% and 95.1% respectively (Van Nieuwenhove *et al.*, 2013), which were both tested in an indirect antibody detection ELISA format. The CATL antigens resulted in a low sensitivity when compared to the ISG75 antigen which is used for the diagnosis of *T. evansi* infections, which resulted in a sensitivity of 94.6% and specificity of 98.9% respectively (Tran *et al.*, 2009). However, the high specificities of the CATL antigens (88.89 to 95.45%) were close to those reported in both the previously mentioned HAT and AAT serodiagnostic antibody detection ELISAs.

The C-terminal extension present in TcrCATL, cruzipain, was demonstrated to be highly immunogenic (Cazzulo and Frasch, 1992). Thus the majority of the immune response should be directed towards the C-terminal extension (Caffrey *et al.*, 2011). Since the TcCATL antigen was only comprised of the prodomain and the catalytic domain, it follows that the full length $TcCATL_{FL}$ antigen, which included the C-terminus, yielded higher sensitivity and specificity values compared to those obtained for the TcCATL antigen. Although the TvCATL antigen performed better than both the *T. congolense* CATL antigens, the full length $TvCATL_{FL}$ was not available for testing and comparison, thus this hypothesis cannot be confirmed.

It was necessary to test the antigens in both the inhibition and indirect antibody detection ELISA formats, as both have been used by other researchers with variable levels of success. In the *T. congolense* blinded serum panel, favourable results were obtained in both the inhibition and indirect antibody detection ELISA formats using the $TcCATL_{FL}$ antigen. However, those resulting from the indirect ELISAs were more promising for further application. Thus only the indirect antibody detection ELISA format was used in the *T. vivax* blinded serum panel.

The maltose binding protein (MBP)-HSP70/BiP antigen, from *T. congolense,* was used in an inhibition antibody detection ELISA for the detection of AAT infections in cattle using monoclonal antibodies (Bossard *et al.*, 2010). It was demonstrated by Bossard and co-workers (2010) that the HSP70/BiP inhibition ELISA was characterised by a higher sensitivity than the HSP70/BiP indirect ELSA (Boulangé *et al.*, 2002). A higher sensitivity was obtained for sera from secondary infections than in primary infections making the test more useful in endemic areas where rechallenge is common. Cross-reactivity occurred between *T. b. brucei, T. congolense* and *T. vivax* but not with *Anaplasma, Babesia* or *T. theileria*, thus making this ELISA a possible pan-*Trypanozoon* diagnostic tool (Bossard *et al.*, 2010). This is thought to be caused

by the simultaneous detection of IgG and IgM in the inhibition antibody detection ELISA format whilst only IgG is detected in the indirect antibody detection ELISA format (Bossard *et al.*, 2010). The downfall of the use of the indirect antibody detection ELISA in serodiagnosis is the requirement of species specific reagents, e.g. anti-bovine/camel/goat IgG HRPO conjugated detection antiodies, whilst only one set of reagents are required for the inhibition antibody detection ELISA, e.g. rabbit anti-chicken IgY HRPO conjugate detection antibody (Bossard *et al.*, 2010).

The CATL antigens were able to discriminate between infected and non-infected serum samples more effectively than the OPB and PGP antigens as indicated by their high sensitivity, specificity and accuracy values along with favourable Youden indices and AUCs from the ROC analyses. Due to the promising performance of the CATL antigens in the blinded serum panels, these antigens will be taken forward to determine the species specificity and cross-reactivity of these antigens. Cross-reactions may occur in serodiagnostic techniques in areas where the *T. equiperdum* and *T. vivax* species occur, which are not transmitted by the tsetse fly (OIE, 2013). Thereafter, it is possible that the CATL antigens may be suitable candidates for the development of a pan-*Trypanozoon* or species-specific lateral flow test. As proposed by Manful and co-workers (2010), an increase in the diagnostic accuracy of HSP70 might be achieved if used in tandem with other potential diagnostic antigens in a multiplex diagnostic tool. It follows that the combination of the CATL, OPB and PGP antigens might result in higher diagnostic accuracies. However, the development of species specific ELISAs can be achieved only if species specific antigens are used (Desquesnes and Dávila, 2002).

Despite PGP showing strong potential in the optimisation ELISAs using infected and non-infected sera, poor results were obtained when tested in the *T. congolense* blinded serum panel. At the second cut-off the PGP antigen correctly identified 9/39 infected and 37/38 non-infected serum samples in the inhibition ELISA format and 1/39 infected and 37/38 non-infected serum samples in the indirect ELISA format. The ROC analyses indicated that diagnosis, using the PGP antigen, was by chance due to the low AUC (± 0.50) and high p values.

The OPB antigen, at the second cut-off was able to correctly identify 0/39 infected and 30/38 non-infected serum samples in the inhibition ELISA format and 16/39 infected and 30/38 non-infected serum samples in the indirect ELISA format. The ROC analysis of the indirect antibody detection ELISA results was favourable, with an average AUC

value and low p value, this however was not the case for the inhibition ELISA analysis, with diagnosis occurring by chance (AUC values close to 0.5). This result was unexpected as it has been demonstrated that the trypanocides, pentamidine, diminazene, and suramin target OPB (Morty *et al.*, 1998). However it has been suggested that the trypanocides target multiple molecules rather than just OPB (Morty *et al.*, 1998). It was also shown that OPB remains active in the bloodstream of infected hosts (Morty *et al.*, 2001) but the results presented in the present study suggest that OPB is not sufficiently immunogenic to elicit antibodies.

Since *T. congolense* and *T. vivax* are strictly vascular parasites (Taylor and Authié, 2004) the activity of PGP and OPB would be based on the concentration of hormones in the bloodstream as they are not affected by host plasma inhibitors (Morty *et al.*, 2005; Morty *et al.*, 2006). Mammalian PGP cleaves L-pGlu from thyrotropin-releasing hormone, luteinizing hormone releasing hormone, neurotensin, bombesin and leukopyrokinin (Dando *et al.*, 2003) whilst OPB cleaves peptide hormones, not bigger than 30 residues long (Fülöp *et al.*, 1998; Coetzer *et al.*, 2008), some of which are present in the bloodstream. It has been suggested by Bastos and co-workers (2010) that PGP and OPB function synergistically to cleave gonadotropin-releasing hormone. Thus these antigens might be used in HAT stage determination as endocrine disorders during the course of trypanosomal infection have been observed in humans (Bouteille and Buguet, 2012) and animals (Uilenberg and Boyt, 1998). From the antibody detection ELISA results with the blinded serum panels, and considering their identities as virulence factors, OPB and PGP might be suitable as chemotherapeutic targets for AAT. However, OPB and PGP may also be good targets for an antigen detection ELISA provided high titre of antibodies could be produced in experimental animals. Future work with regard to these antigens will be aimed at investigating phage display scFV-libraries to identify such monoclonal antibodies (Nissim *et al.*, 1994; Pansri *et al.*, 2009; Ferrara *et al.*, 2012).

Future work for the evaluation of the diagnostic potential of the CATL antigens includes the determination of their cross-reactivities against other bovine pathogens, *Anaplasma, Babesia* and *T. theileria*, which exist in endemic AT areas. Thereafter, it will be determined if any of the CATL antigens would be suitable candidates for the development of AAT serodiagnostic lateral flow tests.

The diagnostic potential of TcMCA5 still requires validation as pure antigen was not available when the *T. congolense* blinded serum panel was tested. There are still uncharacterised MCAs present in the genomes of *T. congolense* and *T. vivax*, and their

roles in cell death, differentiation and pathogenesis require further study. A MCA4 protein exists in *T. congolense* and is worth investigating should it perform a similar function to the pseudopeptidase and virulence factor from *T. b. brucei*, TbMCA4 (Proto *et al.*, 2011).

The present study has confirmed the successful application of the CATL antigens in an indirect antibody detection ELISA format. With further optimisation studies, they have the potential to be incorporated into lateral flow tests for the diagnosis of AAT. The *in vivo* presence of putative TcMCA5 was confirmed in procyclic *T. congolense* parasites (strain IL 3000) and further research into their mechanism of action and diagnostic potential is required.

APPENDIX A

The DNA sequence of the *MCA5* gene from *T. congolense* (EMBL accession: CCC93200.1, GeneDB: TcIL3000.9.6120) and the position of the specific primers are highlighted in Fig. A.1.

```
   1 CAACGTCACA ATGGATCTTG CTGTTGGGCT TCTGTTGGGA CAGCTGGCGT
  51 CCAGCGCCCT GCCTTACCTT GTTGAGAGCA TTGGTAAGGT GAAGCGGCCC
 101 AAGCGGGTCG ATGTGAAAAA GGCGATGAGT GAGGCACACA CGTGTCGCCC
 151 GGTGGTTCCC TACCATGCTC CCAGACCCTA CACGGAGGGC CGTGTGAAGG
 201 CTCTTTTCAT TGGAATCAAT TACACGGGAA GGAAAGGGCA ACTTAGTGGG
 251 TGCATCAACG ATGTGAAGCA AATGCTGAAC ACGCTCCAGC AAATTCAGTT
 301 CCCCATATCA TCGTGTTGTA TTCTTGTCGA CGACCCCAGG TTCCCGAATT
 351 ACACCGCTAT GCCGACCCGG GCGAACATCA TTAAGCACAT GGCCTGGTTG
 401 GTGTACGACG CACGTCCGGG GGACGTTCTG TTTTTTCACT ACTCTGGGCA
 451 CGGTGCGGAG ACGACTGGCG GCCGCGACTC CGAGGAGGAA AACGACCAGT
 501 GCCTCATTCC GTTGGACTAC GAGAAGGAGG GATCTATTTT AGACGACGAC
 551 TTGTTTGAGC TAATGGTAAA GGGCCTGCCA GCGGGCGTGC GTATGACGGC
 601 CGTCTTTGAT TGCTGCCACT CTGCCTCTCT TCTCGACCTC CCGTTTGCAT
 651 TTGTTGCTGG AAGGAACGCA CTGTCGAGTC ACCGGCAGGA GATGCGGATG
 701 GTTCGAAAGG GCAATTTTTC TCGTGCCGAC GTTGTCATGT TCAGTGGCTG
 751 TGAGGACTCA GGTACCAGTG CTGATGTGCA GAACACGGCG TCTTTCGGCA
 801 ACGGGACTAG GGTCCCTGGT GGGGCAGCTA CACAGGCACT TACCTGGGCG
 851 CTGCTTAACA CGTCAGGGTA CAACTACGCA GATATATTTA TGAGGATGAG
 901 GGATGTGCTC CGGAATAAGG GCTATAGGCA GGTGCCACAG CTCTCGAGCT
 951 CGAAGCCGAT CGATTTATAC AAACCATTTT CTTTGTTTGG AACTTTGACT
1001 ATGAATACAA ACCTTATTCA GAATGTACCC GTAGAATATA CCAACGCATG
1051 GAATGCACAA CCGCCACAGC ACTCCTATCC GCAGTTGCCG CAACAGCAAC
1101 AGGTACCGGT ACCTACTCCG CAGAATGATG GCCCTGTGAT GGGTATTCCT
1151 ATTTCTTCGA GCACCAATGA TCAAAACTCT GGAAACCCTC CCGCTGCTGC
1201 CGCGCCGACA AACGTGGTCA CTCCAGTACA ATACCCCTCT CAACCGCCCT
1251 CACACCAACC GCAGCAGGGC TACTACTCGG CACCTCAGCA GCAGCCACCG
1301 CAGCAGGGCT ACTATTCGGC GCCTCAGCAG TACCCACCGC AGCAGGGCTA
1351 CTACGCGGCA CCTCAGCAGT ACCCACCGCA GCAGGGCTAC TATTCGGCAC
1401 CTCAGCAATA CCCACCGCAG CAGGGCTACT ATTCGGCACC TCAGCAATAC
1451 CCACCGCAGC AGGGCTACTA TTCGGCACCT CAGCAATACC CACCGCAGCA
1501 GGGCTACTAT TCGGCGCCTC AGCAGTACCC ACCGCAGCAG TCACGACCGG
1551 CACAGGCCCA GAAGCCGTCT CGATCAGGGT ATCCGATTGA TTTTTTGAAG
1601 GGCTCCAAGT GAGGGACCGG
```

Figure A.1: The coding sequence for the *MCA5* gene found in *T. congolense* (strain IL 3000). The DNA sequence was obtained from EMBL (http://www.ncbi.nlm.nih.gov/nuccore/HE575322, accessed 16/04/2012), *T. congolense MCA5*, CCC93200.1. The positions of the forward and reverse primer annealing sites are highlighted in pink whilst the start and stop codons are in bold.

APPENDIX B

SERA ANNOTATIONS

Serum name (ClinVet)	Abbreviation	Infection status
	Trypanosoma congolense	
	STUDY CV12/884	
CV12/884 18 (-7)	18 (-7)	Negative
CV12/884 18 (+7)	18 (+7)	Positive
CV12/884 18 (+23) *T0	18 (+23)	Positive
CV12/884 18 (+37) *T14	18 (+37)	Positive
CV12/884 18 (+51) *T25	18 (+51)	Positive
CV12/884 53 (-7)	53 (-7)	Non-infected
CV12/884 53 (+28)	53 (+28)	Non-infected
CV12/884 81 (-7)	81 (-7)	Negative
CV12/884 81 (+28) *T0	81 (+28)	Positive
CV12/884 81 (+49) *T14	81 (+49)	Positive
CV12/884 109 (-7)	109 (-7)	Non-infected
CV12/884 109 (+7)	109 (+7)	Non-infected
CV12/884 109 (+28) *T0	109 (+28)	Non-infected
CV12/884 109 (+49) *T14	109 (+49)	Non-infected
CV12/884 CVB 149 (-7)	149 (-7)	Negative
CV12/884 CVB 149 (+7)	149 (+7)	Positive
CV12/884 CVB 149 (+28)	149 (+28)	Positive
CV12/884 CVB 149 (+42) *T7	149 (+42)	Positive
CV12/884 CVB 149 (+49) *T14	149 (+49)	Positive
CV12/884 CVB 150 (-7)	150 (-7)	Non-infected
CV12/884 CVB 150 (+7)	150 (+7)	Non-infected
CV12/884 CVB 150 (+28) *T0	150 (+28)	Non-infected
CV12/884 CVB 150 (+42) *T14	150 (+42)	Non-infected
CV12/884 CVB 150 (+49) *T21	150 (+49)	Non-infected
CV12/884 CVB 151 (-7)	151 (-7)	Negative
CV12/884 CVB 151 (+28) *T0	151 (+28)	Positive
CV12/884 CVB 151 (+42) *T14	151 (+42)	Positive
CV12/884 CVB 152 (-7)	152 (-7)	Negative
CV12/884 CVB 152 (+14)	152 (+14)	Positive
CV12/884 CVB 152 (+28) *T0	152 (+28)	Positive

Serum name (ClinVet)	Abbreviation	Infection status
CV12/884 CVB 152 (+45) *T14	152 (+45)	Positive
CV12/884 CVB 152 (+63) *T28	152 (+63)	Positive
CV12/884 CVB 153 (-7)	153 (-7)	Negative
CV12/884 CVB 153 (+28) *T0	153 (+28)	Positive
CV12/884 CVB 153 (+42) *T7	153 (+42)	Positive
CV12/884 CVB 153 (+49) *T14	153 (+49)	Positive
CV12/884 CVB 153 (+63) *T28	153 (+63)	Positive
	STUDY CV12/885	
CV12/885 CVB 178 (-6)	178 (-6)	Negative
CV12/885 CVB 178 (+19) *T10	178 (+19)	Positive
CV12/885 CVB 178 (+25) *T16	178 (+25)	Positive
CV12/885 CVB 178 (+39) *T30	178 (+39)	Positive
CV12/885 CVB 179 (-7)	179 (-7)	Negative
CV12/885 CVB 179 (+19) *T10	179 (+19)	Positive
CV12/885 CVB 179 (+25) *T16	179 (+25)	Positive
CV12/885 CVB 179 (+39) *T30	179 (+39)	Positive
CV12/888 CVB 180 (-8)	180 (-8)	Negative
CV12/885 CVB 180 (+7)	180 (+7)	Positive
CV12/885 CVB 180 (+10) *T10	180 (+10)	Positive
CV12/885 CVB 180 (+25) *T16	180 (+25)	Positive
CV12/885 CVB 181 (-6)	181 (-6)	Negative
CV12/885 CVB 181 (+19) *T10	181 (+19)	Positive
CV12/885 CVB 182 (-6)	182 (-6)	Non-infected
CV12/885 CVB 182 (+25) *T16	182 (+39)	Non-infected
CV12/885 CVB 182 (+39) *T30	182 (+39)	Positive
CV12/885 CVB 183 (-10)	183 (-10)	Non-infected
CV12/885 CVB 183 (+19) *T10	183 (+19)	Non-infected
CV12/885 CVB 184 (-6)	184 (-6)	Non-infected
CV12/885 CVB 185 (-6)	185 (-6)	Non-infected
CV12/885 CVB 186 (-7)	186 (-7)	Negative
CV12/885 CVB 186 (+7)	186 (+7)	Positive
CV12/885 CVB 187 (-7)	187 (-7)	Negative
CV12/885 CVB 187 (+25) *T16	187 (+25)	Positive
CV12/885 CVB 187 (+39) *T30	187 (+39)	Positive
CV12/885 CVB 188 (-6)	188 (-6)	Negative

Serum name (ClinVet)	Abbreviation	Infection status
CV12/885 CVB 188 (+7)	188 (+7)	Positive
CV12/885 CVB 190 (-9)	190 (-9)	Negative
CV12/885 CVB 190 (+7)	190 (+7)	Positive
CV12/885 CVB 190 (+19)	190 (+19)	Positive
CV12/885 CVB 190 (+25)	190 (+25)	Positive
CV12/885 CVB 191 (-7)	191 (-7)	Negative
CV12/885 CVB 191 (+7)	191 (+7)	Negative
CV12/885 CVB 191 (+19) *T10	191 (+19)	Positive
CV12/885 CVB 191 (+25) *T16	191 (+25)	Positive
CV12/885 CVB 192 (-8)	192 (-8)	Negative
CV12/885 CVB 192 (+7)	192 (+7)	Positive
CV12/885 CVB 192 (+19) *T10	192 (+19)	Positive
CV12/885 CVB 192 (+25) *T16	192 (+25)	Positive
CV12/885 CVB 193 (-6)	193 (-6)	Negative
CV12/885 CVB 193 (+7)	193 (+7)	Positive
CV12/885 CVB 193 (+19) *T10	193 (+19)	Positive
CV12/885 CVB 193 (+25) *T16	193 (+25)	Positive
CV12/885 CVB 194 (-7)	194 (-7)	Negative
CV12/885 CVB 194 (+7)	194 (+7)	Positive
CV12/885 CVB 194 (+19) *T10	194 (+19)	Positive
CV12/885 CVB 194 (+25) *T14	194 (+25)	Positive
CV12/885 CVB 195 (-7)	195 (-7)	Non-infected
CV12/885 CVB 195 (+19) *T10	195 (+19)	Non-infected
CV12/885 CVB 196 (-6)	196 (-6)	Non-infected
CV12/885 CVB 196 (+25) *T16	196 (+25)	Positive
CV12/885 CVB 196 (+39) *T30	196 (+39)	Positive
CV12/885 CVB 197 (-9)	197 (-9)	Negative
CV12/885 CVB 198 (+7)	198 (+7)	Positive
CV12/885 CVB 198 (+19) *T10	198 (+19)	Positive
CV12/885 CVB 198 (+25) *T16	198 (+25)	Positive
CV12/885 CVB 198 (-8)	198 (-8)	Negative
CV12/885 CVB 198 (+7)	198 (+7)	Positive
CV12/885 CVB 198 (+19) *T10	198 (+19)	Positive
CV12/885 CVB 198 (+25) *T16	198 (+25)	Positive
CV12/885 CVB 199 (-9)	199 (-9)	Negative
CV12/885 CVB 199 (+7)	199 (+7)	Positive

Serum name (ClinVet)	Abbreviation	Infection status
CV12/885 CVB 199 (+19) *T10	199 (+19)	Positive
CV12/885 CVB 199 (+25) *T16	199 (+25)	Positive
CV12/885 CVB 200 (-8)	200 (-8)	Negative
CV12/885 CVB 200 (+7)	200 (+7)	Positive
CV12/885 CVB 200 (+19) *T10	200 (+19)	Positive
CV12/885 CVB 200 (+25) *T16	200 (+25)	Positive
CV12/885 CVB 201 (-8)	201 (-8)	Negative
CV12/885 CVB 201 (+7)	201 (+7)	Positive
CV12/885 CVB 201 (+19) *T10	201 (+19)	Positive
CV12/885 CVB 201 (+25) *T16	201 (+25)	Positive
CV12/885 CVB 201 (+39) *T30	201 (+39)	Positive
CV12/885 CVB 202 (-6)	202 (-6)	Negative
CV12/885 CVB 202 (+7)	202 (+7)	Positive
CV12/885 CVB 202 (+19) *T10	202 (+19)	Positive
CV12/885 CVB 202 (+25) *T16	202 (+25)	Positive
CV12/885 CVB 203 (-9)	203 (-9)	Negative
CV12/885 CVB 203 (+25) *T16	203 (+25)	Positive
CV12/885 CVB 203 (+39) *T30	203 (+39)	Positive
CV12/885 CVB 204 (-7)	204 (-7)	Negative
CV12/885 CVB 204 (+7)	204 (+7)	Positive
CV12/885 CVB 204 (+19) *T10	204 (+19)	Positive
CV12/885 CVB 204 (+25) *T16	204 (+25)	Positive
CV12/885 CVB 205 (-7)	205 (-7)	Negative
CV12/885 CVB 205 (+7)	205 (+7)	Positive
CV12/885 CVB 205 (+19) *T10	205 (+19)	Positive
CV12/885 CVB 205 (+25) *T16	205 (+25)	Positive
CV12/885 CVB 206 (-8)	206 (-8)	Negative
CV12/885 CVB 206 (+7)	206 (+7)	Positive
CV12/885 CVB 207 (-6)	207 (-6)	Positive
CV12/885 CVB 207 (+7)	207 (+7)	Positive
CV12/885 CVB 207 (+19) *T10	207 (+19)	Positive
CV12/885 CVB 208 (-10)	208 (-10)	Negative
CV12/885 CVB 208 (+7)	208 (+7)	Positive
CV12/885 CVB 208 (+19) *T10	208 (+19)	Positive
CV12/885 CVB 208 (+25) *T16	208 (+25)	Positive
CV12/885 CVB 210 (-9)	210 (-9)	Negative

Serum name (ClinVet)	Abbreviation	Infection status
CV12/885 CVB 210 (+19) *T10	210 (+19)	Positive
CV12/885 CVB 210 (+25) *T16	210 (+25)	Positive
CV12/885 CVB 210 (+39) *T30	210 (+39)	Positive
CV12/885 CVB 211 (-7)	211 (-7)	Non-infected
CV12/885 CVB 211 (+25) *T16	211 (+25)	Non-infected
CV12/885 CVB 211 (+39) *T30	211 (+39)	Non-infected
CV12/885 CVB 213 (-7)	213 (-7)	Non-infected
CV12/885 CVB 213 (+19) *T10	213 (+19)	Non-infected
CV12/885 CVB 214 (-10)	214 (-10)	Negative
CV12/885 CVB 214 (+7)	214 (+7)	Positive
CV12/885 CVB 214 (+19) *T10	214 (+19)	Positive
CV12/885 CVB 214 (+25) *T16	214 (+25)	Positive
CV12/885 CVB 215 (-7)	215 (-7)	Non-infected
CV12/885 CVB 215 (+19) *T10	215 (+19)	Non-infected
CV12/885 CVB 218 (-10)	218 (-10)	Negative
CV12/885 CVB 218 (+25) *T16	218 (+25)	Positive
CV12/885 CVB 218 (+39) *T30	218 (+39)	Positive
	STUDY CV12/928	
CV12/928 14 (-8)	14 (-8)	Non-infected
CV12/928 47 (-8)	47 (-8)	Negative
CV12/928 47 (+16)	47 (+16)	Positive
CV12/928 47 (+37)	47 (+37)	Positive
CV12/928 47 (+44)	47 (+44)	Positive
CV12/928 47 (+51)	47 (+51)	Positive
CV12/928 48 (-7)	48 (-7)	Negative
CV12/928 48 (+14)	48 (+14)	Positive
CV12/928 48 (+28)	48 (+28)	Positive
CV12/928 48 (+42) *T9	48 (+42)	Positive
CV12/928 48 (+49) *T16	48 (+49)	Positive
CV12/928 48 (+98) *T65	48 (+98)	Positive
CV12/928 62 (-7)	62 (-7)	Negative
CV12/928 62 (+16)	62 (+16)	Positive
CV12/927 62 (+37)	62 (+37)	Positive
CV12/928 62 (+51) *T7	62 (+51)	Positive
CV12/928 CVB 161 (-7)	161 (-7)	Negative

Serum name (ClinVet)	Abbreviation	Infection status
CV12/928 CVB 161 (+7)	161 (+7)	Positive
CV12/928 CVB 161 (+28)	161 (+28)	Positive
CV12/928 CVB 161 (+78) *T43	161 (+78)	Positive
CV12/928 CVB 162 (-8)	162 (-8)	Non-infected
CV12/928 CVB 162 (+7)	162 (+7)	Non-infected
CV12/928 CVB 162 (+16)	162 (+16)	Non-infected
CV12/928 CVB 162 (+42) *T9	162 (+42)	Non-infected
CV12/928 CVB 163 (-8)	163 (-8)	Negative
CV12/928 CVB 163 (+14)	163 (+14)	Positive
CV12/928 CVB 163 (+28)	163 (+28)	Positive
CV12/928 CVB 164 (-7)	164 (-7)	Negative
CV12/928 CVB 164 (+14)	164 (+14)	Positive
CV12/928 CVB 164 (+24) *T7	164 (+24)	Positive
CV12/928 CVB 164 (+31) *T14	164 (+31)	Positive
CV12/928 CVB 164 (+45) *T28	164 (+45)	Positive
CV12/928 CVB 164 (+101) *T84	164 (+101)	Positive
CV12/928 CVB 165 (-8)	165 (-8)	Negative
CV12/928 CVB 165 (+28)	165 (+28)	Positive
CV12/928 CVB 165 (+105) *T71	165 (+105)	Positive
CV12/928 CVB 166 (-8)	166 (-8)	Non-infected
CV12/928 CVB 167 (-7)	167 (-7)	Negative
CV12/928 CVB 167 (+28)	167 (+28)	Positive
CV12/928 CVB 167 (+105) *T70	167 (+105)	Positive
CV12/928 CVB 168 (-7)	168 (-7)	Negative
CV12/928 CVB 168 (+7)	168 (+7)	Positive
CV12/928 CVB 168 (+28)	168 (+28)	Positive
CV12/928 CVB 168 (+35) *T0	168 (+35)	Positive

Serum name (ClinVet)	Abbreviation	Infection status
	Trypanosoma vivax	
	STUDY CV13/001	
CV13/001 CVB263 (+28)	263 (+28)	Positive
CV13/001 CVB315 (+28)	315 (+28)	Positive
CV13/001 CVB321 (+28)	321 (+28)	Positive

Non-infected = immunisation with saline solution instead of with parasite isolate.

Negative = sera collected before infection with parasite isolate.

Positive = confirmed presence of parasites in the sera after infection.

*T = days after treatment commenced.

(±) = days before/after infection.

APPENDIX C

The absorbance values at 405 nm were used to calculate the percentage inhibition for the inhibition format and the percentage positivity for the indirect format as described in sections 4.2.2.1 and 4.2.3.1 respectively.

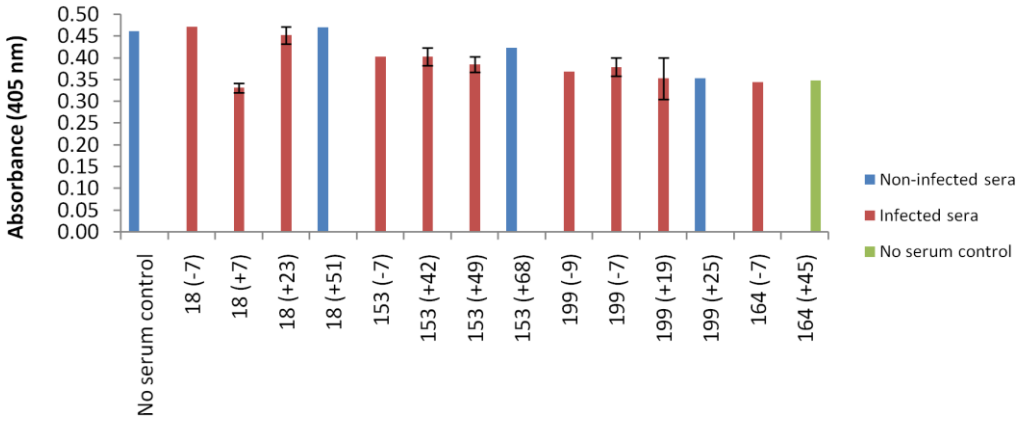

Figure C.1: Inhibition TcOPB ELISA using anti-TcOPB IgY antibodies with infected and non-infected sera. ELISA plates were coated with TcOPB (1 µg/ml in PBS, pH 7.4) blocked with 0.5% (w/v) BSA-PBS, 0.1% (v/v) Tween-20 and incubated with sera (1:10 dilution). Thereafter anti-TcOPB IgY primary antibodies from chicken 3, week 10 (1 µg/ml) were added. Rabbit anti-chicken IgY HRPO secondary antibody (1:15 000) and ABTS·H_2O_2 were used as the detection system. The absorbance readings at 405 nm represent the average of triplicate experiments after 30 min development. Each plate had a no serum control in quadruplicate.

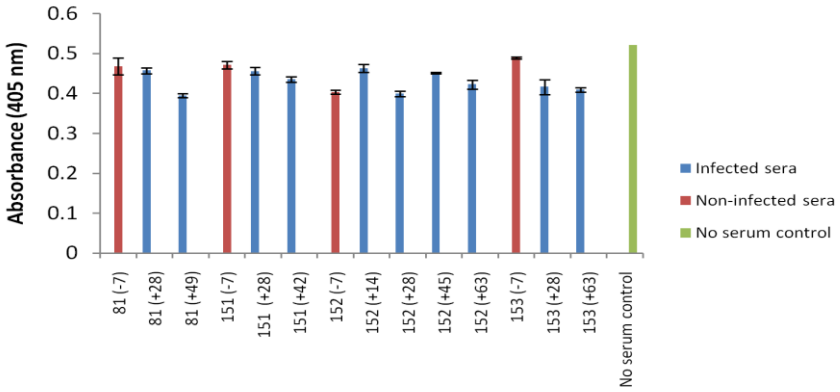

Figure C.2: Inhibition TcPGP ELISA and anti-TcPGP IgY antibodies with infected and non-infected sera. ELISA plates were coated with TcPGP (1 µg/ml in PBS, pH 7.4), blocked with 0.5% (w/v) BSA-PBS, 0.1% (v/v) Tween-20 and incubated with sera (1:10 dilution). Thereafter anti-TcPGP IgY from chicken 3, week 6 to 8 pool (5 µg/ml in blocking buffer, 100 µl/well, 37 °C, 1 hr) was added. Rabbit anti-chicken IgY HRPO secondary antibody (1:5 000) and ABTS·H_2O_2 were used as the detection system. The absorbance readings at 405 nm represent the average of triplicate experiments after 60 min development. Each plate had a no serum control in quadruplicate.

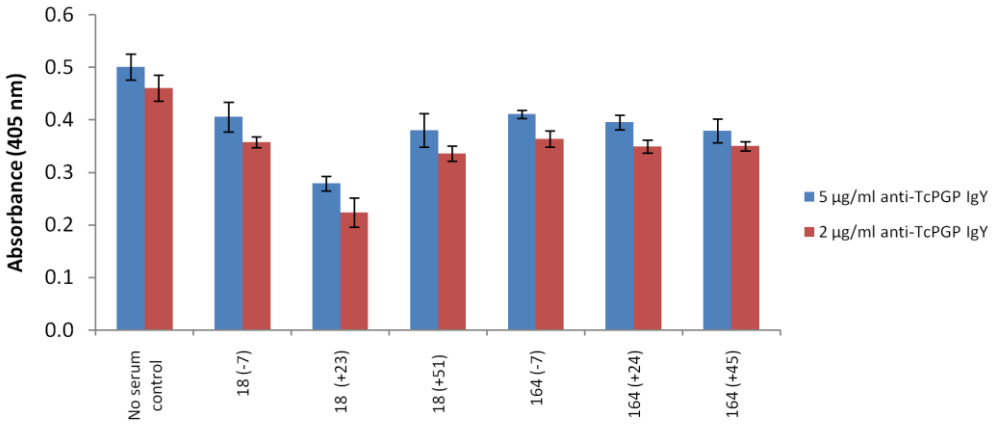

Figure C.3: Inhibition TcPGP ELISA comparing anti-TcPGP IgY antibody concentrations with infected and non-infected sera. ELISA plates were coated with TcPGP (1 µg/ml in PBS, pH 7.4), blocked with 0.5% (w/v) BSA-PBS, 0.1% (v/v) Tween-20 and incubated with sera (1:10). Thereafter anti-TcPGP IgY from chicken 3, week 6 to 8 pool (5 and 2 µg/ml) was added. Rabbit anti-chicken IgY HRPO secondary antibody (1:15 000) and ABTS·H_2O_2 were used as the detection system. The absorbance readings at 405 nm represent the average of triplicate experiments after 60 min development. Each plate had a no serum control in quadruplicate.

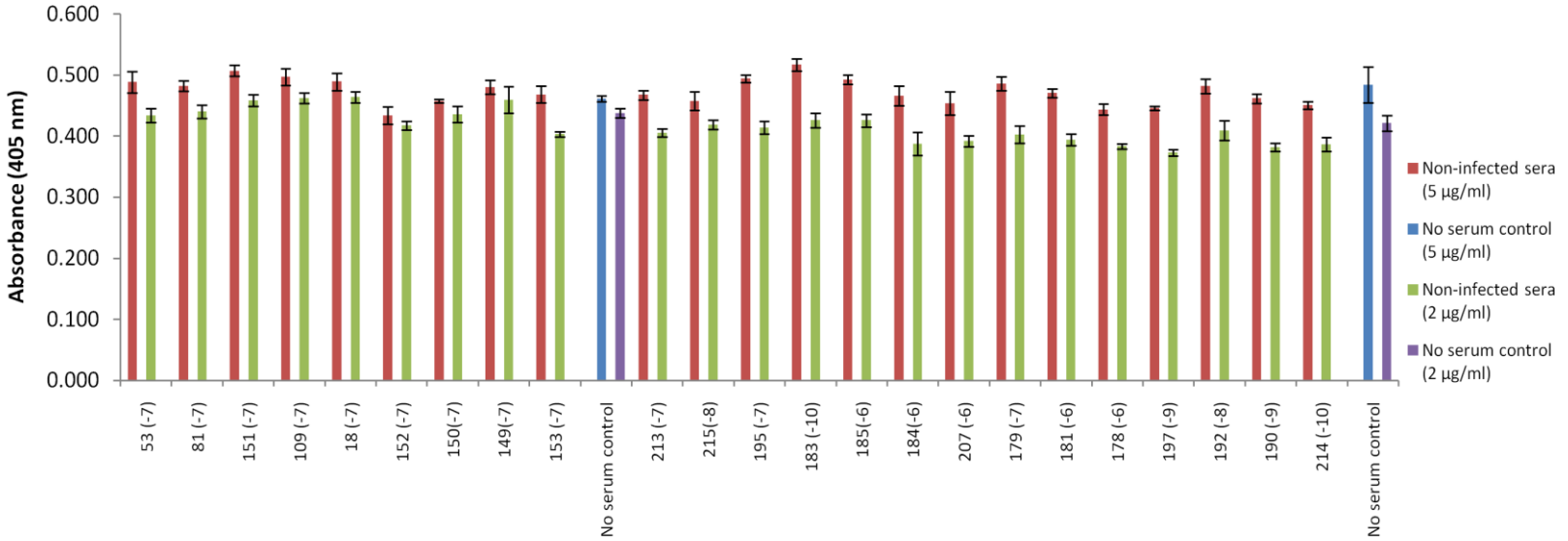

Figure C.4: Inhibition ELISA using TcPGP and anti-TcPGP IgY antibodies against non-infected sera to obtain a cut-off value. ELISA plates were coated with TcPGP (1 µg/ml in PBS, pH 7.4), blocked with 0.5% (w/v) BSA-PBS, 0.1% (v/v) Tween-20 and incubated with sera (1:10 dilution). Thereafter anti-TcPGP IgY from chicken 3, week 6 to 8 pool (5 and 2 µg/ml) was added. Rabbit anti-chicken IgY HRPO secondary antibody (1: 15 000) and ABTS·H_2O_2 were used as the detection system. The absorbance readings at 405 nm represent the average of triplicate experiments after 60 min development. Each plate had a no serum control in quadruplicate.

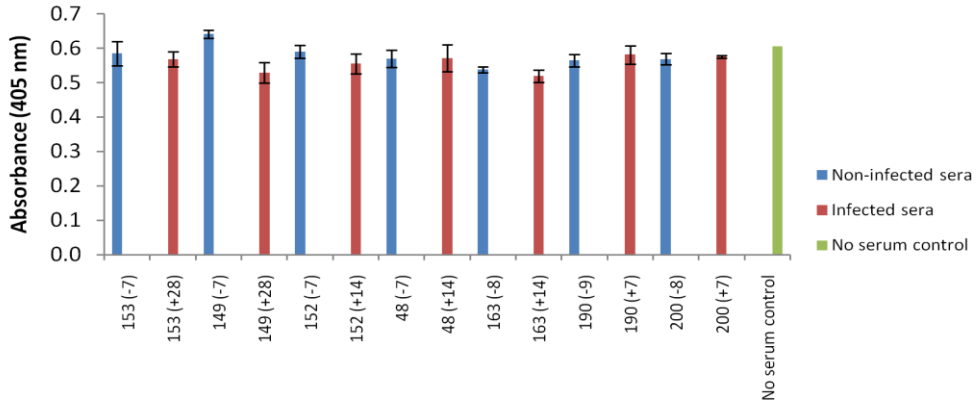

Figure C.5: Inhibition $TcCATL_{FL}$ ELISA using affinity purified anti-$TcCATL_{FL}$ IgY antibodies with infected and non-infected sera. ELISA plates were coated with $TcCATL_{FL}$ (0.05 µg/ml in PBS, pH 7.4), blocked with 0.5% (w/v) BSA-PBS and incubated with sera (1:10). Thereafter affinity purified anti-$TcCATL_{FL}$ IgY from chicken 3, week 6 (0.5 µg/ml) was added. Rabbit anti-chicken IgY HRPO secondary antibody (1:20 000) and ABTS·H_2O_2 were used as the detection system. The absorbance readings at 405 nm represent the average of triplicate experiments after 60 min development. Each plate had a no serum control in quadruplicate.

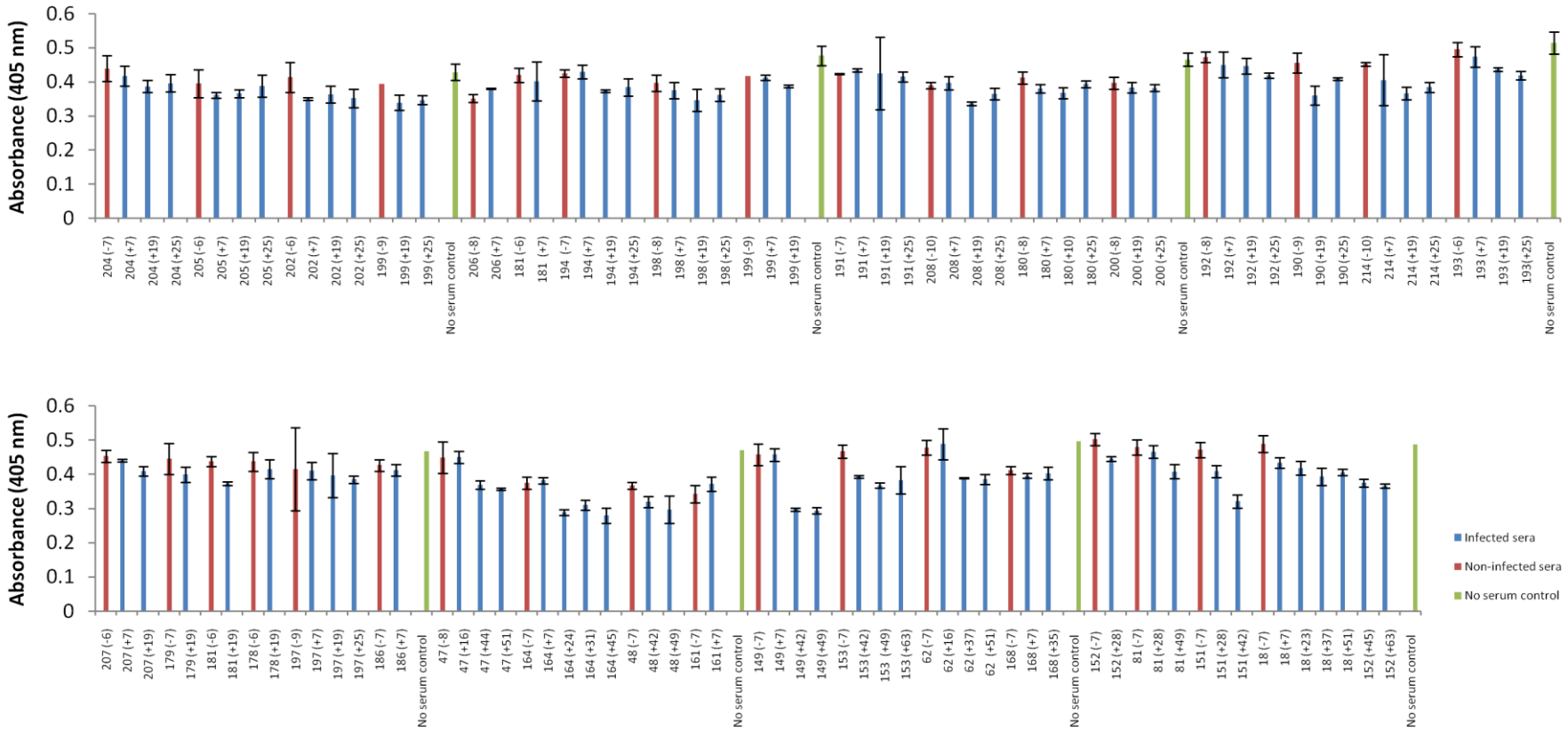

Figure C.6: Mass inhibition $TcCATL_{FL}$ ELISA using affinity purified anti-$TcCATL_{FL}$ IgY antibodies with infected and non-infected sera. ELISA plates were coated with $TcCATL_{FL}$ (0.05 µg/ml in PBS, pH 7.4), blocked with 0.5% (w/v) BSA-PBS and incubated with sera (1:10 dilution). Thereafter affinity purified anti-$TcCATL_{FL}$ IgY from chicken 3, week 6 (0.5 µg/ml) was added. Rabbit anti-chicken IgY HRPO secondary antibody (1:15 000) and ABTS·H_2O_2 were used as the detection system. The absorbance readings at 405 nm represent the average of triplicate experiments after 60 min development. Each plate had a no serum control in quadruplicate.

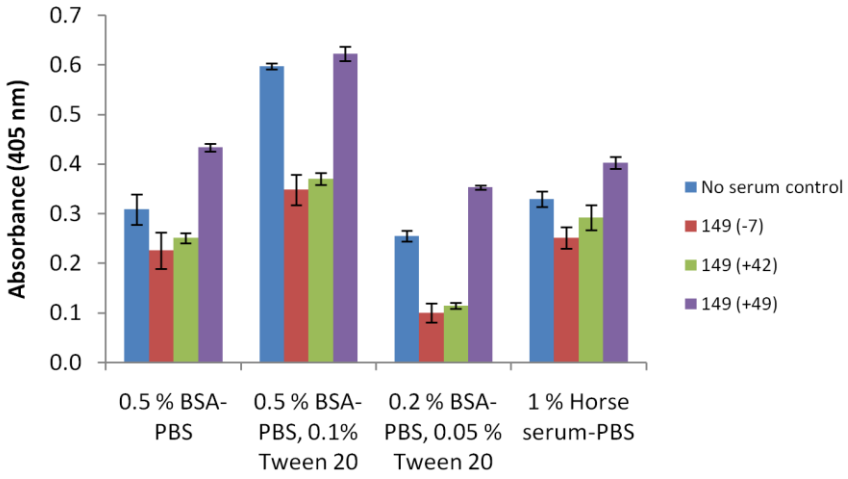

Figure C.7: Inhibition $TcCATL_{FL}$ ELISA using affinity purified anti-$TcCATL_{FL}$ IgY antibodies in different blocking buffers with infected and non-infected sera. ELISA plates were coated with $TcCATL_{FL}$ (0.05 µg/ml in PBS, pH 7.4), blocked with (A) 0.5% (w/v) BSA-PBS, (B) 0.5% (w/v) BSA-PBS, 0.1% (v/v) Tween-20, (C) 0.2% (w/v) BSA-PBS, 0.05% (v/v) Tween-20 and (D) 1% (v/v) horse serum-PBS and incubated with sera (1:10 dilution). Thereafter affinity purified anti-$TcCATL_{FL}$ IgY from chicken 3, week 6 (0.5 µg/ml) was added. Rabbit anti-chicken IgY HRPO secondary antibody (1:15 000) and ABTS·H_2O_2 were used as the detection system. The absorbance readings at 405 nm represent the average of triplicate experiments after 60 min development. Each plate had a no serum control in quadruplicate.

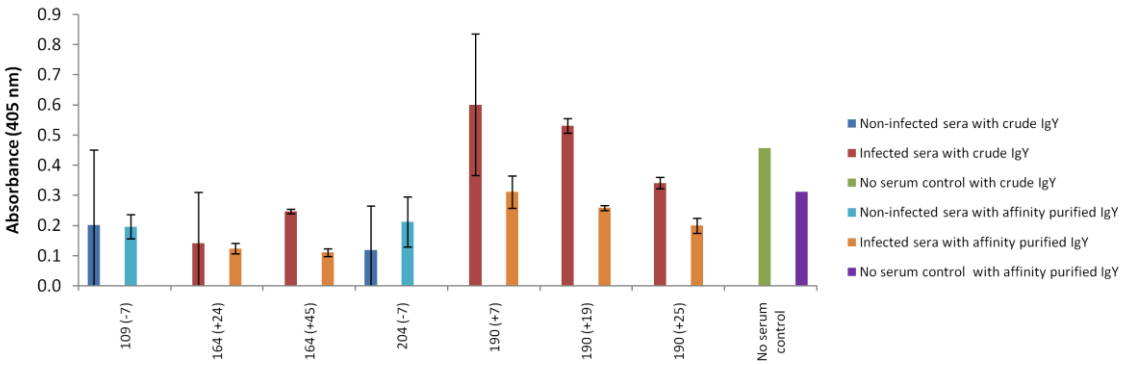

Figure C.8: Inhibition $TcCATL_{FL}$ ELISA using crude and affinity purified anti-$TcCATL_{FL}$ IgY antibodies with infected and non-infected sera. ELISA plates were coated with $TcCATL_{FL}$ (0.05 µg/ml in PBS, pH 7.4), blocked with 0.5% (w/v) BSA-PBS, 0.1% (v/v) Tween-20 and incubated with sera (1:10 dilution). Thereafter affinity purified anti-$TcCATL_{FL}$ IgY from chicken 3, week 6 (0.1 µg/ml) and crude anti-$TcCATL_{FL}$ from chicken 3, week 8 (10 µg/ml) were added. Rabbit anti-chicken-HRPO secondary antibody (1:15 000) and ABTS·H_2O_2 were used as the detection system. The absorbance readings at 405 nm represent the average of triplicate experiments after 45 min development. Each plate had a no serum control in quadruplicate.

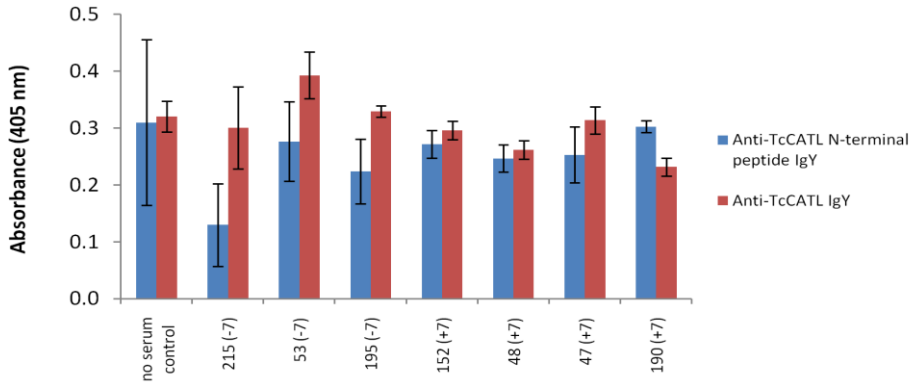

Figure C.9: Inhibition TcCATL ELISA using anti-TcCATL and affinity purified anti-TcCATL N-terminal peptide IgY antibodies with infected and non-infected sera. ELISA plates were coated with TcCATL (0.1 µg/ml in PBS, pH 7.4), blocked with 0.5% (w/v) BSA-PBS and incubated with sera (1:10 dilution). Thereafter anti-TcCATL IgY from chicken 3, week 11 and affinity purified anti-TcCATL N-terminal peptide IgY from pool 1 (2.5 µg/ml) were added. Rabbit anti-chicken IgY HRPO secondary antibody (1:20 000) and ABTS·H_2O_2 were used as the detection system. The absorbance readings at 405 nm represent the average of triplicate experiments after 60 min development. Each plate had a no serum control in quadruplicate.

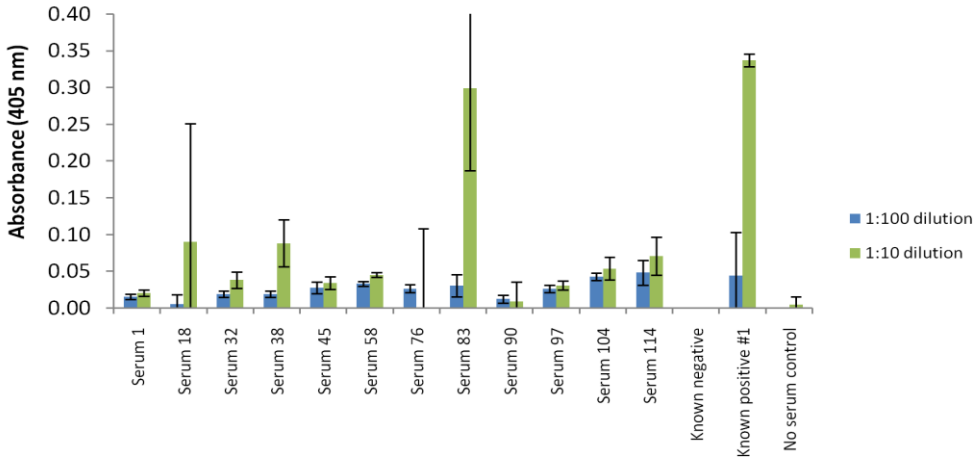

Figure C.10: Comparison of serum dilutions in the indirect TvCATL ELISA testing a selection of serum samples from the *T. vivax* blinded serum panel. ELISA plates were coated with TcCATL (0.5 µg/ml in PBS, pH 7.4), blocked with 0.5% (w/v) BSA-PBS, 0.1% (v/v) Tween-20 and incubated with sera (1:10 dilution). Rabbit anti-bovine IgG HRPO secondary antibody (1:5 000) and ABTS·H_2O_2 were used as the detection system. The absorbance readings at 405 nm represent the average of triplicate experiments after 30 min development. Each plate had a no serum control in quadruplicate.

REFERENCES

Abdulla, M. H., Lim, K. C., Sajid, M., McKerrow, J. H., Caffrey, C. R. (2007). *Schistosomiasis mansoni*: novel chemotherapy using a cysteine protease inhibitor. *PLOS Medicine*. **4**, e14.

Alexander, J., Coombs, G. H., Mottram, J. C. (1998). *Leishmania mexicana* cysteine proteinase-deficient mutants have attenuated virulence for mice and potentiate a Th1 response. *Journal of Immunology*. **161**, 6794-6801.

Alvarez, V., Niemirowicz, G. T., Cazzulo, J. J. (2011). The peptidases of *Trypanosoma cruzi*: digestive enzymes, virulence factors, and mediators of autophagy and programmed cell death. *Biochimica et Biophysica Acta*. **1824**, 195-206.

Ambit, A., Fasel, N., Coombs, G. H., Mottram, J. C. (2008). An essential role for the *Leishmania major* metacaspase in cell cycle progression. *Cell Death and Differentiation*. **15**, 113-122.

Anene, B. M., Onah, D. N., Nawa, Y. (2001). Drug resistance in pathogenic African trypanosomes: what hopes for the future? *Veterinary Parasitology*. **96**, 83-100.

Anene, B. M., Ezeokonkwo, R. C., Mmesirionye, T. I., Tetley, L., Brock, J. M., Barrett, M. P., De Koning, H. P. (2006). A diminazene-resistant strian of *Trypanosoma brucei brucei* from a dog is cross-resistnat to pentamidine in experimentally infected albino rats. *Parasitology*. **132**, 127-133.

Anosa, V. O., Isoun, T. T. (1976). Serum proteins, blood and plasma volumes in experimental *Trypanosoma vivax* infections of sheep and goats. *Tropical Animal Health and Production*. **8**, 14-19.

Antoine-Moussiaux, N., Magez, S., Desmecht, D. (2008). Contributions of experimental mouse models to the understanding of African trypanosomiasis. *Trends in Parasitology*. **24**, 411-418.

Antoine-Moussiaux, N., Büscher, P., Desmecht, D. (2009). Host-parasite interactions in trypanosomiasis: on the way to an anti-disease strategy. *Infection and Immunity*. **77**, 1276–1284.

Aparicio, I. M., Scharfstein, J., Lima, A. P. (2004). A new cruzipain-mediated pathway of human cell invasion by *Trypanosoma cruzi* requires trypomastigote membranes. *Infection and Immunity*. **72**, 5892-5902.

Apted, F. I. C. (1970). Clinical manifestations and diagnosis of sleeping sickness, In: The African Trypanosomiasias, (Mulligan, H. W. (Ed.) 661-683

Aravind, L., Koonin, V. E. (2002). Classification of the caspase-hemoglobinase fold: detection of new families and implication for the origin of the eukaryotic separins. *Proteins*. **46**, 355-367.

Arnold, T., Linke, D. (2007). Phase separation in the isolation and purification of membrane proteins. *Biotechnology*. **43**, 427-440.

Asonganyi, T., Doua, F., Kibona, S. N., Nyasulu, Y. M., Masake, R., Kuzoe, F. A. S. (1998). A multi-centre evaluation of the card indirect agglutination test for trypanosomiasis (TrypTect CIATT). *Annals of Tropical Medicine and Parasitology*. **92**, 837-844.

Atkinson, H. J., Babbitt, P. C., Sajid, M. (2009). The global cysteine peptidase landscape in parasites. *Trends in Parasitology*. **25**, 573-581.

Authié, E., Muteti, D., Mbawa, Z. R., Lonsdale-Eccles, J. D., Webster, P., Wells, C. (1992). Identification of a 33-kilodalton immunodominant antigen of *Trypanosoma congolense* as a cysteine protease. *Molecular and Biochemical Parasitology*. **56**, 103-116.

Authié, E., Duvallet, G., Robertson, C., Williams, D. J. L. (1993a). Antibody responses to a 33 kDa cysteine protease of *Trypanosoma congolense*: relationship to 'trypanotolerance' in cattle. *Parasite Immunology*. **15**, 465-474.

Authié, E., Muteti, D. K., Williams, D. J. L. (1993b). Antibody response to invariant antigens of *Trypanosoma congolense* in cattle of differing susceptibility to trypanosomiasias. *Parasite Immunology*. **15**, 101-111.

Authié, E. (1994). Bovine trypanosomiasias and trypanotolerance: a role for congopain? *Parasitology Today*. **10**, 360-364.

Authié, E., Boulangé, A., Muteti, D., Lalmanach, G., Gauthier, F., Musoke, A. J. (2001). Immunisation of cattle with cysteine proteinases of *Trypanosoma congolense*: targeting the disease rather than the parasite. *International Journal for Parasitology*. **31**, 1429-1433.

Awadé, A. C., Cleuziat, P., Gonzales, T., Robert-Baudouy, J. (1994). Pyrrolidone carboxyl peptidase (Pcp): an enzyme that removes pyroglutamic acid (pGlu) from pGlu-peptides and pGlu-proteins. *Proteins*. **20**, 34-51.

Bacchi, C. J. (1993). Resisitance to clinical drugs in African trypanosomes. *Parasitology Today*. **9**, 190-193.

Bailey, J. W., Smith, D. H. (1992). The use of the acridine orange QBC technique in the diagnosis of African trypanosomiasis. *Transactions of the Royal Society of Tropical Medicine and Hygiene*. **86**, 630.

Baral, T. N. (2010). Immunobiology of African trypanosomes: need of alternative interventions. *Journal of Biomedicine and Biotechnology*, 24.

Barrett, A. J., Rawlings, N. D. (1992). Oligopeptidases, and the emergence of the prolyl oligopeptidase family. *Biological Chemistry Hoppe Seyler*. **373**, 353-360.

Barrett, A. J., Rawlings, N. D. (2004). The clans and families of cysteine peptidases, In: Handbook of proteolytic enzymes, (Barret, A. J., Rawlings, N. D., Woessner, J. F. (Eds.)): London, Elsevier.

Barrett, M. P., Burchmore, R. J., Stich, A., Lazzari, J. O., Frasch, A. C., Cazzulo, J. J., Krishna, S. (2003). The trypanosomiases. *Lancet*. **362**, 1469-1480.

Barrett, M. P. (2010). Potential new drugs for human African trypanosomiasis: some progress at last. *Current Opinion in Infectious Diseases*. **23**, 603–608.

Barry, J. D., McCulloch, R. (2001). Antigenic variation in trypanosomes: enhanced phenotypic variation in a eukaryotic parasite. *Advances in Parasitology*. **49**, 1-70.

Barry, J. D., Marcello, L., Morrison, L. J., Read, A. F., Lythgoe, K., Jones, N., Carrington, M., Blandin, G., Böhme, U., Caler, E., Hertz-Fowler, C., Renauld, H., El-Sayed, N., Berriman, M. (2005). What the genome sequence is revealing about trypanosome antigenic variation. *Biochemical Society Transactions*. **33**, 986-989.

Bastos, I. M., Motta, F. N., Grellier, P., Santana, J. M. (2013). Parasite prolyl oligopeptidases and the challenge of designing chemotherapeuticals for Chagas disease, Leishmaniasis and African trypanosomiasis. *Current Medicinal Chemistry*. **20**, 3103-3115.

Bastos, I. M. D., Motta, F. N., Charneau, S., Santana, J. M., Dubost, L., Augustyns, K., Grellier, P. (2010). Prolyl oligopeptidase of *Trypanosoma brucei* hydrolyzes native

collagen, peptide hormones and is active in the plasma of infected mice. *Microbes and Infection*. **12**, 457-466.

Bell, D., Peeling, R. W. (2006). Evaluation of rapid diagnostic tests: malaria. *Nature Reviews Microbiology*, S34-S38.

Berasain, P., Carmona, C., Frangione, F., Cazzulo, J. J., Goni, F. (2003). Specific cleavage sites on human IgG subclasses by cruzipain, the major cysteine proteinase from *Trypanosoma cruzi*. *Molecular & Biochemical Parasitology*. **130**, 23-29.

Berriman, M., Ghedin, E., Hertz-Fowler, C. (2005). The genome of the African trypanosome *Trypanosoma brucei*. *Science*. **309**, 416-422.

Bertone, P., Kluger, Y., Lan, N., Zheng, D., Christendat, D., Yee, A., Edwards, A. M., Arrowsmith, C. H., Montelione, G. T., Gerstein, M. (2001). SPINE: an integrated tracking database and data mining approach for identifying feasible targets in high-throughput structural proteomics. *Nucleic Acids Research*. **29**, 2884-2898.

Biron, D. G., Moura, H., Marche, L., Hughes, A. L., Thomas, F. (2005). Towards a new conceptual approach to "parasitoproteomics". *Trends in Parasitology*. **21**, 162-168.

Bisser, S., N'Siesi, F., Lejon, V., Preux, P., Van Nieuwenhove, S., Miaka Mia Bilenge, C., Buscher, P. (2007). Equivalence trial of melarsoprol and nifurtimox monotherapy and combination therapy for the treatment of second-stage *Trypanosoma brucei gambiense* sleeping sickness. *Journal of Infectious Diseases*. **195**, 322 - 329.

Bizaaré, L. C., (2008). Evaluation of congopain and oligopeptidase B as anti-disease vaccines for African trypanosomiasis. University of KwaZulu-Natal, Pietermaritzburg. MSc.

Black, S. J., Sendashonga, C. N., Webster, P. (1986). Regulation of parasite-specific antibody responses in resistant (C57BL/6) and susceptible (C3H/He) mice infected with *Trypanosoma (trypanozoon) brucei brucei*. *Parasite Immunology*. **8**, 425-442.

Blum, B., Beier, H., Gross, H. J. (1987). Improved silver staining of plant proteins, RNA and DNA in polyacrylamide gels. *Electrophoresis*. **8**, 93-99.

Bonaldo, M. C., d'Escoffier, L. N., Salles, J. M., Goldenberg, S. (1991). Characterization and expression of proteases during *Trypanosoma cruzi* metacyclogenesis. *Experimental Parasitology*. **73**, 44-51.

Bossard, G., Boulangé, A., Hölzmuller, P., Thévenon, S., Patrel, D., Authié, E. (2010). Serodiagnosis of bovine trypanosomosis based on HSP70/BiP inhibition ELISA. *Veterinary Parasitology*. **173**, 39-47.

Boulangé, A., Katende, J., Authié, E. (2002). *Trypanosoma congolense*: expression of a heat shock protein 70 and initial evaluation as a diagnostic antigen for bovine trypanosomosis. *Experimental Parasitology*. **100**, 6-11.

Bouteille, B., Buguet, A. (2012). The detection and treatment of human African trypanosomiasis. *Research and Reports in Tropical Medicine*. **3**, 35-45.

Bouyer, J., Bouyer, F., Donadeu, M., Rowan, T., Napier, G. B. (2013). Community- and farmer-based management of animal African trypanosomiasis in cattle. *Trends in Parasitology*. **29**, 1-4.

Bowden, G. A., Paredes, A. M., Georgiou, G. (1991). Structure and morphology of protein inclusion bodies in *E. coli*. *Biotechnology*. **9**, 725-730.

Bozhkov, P. V., Smertenko, A. P., Zhivotovsky, B. (2010). Apasing out metacaspases and caspases: proteases of many trades. *Science Signalling*. **3**, pe48.

Bradford, M. M. (1976). A rapid and sensitive method for the quantitation of microgram quantities of protein utilizing the principle of protein-dye binding. *Analytical Biochemistry*. **72**, 248-254.

Brandenberger, G., Buguet, A., Spiegel, K., Stanghellini, A., Muanga, G., Bogui, P., Dumas, M. (1996). Disruption of endocrine rhythms in sleeping sickness with preserved relationship between hormonal pulsatility and the REM-NREM sleep cycles. *Journal of Biological Rhythms*. **11**, 258-267.

Brun, R., Schumacher, R., Schmid, C., Kunz, C., Burri, C. (2001). The phenomenon of treatment failures in human African trypanosomiasis. *Tropical Medicine and International Health*. **6**, 906-914.

Brun, R., Don, R. H., Jacobs, R. T., Wang, M. Z., Barrett, M. P. (2011). Development of novel drugs for human African trypanosomiasis. *Future Microbiology*. **6**, 677-691.

Burgess, R. R. (2009). Refolding solubilized inclusion body proteins. *Methods in Enzymology*. **463**, 259-282.

Burleigh, B. A., Caler, E. V., Webster, P., Andrews, N. W. (1997). A cytosolic serine endopeptidase from *Trypanosoma cruzi* is required for the generation of Ca^{2+} -signaling in mammalian cells. *Journal of Cell Biology*. **136**, 609-620.

Burri, C., Stich, G., Brun, R. (2004). Current chemotherapy of human African trypanosomiasis, In: Trypanosomiasis, (Maudlin, I., Holmes, P. H., Miles, M. A. (Eds.)): Wallingford, U.K., CABI Publishing.

Burri, C. (2010). Chemotherapy against human African trypanosomiasis: is there a road to success? *Parasitology*. **137**, 1987-1994.

Busby Jr., W. H., Youngblood, W. W., Kizer, J. S. (1982). Studies of substrate requirements, kinetic properties, and competive inhibitor of the enzymes catabolizing TRH in rat brain. *Brain Research*. **242**, 261-270.

Büscher, P., Gilleman, Q., Lejon, V. (2013). Rapid diagnostic test for sleeping sickness. *New England Journal of Medicine*. **368**, 1069-1070.

Buyst, H. (1975). The diagnosis of sleeping sickness in a district hospital in Zambia. *Annales de la Societe Belge de Medecine Tropicale*. **55**, 551-557.

Cabrera, L., De Witte, J., Victor, B., Vermeiren, L., Zimic, M., Brandt, J., Geysen, D. (2009). Specific detection and identification of African trypanosomes in bovine peripheral blood by means of a PCR-ELISA assay. *Veterinary Parasitology*. **164**, 111-117.

Caffrey, C. R., Scory, S., Steverding, D. (2000). Cysteine proteinases of trypanosome parasites: novel targets for chemotherapy. *Current Drug Targets*. **1**, 155-162.

Caffrey, C. R., Hansell, E., Lucas, K. D., Brinen, L. S., Hernandez, A. A., Cheng, J., Gwaltney, S. L., Roush, W. R., Stierhof, Y. D., Bogyo, M., Steverding, D., McKerrow, J. H. (2001). Active site mapping, biochemical properties and subcellular localization of rhodesian, the major cysteine protease of *Trypanosoma brucei rhodesiense*. *Molecular and Biochemical Parasitology*. **118**, 61-73.

Caffrey, C. R., Steverding, D. (2009). Kinetoplastid papain-like cysteine peptidases. *Molecular and Biochemical Parasitology*. **167**, 12-19.

Caffrey, C. R., Lima, A. P., Steverding, D. (2011). Cysteine peptidases of kinetoplastid parasites, In: Cysteine Proteases of Pathogenic Organisms, (Robinson, M. W., Dalton, J. P. (Eds.)), Landes Bioscience and Springer Science.

Caler, E. V., de Avalos, S. V., Haynes, P. A., Andrews, N. W., Burleigh, B. A. (1998). Oligopeptidase B-dependent signalling mediates host cell invasion by *Trypanosoma cruzi*. *EMBO Journal*. **17**, 4975-4986.

Canning, P., Rea, D., Morty, R. E., Fülöp, V. (2013). Crystal structure of *Trypanosoma brucei* oligopeptidase B broaden the paradigm of catalytic regulation in prolyl oligopeptidase family enzymes. *PLOS ONE*. **8**, e79349.

Cattand, P., Miezan, B. T., de Raadt, P. (1988). Human African trypanosomiasis: use of double centrifugation of cerebrospinal fluid to detect trypanosomes. *Bulletin of the World Health Organization*. **66**, 83.86.

Cattand, P., Jannin, J., Lucas, P. (2001). Sleeping sickness surveillance: an essential step towards elimination. *Tropical Medicine and International Health*. **6**, 348-361.

Cazzulo, J. J., Cazzulo Franke, M. C., Martínez, J., Franke de Cazzulo, B. M. (1990). Some kinetic properties of a cysteine proteinase (cruzipain) from *Trypanosoma cruzi*. *Biochimica et Biophysica Acta*. **1037**, 186-191.

Cazzulo, J. J., Frasch, A. C. (1992). SAPA/trans-sialidase and cruzipain: two antigens from *Trypanosoma cruzi* contain immunodominant but enzymatically inactive domains. *FASEB Journal*. **14**, 3259-3264.

Cereghino, G. P. L., Cereghino, J. L., Ilgen, C., Cregg, J. M. (2002). Production of recombinant proteins in fermenter cultures of the yeast *Pichia pastoris*. *Current Opinion in Biotechnology*. **13**, 329-332.

Chagas, J. R., Authié, E., Serveau, C., Lalmanach, G., Juliano, L., Gauthier, F. (1997). A comparison of the enzymatic properties of the major cysteine proteinases from *Trypanosoma congolense* and *Trypanosoma cruzi*. *Molecular and Biochemical Parasitology*. **88**, 85-94.

Chan, A. B., Fox, J. D. (1999). NASBA and other transcription-based amplification methods for research and diagnostic microbiology. *Reviews in Medical Microbiology*. **10**, 185-196.

Chan, V. J., Selzer, P. M. M., J. H., Sakanari, J. A. (1999). Expression and alteration of the S2 subsite of the *Leishmania major* cathepsin B-like cysteine protease. *Biochemical Journal*. **340**, 113-117.

Chappuis, F., Loutan, L., Simarro, P. P., Lejon, V., Büscher, P. (2005a). Options for field diagnosis of human African trypanosomiasis. *Clinical Microbiology Reviews*. **18**, 133-146.

Chappuis, F., Udayraj, N., Stietenroth, K., Meussen, A., Bovier, P. A. (2005b). Efluornithine is safer than melarsoprol for the treatment of second-stage *Trypanosoma brucei gambiense* human African trypanosomiasias. *Clinical Infectious Diseases*. **41**, 748-751.

Chitanga, S., Marcotty, T., Namangala, B., Van den Bossche, P., Van Den Abbeele, J., Delespaux, V. (2011). High prevalence of drug resistance in animal trypanosomes without a history of drug exposure. *PLOS Neglected Tropical Diseases*. **5**, e1454.

Chothia, C., Lesk, A. M. (1986). The relation between the divergence of sequence and structure in proteins. *EMBO Journal*. **5**, 823e826.

Chowdhury, I., Tharakan, B., Bhat, G. K. (2008). Caspases - an update. *Comparative Biochemistry and Physiology Part B: Biochemistry and Molecular Biology*. **151**, 10.

Christendat, D., Yee, A., Dharamsi, A., Kluger, Y., Savchenko, A., Cort, J. R., Booth, V., Mackereth, C. D., Saridakis, V., Ekiel, I., Kozlov, G., Maxwell, K. L., Wu, N., McIntosh, L. P., Gehring, K., Kennedy, M. A., Davidson, A. R., Pai, E. F., Gerstein, M., Edwards,

A. M., Arrowsmith, C. H. (2000). Structural proteomics of an archaeon. *Natural Structural Biology*. **7**, 903-909.

Clark, E. B. (1998). Refolding of recombinant proteins. *Current Opinion in Biotechnology*. **9**, 157-163.

Clayton, C., Hausler, T., Blattner, J. (1995). Protein trafficking in kinetoplastid protozoa. *Microbiological Reviews*. **59**, 325-344.

Clayton, C. E. (1992). Developmental regulation of nuclear gene expression in *Trypanosoma brucei*. *Progress in Nucleic Acids Research and Molecular Biology*. **43**, 37-66.

Clerinx, J., Vlieghe, E., Asselman, V., Van de Casteele, S., Maes, M. B., Lejon, V. (2012). Human African trypanosomiasis in a Belgian traveller returning from the Masai Mara area, Kenya, February 2012. *Euro Surveillance*. **17**, 20111.

Coetzer, T. H. T., Goldring, J. P., Huson, L. E. J. (2008). Oligopeptidase B: a processing peptidase involved in pathogenesis. *Biochimie*. **90**, 336-344.

Cohen, S. N., Chang, A. C. Y., Hsu, L. (1972). Nonchromosomal antibiotic resistance in bacteria: genetic transformation of *Escherichia coli* by R-factor DNA. *Proceedings of the National Academy of Sciences*. **69**, 2110-2114.

Coll, N. S., Vercammen, D., Smidler, A., Clover, C., Van Breusegem, F., Dangl, J. L., Epple, P. (2010). *Arabidopsis* type I metacaspases control cell death. *Science*. **330**, 1393-1397.

Cornelissen, A., Bakkeren, G. A., Barry, J. D., Michels, P., Borst, P. (1985). Characteristics of trypanosome varient antigen genes active in the tsetse fly. *Nucleic Acids Research*. **13**, 4661-4676.

Cortez, A. P., Rodrigues, A. C., Garcia, H. A., Neves, L., Batista, J. S., Bengaly, Z., Paiva, F., Teixeira, M. M. G. (2009). Cathepsin L-like genes of *Trypanosoma vivax* from Africa and South America - characterization, relationships and diagnostic implications. *Molecular and Cellular Probes*. **23**, 44-51.

Courtin, F., Rayaissé, J. B., Tamboura, I., Serdébéogo, O., Koudougou, Z., Solano, P., Sidibé, I. (2010). Updating the northern tsetse limit in Burkina Faso (1949–2009): impact of global change. *International Journal of Environmental Research and Public Health* **7**, 1708-1719.

Cregg, J. M., Madden, K. R. (1988). Development of the methylotrophic yeast, *Pichia pastoris*, as a host for the production of foreign proteins. *Developments in Industrial Microbiology* **29**, 33-41.

Cross, G. A. M. (1975). Identification, purification and properties of clone specific glycoprotein antigens constituting the surface coat of *Trypanosoma brucei*. *Parasitology*. **71**, 393-417.

Cross, G. A. M. (1990). Cellular and genetic aspects of antigenic variation in African trypanosomes. *Annual Review of Immunology*. **8**, 83-110.

Crowe, J. S., Lamont, A. G., Barry, J. D., Vickerman, K. (1984). Cytotoxicity of monoclonal antibodies to *Trypanosoma brucei*. *Transactions of the Royal Society of Tropical Medicine and Hygiene*. **78**.

Crowther, J. R. (2000). The ELISA Guidebook, Vol 149. Humana Press Inc., Totowa, NJ.

Cummins, P. M., O'Connor, B. (1998). Pyroglutamyl peptidase: an overview of the three known enzymatic forms. *Biochimica et Biophysica Acta*. **1429**, 1-17.

da Silva-Lopez, R. E., Morgado-Díazb, J. A., dos Santosa, P. T., Giovanni-De-Simonea, S. (2008). Purification and subcellular localization of a secreted 75 kDa *Trypanosoma cruzi* serine oligopeptidase. *Acta Tropica*. **107**, 159-167.

Dando, P. M., Fortunato, M., Strand, G. B., Smith, T. S., Barrett, A. J. (2003). Pyroglutamyl-peptidase I: cloning, sequencing, and characterisation of the recombinant human enzyme. *Protein Expression and Purification*. **28**, 111-119.

Das, M., Mukherjee, S. B., Shaha, C. (2001). Hydrogen peroxide induces apoptosis-like death in *Leishmania donovani* promastigotes. *Journal of Cell Science*. **114**, 2461-2469.

De Greef, C., Chimfwembe, E., Wabacha, J. K., Songa, E. B., Hamers, R. (1992). Only the serum-resistant bloodstream forms of *Trypanosoma brucei rhodesiense* express the serum resistance associated (SRA) protein. *Annales de la Societe Belge de Medecine Tropicale*. **72**, 13-21.

Deborggraeve, S., Claes, F., Laurent, T., Mertens, P., Leclipteux, T., Dujardin, J. C., Herdewijn, P., Büscher, P. (2006). Molecular dipstick test for diagnosis of sleeping sickness. *Journal of Clinical Microbiology*. **44**, 2884-2889.

Deborggraeve, S., Büscher, P. (2010). Molecular diagnostics for sleeping sickness: what is the benefit for the patient? *Lancet Infectious Diseases*. **10**, 433-439.

Debrabant, A., Lee, N., Bertholet, S., Duncan, R., Nakhasi, H. L. (2003). Programmed cell death in trypanosomatids and other unicellular organisms. *International Journal for Parasitology*. **33**, 257.

Delespaux, V., Geerts, S., Brandt, J., Elyn, R., Eisler, M. C. (2002). Monitoring the correct use of isometamidium by farmers and veterinary assistants in Eastern Province of Zambia using isometamidium-ELISA. *Veterinary Parasitology*. **110**, 117-122.

Delespaux, V., Geysen, D., van den Bossche, P., Geerts, S. (2008). Molecular tools for the rapid detection of drug resistance in animal trypanosomes. *Trends in Parasitology*. **24**, 236-242.

Desquesnes, M., McLaughlin, G., Zoungrana, A., Davila, A. M. (2001). Detection and identification of *Trypanosoma* of African livestock through a single PCR based on internal transcribed spacer 1 of rDNA. *International Journal for Parasitology*. **31**, 610-614.

Desquesnes, M., Dávila, A. M. R. (2002). Applications of PCR-based tools for detection and identification of animal trypanosomes: a review and perspectives. *Veterinary Parasitology*. **109**, 213-231.

Desquesnes, M. (2004). Livestock trypanosomoses and their vectors in latin America. OIE and CIRAD (Centre de coopération internationale en recherche agronomique pour le développement). World Organisation for Animal Health (OIE), Paris, France.

Donelson, J. E. (2003). Antigenic variation and the African trypanosome genome. *Acta Tropica*. **85**, 391-404.

Doolittle, R. F., Armentrout, R. W. (1968). Pyrrolidonyl peptidase. An enzyme for selective removal of pyrrolidonecarboxylic acid residues from polypeptides. *Biochemistry*. **7**, 516-521.

Dorta, M. L., Ferreira, A. T., Oshiro, M. E., Yoshida, N. (1995). Ca^{2+} signal induced by *Trypanosoma cruzi* metacyclic trypomastigote surface molecules implicated in mammalian cell invasion. *Molecular and Biochemical Parasitology*. **73**, 285-289.

dos Santos, A. L. S., Sodré, C. L., Branquinha, M. H., d'Avila-Levy, C. M. (2013). Proteolytic inhibitors: implications on microorganisms development, virulence and pathogenesis. *Current Medicinal Chemistry*. **20**, 3035-3040.

Doyle, P. S., Zhou, Y. M., Engel, J. C., McKerrow, J. H. (2007). A cysteine protease inhibitor cures Chagas' disease in an immunodeficient-mouse model of infection. *Antimicrobial Agents and Chemotherapy*. **51**, 3932-3939.

Dukes, P., Gibson, W. C., Gashumba, J. K., Hudson, K. M., Bromidge, T. J., Kaukus, A., Asonganyi, T., Magnus, E. (1992). Absence of the LiTat 1.3 (CATT antigen) gene in *Trypanosoma brucei gambiense* stocks from Cameroon. *Acta Tropica*. **51**, 23-34.

Dumas, M., Bisser, S. (1999). Clinical aspects of human African trypanosomiasias, In: Progress in Human African Trypasomiasias, Sleeping Sickness, (Dumas, M., Bouteille, B., Buguet, A. (Eds.)) 215-233: Paris, Springer-Verlag.

Duszenko, M., Figgarella, K., Macleod, E., Welburn, S. C. (2006). Death of a trypanosome: a selfish altruism. *Trends in Parasitology*. **22**, 536-542.

Dvorák, J., Delcroix, M., Rossi, A., Vopalensky, V., Pospíšek, M., Šedinova, M., Mikeš, L., Sajid, M., Sali, A., McKerrow, J. H. (2005). Multiple cathepsin B isoforms in schistosomula of *Trichobilharzia regenti*: identification, characterisation and putative role in migration and nutrition. *International Journal for Parasitology*. **35**, 895-910.

Eisler, M. C., Lessard, P., Masake, R. A., Moloo, S. K., Peregrine, A. S. (1998). Sensitivity and specificity of antigen-capture ELISAs for diagnosis of *Trypanosoma congolense* and *Trypanosoma vivax* infections in cattle. *Veterinary Parasitology*. **79**, 187-201.

Eisler, M. C., Dwinger, R. H., Majiwa, P. A. O., Picozzi, K. (2004). Diagnosis and epidemiology of African animal African trypanosomiasis, In: The Trypanosomiases, (Maudlin, I., Holmes, P. H., Miles, M. A. (Eds.)): Wallingford, CAB International.

Ellis, J. R., Scott, J. R., Machugh, N. D. (1987). Peripheral blood leucocytes subpopulation dynamics during *Trypanosoma congolense* infection in Boran and N'Dama cattle: an analysis using monoclonal antibodies and flow cytometry. *Parasite Immunology*. **9**, 363-378.

Engstler, M., Pfohl, T., Herminghaus, S., Boshart, M., Wiegertjies, G., Heddergott, N., Overath, P. (2007). Hydrodynamic flow-mediated protein sorting on the cell surface of trypanosomes. *Cell*. **131**, 505-515.

Enyaru, J. C., Matovu, E., Akol, M., Sebikali, C., Kyambadde, J., Schmidt, C., Brun, R., Kaminsky, R., Ogwal, L. M., Kansiime, F. (1998). Parasitological detection of *Trypanosoma brucei gambiense* in serologically negative sleeping-sickness suspects from north-western Uganda. *Annales of Tropical Medicine and Parasitology*. **92**, 845-850.

Erez, E., Fass, D., Bibi, E. (2009). How intramembrane proteases bury hydrolytic reactions in the membrane. *Nature*. **459**, 371-378.

Ersfeld, K. (2011). Nuclear architecture, genome and chromatin organisation in *Trypanosoma brucei*. *Research in Microbiology*. **20**, 1-11.

Esposito, D., Chatterjee, D. K. (2006). Enhancement of soluble protein expression through the use of fusion tags. *Current Opinion in Biotechnology*. **17**, 353-358.

Eyford, B. A., Sakurai, T., Smith, D., Loveless, B., Hertz-Fowlerd, C., Donelson, J. E., Inoue, N., Pearson, T. W. (2011). Differential protein expression throughout the life cycle of *Trypanosoma congolense*, a major parasite of cattle in Africa. *Molecular and Biochemical Parasitology*. **177**, 116-125.

Eyford, B. A., Ahmad, R., Enyaru, J. C., Carr, S. A., Pearson, T. W. (2013). Identification of trypanosome proteins in plasma from African sleeping sickness patients infected with *T. b. rhodesiense*. *PLOS ONE*. **8**, e71463.

Facer, C. A., Crossley, J. M., Clarkson, M. J., Jenkins, G. C. (1982). Haemolytic anaemia in bovine trypanosomiasias. *Journal of Comparative Pathology*. **92**, 393-401.

Ferrara, F., Naranjo, L. A., Kumar, S., Gaiotto, T., Mukundae, H., Swanson, B., Bradbury, A. R. M. (2012). Using phage and yeast display to select hundreds of monoclonal antibodies: application to antigen 85, a, Tuberculosis biomarker. *PLOS ONE*. **7**, e49535.

Févre, E. M., Wissmann, B. V., Welburn, S. C., Lutumba, P. (2008). The burden of Human African Trypanosomiasis. *PLOS Neglected Tropical Diseases*. **2**, e333.

Field, M. C., Lumb, J. H., Adung'a, V. O., Jones, N. G., Engstler, M. (2009). Macromolecular trafficking and immune invasion in African trypanosomes. *International Review of Cell and Molecular Biology*. **278**, 1-67.

Fülöp, V., Böcskei, Z., Polgár, L. (1998). Prolyl oligopeptidase: an unusual β-propeller domain regulates proteolysis. *Cell*. **94**, 161-170.

Gasteiger, E., Hoogland, C., Gattiker, A., Duvaud, S., Wilkins, M. R., Appel, R. D., Bairoch, A. (2005). Protein identification and analysis tools on the ExPASy server, In: The Proteomics Protocols Handbook, (Walker, J. M. (Ed.), Humana Press.

Geerts, S., Holmes, P. H. (1998). Drug management and parasite resistance in bovine trypanosomiasis in Africa. *PAAT Technical and Scientific Series*. **1**.

Geerts, S., Holmes, P. H., Diall, O., Eisler, M. C. (2001). African bovine trypanosomiasis: the problem of drug resistance. *Trends in Parasitology*. **17**, 25-28.

Gérczei, T., Keserü, G. M., Náray-Szabó, G. (2000). Construction of a 3D model of oligopeptidase B: a potential processing enzyme in prokaryotes. *Journal of Molecular Graphics and Modelling*. **18**, 7-17.

Gibson, W., Backhouse, T., Griffiths, A. (2002). The human serum resistance associated gene is ubiquitous and conserved in *Trypanosoma brucei rhodesiense* throughout East Africa. *Journal of Molecular Epidemiology and Evolutionary Genetics in Infectious Diseases*. **1**, 207-214.

Goldring, J. P., Coetzer, T. H. T. (2003). Isolation of chicken immunoglobulins (IgY) from egg yolk. *Biochemistry and Molecular Biology Education*. **31**, 185-187.

Goldring, J. P. D., Thobakgale, C., Hiltunen, T., Coetzer, T. H. T. (2005). Raising antibodies in chickens against primaquine, pyrimethamine, dapsone, tetracycline, and doxycycline. *Immunological Investigations*. **34**, 101-114.

Gonzáles, I. J., Desponds, C., Schaff, C., Mottram, J. C., Fasel, N. (2007). *Leishmania major* metacaspase can replace yeast metacaspase in programmed cell death and has arginine-specific cysteine peptidase activity. *International Journal for Parasitology*. **37**, 161-172.

Granér, T., (2005). Understanding chromatographic behaviour of glycosylated proteins. Uppsala University, Uppsala. MSc.

Greiner, M., Sohr, D., Göbel, P. (1995). A modified ROC analysis for the selection of cut-off values and the definition of intermediate results of serodiagnostic tests. *Journal of Immunological Methods*. **185**, 123-132.

Greiner, M., Kumar, S., Kyeswa, C. (1997). Evaluation and comparison of antibody ELISAs for serodiagnosis of bovine trypanosomosis. *Veterinary Parasitology*. **73**, 197-205.

Gruszynski, A. E., DeMaster, A., Hooper, N. M., Bangs, J. D. (2003). Surface coat remodelling during differentiation of *Trypanosoma brucei*. *Journal of Biological Chemistry*. **278**, 24665-24672.

Grutter, M. G. (2000). Caspases: key players in programmed cell death. *Current Opinion in Structural Biology*. **10**, 649-655.

Haag, J., O'hUigin, C., Overath, P. (1998). The molecular phylogeny of trypanosomes: evidence for an early divergence of the Salivaria. *Molecular and Biochemical Parasitology*. **91**, 37 - 49.

Hargrove, J. W., Torr, S. J., Kindness, H. M. (2003). Insecticide-treated cattle against tsetse (Diptera: Glossinidae): what governs success? *Bulletin of Entomological Research*. **93**, 203-217.

Hargrove, J. W., Ouifki, R., Kajunguri, D., Vale, G. A., Torr, S. J. (2012). Modelling the control of trypanosomiasis using trypanocides or insecticide-treated livestock. *PLOS Neglected Tropical Diseases*. **5**, e1615.

Hasker, E., Lutumba, P., Chappuis, F., Kande, V., Potet, J., De Weggheleire, A., Kambo, C., Depoortere, E., Pécoul, B., Boelaert, M. (2012). Human African trypanosomiais in the Democratic Republic of the Congo: a looming emergency? *PLOS Neglected Tropical Diseases*. **6**, e1950.

Hedstrom, L. (2002). Serine protease mechanism and specificity. *Chemical Review*. **102**, 4501-4524.

Helms, M. J., Ambit, A., Appleton, P., Tetley, L., Coombs, G. H., Mottram, J. C. (2006). Bloodstream form *Trypanosoma brucei* depend on multiple metacaspases associated with RAB-11 positive endosomes. *Journal of Cell Science*. **119**, 1105-1117.

Hertz-Fowler, C., Ersfeld, K., Gull, K. (2001). CAP5.5, a life-cycle-regulated, cytoskeleton-associated protein is a member of a novel family of calpain-related proteins in *Trypanosoma brucei*. *Molecular and Biochemical Parasitology*. **116**, 25-34.

Hertz, C. J., Filutowicz, H., Mansfield, J. M. (1998). Resistance to the African trypanosomes is IFN-γ dependent. *Journal of Immunology*. **161**, 6775-6783.

Heussen, C., Dowdle, E. B. (1980). Electrophoretic analysis of plasminogen activators in polyacrylamide gels containing sodium dodecyl sulfate and copolymerized substrates. *Analytical Biochemistry*. **102**, 196-202.

Hirumi, H., Hirumi, K. (1991). *In vitro* cultivation of *Trypanosoma congolense* bloodstream forms in the absence of feeder cell layers. *Parasitology*. **102(Suppl. 2)**, 225-236.

Hölzmuller, P., Grebaut, P., Brizard, J. P., Berthier, D., Chantal, I., Bossard, G., Bucheton, B., Vezilier, F., Chuchana, P., Bras-Gonçalves, R., Lemesre, J.-L., Vincendeau, P., Cuny, G., Frutos, R., Birond, D. G. (2008). Pathogeno-proteomics. *Annals of the New York Academy of Sciences*. **1149**, 66-70.

Hopkins, J. S., Chitambo, H., Machila, N., Luckins, A. G., Rae, P. F., van den Bossche, P., Eisler, M. C. (1998). Adaptation and validation of antibody ELISAs using dried blood spots on filter paper for epidemiological surveys of tsetse-transmitted trypanosomosis in cattle. *Preventive Veterinary Medicine*. **37**, 91-99.

Horn, D., Cross, G. A. M. (1997). Analysis of *Trypansoma brucei* VSG expression site switching *in vitro*. *Molecular and Biochemical Parasitology*. **84**, 189-201.

The TDR targets database v5, http://tdrtargets.org/targets/view?gene_id=48009, accessed 20/10/2103.

The first rapid test to screen for sleeping sickness is launched, http://www.finddiagnostics.org/media/press/121206.html, accessed 7/06/2013.

Loop-mediated isothermal amplification (LAMP), http://www.finddiagnostics.org/programs/hat-ond/hat/molecular_diagnosis.html, accessed 7/06/2013.

Tests for parasite detection, http://www.finddiagnostics.org/programs/hat-ond/hat/parasite_detection/, accessed 7/06/2013.

Trypanosoma congolense IL 3000 annotated genomic contig, chromosome 9, http://www.ncbi.nlm.nih.gov/nuccore/HE575322, accessed 16/04/2012.

Huson, L., (2006). Antibody-mediated inhibition of proteases of African trypasomes. University of KwaZulu-Natal, Pietermaritzburg. PhD.

Iwamoto, T., Sonobe, T., Hayashi, K. (2003). Loop-mediated isothermal amplification for direct detection of *Mycobacterium tuberculosis* complex, *M. avium*, and *M. intracellulare* in sputum samples. *Journal of Clinical Microbiology*. **41**, 2616-2622.

Jackson, D. G., Windle, H. J., Voorheis, H. P. (1993). The identification, purification, and characterization of two invariant surface glycoproteins located beneath the surface coat barrier of bloodstream forms of *Trypanosoma brucei*. *Journal of Biological Chemistry*. **268**, 8085-8095.

Jackson, L., (2011). Enzymatic and crystallisation studies of CATL-like trypanosomal cysteine peptidases. University of KwaZulu-Natal, Pietermaritzburg. MSc.

Jaffe, C. L., Dwyer, D. M. (2003). Extracellular release of the surface metalloprotease, gp63, from *Leishmania* and insect trypanosomatids. *Parasitology Research*. **91**, 229-237.

Jamonneau, V., Truc, P., Garcia, A., Magnus, E., Büscher, P. (2000). Preliminary evaluation of LATEX/*T. b. gambiense* and alternative versions of CATT/*T. b. gambiense* for the serodiagnosis of human African trypanosomiasis of a population at risk in Cote d'Ivoire: considerations for mass screening. *Acta Tropica*. **76**, 175-183.

Jordan, F. (1976). Tsetse flies as vectors of trypanosomes. *Veterinary Parasitology*. **2**, 143-152.

Kagira, J. M., Maina, N. (2007). Occurance of multiple drug resistance in *Trypanosoma brucei rhodesiense* from sleeping sickness patients. *Onderstepoort Journal of Veterinary Research*. **74**, 17-22.

Kangethe, R. T., Boulangé, A. F., Coustou, V., Baltz, T., Coetzer, T. H. T. (2012). *Trypanosoma brucei brucei* oligopeptidase B null mutants display increased prolyl oligopeptidase-like activity. *Molecular and Biochemical Parasitology*. **182**, 7-16.

Kaushik, R. S., Uzonna, J. E., Gordon, J. R., Tabel, H. (1999). Innate resistance of *Trypanosoma congolense* infections: differential production of nitric oxide by macrophages from susceptible BALB/c and resistant C57BL/6 mice. *Experimental Parasitology*. **92**, 131-143.

Kennedy, P. G. (2004). Human African trypanosomiasis of the CNS: current issues and challenges. *Journal of Clinical Investigation*. **113**, 496-504.

Kennedy, P. G. (2008). Diagnosing central nervous system trypanosomiasis: two stage or not to stage? *Transactions of the Royal Society of Tropical Medicine and Hygiene*. **102**, 306-307.

Kerr, I. D., Lee, J. H., Farady, C. J., Marion, R., Ricket, M., Sajid, M., Pandey, K. C., Caffrey, C. R., Legac, J., Hansell, E., McKerrow, J. H., Craik, C. S., Rosenthal, P. J., Brinen, L.

S. (2009). Vinyl sulfones as antiparasitic agents and a structural basis for drug design. *Journal of Biological Chemistry*. **284**, 25697-25703.

Kinabo, L. D. (1993). Pharmacology of existing drugs for animal trypanosomiasias. *Acta Tropica*. **54**, 169-183.

Kitagawa, T., Aikawa, T. (1976). Enzyme coupled immunoassay of insulin using a novel coupling reagent. *Journal of Biochemistry*. **79**, 233-236.

Klemba, M. W., Goldberg, D. E. (2002). Biological roles of proteases in parasitic protozoa. *Annual Review of Biochemistry*. **71**, 275-305.

Kosec, G., Alvarez, V., Cazzulo, J. J. (2006a). Cysteine proteinases of *Trypanosoma cruzi*: from digestive enzymes to programmed cell death mediators. *Biocell*. **30**, 479-490.

Kosec, G., Alvarez, V. E., Agüero, F., Sánchez, D., Doliinar, M., Turk, B., Cazzulo, J. J. (2006b). Metacaspases of *Trypanosoma cruzi*: Possible candidates for programmed cell death mediators. *Molecular and Biochemical Parasitology*. **145**, 18-28.

KPL. (2013). Technical Guide for ELISA: Protocols and Troubleshooting.

Kuboki, N., Inoue, N., Sakurai, T., Di Cello, F., Grab, D. J., Suzuki, H., Sugimoto, C., Igarashi, I. (2003). Loop-mediated isothermal amplification for detection of African trypanosomes. *Journal of Clinical Microbiology*. **41**, 5517-5524.

Kuzoe, F. A. S. (1993). Current situation of African trypanosomiasias. *Acta Tropica*. **54**, 153-162.

La Greca, F., Magez, S. (2011). Vaccination against trypanosomiasis, can it be done or is the trypanosome truly the ultimate immune destroyer and escape artist? *Human Vaccines*. **7**, 1225-1233.

LaCount, D. J., Gruszynski, A. E., Grandgenett, P. M., Bangs, J. D., Donelson, J. E. (2003). Expression and function of the *Trypanosoma brucei* major surface protease (GP63) genes. *Journal of Biological Chemistry*. **278**, 24658-24664.

Laemmli, U. K. (1970). Cleavage of structural proteins during the assembly of the head of bacteriophage T4. *Nature*. **277**, 680-685.

Lalmanach, G., Boulangé, A., Serveau, C., Lecaille, F., Scharfstein, J., Gauthier, F., Authié, E. (2002). Congopain from *Trypanosoma congolense*: drug target and vaccine candidate. *Biological Chemistry*. **383**, 739-749.

Lam, E., Zhang, Y. (2012). Regulating the reapers: activating metacaspases for programmed cell death. *Trends in Plant Science*. **17**, 487-494.

Lambert, C., Léonard, N., De Bolle, X., Depiereux, E. (2002). ESyPred3D: Prediction of proteins 3D structures. *Bioinformatics*. **18**, 1250-1256.

Lamkanfi, M., Festjens, N., Declercq, W., Van den Berghe, T., Vandenabeele, P. (2007). Caspases in cell survival, proliferation and differentiation. *Cell Death and Differentiation*. **14**, 44-55.

Lanham, S. M., Godfrey, D. G. (1970). Isolation of salivarian trypanosomes from man and other mammals using DEAE-cellulose. *Experimental Parasitology*. **28**, 521-534.

Lantz, M. S., Ciborowski, P. (1994). Zymographic techniques for detection and characterization of microbial proteases. *Methods in Enzymology*. **235**, 563-594.

Lança, A. S., de Sousa, K. P., Atouguia, J., Prazeres, D. M., Monteiro, G. A., Silva, M. S. (2011). *Trypanosoma brucei*: immunisation with plasmid DNA encoding invariant surface glycoprotien gene is able to induce partial protection in experimental African trypanosomiasis. *Experimental Parasitology*. **127**, 18-24.

Larkin, M. A., Blackshields, G., Brown, N. P., Chenna, R., McGettigan, P. A., McWilliam, H., Valentin, F., Wallace, I. M., Wilm, A., Lopez, R., Thompson, J. D., Gibson, T. J., Higgins, D. G. (2007). Clustal W and Clustal X version 2.0. *Bioinformatics*. **23**, 2947-2948.

Lauffart, B., Mantle, D. (1998). Rationalization of aminopeptidase activities in human skeletal muscle soluble extract. *Biochimica et Biophysica Acta*. **956**, 300-306.

Laverrière, M., Cazzulo, J. J., Alvarez, V. E. (2012). Antagonic activities of *Trypanosoma cruzi* metacaspases affect the balance between cell proliferation, death and differentiation. *Cell Death and Differentiation*. **19**, 1358-1369.

Lecaille, F., Kaleta, J., Brömme, D. (2002). Human and parasitic papain-like cysteine proteases: their role in physiology and pathology and recent developments in inhibitor design. *Chemical Review*. **102**, 4459-4488.

Lee, N., Gannavaram, S., Selvapandiyan, A., Debrabant, A. (2007). Characterization of metacaspases with trypsin-like activity and their putative role in programmed cell death in the protozoan parasite *Leishmania*. *Eukaryotic Cell*. **6**, 1745-1757.

Leibly, D. J., Nguyen, T. N., Kao, L. T., Hewitt, S. N., Barrett, L. K., Van Voorhis, W. C. (2012). Stabilizing additives added during cell lysis aid in the solubilization of recombinant proteins. *PLOS ONE*. **7**, e52482.

Lejon, V., Büscher, P., Magnus, E., Moons, A., Wouters, I., Van Meirvenne, N. (1998). A semi-quantitative ELISA for detection of *Trypanosoma brucei gambiense* specific antibodies in serum and cerebrospinal fluid of sleeping sickness patients. *Acta Tropica*. **69**, 151-164.

Lejon, V., Büscher, P. (2001). Stage determination and follow-up in sleeping sickness. *Médecine tropicale: revue du Corps de santé colonial*. **61**, 355-360.

Lejon, V., Kwete, J., Büscher, P. (2003). Towards saliva-based screening for sleeping sickness? *Tropical Medicine and International Health*. **8**, 585-588.

Lejon, V., Ngoyi, D. M., Boelaert, M., Büscher, P. (2010). A CATT negative result after treatment for human African trypanosomiasis is not indication for cure. *PLOS Neglected Tropical Diseases*. **4**, e590.

Levine, R. A., Wardlaw, S. C., Patton, C. L. (1989). Detection of haematoparasites using quantitative buffy coat analysis tubes. *Parasitology Today*. **5**, 132-134.

Lima, A. P., dos Reis, F. C., Serveau, C., Lalmanach, G., Juliano, L., Ménard, R., Vernet, T., Thomas, D. Y., Storer, A. C., Scharfstein, J. (2001). Cysteine protease isoforms from *Trypanosoma cruzi*, cruzipain 2 and cruzain, present different substrate preference and susceptibility to inhibitors. *Molecular and Biochemical Parasitology*. **114**, 41-52.

Lonsdale-Eccles, J. D., Grab, D. J. (2002). Trypanosome hydrolases and the blood–brain barrier. *Trends in Parasitology*. **18**, 17-19.

Luckins, A. G., Mehlitz, D. (1978). Evaluation of an indirect fluorescent antibody test, enzyme-linked immunosorbent assay and quantification of immunoglobulins in the diagnosis of bovine trypanosomiasis. *Tropical Animal Health and Production*. **10**, 149-159.

Luckins, A. G. (1988). *Trypanosoma evansi* in Asia. *Parasitology Today*. **4**, 137-142.

Luckins, A. G. (1992). Methods for diagnosis of trypanosomiasis in livestock. *World Animal Review*. **70/71**, 15-20.

Luckins, A. G. (1997). Detection of antibodies in trypanosome-infected cattle by means of a microplate enzyme-linked immunosorbent assay. *Tropical Animal Health and Production*. **9**, 53-62.

Lumsden, W. H., Kimber, C. D., Evans, D. A., Doig, S. J. (1979). *Trypanosoma brucei*: miniature anion-exchange centrifugation technique for detection of low parasitaemias: adaptation for field use. *Transactions of the Royal Society of Tropical Medicine and Hygiene*. **73**, 312-317.

Lumsden, W. H., Kimber, C. D., Dukes, P., Haller, L., Stanghellini, A., G. D. (1981). Field diagnosis of sleeping sickness in the Ivory Coast. I. Comparison of the miniature anion-exchange/centrifugation technique with other protozoological methods. *Transactions of the Royal Society of Tropical Medicine and Hygiene*. **75**, 242-250.

Machado, M. F. M., Marcondes, M. F., Juliano, M. A., McLuskey, K., Mottram, J. C., Moss, C. X., Juliano, L., Oliveira, V. (2013). Substrate specificity and the effect of calcium on *Trypanosoma brucei* metacaspase 2. *FEBS Journals*. **280**, 2608-2621.

Machila, N., Sinyangwe, L., Mubanga, J., Hopkins, J. S., Robinson, T., Eisler, M. C. (2001). Antibody-ELISA seroprevalence of bovine trypanosomosis in eastern province of Zambia. *Preventive Veterinary Medicine*. **49**, 249-257.

Mackey, Z. B., O' Brien, T. C., Greenbaum, D. C., Blank, R. B., McKerrow, J. H. (2004). A cathepsin B-like protease is required for host protein degradation in *Trypanosoma brucei*. *Journal of Biological Chemistry*. **279**, 48426-48433.

Madeo, F., Herker, E., Maldener, C. (2002). A caspase-related protease regulates apoptosis in yeast. *Molecular Cell*. **9**, 911-917.

Magez, S., Lucas, R., Darji, A., Songa, E. B., Hamers, R., De Baetselier, P. (1993). Murine tumor necrosis factor plays a protective role during the initial phase of the experimental infection with *Trypanosoma brucei brucei*. *Parasite Immunology*. **15**, 635-641.

Magez, S., Geuskens, M., Beschin, A., del Favero, H., Verschueren, H., Lucas, R., Pays, E., De Baetselier, P. (1997). Specific uptake of tumor necrosis factor-α is involved in growth control of *Trypanosoma brucei*. *Journal of Cell Biology*. **137**, 715-727.

Magez, S., Radwanska, M., Beschin, A., Sekikawa, K., De Baetselier, P. (1999). Tumor necrosis factor alpha is a key mediator in the regulation of experimental *Trypanosoma brucei* infections. *Infection and Immunity*. **67**, 3128-3132.

Magez, S., Radwanska, M., Drennan, M., Fick, L., Baral, T. N., Brombacher, F., De Baetselier, P. (2006). Interferon-γ and nitric oxide in combination with antibodies are key protective host immune factors during *Trypanosoma congolense* Tc13 infections. *Journal of Infectious Diseases*. **193**, 1575-1583.

Magez, S., Caljon, G., Tran, T., Stijlemans, B., Radwanska, M. (2010). Current status of vaccination against African trypanosomiasis. *Parasitology*. **137**, 2017-2027.

Magnus, E., Vervoort, T., Van Meirvenne, N. (1978). A card-agglutination test with stained trypanosomes (C.A.T.T.) for the serological diagnosis of *T. b. gambiense* trypanosomiasis. *Annales de la Societe Belge de Medecine Tropicale*. **58**, 169-176.

Magona, J. W., Mayende, J. S. P., Walubengo, J. (2002). Comparative evaluation of the antibody-detection ELISA technique using microplates precoated with denatured crude antigens from *Trypanosoma congolense* or *Trypanosoma vivax*. *Tropical Animal Health and Production*. **34**, 295-308.

Manchenko, G. P. (2003). Handbook of detection of enzymes on electrophoresis gels, 2nd Edition. CRC Press, USA.

Manful, T., Mulindwa, J., Frank, F. M., Clayton, C. E., Matovu, E. (2010). A search for *Trypanosoma brucei rhodesiense* diagnostic antigens by proteomic screening and targetted cloning. *PLOS ONE*. **5**, e9630.

Mantle, D., Lauffart, B., McDermott, J., Gibson, A. (1990). Characterization of aminopeptidases in human kidney soluble fraction. *Clinica Chimica Acta*. **187**, 105-114.

Marcello, L., Barry, J. D. (2007). Analysis of the VSG gene silent archive in *Trypanosoma brucei* reveals that mosaic gene expression is prominent in antigenic variation and is favored by archive substructure. *Genome Research*. **17**, 1344-1352.

Mathieu-Daude, F., Bicart-See, A., Bosseno, M. F., Breniere, S. F., Tibayrenc, M. (1994). Identification of *Trypanosoma brucei gambiense* group I by a specific kinetoplast DNA probe. *American Journal of Tropical Medicine and Hygiene*. **50**, 13-19.

Matovu, E., Mugasa, C. M., Ekangu, R. A., Deborggraeve, S., Lubega, G. W., Laurent, T., Schoone, G. J., Schallig, H. D., Büscher, P. (2010). Phase II evaluation of sensitivity and specificity of PCR and NASBA followed by oligochromatography for diagnosis of human African trypanosomiasis in clinical samples from D.R. Congo and Uganda. *PLOS Neglected Tropical Diseases*. **4**, e737.

Matthews, K. R., Gull, K. (1994). Cycles within cycles: the interplay between differentiation and cell division in *Trypanosoma brucei*. *Parasitology Today*. **10**, 473-476.

Matthews, K. R. (1999). Developments in the differentiation of *Trypanosoma brucei*. *Parasitology Today*. **15**, 76-80.

Matthews, K. R., Ellis, J. R., Paterou, A. (2004). Molecular regulation of the life cycle of African trypanosomes. *Trends in Parasitology*. **20**, 40-47.

Matthews, K. R. (2005). The developmental cell biology of *Trypanosoma brucei*. *Journal of Cell Science*. **118**, 283-290.

Mattioli, R. C., Feldmann, U., Hendrickx, G., Wint, W., Jannin, J., Slingenbergh, J. (2004). Tsetse and trypanosomiasis intervention policies supporting sustainable animal-agricultural development. *Journal of Food Agriculture and Environment*. **2**, 310-314.

Mbawa, Z. R., Webster, P., Lonsdale-Eccles, J. D. (1991). Immunolocalization of a cysteine protease within the lysosomal system of *Trypansoma congolense*. *European Journal of Cell Biology*. **56**, 243-250.

McDermott, J. J., Coleman, P. G. (2001). Comparing apples and oranges - model-based assessment of different tsetse-transmitted trypanosomis control strategies. *International Journal for Parasitology*. **31**, 603-609.

McKerrow, J. H., Engel, J. C., Caffrey, C. R. (1999). Cysteine protease inhibitors as chemotherapy for parasitic infections. *Bioorganic and Medicinal Chemistry*. **7**, 639-644.

McKerrow, J. H., Caffrey, C. R., Kelley, L. A., Loke, P., Sajid, M. (2006). Proteases in parasitic diseases. *Annual Review of Pathology*. **1**, 497-536.

McLintock, L. M. L., Turner, C. M. R., Vickerman, K. (1993). Comparison of the effects of immune killing mechanisms on *Trypanosoma brucei* parasites of slender and stumpy morphology. *Parasite Immunology*. **15**, 475-480.

McLuskey, K., Paterson, N. G., Bland, N. D., Isaacs, N. W., Mottram, J. C. (2010). Crystal stucture of *Leishmania major* oligopeptidase B gives insight into the enzymatic properties of a trypanosomatid virulence factor. *Journal of Biological Chemistry*. **285**, 39249-39259.

McLuskey, K., Rudolf, J., Proto, W. R., Isaacs, N. W., Coombs, G. H., Moss, C. X., Mottram, J. C. (2012). Crystal structure of a *Trypanosoma brucei* metacaspase. *PNAS*. **109**, 7469-7474.

Medina-Acosta, E., Cross, G. A. M. (1993). Rapid isolation of DNA from trypanosomatid protozoa using a simple 'mini-prep' procedure. *Molecular and Biochemical Parasitology*. **59**, 327-329.

Mendoza-Palomares, C., Biteau, N., Giroud, C., Coustou, V., Coetzer, T. H. T., Authié, E., Boulangé, A., Baltz, T. (2008). Molecular and biochemical characterization of a cathepsin B-like protease family unique to *Trypanosoma congolense*. *Eukaryotic Cell*. **7**, 684-697.

Merckelbach, A., Hasse, S., Dell, R., Eschlbeck, A., Ruppel, A. (1994). cDNA sequences of *Schistosoma japonicum* coding for two cathepsin B-like proteins and Sj32. *Tropical Medicine and Parasitology*. **45**, 193-198.

Metz, C. E. (2006). Receiver operating characteristic analysis: a tool for the quantitative evaluation of observer performance and imaging systems. *Journal of the Americal College of Radiology*. **3**, 413-422.

Middleberg, A. (2002). Preparative protein folding. *Trends in Biotechnology*. **20**, 437-443.

Miezan, T. W., Meda, H. A., Doua, F., Dje, N. N., Lejon, V., Büscher, P. (2000). Single centrifugation of cerebrospinal fluid in a sealed pasteur pipette for simple, rapid and sensitive detection of trypanosomes. *Transactions of the Royal Society of Tropical Medicine and Hygiene*. **94**.

Mkunza, F., Olaho, W. M., Powell, C. N. (1995). Partial protection against natural trypanosomiasis after vaccination with a flagellar pocket antigen from *Trypanosoma brucei rhodesiense*. *Vaccine*. **13**, 151-154.

Mochabo, K. M., Zhou, M., Suganuma, K., Kawazu, S., Suzuki, Y., Inoue, N. (2013). Expression, immunlocalization and serodiagnostic value of Tc38630 protein from *Trypanosoma congolense*. *Parasitology Research*. **112**, 3357-3363.

Molyneux, D. H., Pentreath, V., Doua, F. (1996). African trypanosomiasias in man, In: Mason's Tropical Diseases, (Cook, G. C. (Ed.): London, W. B. Suanders Company Ltd.

Morty, R. E., Troeberg, L., Pike, R. N., Jones, R., Nickel, P., Lonsdale-Eccles, J. D., Coetzer, T. H. T. (1998). A trypanosome oligopeptidase as a target for the trypanocidal agents pentamidine, diminazene and suramin. *FEBS Letters*. **433**, 251-256.

Morty, R. E., Lonsdale-Eccles, J. D., Morehead, J., Caler, E. V., Mentele, R., Auerswald, E. A., Coetzer, T. H. T., Andrews, N. W., Burleigh, B. A. (1999). Oligopeptidase B from *Trypanosoma brucei*, a new member of an emerging subgroup of serine oligopeptidases. *The Journal of Biological Chemistry*. **274**, 26149-26156.

Morty, R. E., Lonsdale-Eccles, J. D., Mentele, R., Auerswald, E. A., Coetzer, T. H. T. (2001). Trypanosome-derived oligopeptidase B is released into the plasma of infected rodents, where it persists and retains full catalytic activity. *Infection and Immunity*. **69**, 2757-2761.

Morty, R. E., Pellé, R., Vadász, I., Uzcanga, G. L., Seeger, W., Bubis, J. (2005). Oligopeptidase B from *Trypanosoma evansi*. A parasite peptidase that inactivates atrial natriuretic factor in the bloodstream of infected hosts. *Journal of Biological Chemistry*. **280**, 10925-10937.

Morty, R. E., Bulau, P., Pellé, R., Wilk, S., Abe, K. (2006). Pyroglutamyl peptidase type I from *Trypanosoma brucei*: a new virulence factor from African trypanosomes that de-blocks regulatory peptides in the plasma of infected hosts. *Biochemical Journal*. **394**, 635-645.

Moss, C. X., Westrop, G. D., Juliano, L., Coombs, G. H., Mottram, J. C. (2007). Metacaspase 2 of *Trypanosoma brucei* is a calcium-dependent cysteine peptidase without processing. *FEBS Letters*. **581**, 5635-5639.

Motta, F. N., Bastos, I. M., Faudry, E., Ebel, C., Lima, M. M., Neves, D., Ragno, M., Barbosa, J. A., de Freitas, S. M., Santana, J. M. (2012). The *Trypanosoma cruzi* virulence factor oligopeptidase B (OPBTc) assembles into an active and stable dimer. *PLOS One*. **7**, e30431.

Mottram, J. C., Frame, M. J., Brooks, D. R., Tetley, L., Hutchison, J. E., Souza, A. E., Coombs, G. H. (1997). The multiple cpb cysteine proteinase genes of *Leishmania mexicana* encode isoenzymes that differ in their stage regulation and substrate preferences. *Journal of Biological Chemistry*. **272**, 14285-14293.

Mottram, J. C., Brooks, D. R., Coombs, G. H. (1998). Roles of cysteine proteinases of trypanosomes and *Leishmania* in host-parasite interactions. *Current Opinion in Microbiology*. **1**, 455-460.

Mottram, J. C., Helms, M. J., Coombs, G. H., Sajid, M. (2003). Clan CD cysteine peptidases of parasitic protozoa. *Trends in Parasitology*. **19**, 182-187.

Mottram, J. C., Coombs, G. H., Alexander, J. (2004). Cysteine peptidases as virulence factors of *Leishmania*. *Current Opinion in Microbiology*. **7**, 375-381.

Mucache, H. N., (2012). Functional expression of *Trypanosoma congolense* pyroglutamyl peptidase type I and development of reverse genetics tools. University of KwaZulu-Natal, Pietermaritzburg. MSc.

Murray, M., Murray, P. K., McIntyre, W. I. M. (1977). An improved parasitological technique for the diagnosis of African trypanosomiasis. *Transactions of the Royal Society of Tropical Medicine and Hygiene*. **71**, 325-326.

Namangala, B., De Baetselier, P., Noël, W., Brys, L., Beschin, A. (2001). Alternative versus classical macrophage activation during experimental African trypanosomiasis. *Journal of Leukocyte Biology*. **69**, 387-396.

Nantulya, V. M., Lindqvist, K. J. (1989). Antigen-detection enzyme immunoassays for the diagnosis of *Trypanosoma vivax, T. congolense* and *T. brucei* infections in cattle. *Tropical Medicine and Parasitology*. **40**, 267-272.

Nantulya, V. M. (1990). Trypanosomiasis in domestic animals: the problems of diagnosis. *Revue scientifique et technique (International Office of Epizootics)*. **9**, 357-367.

Nantulya, V. M., Doua, F. (1992). Diagnosis of *Trypanosoma brucei gambiense* sleeping sickness using an antigen detection enzyme-linked immunosorbent assay. *Transactions of the Royal Society of Tropical Medicine and Hygiene*. **86**, 42-45.

Ng'wena, A. G., Patel, N. B., Wango, E. O. (1997). Plasma luteinizing hormone levels in response to gonadotropin-releasing hormone agonist and clonidine in *Trypanosoma congolense*-infected female goats. *Brain Research Bulletin*. **44**, 591-595.

Nguewa, P. A., Fuertes, M. A., Valladares, B., Alonso, C., Pérez, J. M. (2004). Programmed cell death in trypanosomatids: a way to maximize their biological fitness? *Trends in Parasitology*. **20**, 375-380.

Nissim, A., Hoogenboom, H. R., Tomlinson, I. M., Flynn, G., Midgley, C., Lane, D., Winter, G. (1994). Antibody fragments from a 'single pot' phage display library as immunochemical reagents. *EMBO Journal*. **13**, 692-698.

Njiru, Z. K., Mikosza, A. S. J., Armstrong, T., Enyaru, J. C., Ndung'u, J. M., Thompson, R. C. A. (2008a). Loop-mediated isothermal amplification (LAMP) method for rapid detection of T*rypanosoma brucei rhodesiense*. *PLOS Neglected Tropical Diseases*. **2**, e147.

Njiru, Z. K., Mikosza, A. S. J., Matovu, E., Enyaru, J. C., Ouma, J. O., Kibona, S. N., Thompson, R. C. A., Ndung'u, J. M. (2008b). African trypanosomiasis: sensitive and rapid detection of the sub-genus *Trypanozoon* by loop-mediated isothermal amplification (LAMP) of parasite DNA. *International Journal for Parasitology*. **38**, 589-599.

Noël, W., Hassanzadeh, G., Raes, G., Namangala, B., Daems, I., Brys, L., Brombacher, F., De Baetselier, P., Beschin, A. (2002). Infection stage-dependent modulation of macrophage activation in *Trypanosoma congolense*-resistant and -susceptible mice. *Infection and Immunity*. **70**, 6180-6187.

Noireau, F., Lemesre, J. L., Nzoukoudi, M. Y., Louembet, M. T., Gouteux, J. P., Frezil, J. L. (1988). Serodiagnosis of sleeping sickness in the Republic of the Congo: comparison of indirect immunofluorescent antibody test and card agglutination test. *Transactions of the Royal Society of Tropical Medicine and Hygiene*. **82**, 237-240.

Odagaki, Y., Hayashi, A., K., O., Hirotsu, K., Kabashima, T., Ito, K., Yoshimoto, T., Tsuru, D., Sato, M., Clardy, J. (1999). The crystal structure of pyroglutamyl peptidase I from *Bacillus amyloliquefaciens* reveals a new structure for a cysteine protease. *Structure*. **7**, 399-411.

Odiit, M., Kansiime, F., Enyaru, J. C. (1997). Duration of symptoms and case fatality of sleeping sickness caused by *Trypanosoma brucei rhodesiense* in Tororo, Uganda. *East African Medical Journal*. **74**, 792-795.

OIE. (2008). Manual of diagnostic tests and vaccines for terrestrial animals. World Organisation for Animal Health, Paris.

OIE. (2013). Manual of diagnostic tests and vaccines for terrestrial animals. World Organisation for Animal Health, Paris.

Oliver, M., Atayde, V. D., Isnard, A., Hassani, K., Shio, M. T. (2012). *Leishmania* virulence factors: focus on the metalloprotease GP63. *Microbes and Infection*. **14**, 1377-1389.

Pan, W., Ogunremi, O., Wei, G., Shi, M., Tabel, H. (2006). CR3 (CD11b/CD18) is the major macrophage receptor for IgM antibody-mediated phagocytosis of African trypanosomes: diverse effect on subsequent synthesis of tumor necrosis factor alpha and nitric oxide. *Microbes and Infection*. **8**, 1209-1218.

Pansri, P., Jaruseranee, N., Rangnoi, K., Kristensen, P., Yamabhai, M. (2009). A compact phage display human scFV library for selection of antibodies to a wide variety of antigens. *BMC Biotechnology*. **9**.

Paquet, C., Ancelle, T., Gastellu-Etchegorry, M., Castilla, J., Harndt, I. (1992). Persistence of antibodies to *Trypanosoma brucei gambiense* after treatment of human trypanosomiasis in Uganda. *Lancet*. **340**, 250.

Park, S. H., Goo, J. M., Jo, C. H. (2004). Receiver operating characteristic (ROC) curve: practical review for radiologists. *Korean Journal of Radiology*. **5**, 11-18.

Pays, E. (2006). The variant surface glycoprotein as a tool for adaptation in African trypanosomes. *Microbes and Infection*. **8**, 930-937.

Penchenier, L., Simo, G., Grebaut, P., Nkinin, S., Laveissiere, C., Herder, S. (2000). Diagnosis of human trypanosomiasis, due to *Trypanosoma brucei gambiense* in central Africa, by the polymerase chain reaction. *Transactions of the Royal Society of Tropical Medicine and Hygiene*. **94**, 392-394.

Pépin, J., Milord, F. (1994). The treatment of human African trypansomiasis. *Advances in Parasitology*. **33**, 1-47.

Pépin, J., Donelson, J. E. (2006). Human African trypanosomiasis, In: Tropical Infectious Diseases: Principles, Pathogens and Practice, (Guerrant, R., Krogstad, D., Maguire, J., Walker, K., Weller, P. F. (Eds.)): New York, Churchill Livingston.

Petty, K. J. (2001). Metal-chelate affinity chromatography. *Current Protocols in Molecular Biology*. **10**.

Pike, R. N., Dennison, C. (1989). Protein fractionation by three phase partioning (TPP) in aqueous/t-butanol mixtures. *Biotechnology and Bioengineering*. **33**, 221-228.

Pillay, D., (2010). Identification and characterisation of novel pathogenic factors of *Trypanosoma congolense*. University of KwaZulu-Natal, Pietermaritzburg. PhD.

Pillay, D., Boulangé, A., Coetzer, T. H. T. (2010). Expression, purification and characterisation of two variant cysteine peptidases from *Trypanosoma congolense* with active site substitutions. *Protein Expression and Purification*. **74**, 264-271.

Pillay, D., Izotte, J., Fikru, R., Büscher, P., Mucache, H., Neves, L., Boulangé, A., Seck, M. T., Bouyer, J., Napier, G. B., Chevtzoff, C., Coustou, V., Baltz, T. (2013). *Trypanosoma vivax* GM6 antigen: a candidate antigen for diagnosis of animal African trypanosomiasis in cattle. *PLOS ONE*. **8**, e78565.

Playfair, J. H. L., Taverne, J., Bate, C. A. W., De Souza, J. B. (1990). The malaria vaccine: anti-parasite of anti-disease. *Immunology Today*. **11**, 25-29.

Poelvoorde, P., Vanhamme, L., Van Den Abbeele, J., Switzer, W. M., Pays, E. (2004). Distribution of apolipoprotein L-I and trypanosome lytic activity among primate sera. *Molecular and Biochemical Parasitology*. **134**.

Polgár, L. (1987). Structure and function of serine proteases, In: Hydrolytic enzymes, (Neuberger, A., Brocklehurst, K. (Eds.)): Amsterdam, Elsevier.

Polgár, L. (2002). The prolyl oligopeptidase family. *CMLS Cellular and Molecular Life Sciences*. **59**, 349-362.

Polgár, L. (2005). The catalytic triad of serine peptidases. *CMLS Cellular and Molecular Life Sciences*. **62**, 2161-2172.

Posthuma-Trumpie, G., Korf, J., van Amerongen, A. (2009). Lateral flow (immuno)assay: its strengths, weaknesses, opportunities and threats. A literature survey. *Analytical and Bioanalytical Chemistry*. **393**, 569-582.

Proto, W. R., Castanys-Munoz, E., Black, A., Tetley, L., Moss, C. X., Juliano, L., Coombs, G. H., Mottram, J. C. (2011). *Trypanosoma brucei* metacaspase 4 is a pseudopeptidase and a virulence factor. *Journal of Biological Chemistry*. **286**, 39914-39925.

Radwanska, M., Magez, S., Dumont, N., Pays, A., Nolan, D. P., Pays, E. (2000). Antibodies raised against the flagellar pocket fraction of *Trypanosoma brucei* preferentially recognize HSP60 in cDNA expression library. *Parasite Immunology*. **22**, 639-650.

Radwanska, M., Chamekh, M., Vanhamme, L., Claes, F., Magez, S., Magnus, E., de Baetselier, P., Büscher, P., Pays, E. (2002). The serum resistance associated gene as a

diagnostic tool for the detection of *Trypanosoma brucei rhodesiense*. *The American Journal of Tropical Medicine and Hygiene*. **67**, 684-690.

Radwanska, M., Guirnalda, P., De Trez, C., Ryffel, B., Black, S. J., Magez, S. (2008). Trypanosomiasis-induced B cell apoptosis results in loss of protective anti-parasite antibody responses and abolishment of vaccine-induced memory responses. *PLOS Pathogens*. **4**, e1000078.

Rand, K. N. (1996). Crystal violet can be used to visualize DNA bands during gel electrophoresis and to improve cloning efficiency. *Technical Tips Online*. **1**, 23-23.

Rawlings, N. D., Polgár, L., Barrett, A. J. (1991). A new family of serine-type peptidases related to prolyl oligopeptidase. *Biochemical Journal*. **279**, 907-908.

Rawlings, N. D., Barrett, A. J. (1993). Evolutionary families of peptidases. *Biochemical Journal*. **290**, 205-218.

Rawlings, N. D., Morton, F. R., Kok, C. Y., Barrett, A. J. (2008). MEROPS: the peptidase database. *Nucleic Acids Research*. **36**, D320-325.

Rawlings, N. D., Barrett, A. J., Bateman, A. (2012). MEROPS: the database of proteolytic enzymes, their substrates and inhibitors. *Nucleic Acids Research*. **40**, D343-D350.

Rayaisse, J. B., Tirados, I., Kaba, D., Dewhirst, S. Y., Logan, J. G., Diarrassouba, A., Salou, E., Omolo, M. O., Solano, P., Lehane, M. J., Pickett, J. A., Vale, G. A., Torr, S. J., Esterhuizen, J. (2010). Prospects for the development of odour baits to control the tsetse flies *Glossina tachinoides* and *G. palpalis* s.l.. *PLOS Neglected Tropical Diseases*. **4**, e632.

Rebeski, D. E., Winger, E. M., Lelenta, M., Colling, A., Robinson, M. M., Ndamkou, C., Aigner, H., Dwinger, R. H., Crowther, J. R. (1998). Comparison of precoated and freshly coated microtitre plates using denatured antigen for the detection of antibodies against *Trypanosoma congolense* by indirect enzyme-linked immunosorbent assay, In: Proceedings of the Ninth International Conference of the AITVM, (Harare, Zimbabwe, Association of Institutions of Tropical Veterinary Medicine.

Rebeski, D. E., Winger, E. M., Robinson, M. M., Crowther, J. R., Dwinger, R. H. (1999a). Current stautus of improved enzyme-linked immunoassay mehods for diagnosis and control of African trypanosomiasis conducted under the FAO/IAEA coordinated research programme 3.13.D 3.20.13. *Integrated Control of Pathogenic Trypanosomes and their Vectors Newsletter*. **1**.

Rebeski, D. E., Winger, E. M., Rogovic, B., Robinson, M. M., Crowther, J. R., Dwinger, R. H. (1999b). Improved methods of the diagnosis of African trypanosomiasis. *Memórias do Instituto Oswaldo Cruz*. **94**, 249-253.

Rebeski, D. E., Winger, E. M., Van Rooij, E. M., Schöchl, R., Schuller, W., Dwinger, R. H., Crowther, J. R., Wright, P. F. (1999c). Pitfalls in the application of enzyme-linked immunoassays for the detection of circulating trypanosomal antigens in serum samples. *Parasitology Research*. **85**, 550-556.

Rebeski, D. E., Winger, E. M., Okoro, H., Kowalik, S., Bürger, H. J., Walters, D. E., Robinson, M. M., Dwinger, R. H., Crowther, J. R. (2000a). Detection of *Trypanosoma congolense* antibodies with indirect ELISAs using antigen-precoated microtitre plates. *Veterinary Parasitology*. **89**, 187-198.

Rebeski, D. E., Winger, E. M., Robinson, M. M., Gabler, C. M. G., Dwinger, R. H., Crowther, J. R. (2000b). Evaluation of antigen coating procedures of enzyme-linked immunosorbant assay method for detection of trypanosomal antibodies. *Veterinary Parasitology*. **90**, 1-13.

Rebeski, D. E., Winger, E. M., Ouma, J. O., Pages, S. K., Büscher, P., Sanogo, Y., Dwinger, R. H., Crowther, J. R. (2001). Charting methods to monitor the operational performance of ELISA methods for the detection of antibodies against trypanosomes. *Veterinary Parasitology*. **96**, 11-50.

Redpath, M. B., Windle, H. J., Nolan, D. P., Pays, E., Voorheis, H. P., Carrington, M. (2000). ESAG11, a new VSG expression site-associated gene from *Trypanosoma brucei*. *Molecular and Biochemical Parasitology*. **111**, 223-228.

Rising, M. M., Hicks, J. S., Moerke, G. A. (1930). The biuret reaction: II. The biuret reaction of di-acid amides. *Journal of Biological Chemistry*. **89**.

Robays, J., Bilengue, M. M., Van der Stuyft, P., Boelaert, M. (2004). The effectiveness of active population screening and treatment for sleeping sickness control in the Democratic Republic of Congo. *Tropical Medicine and International Health*. **9**, 542-550.

Roberts, R. J., Belfortm, M., Bestor, T., Bhagwat, A. S., Bickle, T. A., Bitinaite, B., Blumenthal, R. M., Degtyarev, S. K., Dryden, D. T. F., Dybvig, K., Firman, K., Gromova, E. S., Gumport, R. I., Halford, S. E., Hattman, S. H., Heitman, J., Hornby, D. P., Janulaitis, A., Jeltsch, A., Josephsen, J., Kiss, A., Klaenhammer, T. R., Kobayashi, I., Kong, H., KruÈger, D. H., Lacks, S., Marinus, M. G., Miyahara, M., Morgan, R. D., Murray, N. E., Nagaraja, V., Piekarowicz, A., Pingoud, A., Raleigh, E., Rao, D. N., Reich, N., Repin, V. E., Selker, E. U., Shaw, P.-C., Stein, D. C., Stoddard, B. L., Szybalski, W., Trautner, T. A., Van Etten, J. L., Vitor, J. M. B., Wilson, G. G., Xu, S.-Y. (2003). A nomenclature for restriction enzymes, DNA methyltransferases, homing endonucleases and their genes. *Nucleic Acids Research*. **31**, 1805-1812.

Rosenthal, P. J. (1999). Proteases of protozoan parasites. *Advances in Parasitology*. **43**, 105-159.

Rosenthal, P. J. (2004). Cysteine proteases of malaria parasites. *International Journal for Parasitology*. **34**, 1489-1499.

Ross, R., Thomson, D. (1910). A case of sleeping sickness studied by precise enumerative methods: regular periodical increase of the parasites disclosed. *Proceedings of the Royal Society B*. **82**, 411-415.

Rozen, S., Skaletsky, H. (2000). Primer3 on the WWW for general users and for the biologist programmers. *Methods in Molecular Biology*. **132**, 365-386.

Sacks, D. L., Askonas, B. A. (1980). Trypanosome-induced suppression of anti-parasite responses during experimental African trypanosomiasis. *European Journal of Immunology*. **10**, 971-974.

Sajid, M., McKerrow, J. H. (2002). Cysteine proteases of parasitic organisms. *Molecular and Biochemical Parasitology*. **120**, 1-21.

Sakanaria, J. A., Nadlerb, S. A., Chana, V. J., Engela, J. C., Leptaka, C., Bouvier, J. (1997). *Leishmania major*: comparison of the cathepsin L- and B-like cysteine protease genes with those of other trypanosomatids. *Experimental Parasitology*. **85**, 63-76.

Sambrook, J., Russell, D. W., Irwin, N. (2001). Molecular cloning: a laboratory manual, 3rd Edition. Cold Spring Harbour Laboratory Press, Cold Spring Harbour, NY.

Santos, C. C., Coombs, G. H., Lima, A. P., Mottram, J. C. (2007). Role of the *Trypanosoma brucei* natural cysteine peptidase inhibitor ICP in differentiation and virulence. *Molecular Microbiology*. **66**, 991-1002.

Sbicego, S., Vassella, E., Kurath, U., Blum, B., Roditi, I. (1999). The use of transgenic *Trypanosoma brucei* to identify compounds inducing the differentiation of bloodstream forms to procyclic forms. *Molecular and Biochemical Parasitology*. **104**, 311-322.

Schaeffer, M., de Miranda, A., Mottram, J. C., Coombs, G. H. (2006). Differentiation of *Leishmania major* is impaired by over-expression of pyroglutamyl peptidase I. *Molecular and Biochemical Parasitology*. **150**, 318-329.

Schileker, C., Bukau, B., Mogk, A. (2002). Prevention and reversion of protein aggregation by molecular chaperones in the *E. coli* cytosol: implications for their applicability in biotechnology. *Biotechnology*. **96**, 13-21.

Schisterman, E. F., Perkins, N. J., Liu, A., Bondell, H. (2005). Optimal cut-point and its corresponding Youden index to discriminate individuals using pooled blood samples. *Epidemiology*. **16**, 73-81.

Schlager, B., Straessle, A., Hafen, E. (2012). Use of anionic denaturing detergents to purify insoluble proteins after overexpression. *BMC Biotechnology*. **12**.

Schmid, C., Nkunku, S., Merolle, A., Vounatsou, P., Burri, C. (2004). Efficacy of 10-day melarsoprol schedule 2 years after treatment for late-stage gambiense sleeping sickness. *Lancet*. **364**, 789-790.

Scory, S., Caffrey, C. R., Steirhof, Y. D., Ruppel, A., Steverding, D. (1999). *Trypanosoma brucei*: killing of bloodstream forms *in vitro* and *in vivo* by the cysteine proteinase inhibitor Z-Phe-Ala-CHN_2. *Experimental Parasitology*. **91**, 327-333.

Seifert, H. S. (1995). Tropical Animal Health. Kluwer Academic Publishers, London.

Selzer, P. M., Pingel, S., Hsieh, I., Ugele, B., Chan, V. J., Engel, J. C., Bogyo, M., Russell, D. G., Sakanari, J. A., McKerrow, J. H. (1999). Cysteine protease inhibitors as chemotherapy: lessons from a parasite target. *Proceedings of the National Academy of Sciences USA*. **96**, 11015-11022.

Shi, M., Wei, G., Pan, W., Tabel, H. (2005). Impaired Kupffer cells in highly susceptible mice infected with *Trypanosoma congolense*. *Infection and Immunity*. **73**, 8393-8396.

Simarro, P. P., Jannin, J., Cattand, P. (2008). Eliminating human African trypanosomiasis: where do we stand and what comes next? *PLOS Medicine*. **5**, e55.

Simarro, P. P., Cecchi, G., Paone, M., Franco, J. R., Diarra, A., Ruiz, J. A., Févre, E. M., Courtin, F., Mattioli, R. C., Jannin, J. (2010). The Atlas of human African trypanosomiasis: a contribution to global mapping of neglected tropical diseases. *International Journal of Health Geographics*. **9**, 57.

Simarro, P. P., Diarra, A., Ruiz Postigo, J. A., Franco, J. R., Jannin, J. G. (2011). The human African trypanosomiasis control and surveillance programme of the World Health Organization 2000–2009: the way forward. *PLOS Neglected Tropical Diseases*. **5**, e1007.

Simarro, P. P., Franco, J., Diarra, A., Postigo, J. A., Jannin, J. (2012). Update on field use of the available drugs for the chemotherapy of human African trypanosomiasis. *Parasitology*. **139**, 842-846.

Simarro, P. P., Franco, J. R., Diarra, A., Ruiz, J. A., Jannin, J. (2013). Diversity of human African trypanosomiasis epidemiological settings requires fine-tuning control strategies to facilitate disease elimination. *Research and Reports in Tropical Medicine*. **4**, 1-6.

Singleton, M., Isupoy, M., Littlechild, J. (1999). X-ray structure of pyrrolidine carboxyl peptidase from the hyperthermophilic archaeon *Thermococcus litoralis*. *Structure*. **15**, 237-244.

Smialowski, P., Martin-Galiano, A. J., Mikolajka, A., Girschick, T., Holak, T. A., Frishman, D. (2006). Protein solubility: sequence based prediction and experimental verification. *Bioinformatics*. **23**.

Smith, M. C., Sherman, D. M. (1994). Blood, lymph and immune system, In: Goat Medicine, (Smith, M. C., Sherman, D. M. (Eds.)): Philadelphia, Lea & Febiger.

Smith, P. K., Krohn, R. I., Hermanson, G. T., Mallia, A. K., Gartner, F. H., Provenzano, M. D., Fujimoto, E. K., Goeke, N. M., Olson, B. J., Klenk, D. C. (1985). Measurement of protein using bicinchoninic acid. *Analytical Biochemistry*. **150**, 76-85.

Songa, E. B., Kageruka, P., Hamers, R. (1987). The use of the card agglutination test (Testryp® CATT) for the serodiagnosis of *T. evansi* infection. *Annales de la Societe Belge de Medecine Tropicale*. **67**, 51-57.

Sørensen, H. P., Mortensen, K. K. (2005). Advanced genetic strategies for recombinant protein expression in *Escherichia coli*. *Journal of Biotechnology*. **115**, 113-128.

Soudan, B., Tetaert, D., Hublart, M., Racadot, A., Croix, D., Boersma, A. (1993). Experimental "chronic" African trypanosomiasis: endocrine dysfunctions generated by parasitic components released during the trypanolytic phase in rats. *Experimental and Clinical Endocrinology*. **101**, 166-172.

Ssenyonga, G. S. Z. (1980). A comparative study on the distribution of *Trypanosoma brucei* and *T. congolense* in tissue of mice and rats. *Bulletin of Animal Health and Production in Africa*. **28**, 3120326.

Stevens, J. R. (2008). Kinetoplastid phylogenetics, with special reference to the evolution of parasitic trypanosomes. *Parasite*. **15**, 226-232.

Steverding, D., Stierhof, Y. D., Chaudhri, M., Ligtenberg, M., Schell, D., Beck-Sickinger, A. G., al, e. (1994). ESAG 6 and 7 products of *Trypanosoma brucei* form a transferrin binding protein complex. *European Journal of Cell Biology*. **64**, 78-87.

Steverding, D. (2008). The history of African trypanosomiasis. *Parasites and Vectors*. **1**, 3.

Steverding, D., Sexton, D. W., Wang, X., Gehrke, S. S., Wagner, G. K., Caffrey, C. R. (2012). *Trypanosoma brucei*: chemical evidence that cathepsin L is essential for survival and a relevent drug target. *International Journal for Parasitology*. **42**, 481-488.

Stijlemans, B., Guilliams, M., Raes, G., Beschin, A., Magez, S., De Baetselier, P. (2007). African trypanosomiasis: from immune escape and immunopathology to immune intervention. *Veterinary Parasitology*. **148**, 3-13.

Stuart, K., Brun, R., Croft, S. L., Fairlamb, A., Gürtler, R. E., McKerrow, J. H., Reed, S., Tarleton, R. (2008). Kinetoplastids: related protozoan pathogens, different diseases. *The Journal of Clinical Investigation*. **118**, 1301-1310.

Sullivan, L., Wall, S. J., Carrington, M., Ferguson, M. A. J. (2013). Proteomic selection of immunodiagnostic antigens for human African trypanosomiasis and generation of a prototype lateral flow immunodiagnostic device. *PLOS Neglected Tropical Diseases*. **7**, e2087.

Sundström, J. F., Vaculova, A., Smertenko, A. P., Savenkov, E. I., Golovko, A., Minina, E., Tiwari, B. S., Rodriguez-Nieto, S., Zamyatnin, J., A. A., Välineva, T., Saarikettu, J., Frilander, M. J., Suarez, M. F., Zavialov, A., Ståhl, U., Hussey, P. J., Silvennoinen, O., Sundberg, E., Zhivotovsky, B., Bozhkov, P. V. (2009). Tudor staphylococcal nuclease is an evolutionarily conserved component of the programmed cell death degradome. *Nature Cell Biology*. **11**, 1347-1354.

Swallow, B. (2000). Impacts of trypanosomiasis on African agriculture. *PAAT Technical Scientific Series*. **2**.

Swenerton, R. K., Zhang, S., Sajid, M., Medzihradszky, K. F., Craik, C. S., Kelly, B. L., McKerrow, J. H. (2011). The oligopeptidase B of *Leishmania* regulates parasite enolase and immune evasion. *Journal of Biological Chemistry*. **286**, 429-440.

Szallies, A., Kubata, B. K., Duszenko, M. (2002). A metacaspase of *Trypanosoma brucei* causes loss of respiration competence and clonal death in the yeast *Saccharomyces cerevisiae*. *FEBS Letters*. **517**, 144-150.

Taylor-Brown, E., Hurd, H. (2013). The first suicides: a legacy inherited by parasitic protozoans from prokaryote ancestors. *Parasites and Vectors*. **6**, 108.

Taylor, K. A. (1998). Immune responses of cattle to African trypanosomes: protective or pathogenic? *International Journal for Parasitology*. **28**, 219-224.

Taylor, K. A., Authié, E. (2004). Pathogenesis of animal trypanosomiasis, In: The Trypanosomiasis, (Maudlin, I., Holmes, P. H., Miles, M. A. (Eds.)): Wallingford, CABI Publishing.

Tetaert, D., Soudan, B., Huet-Duvillier, G., Degand, P., Boersma, A. (1993). Unusual cleavage of peptidic hormones generated by trypanosome enzymes released in infested rat serum. *International Journal for Peptide and Protein Research*. **41**, 147-152.

Tetley, L., Turner, C. M. R., Barry, J. D., Crowe, J. S., Vickerman, K. (1987). Onset of expression of the variant surface glycoproteins of *Trypanosoma brucei* in the tsetse fly studied using immunoelectron microscopy. *Journal of Cell Science*. **87**, 363-372.

Tiberti, N., Hainard, A., Sanchez, J.-C. (2013). Translation of human African trypanosomiasis biomarkers towards field application. *Translational Proteomics*. **1**, 12-24.

Tizard, I., Nielson, K., Seed, J. R., Hall, J. E. (1978). Biologically active products from African Trypanosomes. *Microbiological Reviews*. **42**, 661-681.

Tomas, A. M., Miles, M. A., Kelly, J. M. (1997). Overexpression of cruzipain, the major cysteine proteinase of *Trypanosoma cruzi*, is associated with enhanced metacyclogenesis. *European Journal of Biochemistry*. **244**, 596-603.

Torr, S. J., Hargrove, J. W., Vale, G. A. (2005). Towards a rational policy for dealing with tsetse. *Trends in Parasitology*. **21**, 537-541.

Tran, T., Claes, F., Verloo, D., De Greve, H., Büscher, P. (2009). Towards a new reference test for surra in camels. *Clinical and Vaccine Immunology*. **16**, 999-1002.

Troeberg, L., Pike, R. N., Morty, R. E., Berry, R. K., Coetzer, T. H. T., Lonsdale-Eccles, J. D. (1996). Proteases from *Trypanosoma brucei brucei*. Purification, characterisation and interactions with host regulatory molecules. *European Journal of Biochemistry*. **238**, 728-736.

Trouiller, P., Olliaro, P., Torreele, E., Orbinski, J., Laing, R., Ford, N. (2002). Drug development for neglected diseases: a deficient market and a public-health policy failure. *Lancet*. **359**, 2188-2194.

Truc, P., Lejon, V., Magnus, E., Jamonneau, V., Nangouma, A., Verloo, D., Penchenier, L., Büscher, P. (2002). Evaluation of the micro-CATT, CATT/*Trypanosoma brucei gambiense*, and LATEX/*T. b. gambiense* methods for serodiagnosis and surveillance of human African trypanosomiasis in West and Central Africa. *Bulletin of the World Health Organization*. **80**, 882-886.

Tsiatsiani, L., Van Breusegem, F., Gallois, P., Zavialov, A., Lamm, E., Bozhkov, P. V. (2011). Metacaspases. *Cell Death and Differentiation*. **18**, 1279-1288.

Uilenberg, G., Boyt, W. P. (1998). A field guide for the diagnosis, treatment and prevention of African animal trypanosomosis. *Food and Agriculture Organization of the United Nations*. http://www.fao.org/docrep/006/x0413e/x0413e00.htm.

Uren, G. A., O'Rourke, K., Aravind, L., Pisabarro, T. M., Seshagiri, S., Koonin, V. E., Dixit, M. V. (2000). Identification of paracaspases and metacaspases: two ancient families of caspase-like proteins, one of which plays a key role in MALT lymphoma. *Molecular Cell*. **6**, 961-967.

Urwyler, S., Vassella, E., Van Den Abbeele, J., Renggli, C. K., Blundell, P. B., Roditi, I. (2005). Expression of procyclin mRNAs during cyclical transmission of *Trypanosoma brucei*. *PLOS Pathogens*. **1**, e22.

Urwyler, S., Struder, E., Renggli, C. K., Roditi, I. (2007). A family of stage-specific alanine-rich proteins on the surface of epimastigote forms of *Trypanosoma brucei*. *Molecular Microbiology*. **63**, 218-228.

Uzonna, J. E., Kaushik, R. S., Gordon, J. R., Tabel, H. (1999). Cytokines and antibody responses during *Trypanosoma congolense* infections in two inbred mouse strains that differ in resistance. *Parasite Immunology*. **21**, 57-71.

Van Den Abbeele, J., Claes, Y., van Bockstaele, D., Le Ray, D., Coosemans, M. (1999). *Trypanosoma brucei* spp. development in the tsetse fly: characterization of the post-mesocyclic stages in the foregut and proboscis. *Parasitology*. **118**, 469-478.

Van den Bossche, P., Chigoma, D., Shumba, W. (2000a). The decline of anti-trypanosomal antibody levels in cattle after treatment with trypanocidal drugs and in the absence of tsetse challenge. *Acta Tropica*. **77**, 263-270.

Van den Bossche, P., Doran, M., Connor, R. J. (2000b). An analysis of trypanocidal drug use in Eastern Province of Zambia. *Veterinary Record*. **81**, 567-568.

Van den Bossche, P., Musimbwe, J., Mubanga, J., Jooste, R., Lumamba, D. (2004). A large scale trial to evaluate the efficacy of a 1% pour-on formulation of cyfluthrin (Cylence, Bayer) in controlling bovine trypanosomosis in Eastern Zambia. *Tropical Animal Health and Production*. **36**, 33-43.

Van der Ploeg, L. H. T., Cornelissen, A., Michels, P. A. M., Borst, P. (1984). Chromosome rearrangements in *Trypanosoma brucei*. *Cell*. **39**, 213-221.

Van Meirvenne, N., Magnus, E., Büscher, P. (1995). Evaluation of variant specific trypanolysis tests for serodiagnosis of human infections with *Trypanosoma brucei gambiense*. *Acta Tropica*. **60**, 189-199.

Van Meirvenne, N. (1999). Biological diagnosis of human African trypanosomiasis, In: Progress in human African trypanosomiasis, sleeping sickness, (Dumas, M., Bouteille, B., Buguet, A. (Eds.)): Paris, France, Springer-Verlag.

Van Nieuwenhove, L., Büscher, P., Balharbi, F., Humbert, M., Guisez, Y., Lejon, V. (2013). A LiTat 1.5 variant surface glycoprotein-derived peptide with diagnostic potential for *Trypanosoma brucei gambiense*. *Tropical Medicine and International Health*. **18**, 461-465.

Van Nieuwenhove, S. (1999). Present strategies in the treatment of human African trypanosomiasias, In: Progress in Human African Trypanosomiasis, Sleeping Sickness, (Dumas, M., Bouteille, B., Buguet, A. (Eds.)): Paris, Springer.

Vanhamme, L., Pays, E., McCulloch, R., Barry, J. D. (2001). An update on antigenic variation in African trypanosomes. Trends in Parasitology. 17:338-343. *Trends in Parasitology*. **17**, 338-343.

Vassella, E., Probst, M., Schneider, A., Struder, E., Renggli, C. K., Roditi, I. (2004). Expression of a major surface protein of *Trypanosoma brucei* insect forms is controlled by the activity of mitochondrial enzymes. *Molecular Biology of the Cell*. **15**, 3986-3993.

Vather, P., (2010). Vivapain: a cysteine peptidase from *Trypanosoma vivax*. University of KwaZulu-Natal, Pietermaritzburg. MSc.

Ventura, S., Villaverde, A. (2006). Protein quality in bacterial inclusion bodies. *Trends in Biotechnology*. **24**, 179-185.

Vera, A., González-Montalban, N., Arís, A., Villaverde, A. (2006). The conformational quality of insoluble recombinant proteins is enhanced at low growth temperatures. *Biotechnology and Bioengineering*. **96**, 1101-1106.

Vercammen, D., van de Cotte, B., De Jaeger, G., Eeckhout, D., Casteels, P., Vandepoele, K., Vandenberghe, I., Van Beeumen, J., Inze, D., Van Breusegem, F. (2004). Type II metacaspases Atmc4 and Atmc9 of *Arabidopsis thaliana* cleave substrates after arginine and lysine. *Journal of Biological Chemistry*. **279**, 45329-45336.

Vercammen, D., Belenghi, B., Van De, C. B., Beunens, T., Gavigan, J. A., De Rycke, R., Brackenier, A., Inze, D., Harris, J. L., Van Breusegem, F. (2006). Serpin1 of *Arabidopsis thaliana* is a suicide inhibitor for metacaspase 9. *Journal of Molecular Biology*. **364**, 625-636.

Vercammen, D., Declercq, W., Vandenabeele, P., Van Breusegem, F. (2007). Are metacaspases caspases? *Journal of Cell Biology*. **179**, 375-380.

Verloo, D., Holland, W., My, L. N., Tam, P. T., Goddeeris, B., Vercruysse, J., Büscher, P. (2000). Comparison of serological tests for *Trypanosoma evansi* natural infections in water buffaloes from north Vietnam. *Veterinary Parasitology*. **92**, 87-96.

Verloo, D., Magnus, E., Büscher, P. (2001). General expression of RoTat 1.2 variable antigen type in *Trypanosoma evansi* isolates from different origin. *Veterinary Parasitology*. **97**, 183-189.

Vernet, T., Tessier, D. C., Richardson, C., Laliberté, F., Khouri, H. E., Bell, A. W., Storer, A. C., Thomas, D. Y. (1990). Secretion of functional papain precursor from insect cells. Requirement for *N*-glycosylation of the pro-region. *Journal of Biological Chemistry*. **25**, 16661-16666.

Vickerman, K., Luckins, A. G. (1969). Localization of variable antigens in the surface coat of *Trypanosoma brucei* using ferritin conjugated antibody. *Nature*. **224**, 1125-1126.

Vickerman, K. (1985). Developmental cycles and biology of pathogenic trypanosomes. *British Medical Bulletin*. **41**, 105-114.

Voller, A., Bidwell, D. E., Bartlett, A. (1975). A serological study on human *T. rhodesiense* infections using microscale ELISA. *Tropenmedizin und Parasitologie*. **26**, 247-251.

Walker, J. M. (1996). The bicinchoninic acid (BCA) assay for protein quantitation, In: The Protein Protocols Handbook, (Walker, J. M. (Ed.) 11-14, Humana Press.

Wastling, S. L., Picozzi, K., Kakembo, A. S. L., Welburn, S. C. (2010). LAMP for human African trypanosomiasis: a comparative study of detection formats. *PLOS Neglected Tropical Diseases*. **4**, e865.

Wastling, S. L., Welburn, S. C. (2011). Diagnosis of human sleeping sickness: sense and sensitivity. *Trends in Parasitology*. **27**, 394-402.

Watanabe, N., Lam, E. (2005). Two *Arabidopsis* metacaspases AtMCP1b and AtMCP2b are arginine/lysine-specific cysteine proteases and activate apoptosis-like cell death in yeast. *Journal of Biological Chemistry*. **280**, 14691-14699.

Watanabe, N., Lam, E. (2011). Calcium-dependent activation and autolysis of *Arabidopsis* metacaspase 2d. *Journal of Biological Chemistry*. **286**, 10027-10040.

Welburn, S. C., Coleman, P. G., Févre, E. M., Maudlin, I., Odiit, M., Eisler, M. C. (2006). Crisis, what crisis? Control of Rhodesian sleeping sickness. *Trends in Parasitology*. **22**, 123-128.

Werthein, H., Horby, P., Woodall, J. (2012). Atlas of human infectious diseases. Wiley-Blackwell, Oxford.

Whitesand, E. F. (1960). Recent work in Kenya on control of drug resistant cattle trypanosomiasis. *Proceedings of the 8th ISCTRC Meeting, Jos, Nigeria*, 141-154.

WHO. (1976). Parallel evaluation of serological tests applied in African trypanosomiasis: a WHO collaborative study. *Bulletin of the World Health Organisation*. **54**, 141-147.

WHO. (1986). Epidemiology and control of African trypanosomiasias. *Report of a WHO expert committee: Technical Report Series*. **739**, 1-125.

WHO. (1998). Control and surveillance of African trypanosomiasis. *Report of a WHO expert committee: Technical Report Series*. **881**, 1-120.

WHO. (2006). World Health Organization human african trypanosomiasis (sleeping sickness): epidemiological update. *The Weekly Epidemiological Record*. **81**, 71-80.

Williams, D. J. L., Taylor, K., Newson, J., Gichuki, B., Naessens, J. (1996). The role of anti-variable glycoprotein antibody responses in bovine trypanotolerance. *Parasite Immunology*. **18**, 209-218.

Woo, P. T. (1970). The heamocrit centrifuge technique for the diagnosis of African trypanosomiasis. *Acta Tropica*. **27**, 384-386.

Woo, P. T. (1971). Evaluation of the haematocrit centrifuge and other techniques for the field diagnosis of human trypanosomiasis and filariasis. *Acta Tropica*. **28**, 298-303.

Wragg, W. R., Washbourn, K., Brown, K. N., Hill, J. (1958). Metamidium: a new trypanocidal drug. *Nature*. **182**, 1005-1006.

Wright, P. F., Nilsson, E., van Rooij, E. M. A., Lelenta, M., Jeggo, M. H. (1993). Standardisation and validation of enzyme-linked immunosorbent assay techniques for the detection of antibody in infectious disease diagnosis. *Revue scientifique et technique (International Office of Epizootics)*. **12**, 435-450.

Wuyts, N., Chokesajjawatee, N., Panyim, S. (1994). A simplified and highly specialised detection of *Trypanosoma evansi* in India: the first case report. *The Southeast Asian Journal of Tropical Medicine and Public Health*. **25**, 266-271.

Yoshida, N. (2006). Molecular basis of mammalian cell invasion by *Trypanosoma cruzi*. *Annals of the Brazilian Academy of Sciences*. **78**, 87-111.

Zalila, H., González, I. J., El-Fadili, A. K., Delgado, M. B., Desponds, C., Schaff, C., Fasel, N. (2011). Processing of metacaspase into a cytoplasmic catalytic domain mediating cell death in *Leishmania major*. *Molecular Microbiology*. **79**, 222-239.

Ziegelbauer, K., Overath, P. (1993). Organization of two invariant surface glycoproteins in the surface coat of *Trypanosoma brucei*. *Infection and Immunity*. **61**, 4540-4545.

Zillmann, U., Konstantinov, S. M., Berger, M. R., Braun, R. (1996). Improved performance of the anion-exchange centrifugation technique for studies with human infective African trypanosomes. *Acta Tropica*. **62**, 183-187.

Zweig, M. H., Campbell, G. (1993). Receiver-operating characteristic (ROC) plots: a fundamental evaluation tool in clinical medicine. *Clinical Chemistry*. **39**, 561-577.

Zweygarth, E., Sabwa, C., Rötter, D. (1984). Serodiagnosis of trypanosomiasis in dromadary camels using a card agglutination test set (Testryp CATT). *Annales de la Societe Belge de Medecine Tropicale*. **64**, 309-313.